CHAPTER 1

INTRODUCTION

Paper Recycling

In the early 1990's, the disposal of solid waste material became a significant problem that needed to be addressed by the United States [1]. Between the early 1980's and the early 1990's, the landfill disposal capacity of the United States decreased, causing the average cost of waste disposal to quadruple. More wastepaper was collected in landfills than any other type of material, but wastepaper had the highest percentage of material that was recycled. So, the demand for recycled paper increased in the United States in order to decrease waste disposal and paper recycling became more significant for the paper industry. Also, recovered wastepaper was exported to other countries where the virgin fiber supply was limited, to further decrease the amount of waste material for disposal in the United States [1,2].

Upon recovery of wastepaper, the material is processed so that the paper fibers can be reused in papermaking [3]. The wastepaper is collected and then sorted at a sorting facility, to improve the wastepaper quality before it is used at a recycle mill. The sorted wastepaper is then processed at a recycle mill by pulping, screening, and cleaning. Other equipment may be used in the process, depending on the wastepaper quality and the desired product.

Contaminants in Recycled Paper

Wastepaper generally contains materials, other than paper fibers, that is not desired in the final paper product, referred to as contaminants [2,3]. Removal of contaminants is essential in the recycling of wastepaper for acceptable paper production.

Three sources of contaminants in wastepaper are paper mill additives, converting additives, and consumer debris [3]. Paper mill additives are added to the paper furnish during production and consist of fillers, dyes, and strength agents. Converting additives are added to the paper during the converting of the paper mill product into the final product and consist of inks, adhesives, and staples. Consumer debris consists of any contaminant added to the paper by the consumer.

Methods for controlling contaminants in wastepaper consist of quality control, mechanical removal, and mechanical dispersion [3]. Quality control of wastepaper involves inspecting bales of wastepaper for cleanliness. Mechanical removal involves centrifugal cleaners and fine screens to remove the contaminant particles from the paper fibers. Mechanical dispersion involves kneaders breaking down contaminant particles to sizes that can be removed by washing and flotation.

Adhesive Contaminants in Paper Recycling

One of the most troublesome contaminants in paper recycling is adhesive material [3]. Wastepaper usually contains adhesive material in stamps, labels, and envelopes [3-7]. When wastepaper is repulped, the adhesive material is broken down into small particles called sticky contaminants or stickies [3,6,8-10]. Stickies cause problems in the paper recycling process by depositing on paper machine equipment and by appearing as dirt in the final product and reclaimed pulp [3,5,11-15]. Reported methods for removing stickies from recycled fiber are screening, cleaning, flotation, and washing, each with their own levels of effectiveness [3,5,10,12,15-19].

Stickies have been reported to cost the paper industry almost $700 million per year due to downgrading of the product, mill downtime, and waste disposal [20]. The cost of downgrading is a result of customers refusing to pay the full cost of the product due to the presence of stickies particles. The cost of mill downtime is due to stickies causing breaks in production, decreasing the total amount of product that could be sold. The cost of waste disposal is the cost of landfilling the material rejected during the processing of recycled material.

The two size categories commonly used for stickies classification are “macro” and “micro” [11,21-23]. Macro stickies are defined as the stickies that are retained on a 0.006 inches slotted laboratory screen, whereas micro stickies pass through the slots of a 0.006 inches slotted laboratory screen [11,24,25]. The macro stickies collect on the screen and are analyzed, while the micro stickies flow through the screen and remain with the accepted pulp [5,21-23]. By definition, laboratory screens remove 100% of the macro stickies [21,22]. Micro stickies may agglomerate and deposit on the paper machine, resulting in breaks and downtime [5,21]. In practice, optimizing the pulping process to minimize the generation of micro stickies will improve the removal of adhesive contaminants by recycling operations.

Pressure Sensitive Adhesives

One very difficult to remove class of adhesive is the pressure sensitive adhesive (PSA) [6]. Pressure sensitive adhesives are commonly used in tapes, stamps, labels, and envelopes [6,26]. Pressure sensitive adhesives are defined as “permanently tacky and will adhere to a variety of dissimilar surfaces upon contact” [9].

During the pulping process, pressure sensitive adhesive materials break down into a variety of shapes and sizes that require different types of removal equipment [6,9,10,13,16]. Pressure sensitive adhesive particles commonly have a specific gravity near 1.0, resulting in low removal efficiency by centrifugal cleaners [4,6,12,13,16,27]. The glass transition temperature (T_g) for pressure sensitive adhesives is usually below room temperature [8,9]. Also, pressure sensitive adhesive particles are deformable and elastic at high temperature and pressure [9,13,16]. It has been proposed that these properties allow stickies to change shape and pass through screens, lowering the removal efficiency [4,6,8,9].

United States Postal Service Program

In 1994, the United States Postal Service (USPS) implemented a program entitled “Environmentally Benign Pressure Sensitive Adhesives (PSA) for Postal Applications” to develop adhesives, that have little effect on the environment, for use on stamps [28]. An environmentally benign pressure sensitive adhesive does not cause significant problems during the recycling process. In the program, adhesive manufacturers submitted products to be evaluated for performance on stamps and in laboratory and pilot plant recycling processes. Adhesives that passed the evaluation were labeled environmentally benign and were approved for use by the United States Postal Service. Unfortunately, the relationship between screenability and formulation was never reported, as the project kept the adhesive manufacturers and their formulations confidential.

Pressure Sensitive Adhesive Formulation

Two common types of pressure sensitive adhesives are block copolymer adhesives and acrylic adhesives [26,29]. The adhesive manufacturers sell the block copolymer adhesives as solutions or hot melts and the acrylic adhesives as solutions or emulsions [26].

The block copolymer adhesive chains consist of three blocks involving polystyrene and polyisoprene or polybutadiene [26,29]. The three blocks in the copolymer are in the form of polystyrene-polyisoprene-polystyrene (SIS) or polystyrene-polybutadiene-polystyrene (SBS). The block copolymer formulation involves a base block copolymer, two tackifiers, and other additives. Two tackifiers are used for block copolymers because each of the polymers in the block copolymer requires a different tackifier.

The SIS block copolymer is a “thermoplastic rubber”, or a copolymer containing a polystyrene phase and a polyisoprene phase [30]. In SIS, the polystyrene phase is the thermoplastic phase and the polyisoprene phase is the rubber phase. The polystyrene phases of multiple chains produce crosslinks between each other by forming a sphere containing only polystyrene phases. Varying the concentrations of the polystyrene and polyisoprene phases affects the stress-strain behavior of the copolymer. At 20 to 30% by weight polystyrene, the copolymer is similar to a vulcanized rubber and is soft with a low modulus. Above 33% by weight polystyrene, the copolymer behaves more like a thermoplastic and is hard with a high modulus.

Additives for the thermoplastic block copolymer interact with either the thermoplastic phase or the rubber phase depending on the solubility parameter [30]. In order for two materials to be miscible in each other, the solubility parameters must be similar. Polystyrene and polyisoprene have different solubility parameters, so materials are miscible in one phase or the other. The tackifiers needed for the block copolymers are resins, miscible with either the thermoplastic phase or the rubber phase. In addition to providing tackification, resins also improve the specific adhesion and control the modulus of the miscible phase. Plasticizer is another additive used in block copolymers. Plasticizers that are miscible in the polystyrene phase decrease the cohesive strength and allow the fluid to flow by preventing strong crosslinks from forming.

Typical formulations for block copolymer, pressure sensitive adhesives are shown in **Table 1-1** [31]. The hydrocarbon resin is the isoprene plasticizer and the liquid resin/plasticizer/oil is the styrene plasticizer. The major additive for rubber-based block copolymer pressure sensitive adhesives is antioxidants.

Table 1-1. Typical Formulations for a Block Copolymer PSA [31]

Parts of a Block Copolymer Adhesive	Percentage of Total Formulation, %
SIS or SBS block copolymer	25-40
Hydrocarbon resin	30-50
Liquid resin/plasticizer/oil	25-35
Additives	<1

Acrylic pressure sensitive adhesives are less complex than rubber-based block copolymer adhesives [32]. The major component in an acrylic pressure sensitive adhesive is the acrylic polymer chain, such as butyl acrylate or 2-ethylhexyl acrylate.

Acrylic polymers are naturally tacky and can serve as pressure sensitive adhesives without the addition of other materials, unlike the rubber-based block copolymer adhesives. In order to provide more tack, other monomer units can be incorporated into the polymer chain with butyl acrylate and 2-ethylhexyl acrylate. Also, tackifiers can be added to acrylic adhesives to increase the tack, but tackifiers do not have to be added to provide tack.

The major acrylic adhesives are butyl acrylate and 2-ethylhexyl acrylate [26,29]. Acrylic adhesive formulations involve a base polymer, tackifier, and other additives. Typical formulations for acrylic pressure sensitive adhesives are shown in **Table 1-2** [31]. The additives for acrylic pressure sensitive adhesives consist of defoamers and biocides.

Table 1-2. Typical Formulations for an Acrylic PSA [31]

Parts of an Acrylic Adhesive	Percentage of Total Formulation, %
Acrylic polymer	60-100
Tackifier resin	0-40
Additives	1-5

Properties of Adhesive Materials

Important properties for the performance of adhesives in stamps, labels, or envelopes are the peel, tack, and shear of the adhesive. These properties are not necessarily important for evaluating the removal of adhesive particles in paper recycling. In recycling, where breakage and deformation can occur, the shear and elongation moduli are important properties. All of the above properties depend on the glass transition temperature (T_g), so it is key [30,32]. Above the glass transition temperature, materials are rubbery or liquid-like; while below the glass transition temperature, materials are rigid and glassy.

Three important properties to adhesive manufacturers for the application of pressure sensitive adhesives are peel, shear, and tack [29,32]. Peel is a measure of the force needed to break the bond between the adhesive and the adherend. Shear is a measure of the resistance of the adhesive to a constant shear force. Tack is the stickiness of the adhesive and its ability to stick to the adherend. Peel and shear depend on the adhesive and cohesive strength of the adhesive, respectively. The peel, tack, and shear all depend on the amount of tackifier in the adhesive formulation.

The three mechanical forces affecting all materials are tensile, shear, and cleavage [29]. To test the three different forces, a sample is subjected to forces in different configurations. For tensile, forces are applied in opposite directions perpendicular to the major plane of and at the center of the sample. For shear, forces are applied in opposite directions parallel to the major plane of the sample. For cleavage, a sample with a crack at the edge is subjected to forces in opposite directions perpendicular to and at the crack in the sample.

The tensile and shear forces can be measured using different geometries in the same device [29]. A sample with a measured cross sectional area is subjected to a force perpendicular to the cross sectional area plane. The force divided by the cross sectional area is the stress. The stress is measured versus the strain, which is the change in length of the sample divided by the original length. In the elastic region of the stress versus strain curve, the slope is the Young's modulus or the shear modulus for the tensile and shear curve, respectively. Therefore, a plot of stress versus strain can be generated for both tensile and shear forces. From the curves, the stress at failure can be determined for both tensile and shear forces.

Pressure sensitive adhesives are viscoelastic polymers [29]. Viscoeleastic materials behave like viscous liquids and elastic solids. By applying a time-dependent or sinusoidal stress to a viscoelastic fluid, the dynamic mechanical properties of the fluid can be determined. For a sinusoidal stress, the stress and the strain are each a function of time and are out of phase with each other by a value of δ. If δ is not equal to 90^o, then the stress and strain are partially in phase and partially out of phase with each other. There are two moduli relating the stress and strain out of phase by δ, one for the stress and strain in phase with each other and one for the stress and strain out of phase. When the stress and stain are in phase with each other, energy is stored during part of a cycle, and when the stress and stain are out of phase with each other, energy is lost during a cycle. The modulus for the stress and strain in phase with each other is the storage modulus and the modulus for the stress and strain out of phase with each other is the loss modulus.

The dynamic mechanical properties of a viscoelastic material are measured in a dynamic mechanical spectrometer [29]. The sample is either placed in tension or in shear between two plates. When in tension, the Young's moduli are determined, and when in shear, the shear moduli are determined. One plate is attached to a sinusoidal driver and the other plate is attached to a force transducer. Both the frequency and amplitude of the signals are measured. The storage and loss moduli are measured as functions of either the temperature or the frequency. For measuring the moduli versus temperature, the frequency is held constant, and for measuring the moduli versus frequency, the temperature is held constant.

An important characteristic of polymeric materials is the glass transition temperature (T_g) [29]. At the glass transition temperature, a polymer changes from a glassy material to a rubbery material. At temperatures less than the glass transition temperature, the polymer behaves like a glass, and at temperatures greater than the glass transition temperature, the polymer behaves like a rubber. For pressure sensitive adhesives, the glass transition temperature is usually less than room temperature.

For a polymer containing thermally reversible crosslinks, another important temperature is the terminal relaxation temperature (T_t) [29]. The terminal relaxation temperature is greater than the glass transition temperature. At temperatures between the glass transition temperature and the terminal relaxation temperature the polymer behaves like a rubber. At temperatures greater than the terminal relaxation temperature, a polymer with thermally reversible crosslinks flows like a viscous fluid.

The storage modulus and the loss modulus are both affected by temperature [29]. As the temperature increases, the storage modulus decreases. At the glass transition temperature and the terminal relaxation temperature, the storage modulus decreases at a faster rate than at other temperatures. At the glass transition temperature and the terminal relaxation temperature, the loss modulus is greater than at other temperatures.

Crosslinking between polymer chains has a profound effect on its behavior [29]. By increasing the degree of crosslinking in a polymer, the mobility of the polymer chains decreases. A polymer containing permanent crosslinks will not flow at any temperature and a terminal relaxation temperature will not occur.

Screening of Adhesive Contaminants and Related Materials

Pressure screens are key to the removal of stickies in a recycling operation [33]. For efficient removal of stickies in a screen it is important that the stickies do not disintegrate or extrude through the slots in the screens. It should be noted that screens were originally designed to remove fibrous debris from the pulp slurry, and not elastic, deformable material like stickies.

The most common method for removing stickies is a multistage system of pressure screens [3]. The pressure screen is a cylindrical vessel containing a screen basket and a rotor (see **Figure 1-1**) [3,7,15,34]. The cylindrical vessel has ports for the feed, accept, and reject lines, allowing for continuous flow of material through the pressure screen [15]. The screen basket has either holes or slots designed to allow the acceptable material to pass through, while blocking the large contaminants [15,35]. The size of the holes or slots is the most important screen parameter in the removal of stickies [3,35]. For the removal of small stickies particles, fine screens are used because their narrow slot sizes range from 0.006 to 0.012 inches [33]. To maximize production, pressure screens utilize large pressure gradients and shear forces.

For commercial fine screens, typical stickies removal efficiencies range from 50 to 80% [33,36-38]. It has been proposed that the low removal efficiency in commercial screens is due to the deformable and elastic stickies being able to change shape and pass through the openings of the screen [4,6,8,9,39]. However, recent research has shown that breakage of adhesive particles in pressure screens also contributes to the reported low removal efficiency [38,40]. As a result, it is also important to understand the conditions that promote disintegration of stickies particles and extrusion in pressure screens.

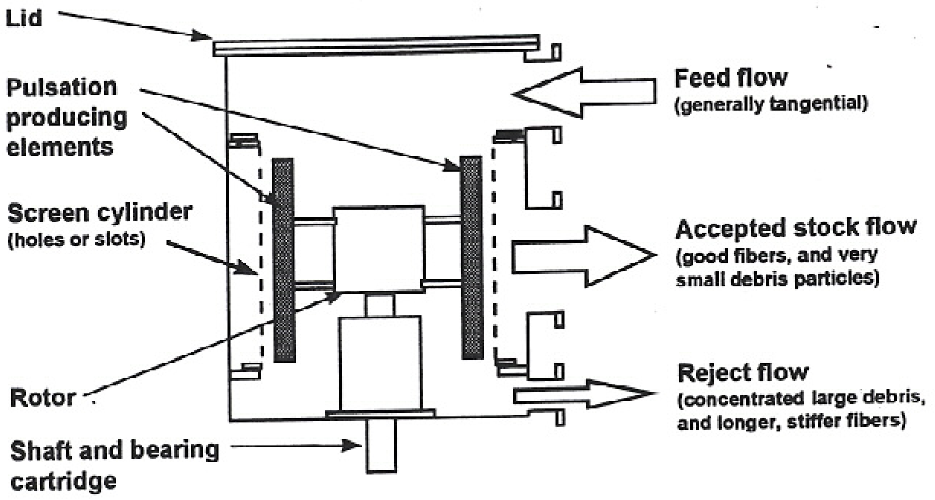

Figure 1-1. Diagram of a Pressure Screen [34]

Pressure Screen Operation

The ideal screen would remove all of the contaminants, while allowing all of the acceptable material to pass through [41]. In order to remove all of the contaminants, a perfect barrier would be required to block all of the contaminants. This is not practical, so screen plates contain holes or slots, to allow acceptable material to pass through. However, some contaminant particles also pass through the holes or slots with the acceptable material. Due to the demand for high fiber processing rates, screens are designed to compromise between production rate and screening efficiency. In this system, a screen accepts some contaminants and rejects some acceptable material. The removal efficiency of contaminants in a pressure screen depends on the rotor, the screen plate, and the operating variables [15,33,42].

Important rotor parameters are the shape of the rotor and the rotor speed [7,15,33,34,42]. Possible rotor shapes include foils, radial vanes, bumps, and tapered surfaces (see **Figure 1-2**) [7,34]. Each rotor shape produces a different pressure pulse at the screen basket [7,34]. Also, the rotor foils may be on the feed or accepts side of the screen basket, or on the inside or the outside of the screen basket (see **Figure 1-3**) [7,34]. A slow rotor can provide a better removal efficiency than a fast rotor by providing fewer pressure pulses [15,33,42].

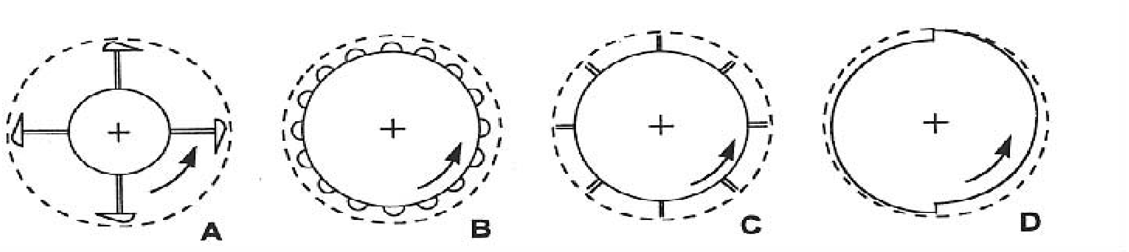

Figure 1-2. Typical Rotor Shapes for Pressure Screens: (A) Foils, (B) Bumps, (C) Radial vanes, (D) Tapered surfaces [34]

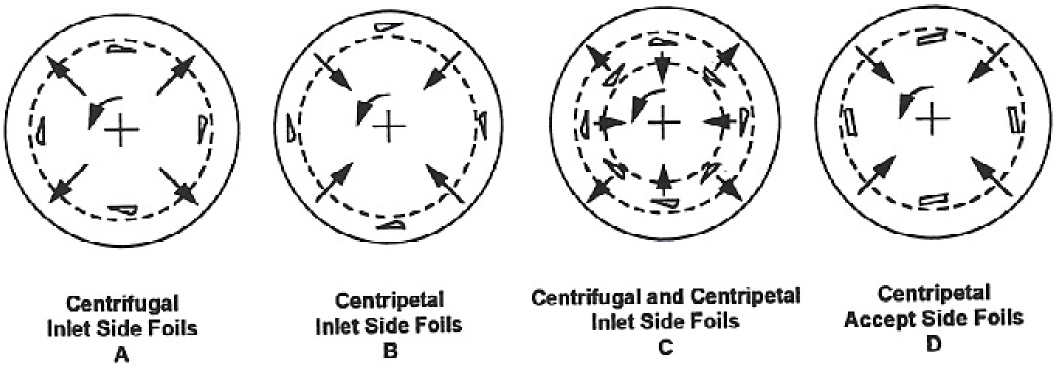
Centrifugal Inlet Side Foils A
Centripetal Inlet Side Foils B
Centrifugal and Centripetal Inlet Side Foils C
Centripetal Accept Side Foils D

Figure 1-3. Flow Designs for Pressure Screens with the Rotor on the Inside (A,C,D) or the Outside (B,C) of the Screen Basket [34]

As the rotor passes over the pressure screen basket, a pressure pulse is generated [43]. The pressure pulse is a result of the rotor tip passing close to the screen basket, followed by a wake to the rotor. The rotor forces material through the openings, while the wake pulls material back through the openings. The rotor and the wake generate positive and negative gauge pressures, respectively. **Figure 1-4** is an example of a pressure pulse. The pressure pulse prevents material from accumulating on the screen basket surface and in the openings due to the material passing back and forth through the openings.

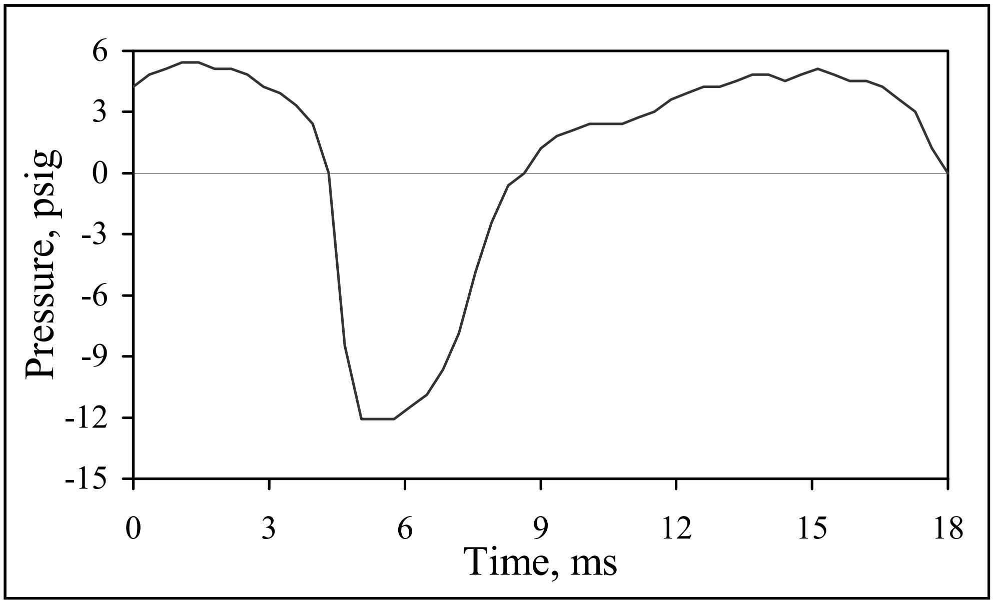

Figure 1-4. A Pressure Pulse in a Pressure Screen [44]

Important screen plate parameters are the shape and size of the openings and the degree of the surface contour [15,33,34,42]. Smaller holes or slots can improve the removal efficiency of a pressure screen by blocking more particles, but plugging is more likely to occur in smaller openings [15,42]. Currently, slot sizes as small as 0.004 to 0.006 inches are in use [39]. A screen basket with more of a contoured surface produces turbulence in the screen, which allows more contaminants to align with and pass through the openings [34].

The feed consistency, reject rate, pressure difference, slot velocity, and temperature have been mentioned as the key operating parameters for pressure screens [15,33,41,42]. The feed consistency affects the operation of a pressure screen by more clogging of the holes or slots occurring as the consistency increases [41]. It has been suggested that a higher consistency is better for contaminant removal [15,33]. The removal efficiency of a pressure screen is better at higher reject rates, but for the same amount of feed material, less material is accepted [15,42]. The pressure difference is the difference between the pressure on the feed side and the pressure on the accept side of the screen. An increase in the pressure difference across the screen basket is suggested to force more material through the openings and decrease the removal efficiency [15]. The slot velocity is a ratio between the volumetric flow rate of material through the screen openings and the total area of the screen openings, reported in velocity units. There is some data showing that as the slot velocity increases, the removal efficiency decreases [33]. Lower stock temperature has been mentioned to provide a better removal efficiency, but no data was offered to support this claim [15]. However, research has been conducted at this facility using a laboratory screen that does support this claim [38].

Two general mechanisms for particle removal are positive size separation and particle alignment with the rotor [7,15,34]. For "pure" positive size separation, rigid particles with all three dimensions larger than the hole or slot size are rejected. For particle alignment with the rotor, the largest dimension of a particle aligns with the rotor so that the largest dimension is parallel to the screen basket surface. Also, the largest dimension faces the hole or is perpendicular to the width of the slot. The particle cannot pass through the hole or slot and is rejected. Real pressure screens use both size separation and particle alignment for the removal of contaminant particles.

Proposed mechanisms for particles with at least one dimension larger than the slot width passing through the slots are particle alignment with the slot, particle bending, and particle extrusion [15,34]. Particle alignment with the slot as a mechanism for particle passage involves turbulence due to the surface contour, allowing the smallest dimension of the particles to align with the width of the slot so that the particles can pass through the slot [15]. Particle bending involves particles, with the smallest dimension less than half the width of the slot, bending in half to pass through the slot [15,34]. Particle extrusion involves particles with a low yield stress and larger size than the slot deforming and passing through the slot [15,34].

Forces in the Pressure Screen

Shear forces and tensile forces exist within a pressure screen [24,40,45]. Shear stresses occur in the wake of the rotor foil moving over the contoured screen basket and within the openings of the screen basket [40,45]. Tensile stresses occur at the entrances of the screen basket openings [24].

The rotor creates shear forces by pulp movement and mechanical action [40,45]. Of special importance is that the rotor breaks up a pulp mat that is formed on the surface of the basket. The pulp mat is at a higher consistency than the feed due to dewatering at the screen openings. As the rotor passes over the mat, the rotor fluidizes the pulp layer so that the fibers can pass through the screen openings. Shear forces in the screen basket openings are due to pulp flowing through the openings.

At the screen basket openings, tensile forces pull the particles into the openings [24,45]. The tensile forces are a result of the fluid velocity being greater in the openings relative to fluid velocity outside of the openings. The tensile forces cause particles to stretch and deform upon entering screen basket openings. Also, particles can break at the screen basket openings if the tensile forces are large enough.

In an analysis of paper fibers in the pressure screen, the two locations for shear stress were compared [45]. The wake of the rotor foil was reported to have a higher shear stress on the fiber wall than the openings of the screen basket. The maximum shear stress on the fiber wall was estimated to be 10^4 Pa for the wake of the rotor foil in the pressure screen, which was second only to the fan pump for wet-end papermaking equipment.

In another analysis of pressure screens, shear stress was calculated for the rotor foil and for the screen basket slots [40]. The shear stress was calculated to be in the 10^5 Pa range for the slots and in the 10^2 Pa range for the rotor foil. To calculate the shear stress for the rotor foil, an equation similar to the shear stress equation for a Newtonian fluid between parallel plates was used, with an apparent viscosity as a function of consistency. However, pulp is not a Newtonian fluid, but a Bingham plastic. To calculate the shear stress for the slots of the screen basket, the Hagen-Poiseuille equation was used, which is for Newtonian fluid flow in pipes.

Kerekes [24] analyzed pulp flocs in pipe constrictions, which could be representative of pulp flocs entering pressure screen slots. It was found that pulp flocs entering pipe constrictions stretched and then ruptured. The fibers in the pulp flocs were not sheared apart, but pulled apart as they entered the pipe constrictions. Due to elongation of the pulp flocs, the lengths increased and the diameters decreased for the pulp flocs.

Shear affects the breakdown of particles by providing the force for fracture. Particles in a suspension break up when the shear stress is greater than their yield stress

[46]. So by increasing the shear to levels greater than the yield stress, particles should break down in a pulp suspension. The maximum shear stress on the surface of papermaking fibers has been estimated for various pieces of equipment in the pulp and paper industry [45]. The fiber wall shear stress, τ_w, can vary from 10^2 Pa for a paper machine to 10^4 Pa for a pressure screen. With the use of high shear mixers and pumps for medium consistency (>10%) pulp processing, the shear is even higher [47].

If an object, such as a fiber or a contaminant, is immersed in a fluid, such as water, shear forces exist on the object. The shear forces resulting from fluid flow around immersed objects are called drag [48]. The two types of drag are skin friction and form drag. Skin friction occurs in flow over the surface of an object and form drag occurs in flow past blunt objects. Skin friction is caused by the formation of a boundary layer at the surface of an object. Form drag usually involves the formation of a wake in the fluid flow beyond the object.

Shear Forces in Rotary Devices

Pulpers, mixers, and screens are all examples of recycling operations that are rotary devices. It is important to understand how the breakage of particles in such devices affects the screening of those particles.

In a stirred vessel, a zone of high energy occurs around the blades of the impeller [25]. The zone of high energy consists of flow acceleration, vortexes, pressure gradients, and variations in shear stress up to one hundred times the average. Aggregate breakup occurs within the zone of high energy due to intense agitation. There is also a zone of low energy, where particles are more likely to collide with and attach to each other, forming aggregates. For a stirred vessel involving turbulent flow, the average shear rate can be calculated using the equation:

$$G = (P/V\mu_f)^{1/2}$$

where G is the shear rate, P is the power input, V is the fluid volume, and μ_f is the fluid viscosity [25]. G is an average value and the actual values can be significantly higher within the zone of high energy.

Using a rotary shear tester, pulp samples have been analyzed to determine the yield stress [46,49]. A relationship was found between the yield stress and the pulp consistency. An equation for the curve fitted to the data was of the form:

$$\tau_y = aC_m^{\ b}$$

where τ_y was the yield stress, a and b were constants, and C_m was the pulp consistency [46,49]. The constants in the equation depended on the type of pulp. Also, apparent viscosity, torque, and power dissipation were found to have relationships to consistency similar to that for yield stress [49,50]. The level of power dissipation was the amount of power required to fluidize a pulp suspension.

Particle Breakage

Dynamic and drag forces act on a particle in a turbulent flow vessel causing breakage to occur [25]. The dynamic forces act across the particle and the drag forces act on the particle surface. The dynamic forces are the local shear stress and the pressure gradient across the particle. The drag forces are the shear forces on the particle surface.

Under high shear conditions, particles can break down into smaller particles by breaking, fragmenting, shedding, stretching, or disintegrating [25,51]. Breaking of particles involves splitting them into two smaller particles. Fragmenting of particles involves splitting them into several smaller particles. Shedding of particles involves erosion of small pieces from the surface. Stretching of particles involves tensile forces causing the particles to change shape into strings or threads and then break. Disintegrating of particles involves splitting the particles into many very small particles. Based on the ways that particles break down, equations have been developed for particle size and number of particles [51-54].

In a study of pulp flocs, different levels of shear stress were considered [51]. Pulp flocs were analyzed for size changes over time. The equation for floc size versus time that was fitted to the data was:

$$S = S_0 \exp[-K_s(t - t_0)]$$

where S was the floc size, S_0 was the initial floc size, t was the time, t_0 was the initial time, and K_s was the rate constant [51]. This equation is in the form of exponential decay, suggesting that erosion caused the flocs to decrease in size. Fitting a curve to the data for the rate constant and shear stress provided the equation:

$$K_s = 3.7(\tau - 6)$$

where K_s was the rate constant in s^{-1} and τ was the shear stress in N/m^2 [51]. The shear stress depended only on the Reynolds number for the fluid flow and the distance across the system. The equation for the rate constant versus the shear stress showed that there was a minimum shear stress required for the floc size to change. According to the two equations, in order for the flocs to disperse, the shear stress had to be greater than 6 N/m^2.

In an analysis of toner deinking, the average diameter of toner particles was analyzed [54]. The average diameter of the toner particles depended on the additives, shear rate, temperature, and time. The additives considered were pure oil and a mixture of oil and surfactant. The additives provided different results for average diameter versus shear rate and temperature. Temperature did not have any effect on average diameter with pure oil, but there was a non-linear relationship between average diameter and temperature with a mixture of oil and surfactant. For average diameter versus time, the curve depended on the temperature.

In the same analysis of toner deinking, models for particle aggregation and particle breakup were considered [54]. The breakup rate depended on the size of the particle and the particle concentration. The parameters were dimensionless and consisted of the ratio between the break up and aggregation rates, the exponent for the breakup rate, and the ratio between the size of a particle before and after breakup. It was found that the only parameter that affected the particle size distribution was the ratio between the breakup and aggregation rates. The equation determined for average particle size was:

$$D = k\rho^{-1/v}$$

where D was the average diameter of the particles, ρ was the ratio between the breakup and aggregation rates, v was the exponent for the breakup rate, and k was a constant [54]. The exponent for the breakup rate, v, depended on the particle size and the volume fraction of particles. An equation for the ratio between the breakup and aggregation rates, ρ, is:

$$\rho = B/\alpha V$$

where B was the breakup rate constant, α was the aggregation efficiency, and V was the volume [54]. The breakup rate, B, depended on the particle size and the volume fraction of particles. The aggregation efficiency, α, was the ratio between the number of aggregation collisions that occurred and the number of theoretical collisions.

Previous Research on Screening of Adhesives and Related Materials

Research has been conducted to understand the effect of operating parameters on the behavior of stickies and related materials in pressure screens [33,40,43,55-57]. The effects of operating parameters on removal efficiency and particle disintegration have been investigated. Operating parameters that were analyzed consisted of consistency, reject rate, rotor speed, slot velocity, and slot width.

In one study of stickies in slotted pressure screens, the effects of consistency, slot velocity, and slot width on the removal efficiency were investigated [55,56]. The pulp furnish consisted of newsprint and address labels. The pressure screen was operated at two consistencies, 0.75% and 1.25%. Slot widths of 0.15, 0.20, and 0.25 mm were considered. For each slot width, the slot velocity was varied from 1 to 5 m/s. The removal efficiency was better at 1.25% consistency than at 0.75% consistency for each slot width and slot velocity. The author did not explain the effect of consistency on removal efficiency. (Presumably, this is due to the fiber matrix preventing contaminant particles from entering the slots of the pressure screen.) Also, the removal efficiency was higher for the 0.15 mm wide slots than for the 0.20 mm and 0.25 mm wide slots at both consistencies and all of the slot velocities. The removal efficiency tended to decrease linearly as the slot velocity increased for each consistency and slot width. The author attributes the effect of slot velocity on removal efficiency as being due to an increase in the fluid forces, which increase the extrusion of the pressure sensitive adhesive particles, but this explanation is not justified by this work.

In another study of stickies in a slotted pressure screen, the effects of reject rate, rotor speed, and slot velocity on the removal efficiency were investigated [33]. Slot widths of 0.25 mm and 0.30 mm were used, but the slot widths were not compared. Reject rates ranged from 10 to 40% by weight and slot velocities ranged from 0.5 to 3.0 m/s. The removal efficiency increased non-linearly as the reject rate increased. Also, the curve of removal efficiency versus reject rate was lower for higher rotor speeds. The author attributes this to increased kinetic stock energy, but again this is not justified. In comparing removal efficiency to slot velocity, the removal efficiency decreased almost linearly as the slot velocity increased. The decrease in removal efficiency versus slot velocity was more for conformable particles than for non-conformable particles, but an explanation was not provided.

In a study of rubber particles representing adhesive contaminants, removal efficiency was evaluated versus consistency, reject rate, rotor speed, slot velocity, and slot width [57]. For consistency, the optimum removal efficiency occurred at about 1.6% consistency. It was theorized, but not proven, that very low consistency caused turbulence and prevented the alignment of the particles with the rotor. The author suggested that as the consistency increased, the turbulence decreased and higher removal efficiencies were achieved. At very high consistencies, the removal efficiency decreased again, but was not explained by the author. The removal efficiency increased as the reject rate increased as expected. The removal efficiency decreased as the rotor speed increased. It was mentioned that lower rotor speeds would reduce the pulse strength and the turbulence, but this was not proven. As the slot velocity increased, the removal efficiency decreased. The effect of slot velocity on the removal efficiency was attributed to fluid drag forces pulling particles through the slot, although no evidence was provided. The removal efficiency decreased as the slot width increased as expected. For the slot width experiments, the accept flow rate was held constant, causing the slot velocity to decrease as the slot width increased. However, the decrease in removal efficiency was more pronounced versus the slot width than versus the slot velocity. This indicates that slot width is more important than slot velocity.

In a study of polyethylene films as contaminants in pulp, the operating parameters of consistency, rotor speed, slot velocity, and slot width were varied for a pressure screen [43]. Three consistencies of 1, 2, and 3% were used. The rotor speed was 17, 20, or 23 m/s. The slot velocity ranged from 0.5 to 4 m/s. The slot width was 0.10, 0.15, 0.20, or 0.25 mm. In these experiments, the removal efficiency decreased as the slot velocity increased. Also, the removal efficiency improved as the slot width decreased. The author mentioned that increasing the slot velocity and the slot width changed the flow pattern and the particle orientation around the entrance to the slot, allowing more particles to flow through the slot, but no evidence was provided related to the flow patterns or the particle orientation. Consistency did not have much of an effect and rotor speed did not have any effect on the removal efficiency of the pressure screen.

In a study of stickies disintegration, three different pressure screens, with each pressure screen operating at a different consistency, were considered [40]. The consistencies at which the pressure screens operated were 2.5, 3.6, and 4.4%. The stickies particles were less likely to disintegrate in the pressure screen at 2.5% consistency than in the pressure screens at 3.6 or 4.4% consistency. The author mentioned that each of the pressure screens had a different rotor design, but the rotor designs were not compared. However, the author claimed that for higher consistency pulps the rotors provided higher shear forces in order to fluidize the pulp, and the higher shear forces increased the particle disintegration, but the shear forces were not measured for the different screens.

SUMMARY

Adhesive materials are found as contaminants in recovered paper and are difficult to remove in paper recycling. One especially troublesome type of adhesive contaminant in paper recycling is the pressure sensitive adhesive. Pressure screens are the most commonly accepted method for removing pressure sensitive adhesive particles from recycled pulp, but show varied removal efficiencies from 50 to 80%. The removal efficiency of the pressure screen depends on the screen rotor and the size and shape of the openings in the screen plate, as well as the operating parameters of feed consistency, reject rate, pressure difference, slot velocity, and operating temperature. Several mechanisms have been suggested to explain the passage of pressure sensitive adhesive materials through a screen, but further research is needed to verify the importance of these mechanisms.

REFERENCES

1. Young, R., "Recovered Paper and the U.S. Solid Waste Dilemma", Chapter 1 in *Secondary Fiber Recycling*, Spangenberg, R. J., ed., TAPPI Press, Atlanta, GA, 1993.

2. Smook, G. A., *Handbook for Pulp & Paper Technologists*, 2nd edition, Angus Wilde Publications, Vancouver, BC, Canada, 1992.

3. McKinney, R. W. J., " Wastepaper Preparation and Contaminant Removal", Chapter 3 in *Technology of Paper Recycling*, McKinney, R. W. J., ed., Blackie Academic & Professional, London, 1995.

4. Pikulin, M. A., "Stickies and Their Impact on Recycled Fiber Content Fine Paper", *Joint Conference to Address Pressure Sensitive Adhesive Issues Proceedings*, United States Postal Service and American Forest & Paper Association, Washington, D.C., June 1996.

5. Doshi, M. R., "Overview-Stickies", *Paper Recycling Challenge*, Vol. I- Stickies, M. R. Doshi and J. M. Dyer, eds., Doshi & Assoc., Inc., Appleton, WI, pp. 3-6, 1997.

6. Scholz, W. F., "Recyclable Pressure Sensitive Adhesives", *1993 Tappi Pulping Conference Proceedings*, Atlanta, GA, TAPPI Press, pp. 501-505, 1993.

7. Bliss, T., "Screening", Chapter 14 in *Secondary Fiber Recycling*, Spangenberg, R. J., ed., TAPPI Press, Atlanta, GA, 1993.

8. Chou, C. S., "Repulpability of Adhesives", *Paper Recycling Challenge, Vol. I- Stickies*, M. R. Doshi and J. M. Dyer, eds., Doshi & Assoc., Inc., Appleton, WI, pp. 304-309, 1997.

9. Scholz, W. F., "Pressure Sensitive Adhesives", *Progress in Paper Recycling*, 4(1):71-73, 1994.

10. Crossley, B. R., Abubakr, S., Grimes, D. B., and Kumar, R., "A Pilot Plant Study of the Recyclability of Pressure Sensitive Adhesives (PSA)", *1998 Tappi Recycling Symposium Proceedings*, New Orleans, LA, TAPPI Press, pp. 469-473, March 1998.

11. Doshi, M. R., "Quantification of Stickies", *Paper Recycling Challenge, Vol. I- Stickies*, M. R. Doshi and J. M. Dyer, eds., Doshi & Assoc., Inc., Appleton, WI, p. 193, 1997.

12. Doshi, M. R., "Properties and Control of Stickies", *Paper Recycling Challenge, Vol. I- Stickies*, M. R. Doshi and J. M. Dyer, eds., Doshi & Assoc., Inc., Appleton, WI, pp. 227-236, 1997.

13. Smith, S. E., "Stickies Properties and the Relationship to Their Removal", *Paper Recycling Challenge, Vol. I- Stickies*, M. R. Doshi and J. M. Dyer, eds., Doshi & Assoc., Inc., Appleton, WI, pp. 237-239, 1997.

14. Douek, M., Guo, X.-Y., and Ing, J., "An Overview of the Chemical Nature of Deposits/Stickies in Mills Using Recycled Fibre", *1997 Tappi Recycling Symposium Proceedings*, Chicago, IL, TAPPI Press, pp. 313-330, April 1997.

15. Bliss, T., and Ostoja-Starzewski, M., “Debris Characteristics and Removal Techniques”, *1997 Tappi Korea Recycling Symposium Proceedings*, Seoul, Korea, TAPPI Press, pp. 1-17, October 1997.

16. Landa, M. R., “PSA Labels and Repulping Paper”, *Joint Conference to Address Pressure Sensitive Adhesive Issues Proceedings*, United States Postal Service and American Forest & Paper Association, Washington, D.C., June 1996.

17. McCool, M. A., and Silveri, L., “Removal of Specks and Nondispersed Ink from a Deinking Furnish”, *Tappi Journal*, 70(11):75-79, 1987.

18. Moss, C. S., “Theory and Reality for Contaminant Removal Curves”, *Tappi Journal*, 80(4):69-74, 1997.

19. Moss, C. S., “The Contaminant Removal Curve – Theory vs Reality”, *1997 Tappi Recycling Symposium Proceedings*, Chicago, IL, TAPPI Press, pp. 1-6, April 1997.

20. Friberg, T., “Cost Impact of Stickies”, *Progress in Paper Recycling*, 6(1):70-72, 1996.

21. Doshi, M. R., “Quantification of Stickies”, *Paper Recycling Challenge, Vol. I-Stickies*, M. R. Doshi and J. M. Dyer, eds., Doshi & Assoc., Inc., Appleton, WI, pp. 176-179, 1997.

22. Dyer, J., “A Summary of Stickies Quantification Methods”, *Paper Recycling Challenge, Vol. I- Stickies*, M. R. Doshi and J. M. Dyer, eds., Doshi & Assoc., Inc., Appleton, WI, pp. 44-51, 1997.

23. Staff, Progress in Paper Recycling, “Methods to Quantify Stickies-A Mill Survey”, *Paper Recycling Challenge, Vol. I- Stickies*, M. R. Doshi and J. M. Dyer, eds., Doshi & Assoc., Inc., Appleton, WI, pp. 171-175, 1997.

24. Kerekes, R. J., “Pulp Floc Behavior in Entry Flow to Constrictions”, *Tappi Journal*, 66(1):88-91, 1983.

25. Shamlou, P. A., and Titchener-Hooker, N., “Turbulent Aggregation and Breakup of Particles in Liquids in Stirred Vessels”, Chapter 1 in *Processing of Solid-Liquid Suspensions*, Shamlou, P. A., ed., Butterworth-Heinemann Ltd., Oxford, 1993.

26. Temin, S. C., “Pressure-Sensitive Adhesives for Tapes and Labels”, Chapter 38 in *Handbook of Adhesives*, 3rd edition, Skeist, I., ed., Van Nostrand Reinhold, New York, 1990.

27. Hsu, N. N.-C., “Stickies-The Importance of Their Chemical and Physical Properties”, *Paper Recycling Challenge, Vol. I- Stickies*, M. R. Doshi and J. M. Dyer, eds., Doshi & Assoc., Inc., Appleton, WI, pp. 256-258, 1997.

28. Peng, J. Y., "United States Postal Service Efforts to Develop an Environmentally Benign Pressure-Sensitive Adhesive for Postage Stamp Applications", *2000 Tappi Recycling Symposium Proceedings*, Washington, D.C., TAPPI Press, pp. 3-20, March 2000.

29. Pocius, A. V., *Adhesion and Adhesives Technology: An Introduction*, Hanser/Gardner Publications, Inc., Cincinnati, OH, 1997.

30. Harlan, J. T., and Petershagen, L. A., "Thermoplastic Rubber (A-B-A Block Copolymers) in Adhesives", Chapter 13 in *Handbook of Adhesives*, 3rd Edition, Skeist, I., ed., Van Nostrand Reinhold, New York, 1990.

31. Leppanen, A., "The Role of Pressure Sensitive Labels in Paper Recycling", *Adhesive and Sealant Council 1999 Spring Convention and Expo Proceedings*, Toronto, ON, Canada, April 1999.

32. Gehman, D. R., "Acrylic Adhesives", Chapter 25 in *Handbook of Adhesives*, 3rd Edition, Skeist, I., ed., Van Nostrand Reinhold, New York, 1990.

33. Heise, O., "Screening Foreign Material and Stickies", *Tappi Journal*, 75(2):78-81, 1992.

34. Bliss, T., "Screening in the Stock Preparation System", *1998 Tappi Stock Preparation Short Course Proceedings*, Atlanta, GA, TAPPI Press, pp. 151-174, April 1998.

35. Kelly, A. F., "Screening Secondary Fiber", *1997 Tappi Improving Screening and Cleaning Efficiencies Short Course Proceedings*, Minneapolis, MN, TAPPI Press, pp. 115-124, June 1997.

36. Heise, O., Kemper, M., Wiese, H., and Krauthauf, E., "Removal of Residual Stickies Applying New Flotation Technology at Haindl Paper - Schongau", *1999 Tappi Conference Proceedings*, Atlanta, GA, TAPPI Press, pp. 693-710, March 1999.

37. Veilleux, S., Chabot, B., and Daneault, C., "Quantification of Macro Stickies and Optimization of the Wastepaper Deinking Process", *5th Research Forum on Recycling Proceedings*, Ottawa, ON, Canada, pp. 241-247, September 1999.

38. Lucas, B. E., Venditti, R. A., and Jameel, H., "Behavior of Pressure Sensitive Adhesive Material in Industrial Pressure Screens and Laboratory Screens", *Tappi Journal*, 84(5):70, 2001.

39. Doshi, M. R., "Reduce The Pressure, Please!", *Progress in Paper Recycling*, 8(4):6, 1999.

40. Heise, O., Schabel, S., Cao, B., and Lorenz, K., "Deformation and Disintegration Physics of Stickies in Pressure Screens", 5th Research Forum on Recycling Proceedings, Ottawa, ON, Canada, pp.187-196, September 1999.

41. Steenberg, B., "Principles of Screening System Design: Studies in Screening Theory I", Svensk Papperstidning, 56(20):771-778, 1953.

42. Sternby, A. J., and Lehman, D. F., "Groundwood Pulp Fractionation and Screening with Pressure Screens at High Consistency", Tappi, 44(6):401-407, 1961.

43. Julien Saint Amand, F., and Perrin, B., "Screening: Experimental Approach and Modelling", 1998 Tappi Pulping Conference Proceedings, Montreal, QC, Canada, TAPPI Press, pp. 1019-1031, October 1998.

44. Wikstrom, T., and Fredriksson, B., "Hydrodynamics in a Pressure Screen – Consequences on the Separation Process", 5th Research Forum on Recycling Proceedings, Ottawa, ON, Canada, pp. 197-202, September 1999.

45. Tam Doo, P. A., Kerekes, J., and Pelton, R. H., "Estimates of Maximum Hydrodynamic Shear Stresses on Fibre Surfaces in Papermaking", Journal of Pulp and Paper Science, 10(4):J80-J88, 1984.

46. Bennington, C. P. J., Kerekes, R. J., and Grace, J. R., "The Yield Stress of Fiber Suspensions", Canadian Journal of Chemical Engineering, 68(10):748-757, 1990.

47. Gullichsen, J., and Harkonen, E., "Medium Consistency Technology: I. Fundamental Data", Tappi Journal, 64(6):69-72, 1981.

48. Geankoplis, C. J., Transport Processes and Unit Operations, 3rd edition, Prentice Hall, Englewood Cliffs, NJ, 1993.

49. Bennington, C. P. J., Kerekes, R. J., and Grace, J. R., "Motion of Pulp Fibre Suspensions in Rotary Devices", Canadian Journal of Chemical Engineering, 69(2):251-258, 1991.

50. Bennington, C. P. J., and Kerekes, R. J., "Power Requirements for Pulp Suspension Fluidization", Tappi Journal, 79(2):253-258, 1996.

51. Lee, C. W., and Brodkey, R. S., "A Visual Study of Pulp Floc Dispersion Mechanisms", A.I.Ch.E. Journal, 33(2):297-302, 1987.

52. Brown, D. L., and Glatz, C. E., "Aggregate Breakage in Protein Precipitation", Chemical Engineering Science, 42(7):1831-1839, 1987.

53. Grabenbauer, G. C., and Glatz, C. E., “Protein Precipitation-Analysis of Particle Size Distribution and Kinetics”, *Chemical Engineering Communications*, 12:203-219, 1981.

54. Snyder, B. A., and Berg, J. C., “Oil-Assisted Agglomeration for Toner Deinking: Population Balance Model and Experiments”, *A.I.Ch.E. Journal*, 43(6):1480-1487, 1997.

55. Vitori, C. M., “Stock Velocity and Stickies Removal Efficiency in Slotted Pressure Screens”, *1st Research Forum on Recycling Proceedings*, Toronto, ON, Canada, pp. 133-142, October 1991.

56. Vitori, C. M., “Stock Velocity and Stickies Removal Efficiency in Slotted Pressure Screens”, *Pulp & Paper Canada*, 94(12):109-112, 1993.

57. Seifert, P., Winkler, J., Vitori, C., Fields, B., and Maze, E., “Removal of Soft and Flexible Contaminants from Recycled Paper, in Screens”, *5th Research Forum on Recycling Proceedings*, Ottawa, ON, Canada, pp. 165-186, September 1999.

CHAPTER 2

RESEARCH OBJECTIVES

One of the major problems in paper recycling is the presence of adhesive contaminants in recycled paper. It has been reported that adhesive contaminants can cost paper recycling about $700 million annually [1]. In 1994, the United States Postal Service (USPS), one of the major contributors of adhesive material to paper recycling, began a program to develop "environmentally benign adhesives" [2].

Screening of pulp is accepted as the best method for adhesive contaminant removal from recycled material. However, individual pressure screens usually provide removal efficiencies below 80% [3-5]. It is of interest to understand the conditions that promote the low removal efficiencies of pressure screens.

There are two main objectives for this research. One objective is to understand the behavior of pressure sensitive adhesive materials in pulp screening devices. The other objective is to identify the important operating conditions and material properties affecting the removal efficiency of pressure sensitive adhesive materials in screens. The results of this study should provide information for adhesive manufacturers, recycling equipment manufacturers, and paper recycling operators to improve the removal of adhesive contaminants from wastepaper.

REFERENCES

1. Friberg, T., "Cost Impact of Stickies", *Progress in Paper Recycling*, 6(1):70-72, 1996.

2. Peng, J. Y., “United States Postal Service Efforts to Develop an Environmentally Benign Pressure-Sensitive Adhesive for Postage Stamp Applications”, *2000 Tappi Recycling Symposium Proceedings*, Washington, D.C., TAPPI Press, pp. 3-20, March 2000.

3. Heise, O., “Screening Foreign Material and Stickies”, *Tappi Journal*, 75(2):78-81, 1992.

4. Heise, O., Kemper, M., Wiese, H., and Krauthauf, E., “Removal of Residual Stickies Applying New Flotation Technology at Haindl Paper - Schongau”, *1999 Tappi Conference Proceedings*, Atlanta, GA, TAPPI Press, pp. 693-710, March 1999.

5. Veilleux, S., Chabot, B., and Daneault, C., “Quantification of Macro Stickies and Optimization of the Wastepaper Deinking Process”, *5th Research Forum on Recycling Proceedings*, Ottawa, ON, Canada, pp. 241-247, September 1999.

CHAPTER 3

BEHAVIOR OF PRESSURE SENSITIVE ADHESIVE MATERIAL IN INDUSTRIAL PRESSURE SCREENS AND LABORATORY SCREENS

ABSTRACT

The objective of this research was to investigate the behavior of adhesive contaminants in industrial and laboratory screens. An acrylate based pressure sensitive adhesive label material was applied to copy paper and pulped in a pilot plant hydropulper. The pulp was then screened using an industrial pressure screen and two laboratory screens, all having 0.006 inches wide slots. A dyeing and image analysis method was utilized to detect the adhesive contaminants in handsheet samples. The industrial pressure screen provided cleanliness efficiencies ranging from 39% to 72%, whereas the two laboratory screens, using the same feed pulp, provided cleanliness efficiencies of greater than 97%. As expected, the laboratory screens were much more efficient than the industrial screen. The industrial pressure screen was found to break down the adhesive particles, which contributed to the lower screening efficiency of the industrial screen. These results indicate that the use of laboratory screens to predict the screenability of adhesive materials is not accurate. Currently, there is not an effective method in the laboratory to predict the screenability of adhesive materials in industrial pressure screens, but it is necessary to develop one.

BACKGROUND

Adhesives enter the wastepaper stream as stamps, labels, envelopes, etc. [1-4]. When wastepaper is repulped, the adhesives are broken down into smaller particles, which are commonly referred to as sticky contaminants or simply stickies [3,5-7]. Stickies deposit on the paper machine equipment, which causes problems in production [2,8-10]. Reported methods for removing stickies from recycled fiber are screening, cleaning, flotation, and washing [2,7,9,11].

One very difficult to remove class of adhesives is the pressure sensitive adhesive (PSA) [3]. Pressure sensitive adhesives are defined as “permanently tacky and will adhere to a variety of dissimilar surfaces upon contact” [6]. To be tacky, PSA materials are formulated with a glass transition temperature less than 20°C. They are deformable and elastic during recycling operations [6,10,11]. PSA materials are typically applied to paper at a thickness of about 0.001 inch. After pulping, this thin film is ruptured, producing either fragments of the thin film or particles in the shape of a sphere or fiber, depending on the pulping conditions [3,6,7,10-12]. It has been proposed that the size, shape, and deformability of the PSA cause removal efficiencies in screening operations to be low [1,3,5,6]. Also, PSA materials often have a specific gravity near one, causing difficulty in removal using cleaners [1,3,9-11,13].

Macro and micro are the two size categories generally used to describe stickies [8,14-16]. Macro stickies are defined as the stickies that are retained on a 0.006 inches slotted laboratory screen, while micro stickies pass through the 0.006 inches slotted laboratory screen [8,14,15]. The macro stickies are collected on the screen and analyzed, while the micro stickies remain with the accepted pulp [2,14-16]. By definition, laboratory screens remove 100% of the macro stickies [14,15]. On the paper machine, micro stickies may agglomerate and deposit on the equipment [2,14].

The commonly held method to remove stickies is the pressure screen in a multistage system [18]. The pressure screen is a cylindrical vessel containing a screen basket, rotor, and multiple ports [4,18]. The screen basket has either holes or slots designed to block large contaminants but allow good fibers to pass through [17]. The size of the holes or slots is the most important screen parameter in the removal of stickies [17,18]. For the removal of small stickies particles, fine screens are used because of their narrow slot sizes ranging from 0.004 to 0.012 inches. A limit exists for the minimum opening size, which is related to the width of a papermaking fiber. Further, operating problems like plugging are more probable at the smaller opening sizes.

For fine screens, typical removal efficiencies of stickies are only 70-80% [19]. To explain this, it has been proposed that some macro stickies extrude through the openings due to the pressure difference across the screen or by shear forces [8,20]. In contrast, laboratory screens do not have appreciable pressure difference or shear forces and therefore have higher removal efficiencies. Due to this difference, the laboratory screens do not provide an adequate representation of industrial pressure screens for stickies removal. This lack of a laboratory test indicative of industrial screening of adhesives limits research by adhesive manufacturers' and the paper industry. Thus, it is important to understand on a detailed level the differences in operating principles and performance between laboratory and industrial screens.

In this study, the removal efficiencies of adhesive contaminants by industrial and laboratory screens were compared. A model system of copy paper and pressure sensitive adhesive labels was prepared in a pilot plant hydropulper and screened in a pilot plant industrial screen and two laboratory screens with the same slot sizes. One of the main findings was that breakage of adhesive particles occurred in the industrial screen and was an important phenomenon contributing to the low screening efficiencies.

EXPERIMENTAL

Pilot Plant Screening

Avery Dennison "White Shipping Labels", product number 5164, were applied to sheets of Weyerhaueser Husky Xerocopy paper to achieve an adhesive content of 0.2% adhesive by weight on OD paper. Through the use of Fourier Transform InfraRed (FTIR) spectroscopy the adhesive material was determined to be an acrylate based PSA (see **APPENDIX 1**). Three batches were prepared, each containing 50 OD lbs. of paper and 0.5 lbs. of labels. Each batch was pulped in a 200 gallon hydropulper from Black Clawson Co. The hydropulper was operated at a consistency of about 6% for 20 minutes at a rotor speed of 800 rpm. The initial temperature of each batch was between 50^{o}C and 55^{o}C. All three batches of pulp were collected in a stock tank and diluted to a consistency of 0.80% with water heated by steam. The pulp was allowed to mix for 20 minutes.

The industrial pressure screen utilized is a cylindrical vessel with feed, accept, and reject valves for flow control. Typical operating parameters for this screen are a 100 gpm feed flow rate and a 1-3% feed consistency. A screen basket with 0.006 inches wide slots and a contoured surface was installed in the vessel. Also, a shower and rotor inside the screen basket are used to prevent the accumulation of material on the face of the basket. The rotor speed is 1800 rpm.

Figure 3-1 shows the pilot plant layout for the experiment. Pulp was pumped from the feed stock tank through a flow meter and the feed valve of the pilot plant screen. The accepts passed through the screen and the accept valve of the pilot plant screen to a second stock tank. During the experiment, feed samples were scooped from the top of the feed stock tank (1). Accepts samples were collected from the outlet of the pipe feeding the second stock tank (2). Rejects samples were collected from the reject valve outlet of the pilot plant screen (3).

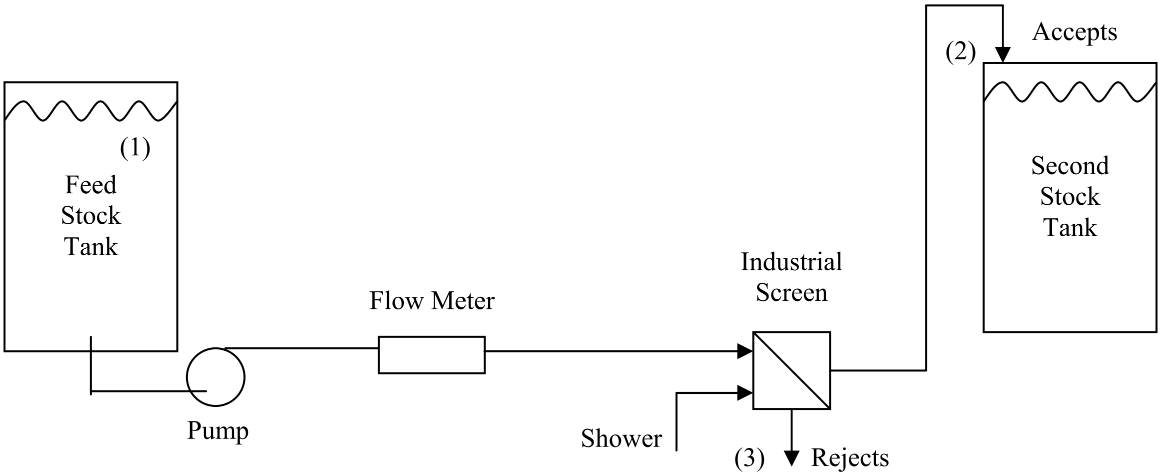

Figure 3-1. Flow Diagram of the Pilot Plant Screening Experiment

The pilot plant screen feed valve was adjusted until the flow rate through the flow meter was 4.4 ft/s, or about 96 gpm. The shower water for the screen was set at 5 gph and the gauge pressures were at 2 and 5 psig for the feed and accept streams, respectively.

The reject valve was adjusted until a reject rate of 10 gpm was achieved, at which point samples of the rejects, accepts and feed were collected. The feed temperature was 50°C and the accept temperature was 51°C. Then, the reject valve was adjusted until a reject rate of 8 gpm was achieved and samples of the rejects, accepts, and feed were collected. The feed temperature was 50°C and the accept temperature was 52°C. Next, the reject rate was decreased to about 5.45 gpm and a third set of rejects, accepts, and feed samples were collected. The feed temperature was 48°C and the accept temperature was 52°C. Samples were stored in a cold room in sealed plastic buckets.

A second pilot plant experiment was used to evaluate the effect of the pilot plant pumps on the adhesive and also to evaluate a different reject rate for the pilot plant screen. **Figure 3-2** shows the pilot plant layout for the pumping experiment. Pulp containing 0.2% adhesive on OD paper was prepared in the hydropulper in a similar manner to the first pilot plant experiment. During the experiment, pulp samples were collected from the top of the pulp in the dilution tank (4), the outlet of the pipe feeding the feed stock tank (5), the top of the pulp in the feed stock tank (6), and the outlet of the pipe back to the feed stock tank (7). Pulp was pumped from the dilution tank to the feed stock tank and then from the feed stock tank through a flow meter and back to the feed stock tank. A valve in the recirculation line was used to set the flow during the recirculation at 96 gpm. With the tank liquid volume of approximately 500 gallons, a quantity of about half of the tank contents was recirculated in this experiment.

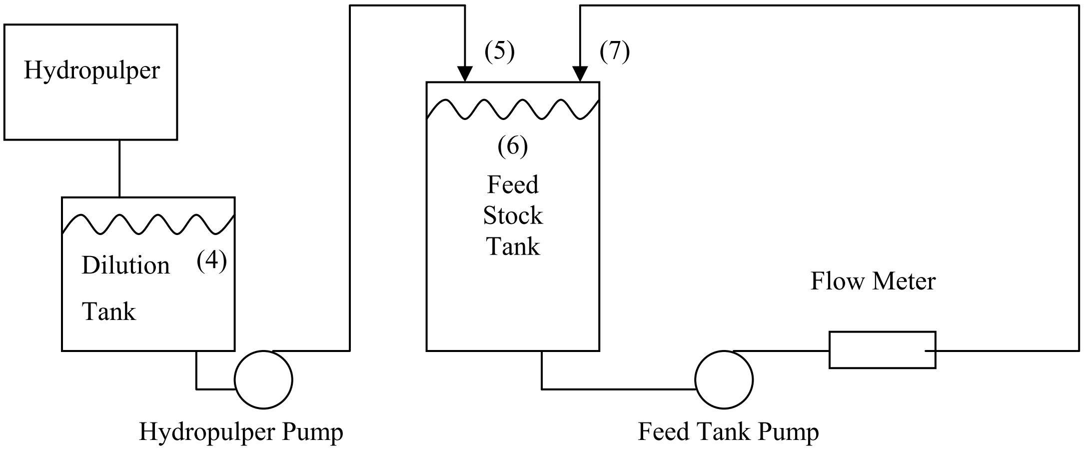

Figure 3-2. Flow Diagram of the Pilot Plant Pump Experiment

After stopping the recirculation flow, pulp from the feed stock tank was directed toward the screen as in **Figure 3-1**. The pilot plant screen feed valve was adjusted until the flow rate through the flow meter was 4.4 ft/s, or about 96 gpm as before. The shower water for the screen was set at 5 gph and the gauge pressures were 2 and 5 psig for the feed and accepts streams, respectively, also as before. The reject valve was adjusted until a reject rate of 15 gpm was achieved, at which point samples of the rejects, accepts, and feed were collected. The feed temperature was 53°C and the accepts temperature was 54°C.

Laboratory Screening: Pulmac MasterScreen

The Pulmac MasterScreen consists of a feed tank, screening chamber, and collection tube. The screening chamber has a screen plate with 0.006 inches slots and a spinning rotor (500 rpm), which agitates the stock and prevents blinding of the screen plate. The collection tube collects the rejects from the screening chamber on coarse filter paper.

Pulp of a known consistency in the plastic sample bucket was stirred to obtain a uniform distribution of contaminants. A pulp sample containing 25 OD g of pulp was taken. The Pulmac MasterScreen was turned on and subjected to two wash cycles. The mesh and screen plates were removed and washed with deionized water and replaced in the screen. A Fischerbrand Filter Paper P8 of measured OD weight was placed in the rejects tube and the Pulmac screening cycle was initiated. The temperatures of the pulp and water were determined to be approximately 25^{o}C for each experiment. The accepts were collected from the accept stream in a 150 mesh basket and the rejects were collected on the filter paper on the mesh plate. The accepts were removed from the basket and placed in a plastic bag for cold storage. The filter paper containing the rejects was placed in a 105^{o}C oven to dry overnight.

Laboratory Screening: Valley Flat Screen

The Valley Flat screen is a rectangular vessel with a rectangular horizontal screening plate containing 0.006 inches slots. A vibrating diaphragm on the accept side of the plate is used to back flush the screen openings on a cyclic basis. A water shower is used to keep the pulp stock diluted throughout a normal screening experiment.

Pulp of a known consistency in the plastic sample bucket was stirred to obtain a uniform distribution of contaminants. A pulp sample containing 25 OD g of pulp was measured. The Valley Flat screen was rinsed out and refilled to above the water shower with deionized water. The water shower supply valve was opened all the way and the motor for the diaphragm was started. The outlet valve was adjusted until the water level was constant. The temperatures of the pulp and water were measured. The water temperature was approximately 25°C for each experiment. The pulp sample was poured onto the screen and the temperature of the diluted pulp was measured. After 5 minutes, the water supply valve was closed. The motor was stopped when the water level was about 1 inch above the screen plate. The remaining water was allowed to drain. The accepts were collected in a 150 mesh basket and then placed in a plastic bag for storage. The rejects remaining on the screen were transferred to Whatman Filter Paper #541 and placed in a 105°C oven to dry overnight.

Another procedure for the Valley Flat screen involved the use of hot water instead of room temperature tap water from the water shower. Five 4 L beakers were filled with deionized water and heated in a microwave to about 48°C. Instead of opening the water supply valve on the shower, one beaker of hot water was poured onto the screen before the pulp was added. Each beaker of heated deionized water was poured onto the screen when the water level dropped to 1 inch above the screen plate. The temperature of the pulp stock during screening was 40-45°C. The screen motor was turned off after the last beaker was added and the water level was about 1 inch above the screen plate.

Dyeing and Rinsing of Handsheets

The dyeing and rinsing method was critical for the image analysis of the handsheets. Undyed white adhesive particles are indistinguishable from the paper fibers by image analysis. An increased contrast between stickies and the handsheets is thus required to detect the stickies properly. A dyeing and rinsing method involving Morplas Blue and Heptane was selected (see **APPENDIX 2**) and was used in this research.

Handsheets containing 1.2 OD g of pulp were prepared in sets of twelve using the TAPPI standard method. After the handsheets had dried overnight, ten handsheets were selected out of each set of twelve for dyeing.

Morplas Blue-Heptane dyeing solution was prepared in a vacuum hood. A mass of 0.670 g of Morplas Blue was weighed out in a metal pan using an analytical balance and poured into a 1000 ml volumetric flask. The flask was filled to the mark with 95% Heptane from Sigma-Aldrich. A magnetic stirrer was placed in the flask and a stopper was placed in the top. The flask was set on a stirring plate to stir overnight.

The Morplas Blue-Heptane dyeing solution was filtered using Whatman Filter Paper #1 in a Buchner funnel. The filtered solution was collected in a 1000 ml Erlenmeyer flask. 250 ml of the filtered dye solution was measured out in a 500 ml graduated cylinder and poured into a crystallizing dish. One handsheet was submerged in the dye solution and swirled for ten seconds. The handsheet was removed with forceps and hung from a string with a binder clip. These steps were repeated for the other nine handsheets to be dyed. The handsheets were allowed to dry overnight.

The next day, the handsheets were removed from the string. 500 ml of 95% Heptane was measured out in a 500 ml graduated cylinder and poured into a crystallizing dish. One handsheet was submerged in the Heptane solution and swirled for ten seconds. The handsheet was removed with forceps and hung from a string with a binder clip. These steps were repeated for the other nine handsheets to be rinsed. Each handsheet was removed as soon as it was dry.

Image Analysis

The SpecScan 2000 program by Apogee Systems Inc. was used to scan each set of ten handsheets, before and after dyeing, to determine the stickies content of the samples. The scanner was a Hewlett Packard Scanjet 4c with a 600 dpi resolution. A standard sample was scanned sixteen times in order to warm up the scanner bulb before image analysis was performed on real samples. The detection threshold was set at 80% of the average grayscale value. Both the felt and wire sides of each of the handsheets in a set were scanned. The parts per million (PPM) of stickies and the average particle size for particles greater than or equal to 0.040 mm^2 for each set of handsheets were determined for each side. Also, a histogram of particle sizes in terms of area and count was recorded. The values for the felt and wire side for each set of handsheets were averaged to obtain values for the total area of the set. An example of image analysis output is shown in **APPENDIX 3**.

RESULTS AND DISCUSSION

The stickies parts per million (PPM) results from the pilot plant screening experiments are shown in **Table 3-1**. The screen was operated at several different reject flow rates. This resulted in different values of the mass reject ratio, R_w:

$$R_W = V_R C_R / V_F C_F$$

where V is the volumetric flow rate and C is the solids consistency and R and F indicate the rejects and feed, respectively. The values of R_w increased with increasing reject flowrate as expected, **Table 3-1**. Samples from the pilot plant feed, accepts, and rejects were screened with the Pulmac and Valley screens. The PPM of the accepts for the Pulmac, Valley 25°C, and Valley 45°C are also shown in **Table 3-1**. Notice that the PPM values for the pilot plant screen feed, accepts, and rejects are much greater than those for the accepts from all of the laboratory screens. This confirms that the lab screens are significantly more effective in removing stickies from pulp.

Table 3-1. Parts Per Million Values of Screening Experiments

		Parts Per Million, PPM			
Feed Flow Rate, gpm		96 gpm	96 gpm	96 gpm	96 gpm
Reject Flow Rate, gpm		5.45 gpm	8 gpm	10 gpm	15 gpm
Mass Reject Ratio, %		4.5 %	12 %	15 %	25 %
Pilot Plant Feed (1)		1600	1840	2260	2940
Pilot Plant Accepts (2)		980	840	1120	830
Pilot Plant Rejects (3)		11300	7770	9620	4080
Pilot Plant Feed (1)	Pulmac	-	14	12	-
	Valley, 25°C	-	22	52	-
	Valley, 45°C	-	2	35	-
Pilot Plant Accepts (2)	Pulmac	40	78	52	-
	Valley, 25°C	67	177	71	-
	Valley, 45°C	228	247	201	-
Pilot Plant Rejects (3)	Pulmac	73	168	42	-
	Valley, 25°C	112	457	88	-
	Valley, 45°C	353	306	432	-

The cleanliness efficiency, E_C, was determined by the following equation [21]:

$$E_C = 1.0 - (S_A / S_F)$$

where S_A and S_F are the PPM of stickies in the accept and feed streams, respectively. (The subscript A indicates accepts.) The cleanliness efficiency indicates how clean the accept stream is relative to the feed stream. The reject efficiency, E_R, can be calculated as either:

$$E_R = (V_R C_R S_R) / (V_F C_F S_F)$$

or equivalently:

$$E_R = 1.0 - (V_A C_A S_A) / (V_F C_F S_F)$$

The reject efficiency measures the fraction of incoming contaminant that is separated into the reject stream. E_R is a better descriptor than E_C of an operation to remove a contaminant because it is based on the material balance of the contaminant, not just the concentrations in the feed and accepts. E_c may be artificially high and misleading in cases where the amount of total reject material is large compared to the accept stream.

The efficiencies described above were calculated from the data in **Table 3-1** and are shown in **Table 3-2**. For the lab screening experiments, it was found that the OD mass of the feed (V_FC_F) essentially equaled the OD mass of the accepts (V_AC_A). This was due to the facts that (a) essentially no fiber was found in the rejects and (b) the mass of the adhesive in the experiment was comparatively small relative to the fiber. If this equality is true, then the reject efficiency and the cleanliness efficiency are equal. Thus, the result from the equation for E_C is shown in **Table 3-2**, but is also equal to E_R.

Table 3-2. Efficiencies of Screening Experiments

		Screening Efficiency, %			
Reject Flow Rate, gpm		5.45 gpm	8 gpm	10 gpm	15 gpm
Mass Reject Ratio, %		4.5 %	12 %	15 %	25 %
Pilot Plant Cleanliness Eff.		38.8	54.5	50.5	71.7
Pilot Plant Reject Eff.		58.8	58.7	55.1	77.4
Pilot Plant Feed (1)	Pulmac	-	99.2	99.5	-
	Valley, 25°C	-	98.8	97.7	-
	Valley, 45°C	-	99.9	98.4	-
Pilot Plant Accepts (2)	Pulmac	95.9	90.6	95.4	-
	Valley, 25°C	93.1	78.8	93.6	-
	Valley, 45°C	76.7	70.4	82.1	-
Pilot Plant Rejects (3)	Pulmac	99.4	97.8	99.6	-
	Valley, 25°C	99.0	94.1	99.1	-
	Valley, 45°C	96.9	96.1	95.5	-

The pilot plant screen provided cleanliness efficiencies between 38.8 and 71.7% and reject efficiencies between 55.1 and 77.4%. This result is similar to a previous investigation in which a 0.012 inches slotted screen was used to remove stickies [19]. In that report, for R_W = 15% the removal efficiency was reported to be about 50%. The stickies removal efficiency of the work herein for the pressure screen experiment is similar, despite the considerable difference in slot sizes. However, the parameters of that study, such as the temperature, consistency, flow rates, and stickies content, were not reported, so an exact comparison is not possible.

In mill data reported by Union Camp for an acrylate PSA, the primary screens provided removal efficiencies of about 74% and the secondary screens provided removal efficiencies of about 59% [1]. In pilot plant experiments by the USDA Forest Service, 0.006 inches slotted pressure screens provided efficiencies of pressure sensitive adhesives between –14.0% and 68.4% [22]. In the data for the upgrade of the Haindl Paper Schongau mill, a fine screen with 0.20 mm wide slots was reported to have a removal efficiency of about 60% [23]. While replacing one of the fine screens at Bowater Pulp and Paper Canada's Gatineau mill, the removal efficiency was reported to increase from 33.7% in the old screen to 62.6-83.4% in the new screen [24]. In experiments conducted on a small commercial unit from Black Clawson Co., negative removal efficiency was reported for small model adhesive particles at 1% consistency [25].

In comparison to the efficiencies of the above industrial screens, all three laboratory screening experiments performed in this report had a E_c of greater than 97% for the pilot plant feed pulp sample (1). These results confirm that both of the laboratory screens are significantly more efficient than the industrial screen in removing adhesive, as expected.

Table 3-2 also shows that the cleanliness efficiency of stickies in the laboratory screens is lower for the pilot plant accepts sample (2) than for the pilot plant feed sample

(1) or rejects sample (3). This was expected because the pilot plant accepts contained stickies that had already passed through the 0.006 inches slotted screen basket in the pilot plant screen. Also, the pilot plant accepts average particle size was significantly smaller than the feed; see **Table 3-3**.

Table 3-3. Average Particle Sizes of Screening Experiments

		Average Particle Size, mm^2			
Reject Flow Rate, gpm		5.45 gpm	8 gpm	10 gpm	15 gpm
Reject Mass Ratio, %		4.5 %	12 %	15 %	25 %
Pilot Plant Feed (1)		2.61	1.97	2.02	1.88
Pilot Plant Accepts (2)		0.38	0.34	0.35	0.31
Pilot Plant Rejects (3)		0.86	0.90	0.90	0.65
Pilot Plant Feed (1)	Pulmac	-	0.08	0.09	-
	Valley, 25°C	-	0.11	0.10	-
	Valley, 45°C	-	0.04	0.09	-
Pilot Plant Accepts (2)	Pulmac	0.12	0.12	0.09	-
	Valley, 25°C	0.12	0.16	0.10	-
	Valley, 45°C	0.18	0.17	0.15	-
Pilot Plant Rejects (3)	Pulmac	0.13	0.12	0.14	-
	Valley, 25°C	0.14	0.17	0.15	-
	Valley, 45°C	0.18	0.18	0.17	-

Temperature appears to be an important parameter in the laboratory screening of stickies. At room temperature, i.e., 25°C, the Pulmac and Valley screens provided similar cleanliness efficiencies for the feed and rejects, **Table 3-2**. However, in general, at higher temperature, 45°C, the cleanliness efficiency of the Valley Flat screen decreased for the pilot plant accepts and rejects relative to screening at 25°C. This decreased efficiency at 45°C was not observed for the pilot plant feed sample. This may be due to the pilot plant feed pulp having a much larger average particle size (about 2 mm^2) than that of the accepts (about 0.3 mm^2) and rejects (about 0.8 mm^2); see **Table 3-3**. The very large particles in the pilot plant feed sample may have prevented the higher temperature from having an effect on the cleanliness efficiency of the Valley Flat screen. It is hypothesized that the higher temperature softens the adhesive, causing adhesive particles that are just slightly too large to pass through the slots at 25°C to be able to pass through at 45°C. The screen may still block significantly larger particles at 45°C despite the softening.

Table 3-3 shows the average particle size of the stickies from the pilot plant and laboratory screening experiments. Notice that the average particle size in the accepts from the laboratory screens is smaller than that in the accepts from the pilot plant screen. The average particle size of the pilot plant accepts ranges from 0.31 to 0.38 mm^2, whereas the laboratory screen accepts range from 0.04 to 0.18 mm^2. This is despite the fact that all of the screens have a slot width of 0.006 inches. It is widely thought that the passage of relatively large adhesive particles through the industrial pressure screen is due to the pressure difference extruding the elastic, deformable adhesives through the screen [1,3,5,6].

Figure 3-3 and **Figure 3-4** are plots of screening efficiency versus particle size for the pilot plant and laboratory screens, respectively. A comparison of these two plots reveals that the removal efficiencies of small particles, those less than 1.00 mm^2, are very different for the pilot plant and the laboratory screens. Unexpectedly, the reject efficiencies of the pilot plant screen are negative for particles < 1.00 mm^2 (**Figure 3-3**). This suggests that small particles are generated in the pilot plant system. This finding suggests another contributing factor that causes the screening reject efficiency of adhesives to be low, i.e., the screen breaks the adhesive particles into sizes that can pass through the screen. In contrast to the pilot plant screen, the cleanliness efficiencies of the laboratory screens for small particles is low, but always positive (**Figure 3-4**). As there is no appreciable pressure difference in the lab screens and the shear is much less than the pilot plant screen, it is expected that less breakage would occur.

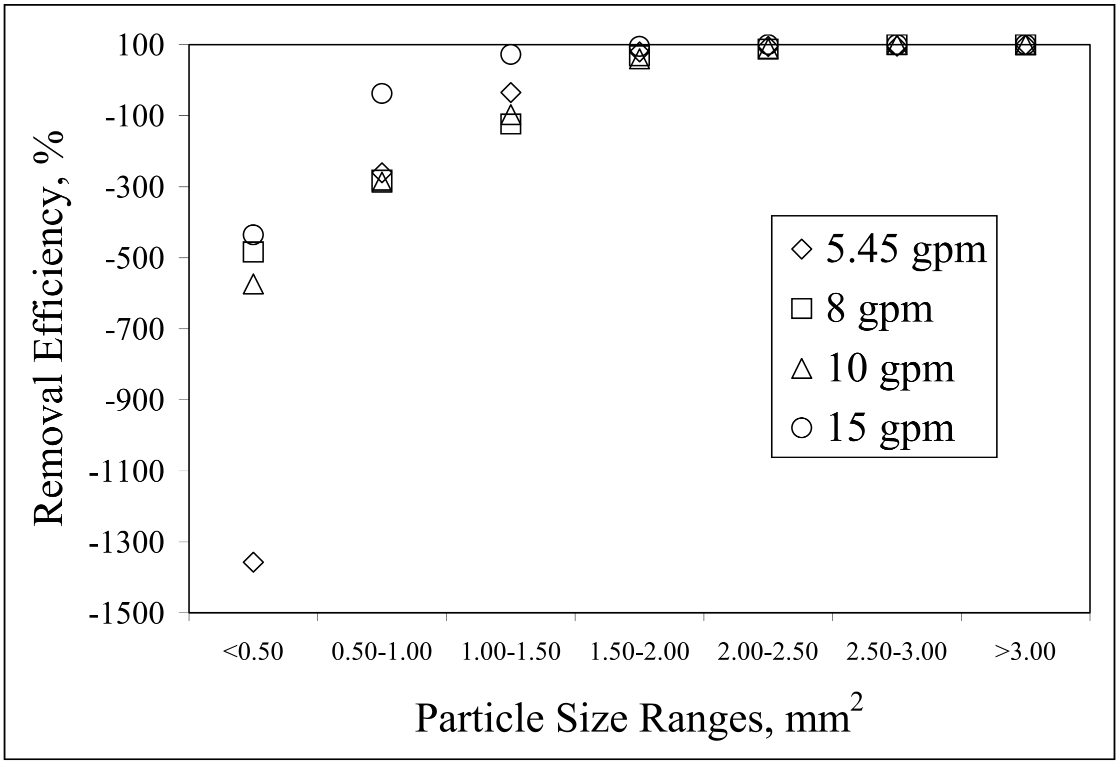

Figure 3-3. Removal Efficiency Versus Particle Size for the Pilot Plant Pressure Screen

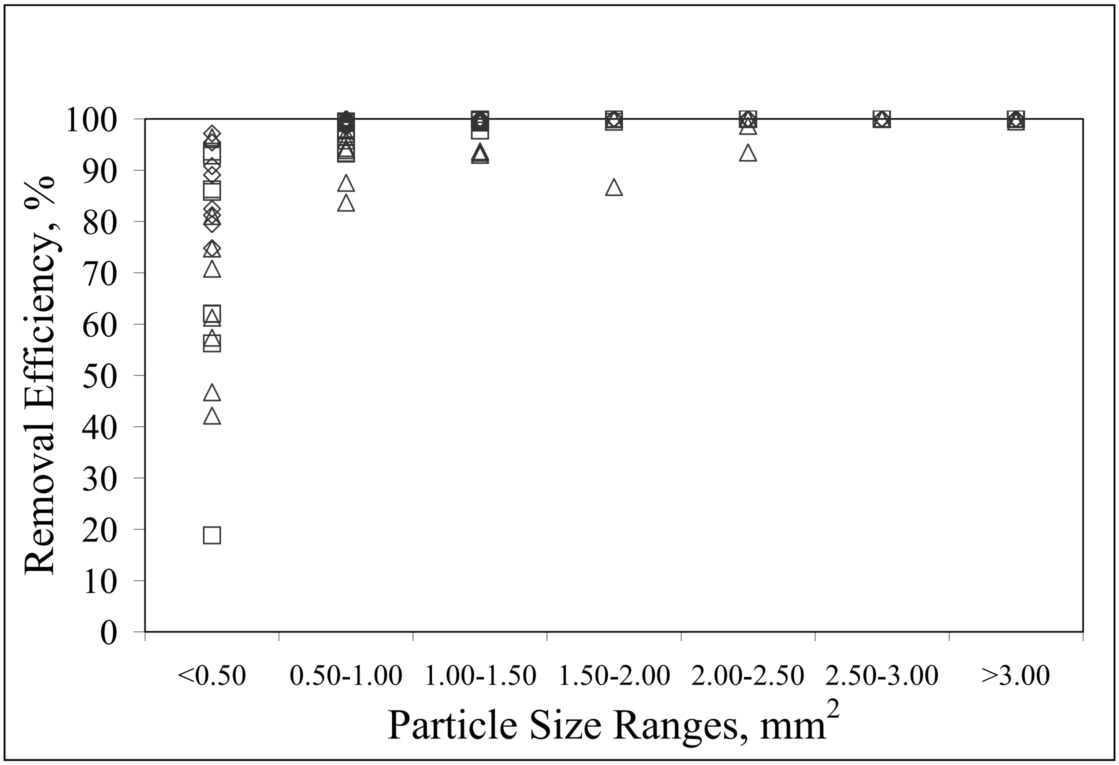

Figure 3-4. Cleanliness Efficiency Versus Particle Size for the Laboratory Screens, Symbols indicate: ◊ Pulmac, ☐Valley at 25°C, and Δ Valley at 45°C

Due to the choice of sampling points illustrated in **Figure 3-1** it was not possible to determine whether the pumps or the pressure screen were actually breaking the adhesive particles. To investigate, another pilot plant experiment was performed as shown in **Figure 3-2** prior to a standard screening experiment. **Table 3-4** shows the average particle size, parts per million, and number of particles at different sampling points according to the experiment illustrated in **Figure 3-2**.

Table 3-4. Pump/Screen Experiment for Reject Rate of 15 gpm

Sample	Average Particle Size, mm^2	Parts Per Million, ppm	Number of Particles in 1 m^2
Hydropulper (4)	1.28	2320	1810
Hydropulper Pump (5)	1.73	2430	1410
Feed Tank (6)	1.67	2770	1660
Feed Tank Pump (7)	1.54	2980	1940
Pilot Plant Screen Feed (1)	1.88	2940	1570
Pilot Plant Screen Accepts (2)	0.31	830	2680
Pilot Plant Screen Rejects (3)	0.65	4080	6300
Pilot Accepts + Rejects (2) + (3)	0.46	1640	3590

The results show that for the five samples taken prior to the pilot plant screen there was no significant difference in the measured average particle size, parts per million, or number of particles in 1 m^2. Thus, it was concluded that the generation of small particles was not due to the pumps. However, for samples during later screening, the values for the pilot plant accepts and rejects are significantly different than those for the pilot plant feed, both having a significantly lower average particle size and higher number of particles in 1 m^2. Accordingly, when the products of the pilot plant accepts and rejects were combined mathematically (2)+(3), i.e., a weighted average with respect to the OD mass flow rate of each stream, it was revealed that the number of particles about doubled and the average particle size decreased significantly relative to the pilot plant feed (1). This result confirms that the screen generated new, smaller adhesive particles.

Figure 3-5 is a plot of the number of particles in 1m^2 versus particle size for the samples from the pump and screening experiment. This plot shows that the mathematically combined pilot plant accepts and rejects contain significantly more small particles than the feed tank, feed tank pump, and pilot plant feed samples. Also, there is not a significant difference between the feed tank, feed tank pump, and pilot plant feed. Therefore, small particles are not generated in the pump, but in the pilot plant screen.

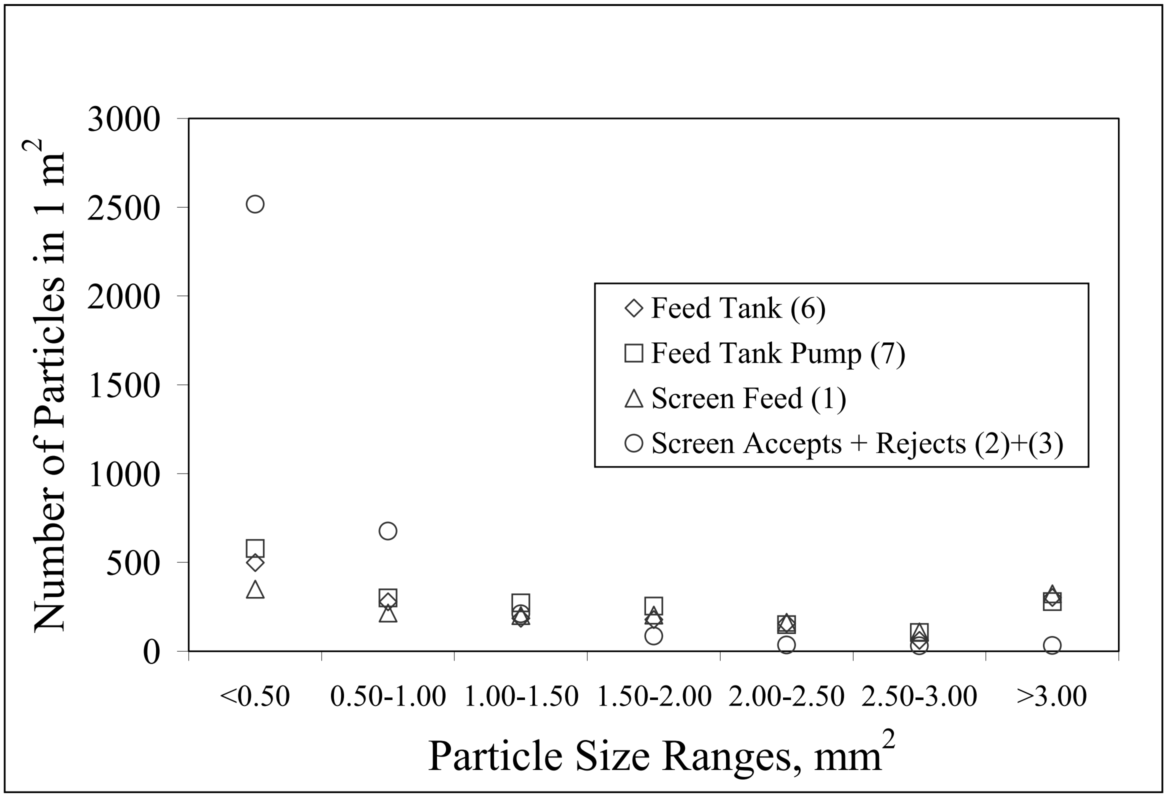

Figure 3-5. Particle Size Distribution Before and After the Pilot Plant Pump and Screen

CONCLUSIONS

Industrial pressure screens can break pressure sensitive adhesive particles, generating significant amounts of small adhesive particles and lowering the removal efficiency. Laboratory screens do not break the adhesive particles and are not good indicators of the screenability of pressure sensitive adhesives. Laboratory screens have a much higher screening efficiency than industrial pressure screens. A new laboratory test method is needed to predict the industrial screenability of pressure sensitive adhesives.

ACKNOWLEDGEMENTS

Support for this research has been provided in part by SCA Corporation and Ecosynthetix. Donations of equipment by Apogee Systems and Pulmac Instruments are also greatly appreciated.

REFERENCES

1. Pikulin, M. A., “Stickies and Their Impact on Recycled Fiber Content Fine Paper”, *Joint Conference to Address Pressure Sensitive Adhesive Issues Proceedings*, United States Postal Service and American Forest & Paper Association, Washington, D.C., June 1996.

2. Doshi, M. R., “Overview-Stickies”, *Paper Recycling Challenge, Vol. I- Stickies*, M. R. Doshi and J. M. Dyer, eds., Doshi & Assoc., Inc., Appleton, WI, pp. 3-6, 1997.

3. Scholz, W. F., “Recyclable Pressure Sensitive Adhesives”, *1993 Tappi Pulping Conference Proceedings*, TAPPI Press, pp. 501-505, 1993.

4. Bliss, T., “Screening”, Chapter 14 in *Secondary Fiber Recycling*, Spangenberg, R. J., ed., TAPPI Press, Atlanta, GA, 1993.

5. Chou, C. S., “Repulpability of Adhesives”, *Paper Recycling Challenge, Vol. I-Stickies*, M. R. Doshi and J. M. Dyer, eds., Doshi & Assoc., Inc., Appleton, WI, pp. 304-309, 1997.

6. Scholz, W. F., “Pressure Sensitive Adhesives”, *Progress in Paper Recycling*, 4(1):71-73, 1994.

7. Crossley, B. R., Abubakr, S., Grimes, D. B., and Kumar, R., “ A Pilot Plant Study of the Recyclability of Pressure Sensitive Adhesives (PSA)”, *1998 Tappi Recycling Symposium Proceedings*, New Orleans, LA, TAPPI Press, pp. 469-473, March 1998.

8. Doshi, M. R., “Quantification of Stickies”, *Paper Recycling Challenge, Vol. I-Stickies*, M. R. Doshi and J. M. Dyer, eds., Doshi & Assoc., Inc., Appleton, WI, p. 193, 1997.

9. Doshi, M. R., “Properties and Control of Stickies”, *Paper Recycling Challenge, Vol. I- Stickies*, M. R. Doshi and J. M. Dyer, eds., Doshi & Assoc., Inc., Appleton, WI, pp. 227-236, 1997.

10. Smith, S. E., “Stickies Properties and the Relationship to Their Removal”, *Paper Recycling Challenge, Vol. I- Stickies*, M. R. Doshi and J. M. Dyer, eds., Doshi & Assoc., Inc., Appleton, WI, pp. 237-239, 1997.

11. Landa, M. R., “PSA Labels and Repulping Paper”, *Joint Conference to Address Pressure Sensitive Adhesive Issues Proceedings*, United States Postal Service and American Forest & Paper Association, Washington, D.C., June 1996.

12. Huo, X., Venditti, R. A., and Chang, H.-m., “Effect of Papermaking Components on Adhesive Contaminant (Stickies) Characteristics After Pulping”, *1999 Tappi Conference Proceedings*, Atlanta, GA, TAPPI Press, pp. 681-692, 1999.

13. Hsu, N. N.-C., “Stickies – The Importance of Their Chemical and Physical Properties”, *Paper Recycling Challenge, Vol. I- Stickies*, M. R. Doshi and J. M. Dyer, eds., Doshi & Assoc., Inc., Appleton, WI, pp. 256-258, 1997.

14. Doshi, M. R., “Quantification of Stickies”, *Paper Recycling Challenge, Vol. I-Stickies*, M. R. Doshi and J. M. Dyer, eds., Doshi & Assoc., Inc., Appleton, WI, pp. 176-179, 1997.

15. Dyer, J., “A Summary of Stickies Quantification Methods”, *Progress in Paper Recycling*, 6(4):44-51, 1997.

16. Staff, Progress in Paper Recycling, “Methods to Quantify Stickies – A Mill Survey”, *Paper Recycling Challenge, Vol. I- Stickies*, M. R. Doshi and J. M. Dyer, eds., Doshi & Assoc., Inc., Appleton, WI, pp. 171-175, 1997.

17. Kelly, A. F., “Screening Secondary Fiber”, *1997 Tappi Improving Screening and Cleaning Efficiencies Short Course Proceedings*, Minneapolis, MN, TAPPI Press, pp. 115-124, June 1997.

18. McKinney, R. W. J., “Wastepaper Preparation and Contamination Removal”, Chapter 3 in *Technology of Paper Recycling*, McKinney, R. W. J., ed., Blackie Academic & Professional, London, pp. 88-95, 1995.

19. Heise, O., “Screening Foreign Material and Stickies”, *Tappi Journal*, 75(2):78-81, 1992.

20. Doshi, M. R., “Reduce the Pressure, Please!”, *Progress in Paper Recycling*, 8(4):6, 1999.

21. Paper Tech Institute, “Screening – Theory and Practice”, *Progress in Paper Recycling*, 8(4):74-78, 1999.

22. Sutherland, N. R., “Stickies Dirt Count and Laboratory Methods”, *Environmentally Benign Pressure Sensitive Adhesives for Postal Applications Conference Proceedings*, United States Postal Service, Potomac, MD, July 1997.

23. Heise, O., Kemper, M., Wiese, H., and Krauthauf, E., “Removal of Residual Stickies Applying New Flotation Technology at Haindl Paper – Schongau”, *1999 Tappi Conference Proceedings*, Atlanta, GA, TAPPI Press, pp. 693-710, 1999.

24. Veilleux, S., Chabot, B., and Daneault, C., “Quantification of Macro Stickies and Optimization of the Wastepaper Deinking Process”, *5th Research Forum on Recycling Proceedings*, Ottawa, ON, Canada, pp. 241-247, September 1999.

25. Seifert, P., Winkler, J., Vitori, C., Fields, B., and Maze, E., “Removal of Soft and Flexible Contaminants from Recycled Paper, in Screens”, *5th Research Forum on Recycling Proceedings*, Ottawa, ON, Canada, pp. 165-186, September 1999.

CHAPTER 4

THE BREAKAGE OF PRESSURE SENSITIVE ADHESIVE CONTAMINANTS IN PAPER RECYCLING OPERATIONS

ABSTRACT

It has been found previously that an industrial pressure screen broke down pressure sensitive adhesive (PSA) contaminants, while laboratory screens did not. It was suspected that the high shear and pressure gradients in the pressure screen caused the breakage. To investigate the effect of operating variables on particle breakage in pressure screens and other recycling operations, a statistically designed experiment was conducted in a laboratory high shear device. An acrylate based PSA label material was applied to copy paper, pulped, and then processed in the high shear device. The operating variables studied in the high shear device were consistency, time, initial temperature, and rotor speed. Handsheets were prepared from treated and untreated pulp samples in the high shear device. Dyeing and image analysis of the treated and untreated adhesive contaminants was performed to obtain the parts per million (PPM), average particle size, and number of particles in 1 m^2. Statistical analysis of the data showed that consistency, time, and initial temperature had a significant effect on the breakage of the adhesive material, whereas rotor speed did not. Empirical models for the average particle size and the number of particles in 1 m^2 were developed using a backward elimination program in the SAS System. Further experiments in which the consistency was varied revealed that at consistencies less than 6%, minimum breakage occurred, but at consistencies greater than 9%, breakage increased with consistency. Increasing the consistency from 9% to

14% reduced the average particle size by half and more than doubled the number of particles in 1 m^2. Also, increasing the initial temperature from 25°C to 75°C increased the breakage and almost doubled the number of particles in 1m^2. These findings provide operational information that is useful in the analysis of recycling equipment with respect to the removal of adhesive contaminants.

INTRODUCTION

Removal of adhesive contaminants is critical to paper recycling. Of the recycling operations, pressure screening is thought to be effective in adhesive removal. However, the removal efficiency of adhesive contaminants has been reported to range from -14 to 83% for industrial and pilot plant operations [1-10]. This wide range may reflect different types of screens, operating conditions, adhesive contaminants, and measurement methods or a combination of these utilized in the different studies. It is of interest to note that in one of these cases negative efficiencies were reported [3].

To investigate these results, screening experiments were performed on industrial and laboratory screening devices at North Carolina State University [11-12]. Copy paper and pressure sensitive adhesive (PSA) labels were prepared in a pilot plant hydropulper. The pulp was then screened in a pilot plant pressure screen, a PulmacMaster screen, and a Valley Flat screen, all having 0.006 inches wide slots. It was found that the PSA contaminants broke down in the pressure screen and not in the laboratory screens. The breakage of PSA contaminants in the pressure screen caused the screening efficiencies to be lower than in the laboratory screens. For small particles, a negative removal efficiency was determined, reflecting the breakage of PSA contaminants.

Among papermaking operations, the pressure screen is second only to the fan pump in the shear stress produced [13]. The shear forces are present in the pressure screen across the screen basket slots and at the rotor [13-14]. Shear forces may cause the breakage of PSA contaminants in the pressure screen [14]. It is the flow conditions in a pulp suspension that determine the shear stress present. At very low consistency, pulp suspensions behave as Newtonian fluids and obey the equation:

$$\tau = \mu(du/dy)$$

where τ is the shear stress, μ is the viscosity, and du/dy is the strain rate. However, at higher consistencies, pulp suspensions behave in a non-Newtonian manner. Head [15] proposed the use of the apparent yield stress, i.e., the shear stress at a shear rate of zero, as a parameter for non-Newtonian fluids such as pulps. Head's apparent yield stress is the same as the Bingham plastic yield stress [16]. The Bingham plastic model equation for shear stress, τ, versus strain rate, du/dy, is:

$$\tau = \tau_y + \mu_s(du/dy)$$

where the variables τ_y and μ_s are yield stress and slope viscosity, respectively [17].

Later, Bennington, Kerekes, and Grace, using a rotary shear tester, presented data comparing the yield stress, τ_y, to the solids consistency, C_m, for pulps. They found that the relationship was of the form:

$$\tau_y = aC_m^{\,b}$$

where *a* and *b* are constants and C_m is a percentage [18-19]. In theory presented by Bennington, Kerekes, and Grace, τ_y is proportional to C_v^3 [18]. However, experimental data indicated that *b* ranged from 2.31 to 3.56 for C_m, and from 2.72 to 3.56 for C_v [18]. Also, Bennington and Kerekes showed that torque and apparent viscosity [19] and ε_f, which is an estimate of the "power dissipation per unit volume for the onset of fluidization" [20], had a similar relationship with the volumetric concentration, C_v. Consistency is a significant variable affecting the shear forces in pulp flow.

In this study, the parameters of pulp consistency, time, initial temperature, and rotor speed were analyzed to determine the effects on the breakage of adhesive contaminants in a laboratory high shear device. These findings will assist in the design and operation of recycling equipment to minimize breakage of stickies for improved removal efficiency.

EXPERIMENTAL

Pilot Plant Pulp Preparation

Acrylate adhesive labels from Avery Dennison were applied to sheets of Quick Copy Xerographic DP paper to achieve an adhesive content of 0.2% adhesive on OD paper. One batch of pulp was prepared containing 80 OD lbs. of paper and 0.8 lbs. of labels. The batch was pulped in a 200 gallon hydropulper from Black Clawson Co. with a high consistency rotor. The hydropulper was operated at about 9% consistency for 20 minutes at a rotor speed of 600 rpm. The initial temperature was 45°C. The pulp was collected in plastic bags and stored in a cold room. Before use in the laboratory, the bags of pulp were filtered, 180 OD g at a time, using Whatman filter paper #1 on a Buchner funnel connected to the house vacuum. Four samples of filtered pulp were left untreated to use as a baseline for comparison.

Statistically Designed Experiments

The laboratory high shear device in this research was a Mark II High Intensity Laboratory Mixer/Reactor by Quantum Technologies, consisting of a mixing chamber, rotor, heating coil, and control system. **Figure 4-1** is an illustration of the high shear device. The dimensions of the mixing chamber are a minimum diameter of 17.0 cm, a maximum diameter of 19.5 cm, and a height of 14.5 cm. The rotor blades are 4.0 cm long and the minimum distance from the rotor to the wall is 2.0 cm.

The independent variables for these experiments were pulp consistency, time, initial temperature, and rotor speed. The dependent variables were average particle size and number of particles in 1 m^2. A full factorial statistically designed set of experiments with a center point was conducted in a random order. The center point experiment was conducted four times. The independent variable values were consistencies of 3, 7.5, and 12%; times of 30, 165, and 300 seconds; initial temperatures of 20, 35, and 50^{o}C; and rotor speeds of 600, 1500, and 2400 rpm.

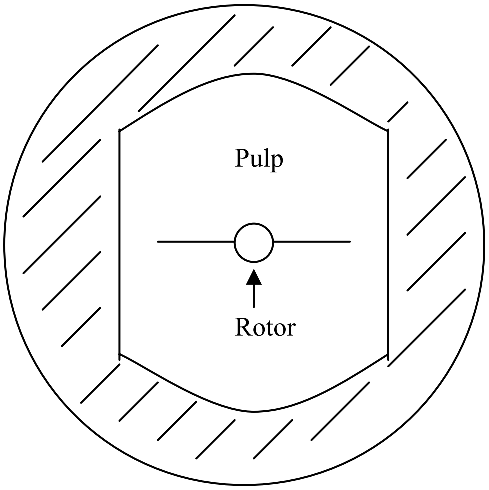

Figure 4-1. Top View of the High Shear Laboratory Device

For each experiment, the mass of a filtered pulp sample, containing the required OD weight of pulp for a consistency of 3, 7.5, or 12% at a total of 3000 g, was measured. Deionized water for dilution was then heated in the microwave depending on the desired initial temperature. A mass of deionized water was added to the pulp for a total of 3000 g for a required consistency. The diluted pulp sample was poured into the chamber with the temperature and rotor speed set for the given experiment. After the pre-determined processing time, the pulp was collected in labeled plastic bags for storage.

Statistical Analysis

A Pareto analysis was performed on the data from the statistically designed experiment. All four of the independent variables and the eleven interactions were considered for the two dependent variables of average particle size and number of particles in 1 m^2. The data for the sixteen full factorial experiments was used in a Yates Algorithm to determine the effect for each of the variables and their interactions. The 2σ limit was calculated using the data from the four center point experiments. The variables with an absolute value of the effect greater than the 2σ limit are significant.

The results from the statistically designed experiments were analyzed using the SAS System from the SAS Institute. All four independent variables and their interactions were considered for average particle size and number of particles in 1 m^2. Also, the squares of the independent variables were considered. The SAS procedures used were maximum R^2 and backward elimination. The R^2 value indicates the fraction of the data that can be explained by a model; the higher the R^2 value the better the fit of the model. The maximum R^2 procedure provides the best fitting model using all the independent variables that have any effect. The backward elimination model uses only variables that are significant at the 0.1000 level to fit a model to the data.

Consistency Experiments

Another set of experiments were performed by varying the consistency while keeping the time, initial temperature, and rotor speed equal to the center point values: 165 seconds, 35^{o}C, and 1500 rpm, respectively. For each experiment, the mass of a filtered pulp sample, containing the required OD weight of pulp for a certain consistency at a total of 3000 g, was measured. However, at 14% consistency, only 360 OD g of filtered pulp were measured for a total mass of 2571.4 g because 3000 g of pulp at 14% consistency did not fit in the mixing chamber.

Temperature Experiments

A third set of experiments were performed by varying the initial temperature while keeping the consistency, time, and rotor speed equal to the center point values of 10%, 165 seconds, and 1500 rpm, respectively.

Dyeing and Rinsing of Handsheets

The dyeing and rinsing method was critical for the image analysis of the handsheets. Undyed white adhesive particles are indistinguishable from the fiber by image analysis. An increased contrast between stickies and the handsheets is thus required to detect the stickies properly. The procedure described below has been found to be effective in improving the contrast [11].

Handsheets containing 1.2 OD g of pulp were prepared in sets of six using the TAPPI standard method. After the handsheets had dried overnight, five handsheets were selected out of each set of six for dyeing, based on irregularities such as wrinkles.

Morplas Blue-Heptane dyeing solution was prepared in a vacuum hood. A mass of 0.670 g of Morplas Blue was weighed out in a metal pan using an analytical balance and poured into a 1000 ml volumetric flask. The flask was filled to the mark with 95% heptane from Sigma-Aldrich. A magnetic stirrer was placed in the flask and a stopper was placed in the top. The flask was set on a stirring plate to stir overnight.

The Morplas Blue-Heptane dyeing solution was filtered using Whatman filter paper #1 in a Buchner funnel. The filtered solution was collected in a 1000 ml Erlenmeyer flask. 250 ml of the filtered dye solution was measured out in a 500 ml graduated cylinder and poured into a crystallizing dish. One handsheet was submerged in the dye solution and swirled for ten seconds. The handsheet was removed with forceps and hung from a string with a binder clip. These steps were repeated for the other four handsheets to be dyed. The handsheets were allowed to dry overnight. The heptane solution remaining in the crystallizing dish was poured into a waste container.

The next day, the handsheets were removed from the string. 500 ml of 95% heptane was measured out in a 500 ml graduated cylinder and poured into a crystallizing dish. One handsheet was submerged in the heptane solution and swirled for ten seconds. The handsheet was removed with forceps and hung from a string with a binder clip. These steps were repeated for the other four handsheets to be rinsed. Each handsheet was removed as soon as it was dry. The heptane solution remaining in the crystallizing dish was poured into a waste container.

Image Analysis

The SpecScan 2000 program by Apogee Systems Inc. was used to scan each set of five handsheets, before and after dyeing, to determine the stickies content of the samples. The scanner was a Hewlett Packard Scanjet 4c with a 600 dpi resolution. A standard sample was scanned sixteen times in order to warm up the scanner bulb before image analysis was performed on real samples. The detection threshold was set at 80% of the average grayscale value. Both the felt and wire sides of each of the handsheets in a set were scanned. The parts per million (PPM) of stickies, number of particles in 1 m^2, and the average particle size for particles greater than or equal to 0.007 mm^2 for each set of handsheets were determined for each side. Also, a histogram of particle sizes in terms of area and count was recorded. The values for the felt and wire side for each set of handsheets were averaged to obtain values for the total area of the set. An example of image analysis output is shown in **APPENDIX 3**.

RESULTS AND DISCUSSION

The operating conditions chosen did affect the breakage of adhesive particles in the high shear device. Examples of the particle size distributions are shown in **Figure 4-2** and **Figure 4-3**. **Figure 4-2** shows the particle size distributions for a sample treated at 3% consistency, 30 seconds, 20^{o}C initial temperature, and 600 rpm and for the average of the untreated samples. **Figure 4-3** shows the particle size distributions for a sample treated at 12% consistency, 300 seconds, 50^{o}C initial temperature, and 2400 rpm and for the average of the untreated samples. At the low conditions (**Figure 4-2**), the particle size distribution is similar to the average of the untreated samples. At the high conditions

(**Figure 4-3**), a significant difference between the treated and untreated distributions exist. Treatment causes the distribution to be shifted to lower particle sizes. In fact, no particles larger than 1.5 mm^2 can be detected after treatment at the high conditions (**Figure 4-3**).

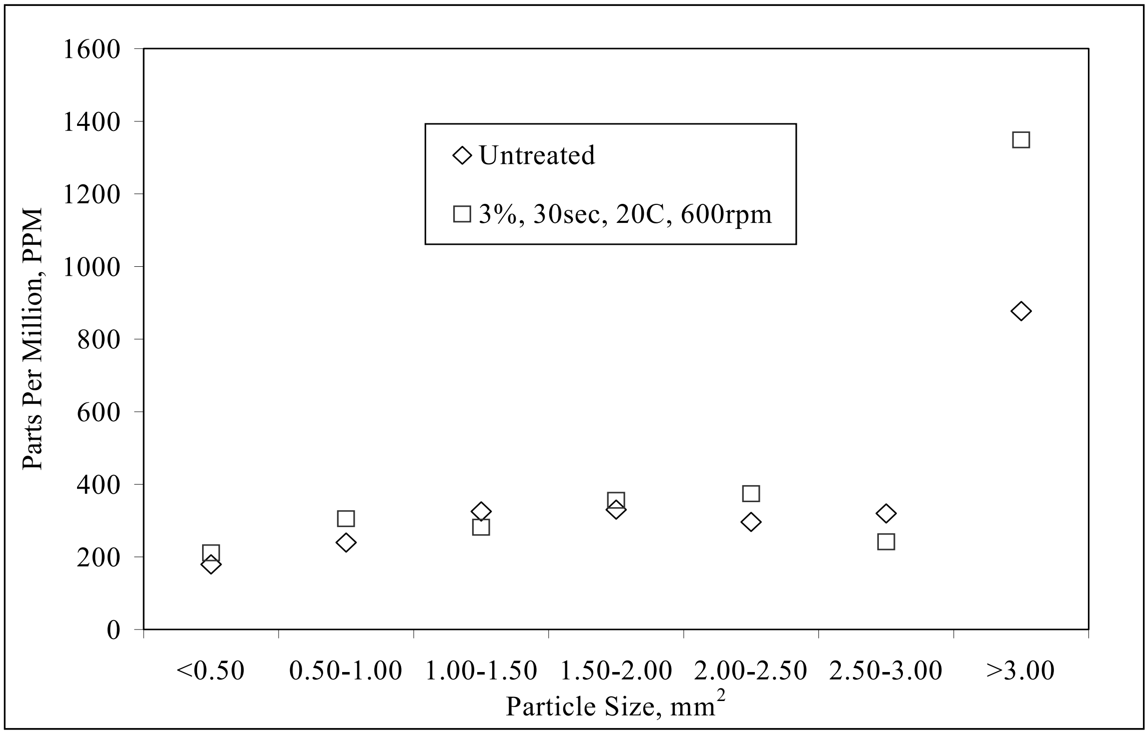

Figure 4-2. PPM Versus Particle Size for Untreated Sample and Sample Treated at Low Conditions

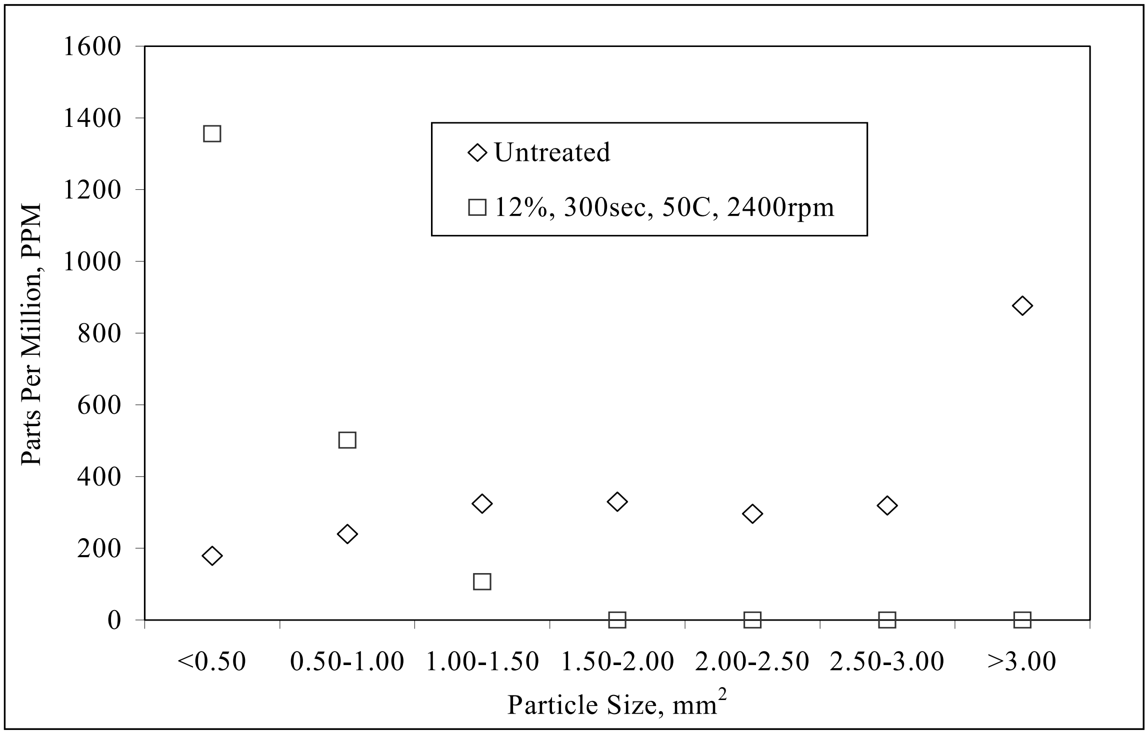

Figure 4-3. PPM Versus Particle Size for Untreated Sample and Sample Treated at High Conditions

The stickies PPM, average particle size, and number of particles in 1 m^2 results from the statistically designed experiments and the four untreated samples are shown in **Table 4-1**. Notice that at high consistency, high time, and high initial temperature, the average particle size is lower and number of particles in 1 m^2 is higher than the other experiments. Also, at low consistency and low time, all of the average particle sizes are about the same. At the center point, there is some variability in PPM, average particle size, and number of particles in 1 m^2; however, the variability is similar to the variability of the untreated samples. The standard deviations of average particle size are 0.13 and 0.16 mm^2 for the center point and untreated samples, respectively. It was found that the precision of the number of particles in 1 m^2 relative to the total range of values measured was better than for the PPM and average particle size.

Table 4-1. Statistically Designed Experiments

Consistency, %	Time, sec	Temperature, °C	Rotor Speed, rpm	Parts Per Million	Average Particle Size, mm^2	Number of Particles in 1 m^2
Untreated	-	-	-	2440	0.90	2710
Untreated	-	-	-	2430	0.52	4670
Untreated	-	-	-	2560	0.63	4040
Untreated	-	-	-	2825	0.75	3760
3	30	20	600	3120	0.63	4920
12	30	20	600	2600	0.67	3890
3	300	20	600	1910	0.44	4370
12	300	20	600	1960	0.17	11350
3	30	50	600	3060	0.62	4940
12	30	50	600	2050	0.33	6140
3	300	50	600	2260	0.45	5060
12	300	50	600	1940	0.13	14520
3	30	20	2400	2690	0.68	3960
12	30	20	2400	2060	0.47	4400
3	300	20	2400	2170	0.96	2260
12	300	20	2400	1920	0.22	8770
3	30	50	2400	2200	0.67	3280
12	30	50	2400	2260	0.38	5880
3	300	50	2400	2700	0.38	7130
12	300	50	2400	1960	0.14	13590
7.5	165	35	1500	2350	0.76	3070
7.5	165	35	1500	2390	0.61	3900
7.5	165	35	1500	2630	0.46	5640
7.5	165	35	1500	2760	0.55	5010

A Pareto analysis was performed on the data from the statistically designed experiments. **Figure 4-4** and **Figure 4-5** show the absolute value of the effects and the 2σ limit for average particle size and number of particles in 1 m^2, respectively. For average particle size (**Figure 4-4**), consistency, time, and temperature were all significant variables. For number of particles in 1 m^2 (**Figure 4-5**), consistency, time, temperature, consistency*time, and time*temperature were all significant variables.

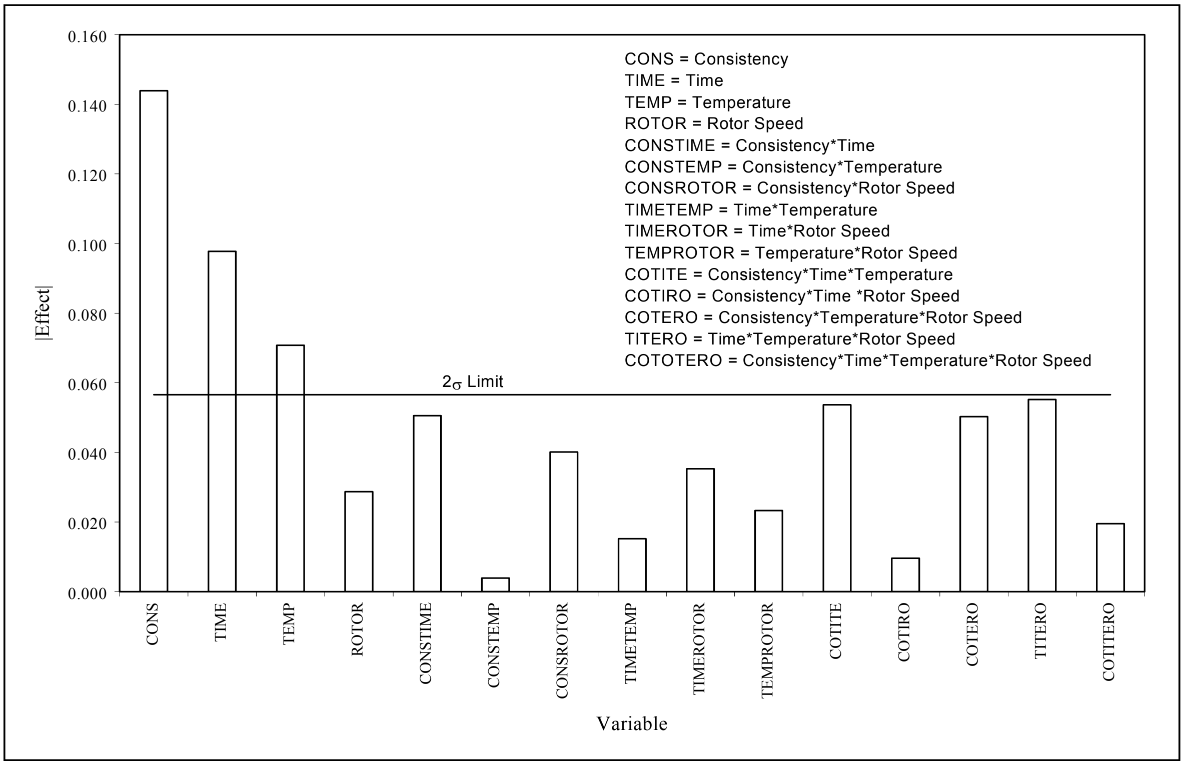

Figure 4-4. Pareto Chart for Average Particle Size

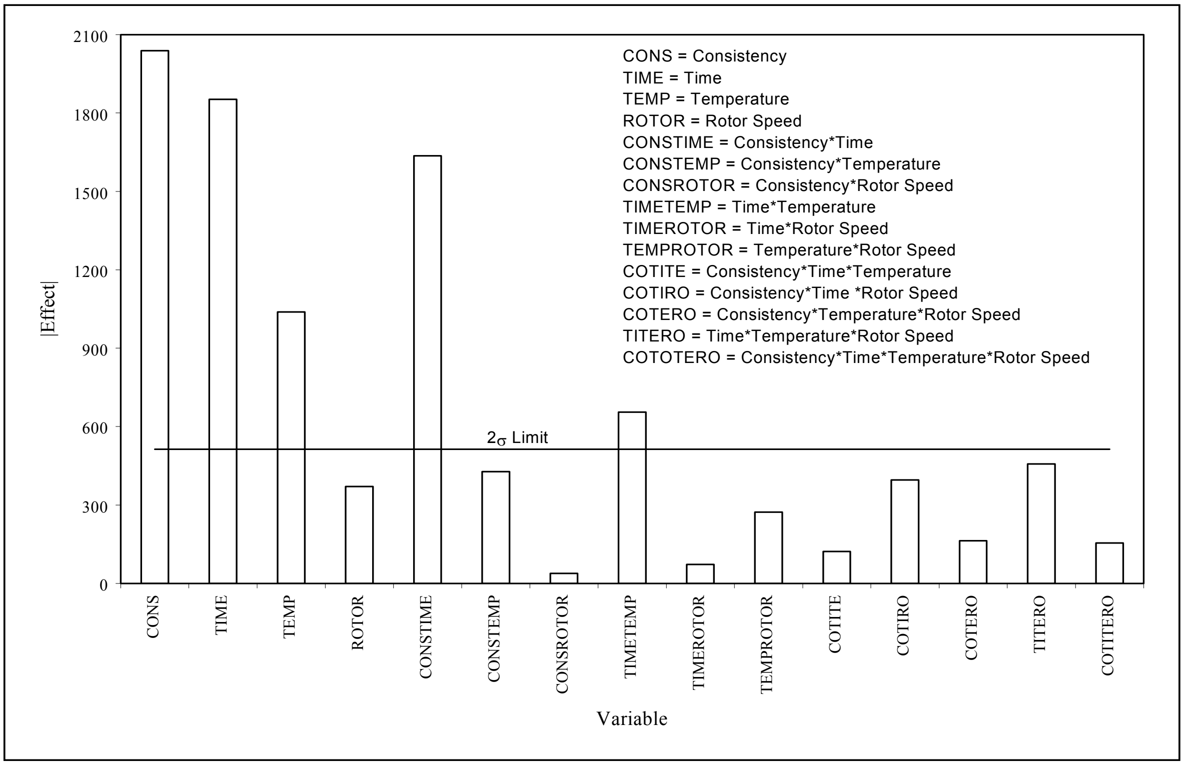

Figure 4-5. Pareto Chart for Number of Particles in 1 m^2

A model was developed for the behavior of the system. SAS modeling was performed using the maximum R^2 and backward elimination procedures. The variables considered were the four independent variables, their eleven interactions, and the two dependent variables. The maximum R^2 procedure provides the best fitting model using all the dependent variables that have any effect. For the maximum R^2 procedure, the R^2 values are 0.87 and 0.91 for average particle size and number of particles in 1 m^2, respectively, and are acceptable. However, fourteen variables are used in each model, and considering that there are a total of fifteen possible variables, there are too many variables for the maximum R^2 procedure to be useful.

The backward elimination procedure uses only variables that are significant at the 0.1000 level to fit a model to the data. The SAS input and output files for backward elimination are available in **APPENDIX 4**. For the backward elimination procedure, the R^2 values are 0.61 and 0.86 for average particle size and number of particles in 1 m^2, respectively. These R^2 values are less than those for the maximum R^2 procedure, but there are fewer variables in each model. The significant variables and their coefficients for average particle size and number of particles in 1 m^2 are shown in **Table 4-2**. The significant variables for average particle size are consistency, time, and temperature. The significant variables for number of particles in 1 m^2 are consistency, time, temperature, consistency*time, and time*temperature. These variables are the same variables that were significant in the Pareto analysis. Interestingly, rotor speed was not a significant variable for average particle size or number of particles in 1 m^2 for the rotor speeds evaluated. In **Table 4-2**, the lower the Pr > F value, the more significant the variable.

Therefore, consistency is the most significant variable for both average particle size and number of particles in 1 m^2.

Table 4-2. SAS Modeling Results for Backward Elimination

	Variable	Range	Coefficient	Pr > F
Average Particle Size	Intercept		1.012	<0.0001
	Consistency	3-12%	-0.03197	0.0015
	Time	30-300 sec	-0.0007241	0.0198
	Temperature	20-50°C	-0.004725	0.0788
Number of Particles in 1 m^2	Intercept		3218	<0.0001
	Consistency	3-12%	8.636	<0.0001
	Time	30-300 sec	-17.80	0.0002
	Temperature	20-50°C	15.89	0.0152
	Consistency*Time	3-12%, 30-300 sec	2.694	0.0007
	Time*Temperature	30-300 sec, 20-50°C	0.3235	0.1034

Equations using the coefficients in **Table 4-2** are:

$$\text{Average Particle Size, mm}^2 = 1.012 - 0.03197*\text{Consistency} - 0.0007241*\text{Time} - 0.004725*\text{Temperature}, \qquad R^2 = 0.61$$

$$\text{Number of Particles in 1 m}^2 = 3218 + 8.636*\text{Consistency} - 17.80*\text{Time} + 15.89*\text{Temperature} + 2.694*\text{Consistency}*\text{Time} + 0.3235*\text{Time}*\text{Temperature}, \qquad R^2 = 0.86$$

for the ranges of the variables shown in **Table 4-2**.

Another model was considered using the squares of the four independent variables for backward elimination in the SAS System since none of the three or four variable interactions were significant. None of the squared terms were significant for the average particle size model, so that model did not change. For the number of particles in 1 m^2 model, the consistency^2 term was significant and the resulting R^2 value was 0.92, indicating an improvement in the model. The equation including consistency^2 is:

$$\begin{aligned}\text{Number of Particles in 1 m}^2 = {} & 7415 - 1563*\text{Consistency} - 17.80*\text{Time} + \qquad R^2=0.92 \\ & 15.89*\text{Temperature} + 2.694*\text{Consistency}*\text{Time} + \\ & 0.3235*\text{Time}*\text{Temperature} + 104.8*\text{Consistency}^2\end{aligned}$$

for the ranges of the variables shown in **Table 4-2**.

The breakage of particles is not expected by itself to change the PPM detected. Ideally, breaking a largely two-dimensional film structure such as PSA film into smaller two-dimensional objects will not change the area of the film. However, phenomena such as folding, irreversible stretching, agglomeration, or deposition on equipment would be expected to change the PPM. A good correlation for PPM versus the operating conditions considered did not exist. From our observations and the statistical results, no significant folding, irreversible stretching, agglomeration, or deposition occurred.

Since the statistical analysis showed that consistency was the most significant variable, additional experiments were performed in which only the consistency was varied. The results from the consistency experiments and the average values for the untreated samples are shown in **Table 4-3**. The average particle size and number of particles in 1 m^2 are plotted versus consistency in **Figure 4-6** and **Figure 4-7**, respectively. At consistencies of 1 to about 6% the average particle size and number of particles in 1 m^2 are similar to the values of the untreated samples and are within the scatter of the duplicated untreated samples. As the consistency increases above about 6%, the average particle size decreases and the number of particles in 1 m^2 increases significantly. The average particle size at 6% consistency is about three times the average particle size at 14% consistency. The number of particles in 1 m^2 at 14% consistency is more than twice the number of particles in 1 m^2 at 9% consistency.

Table 4-3. Consistency Experiments

Consistency, %	Time, sec	Temperature, ^oC	Rotor Speed, rpm	Parts Per Million	Average Particle Size, mm^2	Number of Particles in 1 m^2
Untreated	-	-	-	2570	0.70	3790
1	165	35	1500	3340	0.90	3730
3	165	35	1500	2930	0.70	4170
3	165	35	1500	3060	0.78	3930
4.5	165	35	1500	3100	0.92	3370
6	165	35	1500	2560	0.59	4310
6	165	35	1500	3150	0.71	4430
9	165	35	1500	2300	0.47	4910
9	165	35	1500	2230	0.36	6130
10.5	165	35	1500	2040	0.27	7520
12	165	35	1500	2240	0.29	7600
12	165	35	1500	2160	0.18	11880
14	165	35	1500	2200	0.16	14150
14	165	35	1500	2300	0.17	13770

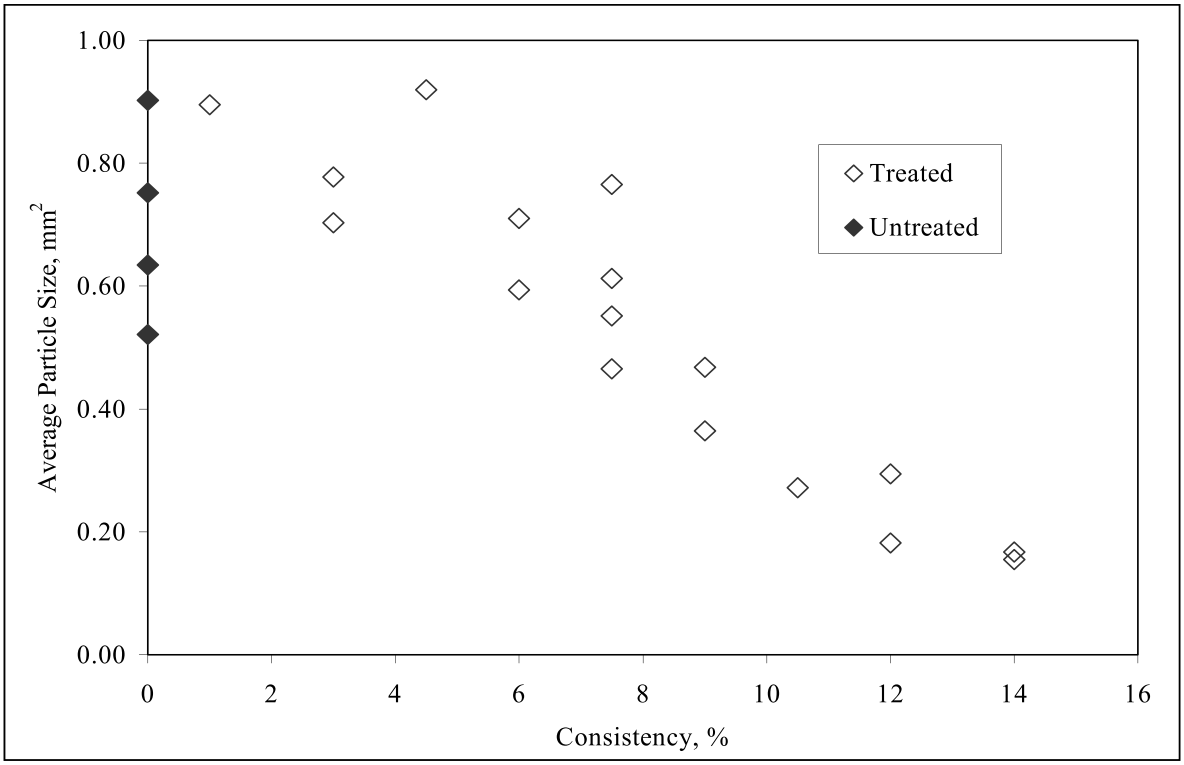

Figure 4-6. Average Particle Size Versus Consistency

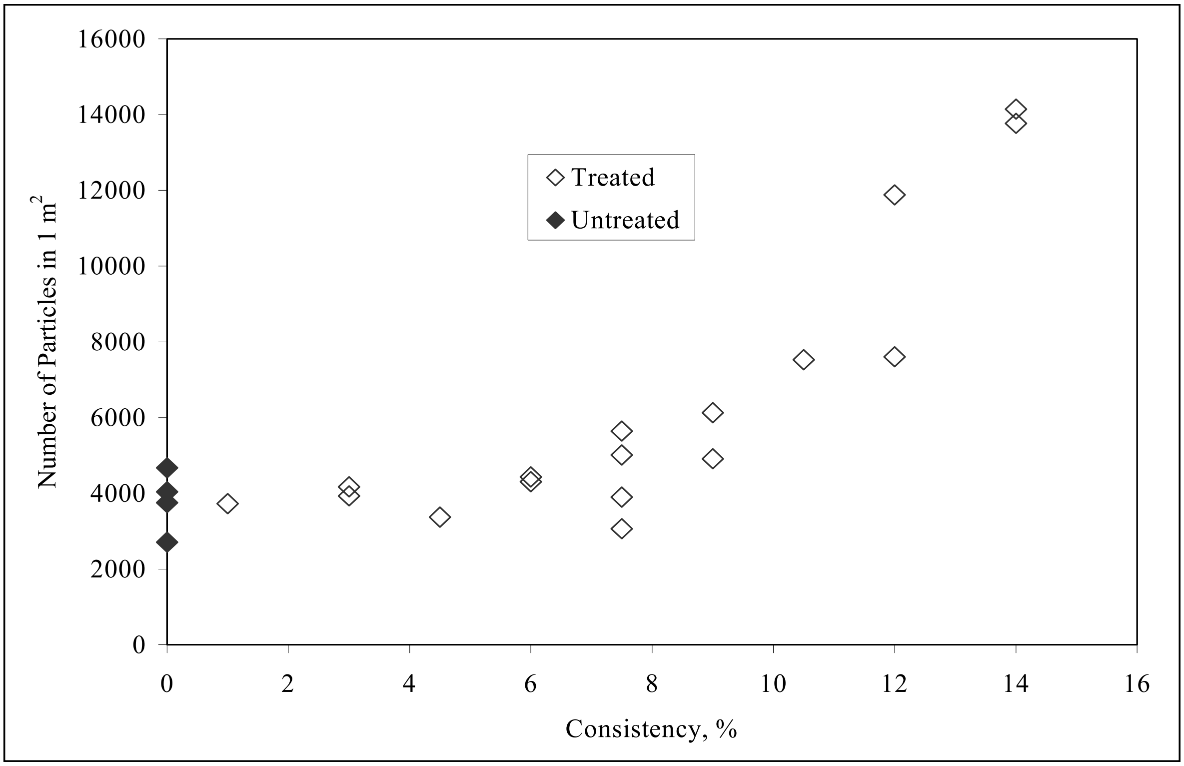

Figure 4-7. Number of Particles in 1 m^2 Versus Consistency

These results are not surprising in that the consistency is known to have a significant effect on the shear stress in a pulp system. This breakage due to shear can exist between fibers, between fibers and the rotor, and between the fibers and the vessel wall. Each of these phenomena is affected by the consistency. At this point, the contribution of each of these phenomena is not known. This type of consideration is also pertinent in industrial screening or in general recycling operations.

The size distribution of particles is shown in **Table 4-4** for the consistency experiments. For experiments conducted at 1 to 4.5% consistency, the particle size distributions are similar to the average particle size distribution for the untreated samples. For particles >3.00 mm^2 and <0.50 mm^2 the percentages are about 35 and 6.5%, respectively. At 9% consistency, there is a significant decrease in the percentage for particles >3.00 mm^2 and a significant increase in the percentage for particles <0.50 mm^2. For the 10.5 to 14% consistency experiments, as the consistency increases, the percentage for particles <0.50 mm^2 increases. At 14% consistency, there are not any particles in the ranges >2.00 mm^2. This data confirms that there is a breakage of large particles that is shifting the size distribution to lower values.

Table 4-4. Contaminant Size Distributions for the Consistency Experiments (Percentages based on PPM)

	Particle Size, mm^2						
Consistency, %	<0.50	0.50-1.00	1.00-1.50	1.50-2.00	2.00-2.50	2.50-3.00	>3.00
Untreated	7.0	9.4	12.7	12.9	11.5	12.4	34.0
1	6.8	9.7	10.9	12.6	12.4	12.6	35.0
3	6.6	9.9	18.0	8.6	11.6	12.7	32.5
3	7.1	11.7	11.8	13.4	9.9	10.3	35.8
4.5	6.4	10.4	11.5	11.9	12.6	10.9	36.3
6	10.4	18.5	18.9	12.3	12.7	5.6	21.6
6	8.2	10.4	16.1	13.1	12.0	7.6	32.7
9	17.9	20.4	21.6	14.0	11.3	9.2	5.5
9	26.6	30.2	15.4	14.4	6.5	3.5	3.4
10.5	38.1	26.5	20.5	7.8	3.1	3.9	0.0
12	43.6	28.8	14.8	6.2	3.6	0.8	2.0
12	45.9	33.7	16.5	3.3	0.7	0.0	0.0
14	73.9	23.7	1.9	0.5	0.0	0.0	0.0
14	63.5	30.7	4.7	1.1	0.0	0.0	0.0

There are two feed consistency ranges for screening, 0.8 to 2.5% and 3 to 5% consistency [1]. Heise et. al. investigated the probability of stickies disintegration in low and high consistency screening [14,21]. They compared screening at 2.5% consistency with 0.15 mm slots to screening at 3.6 and 4.4% consistency with 0.20 mm slots [14]. Different rotor designs were used for each of the three consistencies considered [14]. They found that stickies >1000 μm in diameter have a higher probability to disintegrate at 3.6 and 4.4% consistency, than at 2.5% consistency [14]. In a pressure screen, the consistency of the pulp increases and forms a mat on the screen basket, which may contribute to particle disintegration.

Consistencies in this research that cause breakage are higher than those typically reported as feed consistencies in pressure screens. However, the mat on the face of the screen basket is at a higher consistency (typically not reported) than the pulp entering the pressure screen. A reconciliation of the data presented in this research and the pressure screen conditions may be due to this high-consistency zone in the pressure screens. Other phenomena, such as pressure gradients and fiber-metal or metal-metal friction could also impact the behavior of adhesives in an industrial pressure screen and weaken a correlation between the results herein and observed industrial screening performance.

Experiments were conducted to analyze the effect of initial temperature on the breakage of adhesive contaminants (**Table 4-5**). It should be noted that the temperature rises during the experiments due to the rotor action. As the initial temperature increases, the average particle size decreases and the number of particles in 1m^2 increases. A plot of the average particle size versus temperature for the experiments is shown in **Figure 4-8**. The size distribution of particles is shifted to lower sizes as the initial temperature increases (**Figure 4-9**). The number of particles in 1m^2 approximately doubled by increasing the initial temperature from 25 to 75°C (**Table 4-5**). A typical temperature for recycling operations is 50°C [22], which is in the range that the measured breakage of PSA particles is a function of the temperature. These results indicate that the effect of temperature in an industrial screening operation is a very important processing parameter with regards to PSA contaminants.

Table 4-5. Temperature Experiments

Temp., °C Initial / Final	Consistency, %	Time, sec	Rotor Speed, rpm	Parts Per Million	Average Particle Size, mm^2	Number of Particles in 1 m^2
Untreated	-	-	-	2570	0.70	3790
25 / 40	10	165	1500	2110	0.38	5600
35 / 50	10	165	1500	2790	0.36	7700
55 / 71	10	165	1500	1900	0.20	9380
75 / 97	10	165	1500	1250	0.12	10920

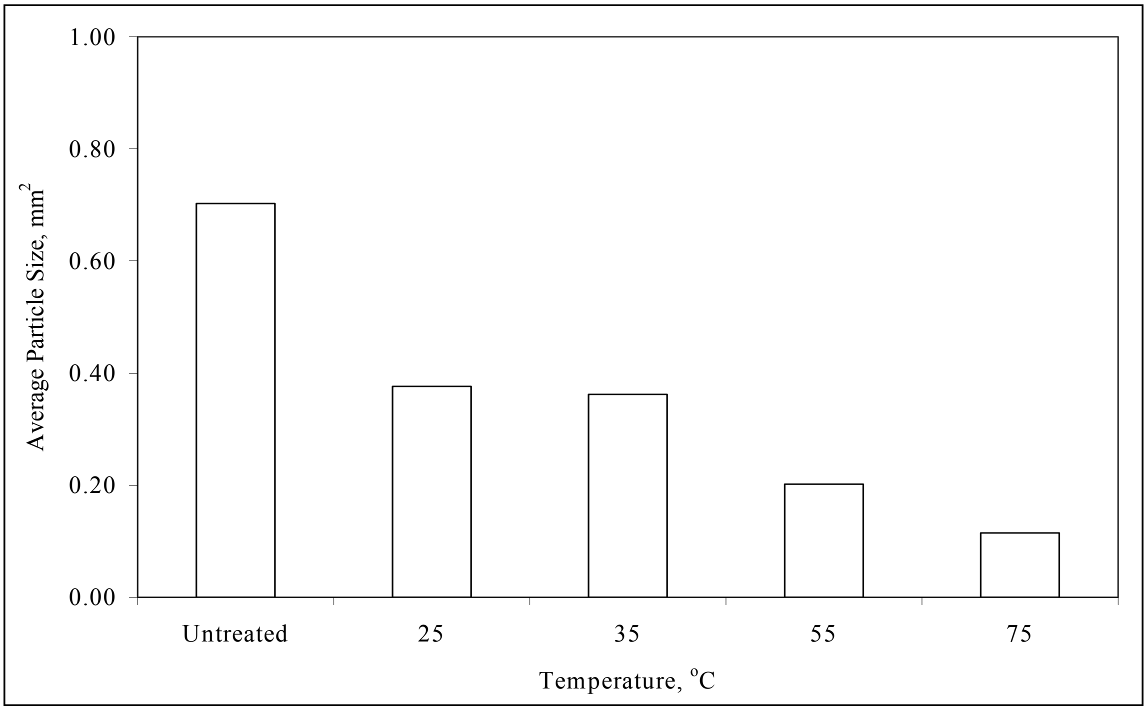

Figure 4-8. Average Particle Size Versus Initial Temperature

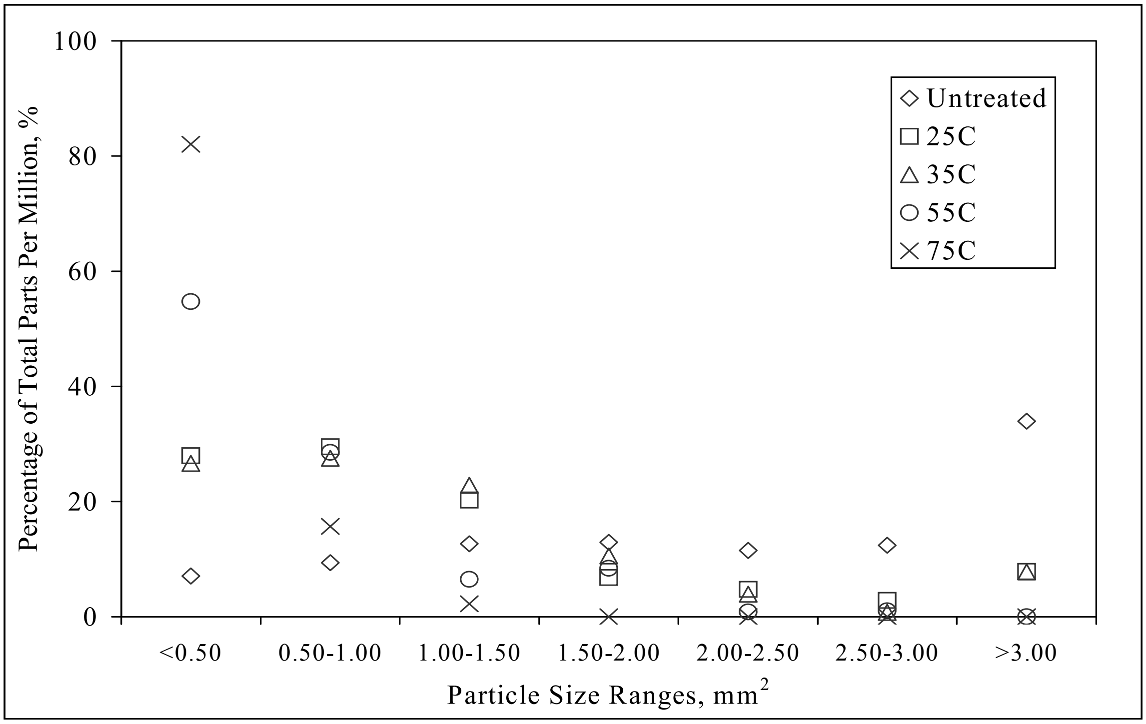

Figure 4-9. Particle Size Distribution for Temperature Experiments

CONCLUSIONS

Experiments with a laboratory high shear device were useful in determining the effect of operating conditions on the breakage of PSA contaminants. Statistical analysis was able to determine that consistency, time, and initial temperature significantly affected the breakage of the PSA contaminants. Rotor speed in the range evaluated did not have a significant effect. At consistencies less than about 6%, breakage of the particles was not detected. However, at consistencies greater than 6%, breakage increased with increasing consistency. Increases in temperature also increased the breakage of the PSA contaminants.

REFERENCES

1. Heise, O., "Screening Foreign Material and Stickies", Tappi Journal, 75(2):78-81, 1992.

2. Pikulin, M. A., "Stickies and Their Impact on Recycled Fiber Content Fine Papers", *Joint Conference to Address Pressure Sensitive Adhesive Issues Proceedings*, United States Postal Service and American Forest & Paper Association, Washington, D.C., June 1996.

3. Sutherland, N. R., "Stickies Dirt Count and Laboratory Methods", *Environmentally Benign Pressure Sensitive Adhesives for Postal Applications Conference Proceedings*, United States Postal Service, Potomac, MD, July 1997.

4. Heise, O., Kemper, M., Wiese, H., and Krauthauf, E., "Removal of Residual Stickies Applying New Flotation Technology at Haindl Paper – Schongau", *1999 Tappi Conference Proceedings*, Atlanta, GA, pp. 693-710, March 1999.

5. Veilleux, S., Chabot, B., and Daneault, C., "Quantification of Macro Stickies and Optimization of the Wastepaper Deinking Process", *5th Research Forum on Recycling Proceedings*, Ottawa, ON, Canada, pp. 241-247, September 1999.

6. Seifert, P., Winkler, J., Vitori, C., Fields, B., and Maze, E., "Removal of Soft and Flexible Contaminants from Recycled Paper, in Screens", *5th Research Forum on Recycling Proceedings*, Ottawa, ON, Canada, pp. 165-186, September 1999.

7. Delagoutte, T., and Julien Saint Amand, F., "Pilot Plant Procedure for the Assessment of the Screening Ability of Pressure Sensitive Adhesive", *2000 Tappi Recycling Symposium Proceedings*, Washington, D.C., pp. 359-374, March 2000.

8. Sutherland, N. R., and Donermeyer, D., "Laboratory- and Pilot-Scale Evaluations of Environmentally Benign PSA Stamps", *2000 Tappi Recycling Symposium Proceedings*, Washington, D.C., pp. 433-470, March 2000.

9. Crossley, B. R., Grimes, D. B., Abubakr S., and Kumar, R., "A Pilot Plant Study of the Recyclability of Pressure Sensitive Adhesives (PSA)", *2000 Tappi Recycling Symposium Proceedings*, Washington, D.C., pp. 594-601, March 2000.

10. Cameron, J., and Forester, W., "Behavior of PSAs: MOW and Sorted Office Paper with High Content of PSAs", *2000 Tappi Recycling Symposium Proceedings*, Washington, D.C., pp. 611-617, March 2000.

11. Lucas, B. E., Venditti, R. A., and Jameel, H., "Behavior of Pressure Sensitive Adhesive Material in Industrial Pressure Screens and Laboratory Screens", Tappi Journal, 84(5):70, 2001.

12. Venditti, R. A., Chang, H.-m., and Jameel, H., "Overview of Stickies Research at North Carolina State University", PaperAge, 115(2):18-20, 1999.

13. Tam Doo, P. A., Kerekes, R. J., and Pelton, R. H., "Estimates of Maximum Hydrodynamic Shear Stresses on Fibre Surfaces in Papermaking", Journal of Pulp and Paper Science, pp. J80-J88, July 1984.

14. Heise, O., Schabel, S., Cao, B., and Lorenz, K., "Deformation and Disintegration Physics of Stickies in Pressure Screens", 5th Research Forum on Recycling Proceedings, Ottawa, ON, Canada, pp. 187-195, September 1999.

15. Head, V. P., "A Shear Criterion for the Hydraulic Behavior of Paper Stocks in Pumps, Pipes, Valves, and Flowmeters", Tappi Journal, 35(6):260-266, 1952.

16. Duffy, G. G., and Titchener, A. L., "The Disruptive Shear Stress of Pulp Networks", Svensk Papperstidning, 78(13):474-479, 1975.

17. Bugliarello, G., and Daily, J. W., "Rheological Models and Laminar Shear Flow of Fiber Suspensions", Tappi Journal, 44(12):881-893, 1961.

18. Bennington, C. P. J., Kerekes, R. J., and Grace, J. R., "The Yield Stress of Fibre Suspensions", Canadian Journal of Chemical Engineering, 68(10):748-757, 1990.

19. Bennington, C. P. J., Kerekes, R. J., and Grace, J. R., "Motion of Pulp Fibre Suspensions in Rotary Devices", Canadian Journal of Chemical Engineering, 69(2):251-258, 1991.

20. Bennington, C. P. J., and Kerekes, R. J., "Power Requirements for Pulp Suspension Fluidization", Tappi Journal, 79(2):253-258, 1996.

21. Heise, O., Cao, B., and Schabel, S., "A Novel Application of TAPPI T 277 to Determine Macro Stickies Disintegration and Agglomeration in the Recycle Process", 2000 Tappi Recycling Symposium Proceedings, Washington, D.C., pp. 631-644, March 2000.

22. Hsu, N. N.-C., "Stickies – The Importance of Their Chemical and Physical Properties", Paper Recycling Challenge, Vol. I- Stickies, M. R. Doshi and J. M. Dyer, eds., Doshi & Assoc., Inc., Appleton, WI, pp. 256-258, 1997.

ACKNOWLEDGEMENTS

Support for this research has been provided in part by SCA Corporation and Ecosynthetix. Donations of equipment by Apogee Systems and Boise Cascade are also greatly appreciated.

CHAPTER 5

BREAKAGE AND EXTRUSION OF PRESSURE SENSITIVE ADHESIVES IN INDUSTRIAL AND LABORATORY SCREENING PROCESSES

ABSTRACT

The objective of this research was to understand the behavior of pressure sensitive adhesive (PSA) materials in industrial recycling equipment and to explain why inefficiencies exist in the removal of pressure sensitive adhesive particles. The devices studied were a hydropulper, an industrial pressure screen, two laboratory screens, and a high shear mixer. An acrylate based PSA label material was applied to copy paper and pulped in a pilot plant hydropulper. The pulp was then screened using an industrial pressure screen and two laboratory screens, all having 0.006 inches wide slots. Pulp from the hydropulper was also processed in a high shear mixer. Using the same feed pulp, the laboratory screens were much more efficient than the industrial screen in removing the PSA particles. This was due to the break down and extrusion of PSA particles in the industrial pressure screen. The combination of a laboratory pulper and high shear mixer was found to break down PSA particles to a particle size reflective of breakage in an industrial pressure screen. Also, ten different PSA formulations were pulped in a laboratory pulper, processed in a high shear mixer, and screened in a laboratory screen. The PSA particles broke down to different average particle sizes and provided different removal efficiencies, depending on the adhesive formulation. The combination of a laboratory pulper, high shear mixer, and laboratory screen could be used to represent the operations in an industrial recycling system.

INTRODUCTION

Pressure sensitive adhesive (PSA) particles are major contaminants in a paper recycling operation. The adhesive material enters the recycling system with the wastepaper in various forms and is broken down into stickies particles during repulping [1-7]. The stickies must then be removed by recycling equipment such as pressure screens. Removal efficiencies for industrial and pilot plant pressure screens have been reported between –14 and 83%, depending on the adhesive material and the pressure screen [8-16]. This wide range in removal efficiencies may be due to the high shear conditions in the pressure screen and possible extrusion of the stickies through the screen openings [17-18]. The high shear conditions have been found to disintegrate the stickies particles in a pressure screen [19]. Also, adhesive formulation may affect the removal of the PSA particles. Initial investigations into screening of PSA contaminants and how they behave in high shear conditions have been conducted at North Carolina State University [20-21].

In this study, pressure sensitive adhesive materials were analyzed for their removal efficiency using industrial and laboratory equipment. Ten different industrial PSA materials were considered in laboratory equipment to evaluate if different adhesive formulations alter the removal efficiency. These findings will assist in understanding why removal efficiencies vary depending on the operating conditions and the adhesive formulation.

EXPERIMENTAL

Industrial screening experiments were conducted using Avery Dennison "White Shipping Labels", product number 5164, applied to alkaline copy paper. Pulp was prepared in a 200 gallon hydropulper and then screened in an industrial pressure screen, with a 0.006 in. slotted screen basket, at different reject rates. For each of the reject flow rates, samples of the feed, accepts, and rejects were collected and analyzed. Details of the industrial experiments are available in reference [20].

The laboratory equipment that was analyzed using pulp from the industrial screening experiments involved a Valley flat screen, Pulmac MasterScreen, and Quantum mixer. Samples of pulp from the industrial screen feed, accepts, and rejects were screened using the two laboratory screens, each containing a 0.006 in. slotted screen plate. The Valley flat screen was operated at two different temperatures, 25°C and 45°C. The Quantum mixer was operated at various consistencies, times, initial temperatures, and rotor speeds to analyze how the adhesive responded to different shear conditions. Details of the laboratory screening experiments are available in reference [20] and details of the Quantum mixer experiments are available in reference [21].

In order to analyze how formulation affected adhesive behavior, ten different pressure sensitive adhesive samples were each examined separately using a 450H pulper, Quantum mixer, and Valley flat screen. The operating conditions for the 450H pulper were 450 OD g of pulp at 12% consistency, 45°C, and 415 rpm, for 60 minutes. The Quantum mixer was operated with 300 OD g of pulp at 10% consistency, 35°C initial temperature, and 1500 rpm, for 165 seconds. The Valley flat screen was operated with 25 OD g of pulp at 45°C for all of the samples and at 25°C for two of the samples.

For each of the industrial and laboratory experiments, sets of handsheets were made for dyeing and image analysis. Handsheets were dyed using a Morplas Blue-Heptane solution and rinsed using Heptane. Each set of handsheets was scanned on both sides before and after dyeing. The parts per million (PPM) of stickies, number of particles in 1 m^2, and average particle size were determined for each set of handsheets by the difference between the before and after dyeing values. Details of the dyeing and image analysis method are available in references [20-21]. An example of image analysis output is shown in **APPENDIX 3**.

RESULTS AND DISCUSSION

Industrial Versus Laboratory Screening

In order to investigate the behavior of PSA's in pressure screens, a series of experiments were conducted using a hydropulper and an industrial pressure screen. The results from the industrial screening experiments are shown in **Table 5-1**. Four different reject flow rates were considered for the industrial pressure screen. The removal efficiencies and average particle sizes of the collected samples for each reject flow rate are shown in **Table 5-1**. The cleanliness efficiency is based only on the parts per million values and increased from 38.8 to 71.7% with increasing mass reject rate [20]. The reject efficiency is based on the parts per million values and mass flow rates and ranged from 55.1 to 77.4% [20]. As expected, increasing the reject rate increased the removal efficiencies.

Table 5-1. Industrial Screening Results [20]

Industrial Reject Flow Rate, gpm	5.45	8	10	15
Industrial Mass Reject Ratio, %	4.5	12	15	25
Industrial Cleanliness Efficiency, %	38.8	54.5	50.5	71.7
Industrial Reject Efficiency, %	58.8	58.7	55.1	77.4
Feed Average Particle Size, mm^2	2.61	1.97	2.02	1.88
Accepts Average Particle Size, mm^2	0.38	0.34	0.35	0.31
Rejects Average Particle Size, mm^2	0.86	0.90	0.90	0.65

The average particle sizes of the feed, accepts, and rejects samples are shown in **Table 5-1**. Notice that the average particle size of the feed ranges from 1.88 to 2.61 mm^2, while the average particle sizes of the accepts ranges from 0.31 to 0.38 mm^2 and the rejects ranges from 0.65 to 0.90 mm^2. Combination of the accepts and rejects, taking into account the accepts and reject flow rates, provided an average particle size of 0.46 mm^2. The average particle sizes of the accepts, rejects and their combination are all less than the average particle size of the feed, indicating that large particles in the feed were broken down into smaller particles in the pressure screen. This should have a significant effect on the removal of these broken particles in the screening process.

The laboratory screening results using the feed samples from the industrial screening experiments appear in **Table 5-2**. All three laboratory screens provided cleanliness efficiencies of greater than 97%, which is much greater than the industrial cleanliness efficiencies for the same pulps and slot sizes. The pseudo reject ratios for the laboratory screens were approximately zero. Despite this, the efficiencies were high.

Table 5-2. Laboratory Results With Industrial Feed Pulp [20]

Industrial Mass Reject Ratio, %	12	15
Industrial Cleanliness Efficiency, %	54.5	50.5
Industrial Reject Efficiency, %	58.7	55.1
Pulmac Cleanliness Efficiency, %	99.2	99.5
Valley, 25°C, Cleanliness Efficiency, %	98.8	97.7
Valley, 45°C, Cleanliness Efficiency, %	99.9	98.4

The differences between industrial and laboratory screens are well known. Laboratory screens have minimal pressure difference and rotor action, if any, compared to an industrial pressure screen. Industrial pressure screens have a pressure pulse and high shear conditions due to the rotor, as well as a pressure difference across it. Also, laboratory screens operate as batch systems, while an industrial pressure screen is a continuous process. These differences impact the relative removal efficiencies of industrial and laboratory screens. Two variables of importance in screening are breakage and extrusion of adhesive particles.

Breakage of PSA Particles

Breakage of particles in a device can easily be observed by comparing particle size distributions of the material before and after the device. If the amount of material in the small particle size ranges increases in the device, then breakage of the larger particles into smaller ones occurred. A plot of the logarithm of number of particles in 1 m^2 versus particle size for the samples from the 25% mass reject ratio industrial screening experiment is shown in **Figure 5-1**. Notice that the mathematically combined industrial accepts and rejects contain approximately ten times more small particles (<0.50 mm^2) than the feed pulp. Similarly, the feed pulp contains about ten times more large particles

(>3.00 mm^2) than the mathematically combined accepts and rejects. This data clearly shows that breakage is a serious issue for PSA materials in an industrial pressure screen.

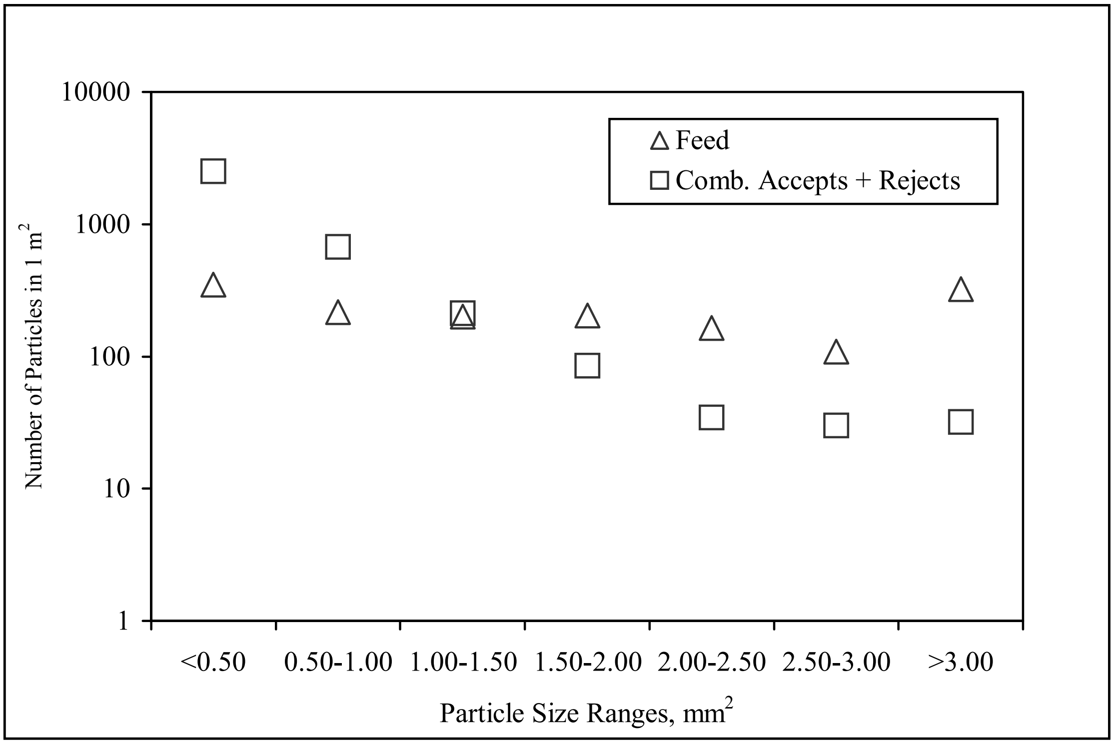

Figure 5-1. Number of Particles in 1 m^2 Versus Particle Size Before and After a Pressure Screen [20]

The removal efficiency of screening devices at different particle sizes for the same feed pulp sample is shown in **Table 5-3**. Notice that the removal efficiencies for particles less than 1.50 mm^2 are negative for the industrial pressure screen. A negative removal efficiency means that particles were generated instead of removed. In order for small particles to be generated in the industrial pressure screen, larger particles must have been broken down.

For all of the particle size ranges, the removal efficiencies for the laboratory screens are all positive and were significantly more efficient in removing adhesive material from the same pulp than the industrial screen (**Table 5-3**). The laboratory screens did not allow any adhesive particles larger than 1.50 mm^2 to pass through the slots.

Table 5-3. Removal Efficiencies of the Industrial and Laboratory Screens for Different Particle Size Ranges [20]

Particle Size Ranges, mm^2	Cleanliness Efficiency, %			
	Industrial, 10 gpm	Pulmac	Valley, 25^{o}C	Valley, 45^{o}C
<0.50	-643.2	81.2	18.8	42.1
0.50-1.00	-326.3	100.0	98.0	100.0
1.00-1.50	-117.1	100.0	99.6	100.0
1.50-2.00	56.0	100.0	100.0	100.0
2.00-2.50	87.9	100.0	100.0	100.0
2.50-3.00	100.0	100.0	100.0	100.0
>3.00	99.2	100.0	100.0	100.0

One parameter that affects the breakage of adhesive particles is the shear field within each device. The average particle size of adhesive particles in pulp after processing with different devices and combinations of devices are shown in **Table 5-4**. Adhesive particles were the largest out of the hydropulper at 1.28 mm^2. The industrial pressure screen then decreased the average particle size to 0.46 mm^2. For pulp from the hydropulper, the Quantum mixer provided a similar average particle size, 0.41 mm^2, to the pressure screen combination of the accepts and rejects. The 450H pulper provided an average particle size similar to the pressure screen and Quantum mixer.

Table 5-4. Breakage of Adhesive Particles in Various Equipment Combinations

Equipment	Average Particle Size, mm^2
Hydropulper [20]	1.28
Hydropulper + Industrial Screen (Combination of Accepts + Rejects) [20]	0.46
Hydropulper + Quantum Mixer (9% K, 165 sec, 35^{o}C, 1500 rpm) [21]	0.41
450H Pulper	0.36
450H Pulper + Quantum Mixer (10% K, 165 sec, 35^{o}C, 1500 rpm)	0.27

The hydropulper produced adhesive particles with an average particle size almost four times that for the 450H pulper (**Table 5-4**). The average particle sizes may be different between the hydropulper and 450H pulper, but the 450H pulper broke down the PSA particles to an average particle size similar to the hydropulper + industrial screen combination. Therefore, if one wants to study the screenability of PSA materials incorporating their tendency to break in the pressure screen, then the 450H pulper will provide similar breakage. The lab screens can then be used to remove the remaining large particles from the pulp. This procedure does not exactly model the industrial screening system, but it reflects the effect of breakage on removal efficiency (see below).

Another parameter that affects the breakage of adhesive particles is the adhesive material itself. The average particle sizes for ten different pressure sensitive adhesives out of the laboratory pulper and Quantum mixer are shown in **Table 5-5**. The operating conditions for the 450H pulper were 450 OD g of pulp at 12% consistency, 45°C, and 415 rpm, for 60 minutes. The Quantum mixer was operated with 300 OD g of pulp at 10% consistency, 35°C initial temperature, and 1500 rpm, for 165 seconds. The average particle sizes range from 0.18 to 1.07 mm^2 out of the pulper and from 0.18 to 0.93 mm^2 out of the mixer. This data indicates the significant effect of PSA formulation on breakage.

Table 5-5. Average Particle Size for Different PSA Materials from the Laboratory Pulper and Mixer

	Average Particle Size, mm^2	
Adhesive Sample	450H Pulper	Quantum Mixer
A	0.49	0.38
B	0.18	0.18
C	0.90	0.84
D	0.49	0.48
E	0.46	0.36
F	1.07	0.93
G	0.76	0.62
Acrylic	0.52	0.42
SIS	0.50	0.39
Labels	0.36	0.27

A plot of removal efficiency of different industrial PSA materials in the Valley flat screen at 45°C versus average particle size of the feed pulp is shown in **Figure 5-2**. The different average particle size values correspond to the average particle sizes out of the Quantum mixer for the different adhesive materials in **Table 5-5**. Notice that the removal efficiencies for the different industrial adhesives range from 26% to 99%, depending on the average particle size of the PSA particles in the feed pulp. As the average particle size decreases, the removal efficiency also decreases. This is because smaller particles are more likely to pass through the 0.006 inches wide slots than larger particles. As expected, feed pulps with lower average particle sizes had lower removal efficiencies in the screens. This indicates that adhesive manufacturers do have an ability to change adhesive formulations to alter the screenability of PSA materials.

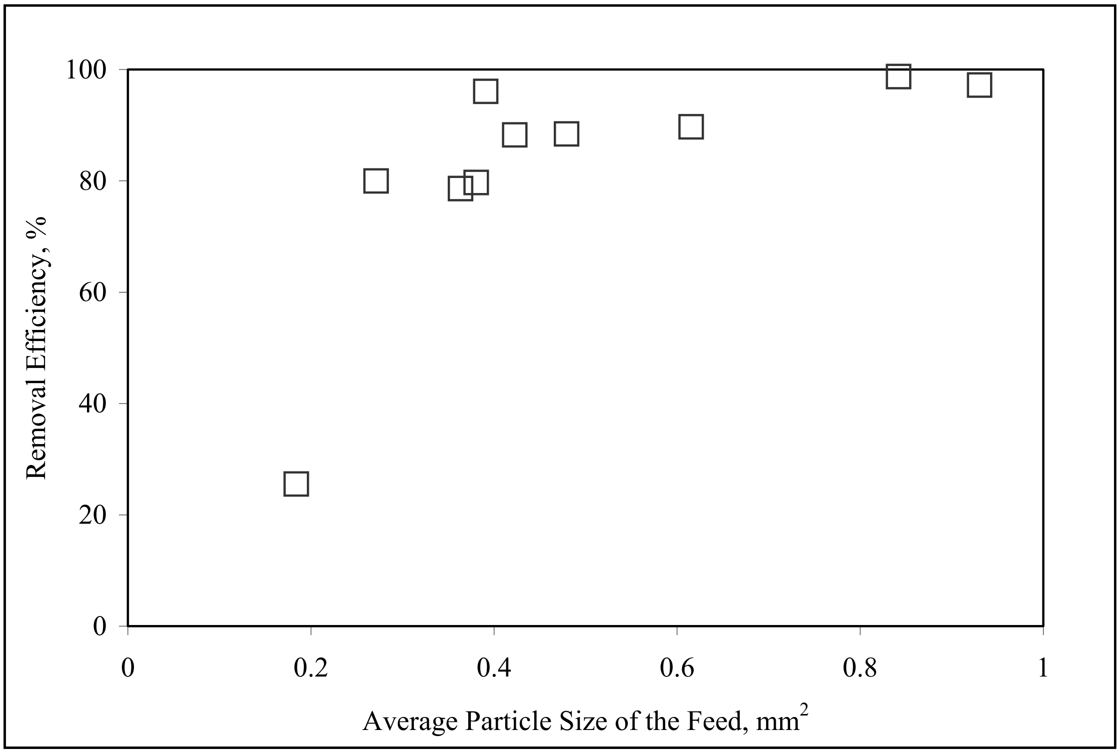

Figure 5-2. Removal Efficiency Versus Average Particle Size of the Feed in the Valley Flat Screen at 45^{o}C (Slot Width of 0.006 inches)

Extrusion of PSA Particles

Extrusion is the forced passage of a particle through a slot or hole that the particle is too large to pass through otherwise. In order to analyze the extrusion effect of the industrial pressure screen, accepts samples from the industrial screening experiments were screened in the laboratory, see **Figure 5-3**.

The cleanliness efficiencies for the laboratory screens using the industrial accepts as the feed samples are shown in **Table 5-6**. The laboratory screen plates had the same size slots, 0.006 in., as the industrial pressure screen basket. The laboratory screening experiments provided cleanliness efficiencies all greater than 70%. That is, at least 70% of the adhesive material that passed through the industrial pressure screen did not pass through the laboratory screens. In other words, 70% of the material that passed through the industrial screen must have extruded through the slots of the industrial pressure screen.

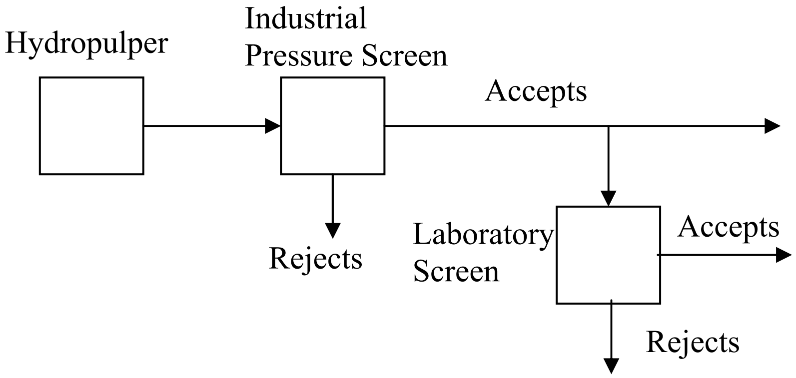

Figure 5-3. Flow Diagram of Industrial Screen Accepts as the Feed for the Laboratory Screens

Table 5-6. Industrial Screening Accepts as the Feed in the Laboratory Screens [20]

Industrial Mass Reject Ratio, %	4.5	12	15
Industrial Accepts in Pulmac Cleanliness Efficiency, %	95.9	90.6	95.4
Industrial Accepts in Valley, 25°C, Cleanliness Efficiency, %	93.1	78.8	93.6
Industrial Accepts in Valley, 45°C, Cleanliness Efficiency, %	76.7	70.4	82.1

Temperature appears to have an effect on laboratory screening of adhesive contaminants (see **Table 5-6** and **Table 5-7**). For the industrial accepts in the Valley flat screen, the cleanliness efficiency was lower at 45°C than at 25°C. Also, for two different adhesives, the removal efficiency was lower at the higher temperature. It is possible that the adhesive particles are softer at higher temperatures, allowing larger particles to extrude through the slots. So, in fact, extrusion also plays a role in laboratory screens. The amount of extrusion that occurs in the laboratory screen is unknown, but it is much less than the extrusion in an industrial pressure screen.

Table 5-7. Removal Efficiency of the Valley Flat Screen at 25^{o}C and 45^{o}C for Two Different Adhesives

Adhesive Samples	25^{o}C	45^{o}C
B	71.4	25.6
Labels	87.7	80.0

A plot of removal efficiency versus particle size for different industrial adhesive samples is shown in **Figure 5-4**. Not all of the adhesives behaved the same in the Valley flat screen at 45^{o}C, especially adhesive B, which had very low removal efficiencies for most of the size ranges. There were a wide range of removal efficiencies for the small particle size ranges, which may be affected by the extrudability and shape of the adhesives. Also note that in the smallest size bins, <0.50 mm^2 and 0.50-1.00 mm^2, there was a wide range of removal efficiencies for the different adhesive materials. For the same size particles, different adhesives provided different removal efficiencies. This was due to the extrusion of different adhesives through the slots of the laboratory screen.

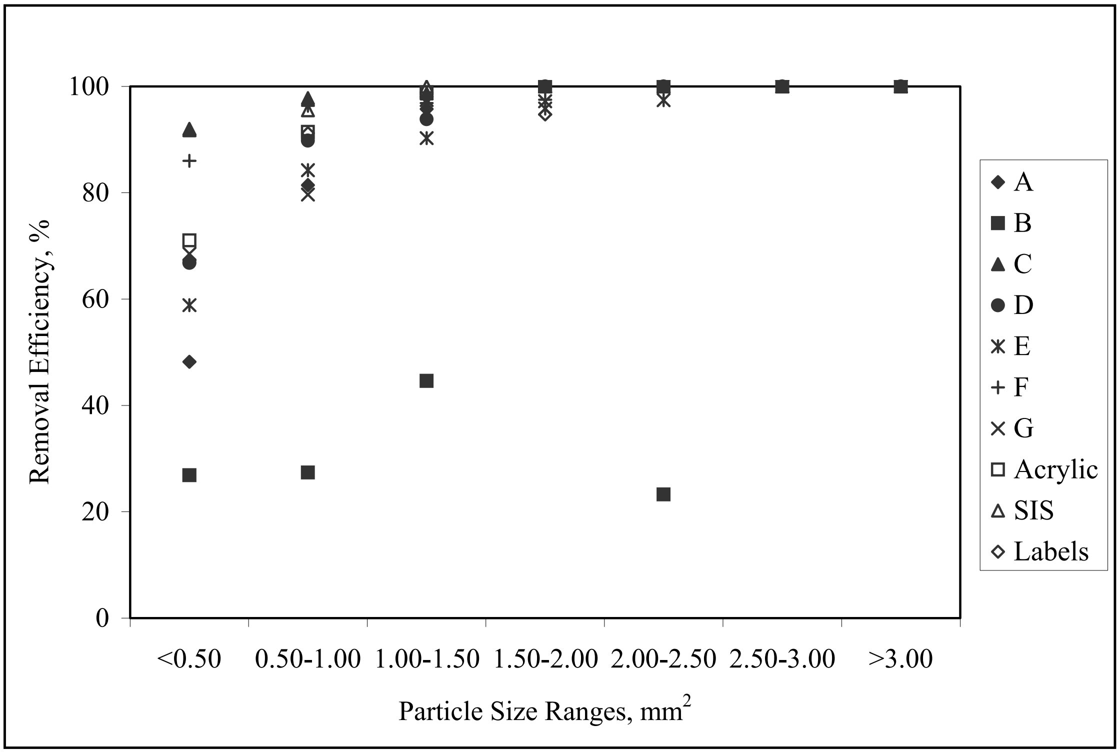

Figure 5-4. Removal Efficiency Versus Particle Size Ranges for Different Adhesive Samples

CONCLUSIONS

Industrial pressure screens and laboratory screens provide different removal efficiencies for pressure sensitive adhesive contaminants. Industrial pressure screens break down PSA particles to smaller particle sizes and particles extrude through the slots. Lab-scale equipment can provide breakage of PSA particles similar to an industrial pressure screen. PSA materials break down to different particle sizes depending on the equipment and the adhesive material itself. Different PSA materials provide different removal efficiencies due to the adhesive formulation. Extrusion of PSA particles can be investigated by screening the accepts from an industrial pressure screen in a laboratory screen and by screening different PSA materials.

REFERENCES

1. Pikulin, M. A., "Stickies and Their Impact on Recycled Fiber Content Fine Paper", *Joint Conference to Address Pressure Sensitive Adhesive Issues Proceedings*, United States Postal Service and American Forest & Paper Association, Washington, D.C., June 1996.

2. Doshi, M. R., "Overview-Stickies", *Paper Recycling Challenge, Vol. I- Stickies*, M. R. Doshi and J. M. Dyer, eds., Doshi & Assoc., Inc., Appleton, WI, pp. 3-6, 1997.

3. Scholz, W. F., "Recyclable Pressure Sensitive Adhesives", *1993 Tappi Pulping Conference Proceedings*, Atlanta, GA, TAPPI Press, pp. 501-505, 1993.

4. Bliss, T., "Screening", Chapter 14 in *Secondary Fiber Recycling*, Spangenberg, R. J., ed., TAPPI Press, Atlanta, GA, 1993.

5. Chou, C. S., "Repulpability of Adhesives", *Paper Recycling Challenge, Vol. I-Stickies*, M. R. Doshi and J. M. Dyer, eds., Doshi & Assoc., Inc., Appleton, WI, pp. 304-309, 1997.

6. Scholz, W. F., "Pressure Sensitive Adhesives", *Progress in Paper Recycling*, 4(1):71-73, 1994.

7. Crossley, B. R., Abubakr, S., Grimes, D. B., and Kumar, R., " A Pilot Plant Study of the Recyclability of Pressure Sensitive Adhesives (PSA)", *1998 Tappi Recycling Symposium Proceedings*, New Orleans, LA, TAPPI Press, pp. 469-473, March 1998.

8. Heise, O., "Screening Foreign Material and Stickies", *Tappi Journal*, 75(2): 78-81, 1992.

9. Sutherland, N. R., "Stickies Dirt Count and Laboratory Methods", *Environmentally Benign Pressure Sensitive Adhesives for Postal Applications Conference Proceedings*, United States Postal Service, Potomac, MD, July 1997.

10. Heise, O., Kemper, M., Wiese, H., and Krauthauf, E., "Removal of Residual Stickies Applying New Flotation Technology at Haindl Paper – Schongau", *Tappi 1999 Conference Proceedings*, Atlanta, GA, TAPPI Press, pp. 693-710, March 1999.

11. Veilleux, S., Chabot, B., and Daneault, C., "Quantification of Macro Stickies and Optimization of the Wastepaper Deinking Process", *5th Research Forum on Recycling Proceedings*, Ottawa, ON, Canada, pp. 241-247, September 1999.

12. Seifert, P., Winkler, J., Vitori, C., Fields, B., and Maze, E., "Removal of Soft and Flexible Contaminants from Recycled Paper, in Screens", *5th Research Forum on Recycling Proceedings*, Ottawa, ON, Canada, pp. 165-186, September 1999.

13. Delagoutte, T., and Julien Saint Amand, F., "Pilot Plant Procedure for the Assessment of the Screening Ability of Pressure Sensitive Adhesive", *2000 Tappi Recycling Symposium Proceedings*, Washington, D.C., TAPPI Press, pp. 359-374, March 2000.

14. Sutherland, N. R., and Donermeyer, D., "Laboratory- and Pilot-Scale Evaluations of Environmentally Benign PSA Stamps", *2000 Tappi Recycling Symposium Proceedings*, Washington, D.C., TAPPI Press, pp. 433-470, March 2000.

15. Crossley, B. R., Grimes, D. B., Abubakr S., and Kumar, R., "A Pilot Plant Study of the Recyclability of Pressure Sensitive Adhesives (PSA)", *2000 Tappi Recycling Symposium Proceedings*, Washington, D.C., TAPPI Press, pp. 594-601, March 2000.

16. Cameron, J., and Forester, W., "Behavior of PSAs: MOW and Sorted Office Paper with High Content of PSAs", *2000 Tappi Recycling Symposium Proceedings*, Washington, D.C., TAPPI Press, pp. 611-617, March 2000.

17. Doshi, M. R., "Quantification of Stickies", *Paper Recycling Challenge, Vol. I-Stickies*, M. R. Doshi and J. M. Dyer, eds., Doshi & Assoc., Inc., Appleton, WI, p. 193, 1997.

18. Doshi, M. R., "Reduce the Pressure, Please!", *Progress in Paper Recycling*, 8(4):6, 1999.

19. Heise, O., Schabel, S., Cao, B., and Lorenz, K., "Deformation and Disintegration Physics of Stickies in Pressure Screens: A compromise between pulp quality and capital investment", *5th Research Forum on Recycling Proceedings*, Ottawa, ON, Canada, pp. 187-195, September 1999.

20. Lucas, B. E., Venditti, R. A., and Jameel, H., "Behavior of Pressure Sensitive Adhesive Material in Industrial Pressure Screens and Laboratory Screens", *Tappi Journal*, 84(5):70, 2001.

21. Lucas, B. E., Venditti, R. A., and Jameel, H., "The Breakage of Pressure Sensitive Adhesive Contaminants in Paper Recycling Operations", *2000 Tappi Pulping/Process & Product Quality Conference Proceedings*, Boston, MA, TAPPI Press, November 2000.

ACKNOWLEDGEMENTS

Support for this research provided by Ecosynthetix. Donations of equipment by Apogee Systems and Pulmac Instruments are also greatly appreciated.

CHAPTER 6

PASSAGE OF PRESSURE SENSITIVE ADHESIVE PARTICLES THROUGH A FINE SLOT

ABSTRACT

The removal of adhesive contaminants using pressure screens is a critical issue in paper recycling. Several hypotheses have been presented to explain the passage of pressure sensitive adhesive (PSA) particles of apparently larger size than the screen openings passing through the screen. The objective of this research was to provide experimental observations to help explore these hypotheses. An acrylate based PSA label material was applied to copy paper and pulped in a laboratory pulper. PSA particles from the pulp were analyzed for passage in a pressurized device containing a single 0.007 inches (0.18 mm) wide slot. The passage of PSA particles through the single slot was determined versus the particle dimensions and pressure difference across the slot. It was found that PSA particles with their smallest dimension less than four times the slot width were able to pass through the slot for pressure differences of up to 75 kPa. These particles were observed to deform and pass through the slot, suggesting that particle extrusion was the method of passage. Increased temperature, which is expected to decrease the modulus of the PSA material, promoted the passage of particles through the slot.

INTRODUCTION

The increased usage of recovered fibers and related problems associated with stickies (potentially tacky contaminants) and other contaminants are a challenge for today's papermaking operations. Stickies are known to deposit on the paper machine wires and felts and also to contaminate the final paper or board product [1-4]. Removing contaminants from recovered fiber is one of the biggest technical barriers to improved paper recycling. Pressure sensitive adhesives (PSA) continue to represent the most challenging contaminant to detect and remove. PSA particles are formed during pulping and other high-shear processing operations and are extremely difficult to remove due to their size, density, and ability to change shape [4-10]. Screening is generally considered to be the most effective removal method, but is known to be less than 100% efficient with PSA particles [11]. Screening has been shown to be sensitive to the size of the PSA particles, and very large particles can be removed at 100% efficiency [12]. PSA particles can also be broken in the screening operation, further decreasing the screening efficiency [12,13,14].

For a wide range of particle sizes larger than the slot or hole size of a screen it has been anecdotally reported that the PSA particles can still pass through. Several theories to explain this phenomenon have been presented [15].

One explanation states that the anecdotal reports stem from the fact that stickies when viewed in a handsheet are pressed flat and thus the largest dimension of the particle is reported. Further, the pressing can increase the apparent size of the particles when pressed from a three dimensional object into a two-dimensional object. Thus, the particles simply look bigger than they actually are.

A second explanation is based on the observation that PSA particles often have different sizes in the three dimensions. The ability of the particle to pass through a slot is explained by the particle aligning its smallest dimension with the slot so that it may pass through the slot.

A third explanation put forth was that particles with one large dimension might bend and fold to fit through the opening [15]. It was calculated using estimates of the PSA properties and expected pressures in a screen that the forces present were sufficient to bend and fold a particle that has its long dimension spanning the width of the slot. No experimental verification was presented.

A fourth explanation that was deemed not probable was the extrusion of the particle through the slot [15]. By extrusion, it was meant that the pressure difference across the slot provides a force that deforms the large particle such that it passes through the opening. The forces existing in a pressure screen, based only on the pressure difference, to extrude typical PSA particles were reported to be less than what was calculated as necessary to extrude the particles. Thus, this concept was rejected previously.

The above study and conclusions were based on theoretical calculations and estimates of material properties. Only forces due to pressure gradients were considered. Other forces, such as the fluid drag and the impact of the rotor was not considered. It was therefore of interest to study these proposed mechanisms experimentally.

Single slotted laboratory experimental equipment has been used previously to understand and visualize the flow patterns near the slot opening and the passage behavior of fibers through the slot [16-18]. In this study a single slot of 0.18 mm (0.007 inches) width was used to evaluate the passage of PSA particles as a function of particle size and pressure difference across the slot under simplified conditions, compared to an industrial pressure screen.

EXPERIMENTAL

Single Slot Apparatus

Figure 6-1 is a schematic of the single slot apparatus. **Figure 6-2** shows the geometry and dimensions of the slot as measured with common calibrated feeler gauges with a precision of 0.025 mm. The key dimension is the 0.18 mm slot width on the feed side of the plate. The length of the slot was 25.4 mm. The metal plate was sealed to the bottom of a plastic Buchner funnel using silicone adhesive. The Buchner funnel was inserted into an Erlenmeyer flask that was connected to a vacuum line with a maximum vacuum of about 80 kPa. A pressure gauge with increments of 1.7 kPa (0.5 inches of Hg) was used to record the vacuum. The vacuum was altered using a standard adjustable manual valve.

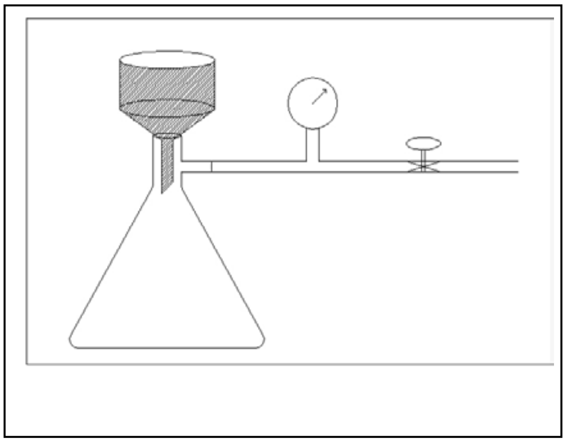

Figure 6-1. Laboratory Single Slot Apparatus

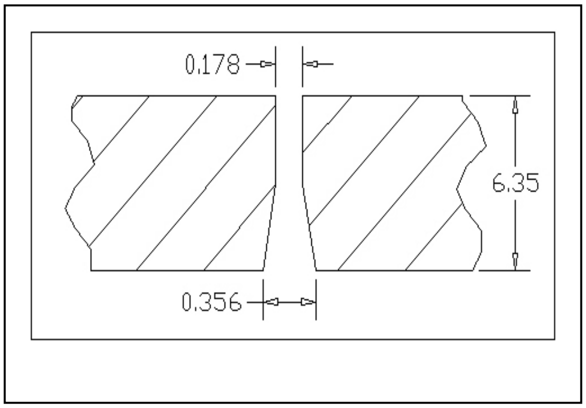

Figure 6-2. Cross-section View of the Slot Showing Important Dimensions in mm

Fluid Velocity in the Slot

The passing velocity (average fluid velocity through the slot) was determined versus the pressure difference across the slot. To do this, a piece of tape was placed over the slot and the Buchner funnel was filled with 1000 mL of water. The vacuum line was opened and once a stable vacuum was achieved the tape was removed. The time for 1000 ml of the water to pass though the slot was measured with a stopwatch. The velocity through the slot was calculated with the following equation:

$$Velocity = V / W\,L\,t \quad (1)$$

where V is the volume (1000 mL), W is the minimum width of the slot, L is the length of the slot, and t is the time.

Pulping

In order to create PSA particles, twelve Avery Dennison 5164 Shipping labels (six labels per 8.5 x 11 inches sheet) were applied on 450 OD grams of copy paper (Quick Copy, Xerographic DP-White, Weyerhaeuser). The pressure sensitive adhesive material is an acrylate-based adhesive. The material was then pulped in a 450H Adirondack laboratory pulper at 12% consistency for 1 hour at 50°C.

Evaluation of the Passage of PSA Particles Through the Slot

Approximately 30 g of pulp containing PSA particles was diluted to 1% consistency with tap water and stirred well. The pulp was poured over a paper machine wire screen and one single particle was removed from the screen and placed on a microscope slide. The particle was covered by a drop of water and manipulated using a small laboratory spatula. The particle was then examined under an optical microscope equipped with a calibrated length scale and measured in three dimensions. It was necessary to keep the particles covered by water so that they did not adhere to the glass slide or spatula. No deformation of the particles was observed during the manipulations.

Immediately after the particle dimensions were measured, the particle was placed on the metal plate with its long dimension (length) parallel to the length of the slot, centered across the width of the slot, and centered on the length of the slot. The Buchner funnel was filled with water at a pre-defined temperature. After 30 seconds, the vacuum was increased until the particle either passed through the slot or the maximum vacuum was achieved. The time to ramp to the maximum vacuum was approximately 30 seconds. This was repeated for other particles with different dimensions. The same procedure was repeated using water temperatures of 5, 25, and 55°C.

RESULTS AND DISCUSSION

Characterization of the Single Slot Apparatus

It was of interest to compare the fluid velocity versus pressure difference of the single slot apparatus relative to industrial screens. In experiments with no adhesive particles present, the pressure difference was varied and the volumetric flowrate was determined. The calculated passing velocity was linearly related to the square root of the pressure difference across the slot (correlation coefficient of 0.995), **Figure 6-3**, as expected. Both the passing velocities determined and the pressure differences utilized herein encompass realistic values of passing velocities and pressure differences found in some industrial pressure screens [19,20]. A detailed description of flow through slotted apertures in pulp screens has been recently presented [16].

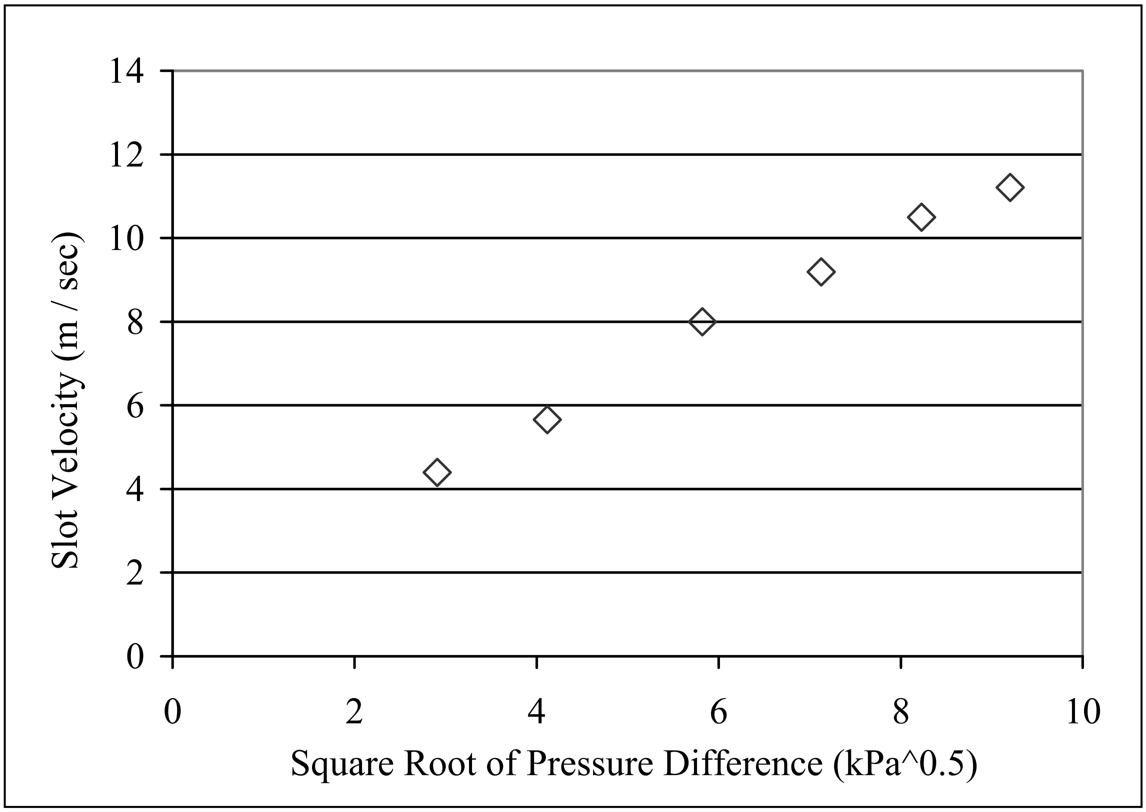

Figure 6-3. Average Fluid Velocity in the Slot Versus the Square Root of the Pressure Difference Across the Slot

PSA Particles

The PSA particles formed during pulping typically had two types of shapes. For qualitative purposes these will be classified as strings and balls, **Figure 6-4** and **6-5**, respectively. The most predominant shape, the "string-like" shape, has a much larger length than width, and typically has a thickness approximately equal to its width. It is important to note that the shorter dimensions (termed width and thickness) of the "string-like" particles were not constant along the length of the particle, **Figure 6-4**. The non-constant nature of the shorter dimension was found to be particularly important to the behavior of the passage of the particle through the slot (see later). The length of these particles was on average two times larger than its width, but for some particles could be as high as eight times larger. The "ball-like" particles had similar length, width, and thickness values. The length (the largest dimension) was never larger than twice the width, and the thickness was almost equal to the width. The ring around the dark object in **Figure 6-4** is water.

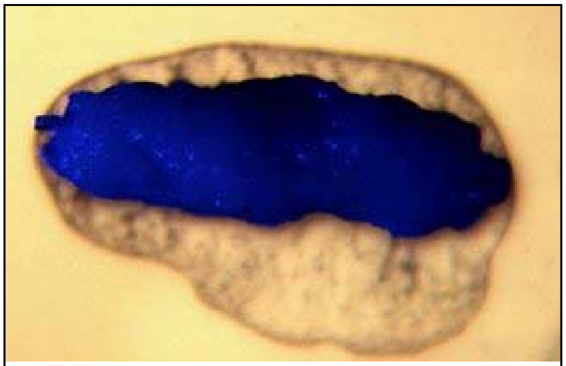

Figure 6-4. Photo-micrograph of a "string-like" PSA Particle (dark object)

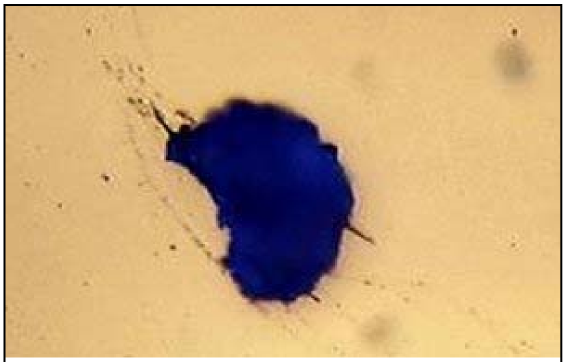

Figure 6-5. Photo-micrograph of a "ball-type" PSA Particle

Passage of PSA Particles through the Slot

Initially, PSA particles were placed on the single slot at various angles to the slot. In all cases, as the vacuum increased the particle rotated until it aligned its longest dimension parallel to the slot (at about 7 kPa pressure difference). There were no indications that the particle by itself would remain perpendicular to the slot. No indications of the PSA particle bending or folding in the long dimension were observed. The observed alignment was due to the symmetric streamlines of the fluid flowing into the slot from both sides. This is a different flow pattern than would be experienced in an industrial screen, in which the flow above the slot is predominantly in the direction of the foil movement (parallel to the screening surface). Also, the flow phenomena due to the contoured screen surface, such as the formation of specifically located vortices or recirculating zones [16,18,20] should be different in our simplified apparatus.

Other differences between these experiments and industrial screening should be noted. In these experiments, no fibers were present, in order to eliminate plugging of the slot. Fibers have an effect on the rheological properties of the suspension. Thus, the range of passing velocities herein, 6-9 m/s for 25-40 kPa pressure difference, is higher than for industrial screens at the same pressure difference, 2-3 m/s for 25-40 kPa difference, for example, in part due to the lower viscosity of the water medium utilized herein. This difference in passing velocities may also be due to the back-flushing of material in a pressure screen with a rotor, not present herein [20]. Fiber mats formed on the surface of the screening basket and fibers lodged in the slots also alter the flow patterns and velocities of the fluid. Also, the time-scale of these experiments was on the order of seconds, much longer than the time scale of milliseconds in a pressure screen due to the positive and negative pressure pulses brought about by the rotor [20]. PSA materials are viscoelastic, meaning that their deformation behavior is affected by the time-scale of the experiment. A PSA material will behave more like an elastic solid at short time-scales and more like a viscous liquid at long-time scales. Despite these differences, these experiments show the effect of pressure difference across a slot on the passage of PSA particles in a simplified system.

For all of the following experiments the PSA particle was aligned with the long dimension (length) parallel to the slot. The vacuum was increased slowly until the maximum pressure difference across the slot with this system, about 80 kPa, was attained. **Figure 6-6** shows that the percentage of particles that passed through the slot decreased with increased particle width (smallest dimension, approximately the same as the thickness). It was found that PSA particles with their smallest dimension greater than approximately four times the slot width did not pass through the slot for pressure differences of up to 80 kPa. A significant percentage of PSA particles with their smallest dimension between the slot width (0.18 mm) and four times the slot width passed through the slot at moderate pressure differences, that are typical for industrial pressure screens. No correlation was found between the particle length and the percentage of particles that passed through the slot (data not shown). Also, there was no correlation found between the particle projected area (length times width) and the percentage of particles that passed through the slot (data not shown).

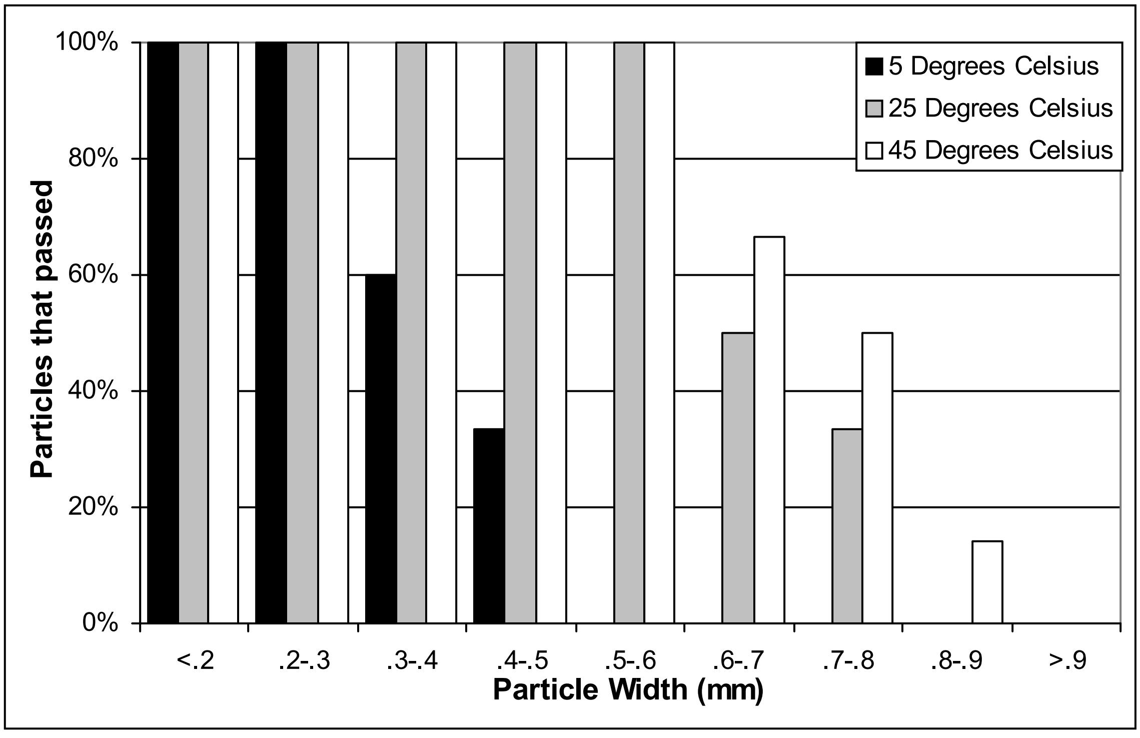

Figure 6-6. Percentage of PSA Particles that Passed Through the Slot Versus the Smallest Particle Dimension (Width) for Different Temperatures

It was observed that increased temperature promoted the passage of particles through the slot, **Figure 6-6**, presumably due to the softening of the particles at higher temperatures. This is in agreement with previous findings in this group [12,21] and by others [22], that lower temperatures improve the screening of PSA contaminants.

The pressure difference that caused passage of the particle versus the smallest particle dimension, the width, is shown in **Figure 6-7** for different temperatures. It is important to note that **Figure 6-7** is a plot of those particles that passed through the slot, those that did not pass through are not represented on this graph. As expected, larger particles required a higher-pressure difference across the slot for passage. It is important to note that there is significant scatter in the data at any given particle width. This is to be expected due to the variability of the three-dimensional shape of the particles and the inherent errors involved in trying to characterize these complex particle shapes using three average dimensions.

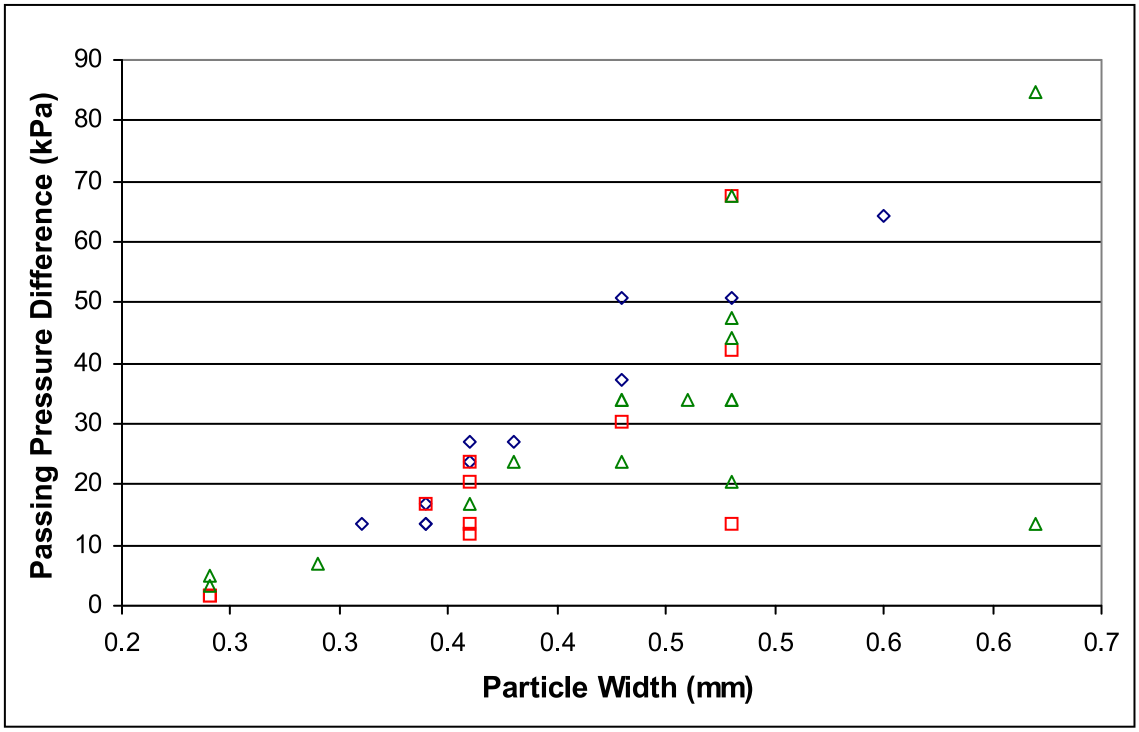

Figure 6-7. Pressure Needed to Force the PSA Particle Through the Slot Versus the Smallest Particle Dimension (Width), Symbols Indicate the Water Temperature: ◊ 5°C, ☐ 25°C, and Δ 55°C

Observations of the stickies that passed through the slot showed a complicated passing process. This was in part due to a non-regular shape of the particles. For string-like particles, the particle is similar to a cylinder, except that the radius of the cylinder is non-constant, **Figure 6-8**. It was observed that a length of the particle cylinder with a relatively small radius would begin to enter the slot while other portions of the particle with larger radii remained anchored above the slot. As the pressure difference increased, these portions with larger radii would then enter the slot and eventually the entire particle would pass through. Regions of small radii were found in the middle of the particle, at one end of the particle and/or at both ends of the particle. Thus, the scatter in the data in **Figure 6-7** is not unusual considering the simplified geometrical descriptions of the particles that were used.

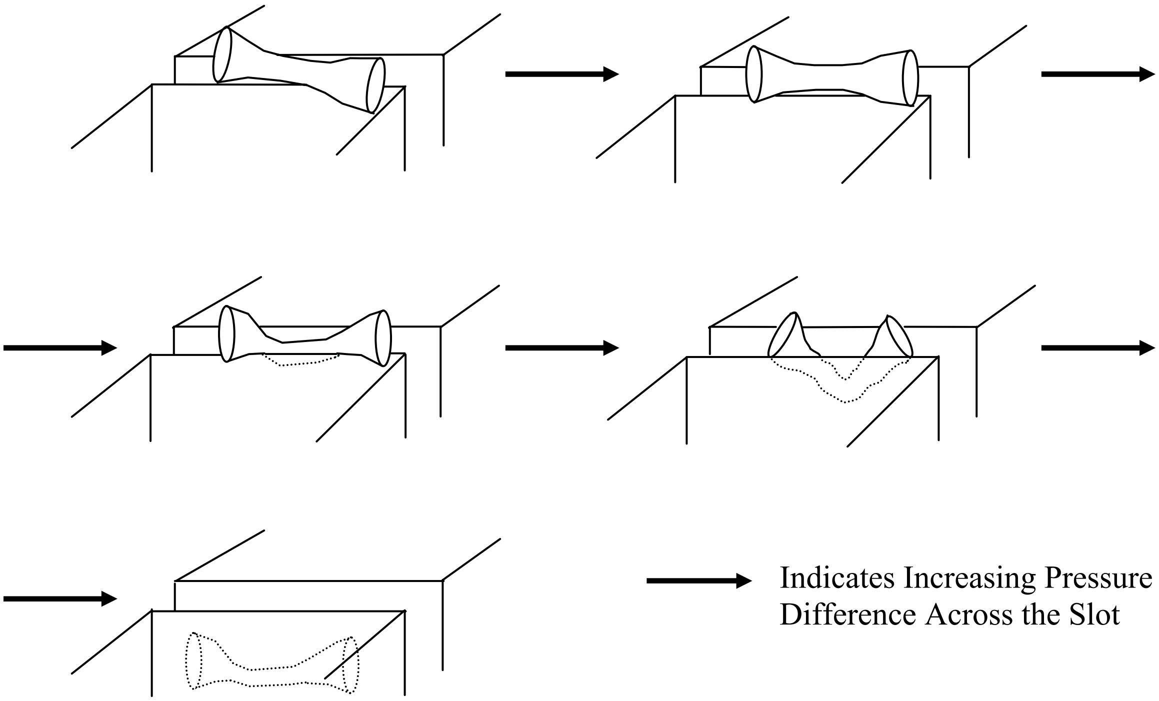

Figure 6-8. Schematic Drawing of a Particle with a Non-constant Radius as the Pressure Difference Increases Across the Slot

The particles were also observed to vary in their “opaqueness” when viewed with a microscope. Qualitatively this was attributed to different “compactness” of the particles; some particles had been folded on themselves during pulping in a tighter fashion than others. This difference in “folded density” of the particles may also contribute to the variability of the results in **Figure 6-7**.

To better demonstrate the trend of pressure difference needed for the passage of particles versus particle size and temperature, the results of particles that passed through the slot with similar particle widths were averaged and are shown in **Figure 6-9**. A significant linear correlation was found for this data for all three temperatures (R^2 values greater than 0.95). From the best fit lines it is observed that the higher temperature of 55°C promoted particle passage.

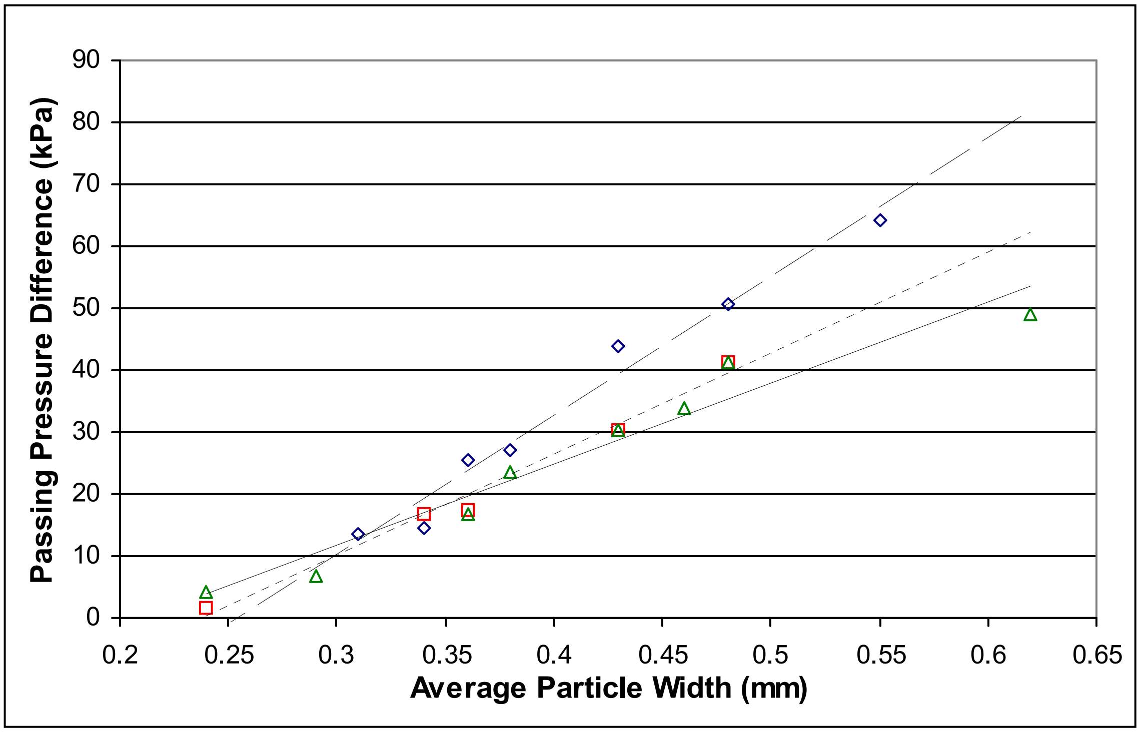

Figure 6-9. Average Pressure Difference (particles of similar width averaged together) Versus Average Particle Width, Symbols Indicate the Water Temperature: ◊ 5°C, ☐ 25°C, and Δ 55°C

In 1987 McCool and Silveri published a qualitative graph on the removal trends of debris removal unit operations [23]. Their illustration suggests that the most important debris dimension during screening and other cleaning operations is its largest dimension. **Figure 6-10** shows the pressure difference needed for the particle passage versus the particle largest dimension (length) does not correlate for these experiments. As was previously stated, the particle length was parallel to the slot length in these experiments. In a screen with micro-turbulence, the longest dimension of the particle would be aligned in many directions relative to the slot. Alignment of the adhesive particles in an industrial pressure screen perpendicular to the slot length is very likely. Thus, the longer dimension is expected to play some role in the determination of passage in a real pressure screen.

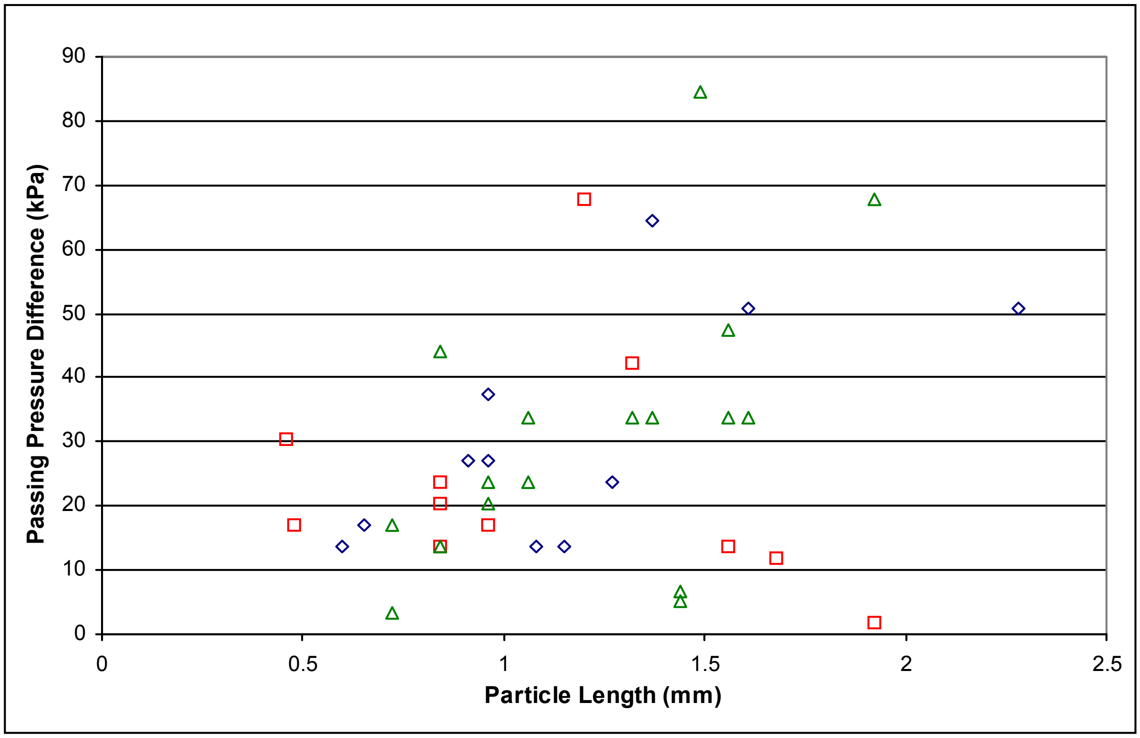

Figure 6-10. Passing Pressure Versus Longest Particle Dimension (Length), Symbols Indicate the Water Temperature: ◊ 5°C, ☐ 25°C, and Δ 55°C

These experiments indicate that the passage of PSA particles can occur due to deformations (similar to extrusion) at moderate pressures that do not involve the folding of the particle across its long dimension. This is in agreement with previous results showing that PSA particles can pass through a pressure screen, but the same particles (from the accepts of the pressure screen) are retained on a laboratory screen in which the pressure difference across the slot is small [21].

RECOMMENDATIONS

This study can potentially lead to further research in the area of PSA particles and screening. Pulping operations may change the size, shape, and composition of the PSA particles and have an effect on their passage through subsequent screening. Similar experiments in which the adhesive is restrained so that its longest dimension is perpendicular to the slot may provide information about a folding/bending phenomenon. It would also be useful to examine the shape and size of the particles before and after passage through the slot versus pressure difference and temperature and determine if plastic deformation has occurred. Causing the fluid flow to be predominantly in one direction perpendicular to the slot length would better simulate the conditions in an industrial pressure screen and the use of visualization techniques would enhance the understanding of the passage process.

CONCLUSIONS

Lab-scale pulping of pressure sensitive adhesive labels and copy paper generated PSA particles that typically had one long dimension and two shorter dimensions of approximately equal magnitude. In experiments with the long dimension aligned with the length of the slot, the passage of the particles through a single 0.178 mm slot was found to depend on the smaller dimension of the particles and not on the longer dimension.

PSA particles with their smallest dimension greater than approximately four times the slot width did not pass through the slot for pressure differences of up to 80 kPa. However, a significant percentage of PSA particles with their smallest dimension between the slot width and four times the slot width passed through the slot at moderate pressure differences. These particles were observed to deform and pass through the slot. Increased temperature, which is expected to decrease the modulus of the PSA material, promoted the passage of particles through the slot. Despite differences between these simplified experiments and pressure screens, these experiments demonstrate the effect of pressure difference across a slot on the passage of PSA particles.

ACKNOWLEDGEMENTS

The laboratory work for this research was conducted by Jeff Flanagan, Nick Wilson, and Nick Weaver and coordinated by Richard Venditti, Hasan Jameel, and Bradley Lucas.

REFERENCES

1. Doshi, M. R., "Overview-Stickies", *Paper Recycling Challenge, Vol. I- Stickies*, M. R. Doshi and J. M. Dyer, eds., Doshi & Assoc., Inc., Appleton, WI, pp. 3-6, 1997.

2. Doshi, M. R., "Quantification of Stickies", *Paper Recycling Challenge, Vol. I- Stickies*, M. R. Doshi and J. M. Dyer, eds., Doshi & Assoc., Inc., Appleton, WI, p. 193, 1997.

3. Doshi, M. R., "Properties and Control of Stickies", *Paper Recycling Challenge, Vol. I- Stickies*, M. R. Doshi and J. M. Dyer, eds., Doshi & Assoc., Inc., Appleton, WI, pp. 227-236, 1997.

4. Smith, S. E., "Stickies Properties and the Relationship to Their Removal", *Paper Recycling Challenge, Vol. I- Stickies*, M. R. Doshi and J. M. Dyer, eds., Doshi & Assoc., Inc., Appleton, WI, pp. 237-239, 1997.

5. Scholz, W. F., "Recyclable Pressure Sensitive Adhesives", *1993 Tappi Pulping Conference Proceedings*, Atlanta, GA, TAPPI Press, pp. 501-505, 1993.

6. Scholz, W. F., "Pressure Sensitive Adhesives", *Progress in Paper Recycling*, 4(1):71-73, 1994.

7. Landa, M. R., "PSA Labels and Repulping Paper", Joint Conference to Address Pressure Sensitive Adhesive Issues Proceedings, United States Postal Service and American Forest & Paper Association, Washington, D.C., June 1996.

8. Pikulin, M. A., "Stickies and Their Impact on Recycled Fiber Content Fine Paper", Joint Conference to Address Pressure Sensitive Adhesive Issues Proceedings, United States Postal Service and American Forest & Paper Association, Washington, D.C., June 1996.

9. Crossley, B. R., Abubakr, S., Grimes, D. B., and Kumar, R., "A Pilot Plant Study of the Recyclability of Pressure Sensitive Adhesives (PSA)", 1998 Tappi Recycling Symposium Proceedings, New Orleans, LA, TAPPI Press, pp. 469-473, 1998.

10. Hsu, N. N.-C., "Stickies-The Importance of Their Chemical and Physical Properties", Paper Recycling Challenge, Vol. I- Stickies, M. R. Doshi and J. M. Dyer, eds., Doshi & Assoc., Inc., Appleton, WI, pp. 256-258, 1997.

11. McKinney, R. W. J., " Wastepaper Preparation and Contaminant Removal", Chapter 3 in Technology of Paper Recycling, McKinney, R. W. J., ed., Blackie Academic & Professional, London, 1995.

12. Lucas, B. E., Venditti, R. A., and Jameel, H., "Behavior of Pressure Sensitive Adhesive Material in Industrial Pressure Screens and Laboratory Screens", Tappi Journal, 84(5):70, 2001.

13. Lucas, B. E., Venditti, R. A., and Jameel, H., "The Breakage of Pressure Sensitive Adhesive Contaminants in Paper Recycling Operations", 2000 Tappi Pulping/Process & Product Quality Conference Proceedings, Boston, MA, TAPPI Press, November 2000.

14. Heise, O., Cao, B., and Schabel, S., "A Novel Application of Tappi 277 to Determine Macro Stickies Disintegration and Agglomeration in the Recycle Process", 2000 Tappi Recycling Symposium Proceedings, Washington, D.C., TAPPI Press, pp. 631-644, March 2000.

15. Bliss, T. and Ostoja-Starzewski, M., "Debris Characteristics and Removal Techniques", 1997 Tappi Korea Recycling Symposium Proceedings, TAPPI Press, Seoul, Korea, October 1997.

16. Gooding, R. W., Kerekes, R. J., and Salcudean, M., "The Flow Resistance of Slotted Apertures in Pulp Screens", in The Science of Papermaking, Volume 1, Transactions of the 12th Fundamental Research Symposium, Oxford, pp. 287-338, September 2001.

17. Kumar, A., Gooding, R. W., and Kerekes, R. J., “Factors Controlling the Passage of Fibers Through Slots”, *Tappi Journal*, 81(5):247-254, 1998.

18. Yu, C. J., and DeFoe, R. J., “Fundamental Study of Screening Hydraulics, Part 2: Fiber Orientation in the Feed Side of a Screen Basket”, *Tappi Journal*, 77(9):119-124, 1994.

19. Kelly, A. F., “Screening Secondary Fiber”, *1997 Improving Screening and Cleaning Efficiencies Short Course Proceedings*, Minneapolis MN, TAPPI Press, June 1997.

20. Yu, C. J., Crossley, B. R., and Silveri, L., “Fundamental Study of Screening Hydraulics, Part 3: Model for Calculating Effective Open Area”, *Tappi Journal*, 77(9):125-131, 1994.

21. Lucas, B. E., Venditti, R. A., and Jameel, H., “Breakage and Extrusion of Pressure Sensitive Adhesives in Industrial and Laboratory Screening Processes”, *2001 Tappi Pulping Conference Proceedings*, Seattle WA, Tappi Press, November 2001.

22. Julien Saint Amand, F., Perrin, B., and de Luca, P., “Stickies Removal Strategy”, *Progress in Paper Recycling*, 7(4):39-53, 1998.

23. McCool, M. A., and Silveri, L., “Removal of Specks and Non-dispersed Ink from a Deinking Furnish”, *Tappi Journal*, 70(11):75, 1987.

CHAPTER 7

FACTORS IN THE PASSAGE OF PRESSURE SENSITIVE ADHESIVE PARTICLES THROUGH A SLOT

ABSTRACT

The objective of this research was to understand the behavior of pressure sensitive adhesive (PSA) particles during passage through a slot in a pressure screen. An acrylate based PSA label material was applied to copy paper and pulped in a laboratory pulper. PSA particles from the pulp were analyzed for passage in a pressurized single slot device at different operating temperatures. Also, particles with a variety of sizes, as a result of pulping time, were considered. The pressurized single slot device had a slot width of 0.007 inches (0.18 mm), which is similar to typical slot widths used in industry of 0.006-0.012 inches (0.15-0.30 mm). Both automated image analysis and manual analysis of particles were used in this study and were found to correlate well with each other. Factors that affected the passage of PSA particles through the slot were temperature and particle width, thickness, and area. Increasing the operating temperature from 5^oC to 50^oC increased particle passage through the slot. These experiments showed that significant fractions of particles with widths greater than the slot width were able to pass through the slot. Also, particle length and area were found to decrease upon particle passage through the slot. However, none of the PSA particles broke down into smaller pieces during the experiments in the single slot device.

INTRODUCTION

One of the major problems in paper recycling is the presence of adhesive contaminants in recycled paper. It has been reported that adhesive contaminants can cost paper recycling about $700 million annually [1]. Industrial pressure screening of recycled material is considered to be the most effective way of removing adhesive contaminants from recycled pulp [2]. For the removal of small adhesive particles, pressure screens use narrow slot sizes ranging from 0.006 inches (0.15 mm) to 0.012 inches (0.30 mm) [2].

In industrial pressure screening experiments, pressure sensitive adhesive particles have been found to break down into smaller particles under high shear conditions such as pressure screening [3-7]. Further investigations have shown that pressure sensitive adhesive particles can extrude through the slots of pressure screens [6]. Also, it has been observed that adhesive particles change shape during passage through a pressure screen [4,8]. Particle extrusion has been mentioned as a possible method of particle passage through the slots of a pressure screen, but particle alignment with the slot and particle bending are considered to be more likely to occur [9].

The purpose of this research is to understand how the adhesive particles extrude through the slots of a pressure screen. A preliminary investigation into particle passage through a slot in a pressurized system found that pressure sensitive adhesive particles, with particle widths up to four times the slot width, were able to extrude through the slot [10]. Also in the preliminary investigation, particle passage was found to increase with temperature and decrease with particle width [10]. In this study, the effects of temperature were further examined, as well as the effect of all three dimensions of the adhesive particles on particle passage. It is acknowledged that there are significant differences between this model screening system and an industrial pressure screen. However, the simplicity of this technique allows for some useful information to be extracted that could not be determined in a more complicated screening system.

EXPERIMENTAL

Single Slot Device

The single slot device consists of a metal plate with a slot cut in the middle, a plastic Buchner funnel, an Erlenmeyer flask attached to the house vacuum, and a vacuum gauge in the line to the house vacuum. Part of the Buchner funnel was cut out of the middle of the funnel that was larger than the slot. The metal plate is attached to the Buchner funnel by silicone and all of the holes in the Buchner funnel are filled with silicone. The slot width for the single slot device is 0.007 inches (0.18 mm). The vacuum gauge has increments of 0.5 inches of Hg and the maximum vacuum pressure of the system is about 21.5 inches of Hg.

Single Slot Temperature Experiments

Pulp containing pressure sensitive adhesive particles was prepared in a 450H laboratory pulper. The pulping material contained 450 OD g of copy paper with ten Avery Dennison 5164 labels applied to sheets of alkaline copy paper. The adhesive material on the labels was an acrylate-based, pressure sensitive adhesive. The 450H pulper was operated at 12% consistency, 45^{o}C, and 415 rpm, for 60 minutes.

Once the pulping was completed, 200 g pulp samples were immediately transferred from the 450H pulper to 1000 mL beakers. The pulp samples were diluted to 1000 mL with deionized water at 5, 20, or 50°C. The beakers were then placed in a temperature control system at the same temperature as the deionized water.

Individual adhesive particles were randomly removed from the diluted pulp samples using forceps. The length, width, and thickness were measured for each particle under a microscope. The particle length was the largest dimension, the particle width was the second largest dimension, and the particle thickness was the smallest dimension. The highest and lowest values were recorded for the width and thickness of each particle. The average width was calculated as the average of the highest and the lowest values recorded for the width. The average thickness was calculated as the average of the highest and the lowest values recorded for the thickness.

After the dimensions were measured, the particle was allowed to soak in 80 mL of deionized water at 5, 20, or 50°C, for five minutes. The particle was then placed on the slot of the single slot device. The device was filled with deionized water at the temperature of the experiment. The valve of the vacuum line was opened. If the particle passed through the slot, the vacuum pressure was recorded. The adhesive particle was recovered from the single slot device and the dimensions were measured again. At least eighty pressure sensitive adhesive particles were analyzed in the single slot device for each of the three temperatures considered.

Pulping Time Experiments

In order to analyze how pulping time affects adhesive particle size and particle passage through a slot, pulp was prepared using the 450H laboratory pulper. The pulping material contained 450 OD g of copy paper with ten Avery Dennison 5164 labels applied to sheets of alkaline copy paper. The 450H pulper was operated at 12% consistency, 45^{o}C, and 415 rpm, for 60 minutes. Pulp samples were collected from the 450H pulper at 0, 5, 10, 20, 40, and 60 minutes for making handsheets and adhesive particle analysis in the single slot device.

For each of the pulping times, sets of handsheets were made for dyeing and image analysis. Handsheets were dyed using a Morplas Blue-Heptane solution and rinsed using Heptane. Each set of handsheets was scanned on both sides before and after dyeing. The parts per million (PPM) of stickies, number of particles in 1 m^2, and average particle size were determined for each set of handsheets by the difference between the before and after dyeing values. An example of image analysis output is shown in **APPENDIX 3**.

For the single slot experiments using particles from different pulping times, 100 g pulp samples were diluted to 1000 mL with deionized water at 50^{o}C. The beakers were placed in a hot water bath at 50^{o}C. Individual adhesive particles were randomly removed from the diluted pulp samples using forceps. The length, width, and thickness were measured for each particle under a microscope. The particle was then allowed to soak in 80 mL of deionized water at 50^{o}C for five minutes. The particle was then placed on the slot of the single slot device. The device was filled with deionized water at 50^{o}C. The valve of the vacuum line was opened. If the particle passed through the slot, the vacuum pressure was recorded. The adhesive particle was recovered from the single slot device and the dimensions were measured again. Twenty adhesive particles were analyzed in the single slot device for each of the six pulping times.

RESULTS AND DISCUSSION

Automated Image Analysis Versus Manual Analysis of Adhesive Particles

The effects of pulping time on the number and average size of adhesive particles from the automated image analysis results are shown in **Figure 7-1**. As the pulping time increased, the number of particles increased and the average particle size decreased, as expected. The minimum particle size for the data that was considered was 0.04 mm^2, the TAPPI standard for dirt. Values are not shown for the 0 minute pulping time data because the handsheets contained a considerable number of large pieces of unpulped paper, which interfered with image analysis.

Particle distributions from the image analysis data for the pulping time experiments are shown in **Figure 7-2** and **Figure 7-3**. The minimum particle size for **Figure 7-2** is 0.04 mm^2, which is the TAPPI standard for dirt. The minimum particle size for **Figure 7-3** is 0.15 mm^2, which was the smallest particle size, as measured manually, for particles randomly removed from the pulp samples for the single slot experiments (see later). The two particle distributions are similar, even though they have different minimum particle sizes. The data shows that as the pulping time increased, the percentage of large particles (>3.00 mm^2) decreased and the percentage of small particles (<0.50 mm^2) increased.

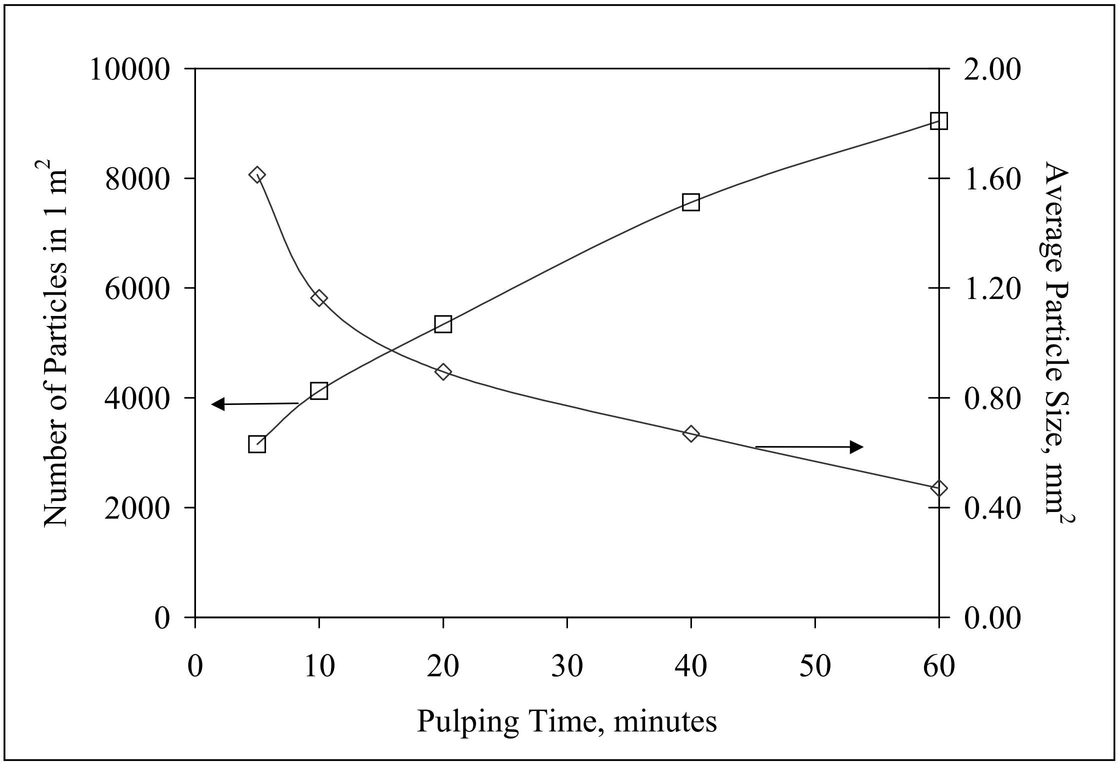

Figure 7-1. Number of Particles in 1 m^2 and Average Particle Size for Particles >0.04 mm^2 Versus Pulping Time

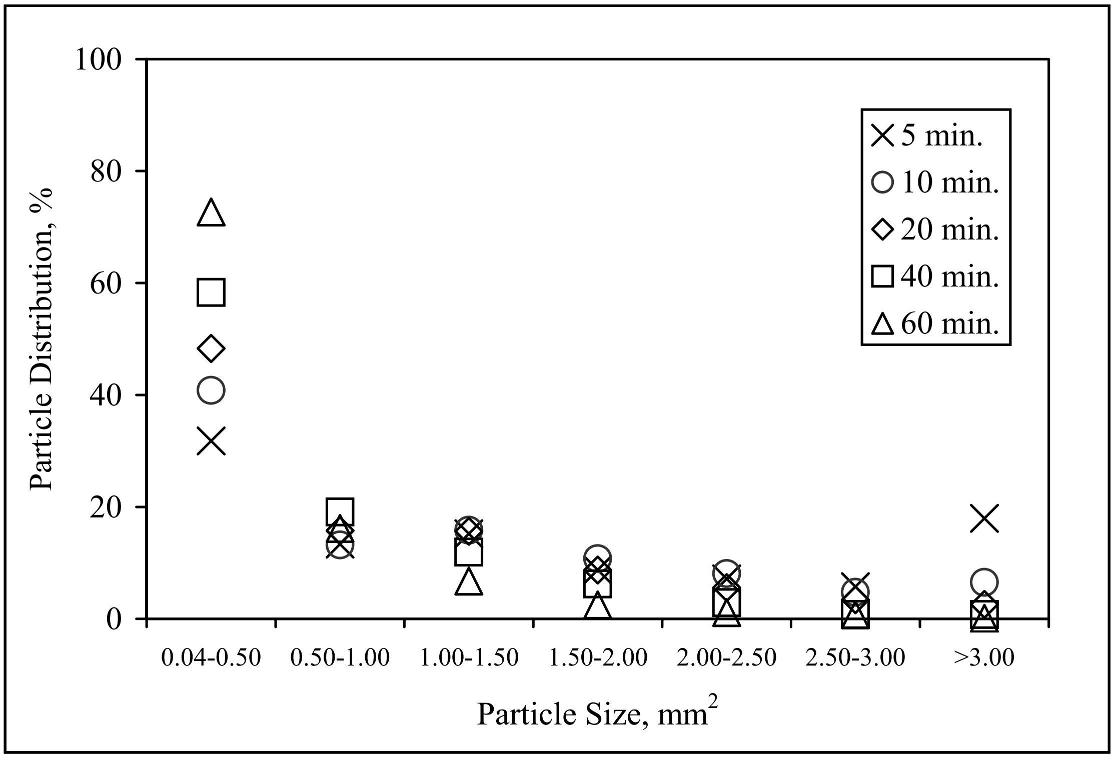

Figure 7-2. Particle Distribution Versus Particle Size (>0.04 mm^2) from Image Analysis Data

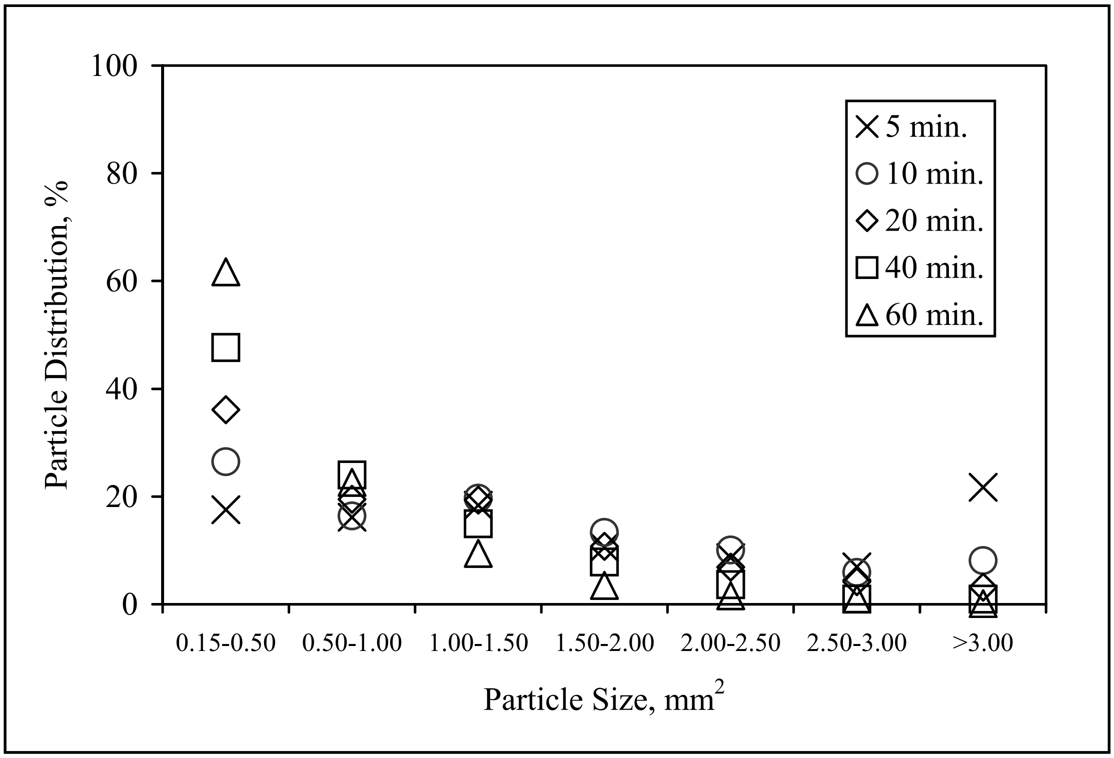

Figure 7-3. Particle Distribution Versus Particle Size (>0.15 mm^2) from Image Analysis Data

Based on the manual particle analysis, particle distributions for different pulping times are shown in **Figure 7-4**. The smallest particle measured manually had an area of 0.15 mm^2, so 0.15 mm^2 is the smallest particle area on the scale. The particle area for the manual measurements was calculated as the particle length times the average particle width. (It is assumed that a particle would normally fall onto a surface, such as a handsheet, with its two largest dimensions parallel to the surface.) As the pulping time increased, the percentage of large particles decreased and the percentage of small particles increased, in agreement with automated image analysis. For pulping times greater than 10 minutes, there were not any particles larger than 2.50 mm^2. For the 40 and 60 minute pulping times, about 50% of the particles were smaller than 0.50 mm^2.

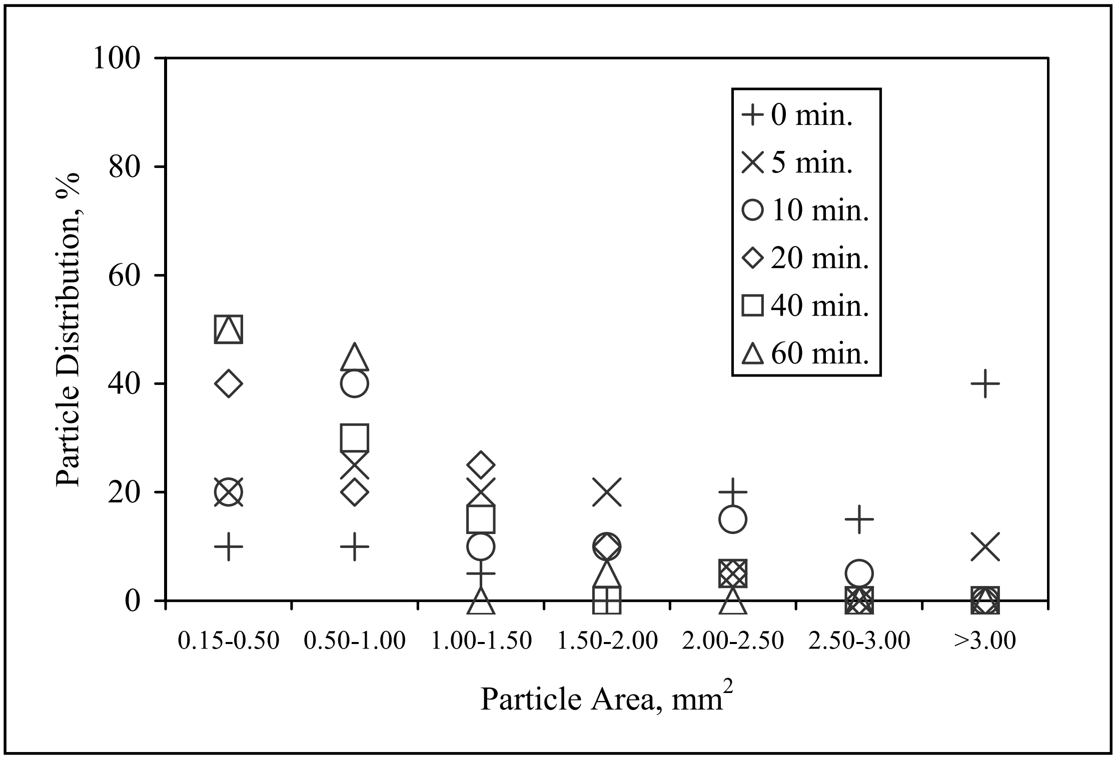

Figure 7-4. Particle Distribution Versus Particle Area from Manual Particle Analysis Data

Figure 7-5 is a plot of the average for each of the manually measured dimensions of length, width, and thickness versus pulping time. The particle length was the largest dimension of the particle, the width was the second largest dimension of the particle, and the thickness was the smallest dimension of the particle. The particle length decreased considerably between 0 and 60 minutes of pulping time. Between 5 and 60 minutes of pulping time, the average width and thickness remained about the same.

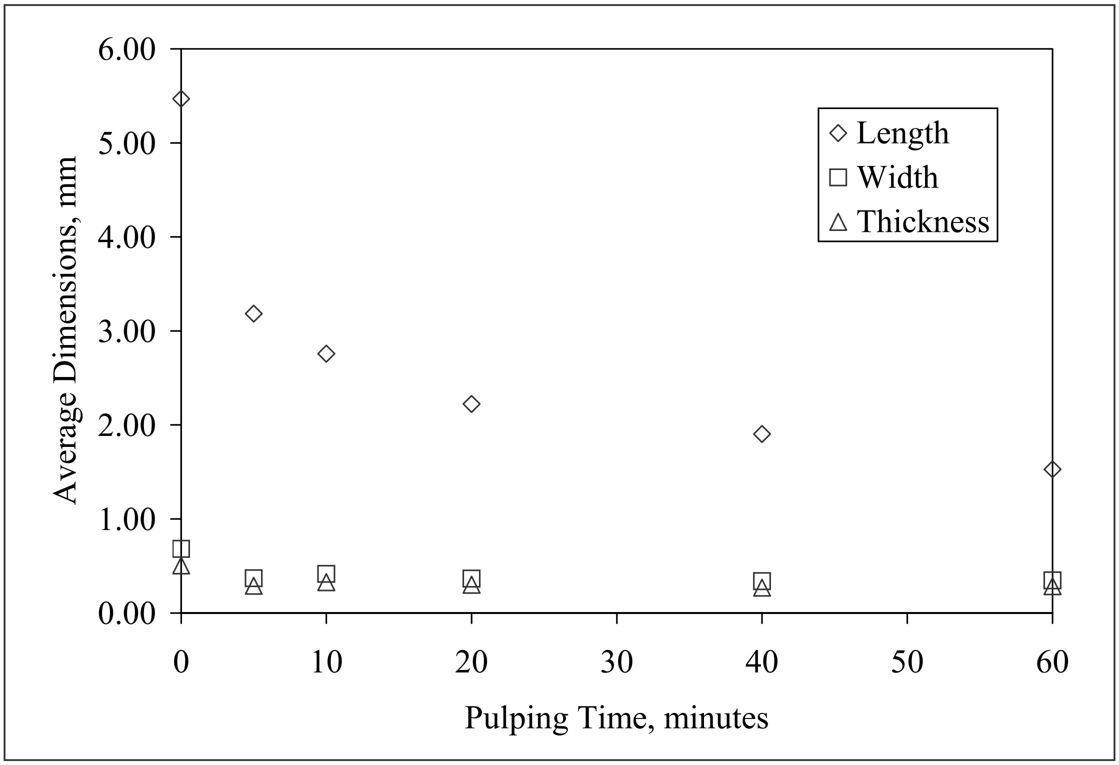

Figure 7-5. Average Particle Dimensions Versus Pulping Time from Manual Particle Analysis

Particle Passage

During all of the single slot experiments in which particles passed through the slot, stages were observed for particle passage. First, the adhesive particle would align its length with the length of the slot. Then, the region of the adhesive particle with the smallest width would enter the slot. Next, the widest part of the adhesive particle would enter the slot. Lastly, the entire particle would pass through the slot.

Figure 7-6 through **Figure 7-9** are plots of particle passage versus particle dimensions and area at operating temperatures of 5, 20, and 50^{o}C. From theses figures there is a trend of particle passage decreasing as average particle width, thickness, and area increase. There does not appear to be a relationship between particle passage and particle length. Increased temperature is observed to promote particle passage when plotting particle passage versus particle width, thickness, and area. Also, notice that a significant percentage of particles with average widths of more than twice the slot width were able to pass through the slot.

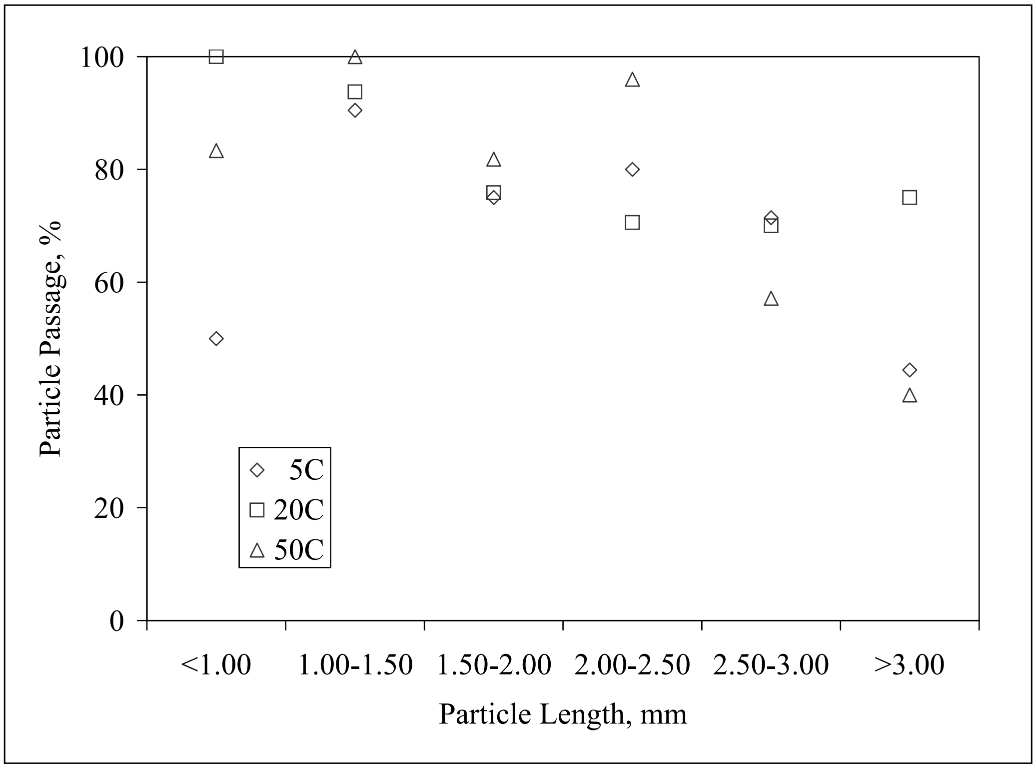

Figure 7-6. Particle Passage Versus Particle Length at Different Operating Temperatures

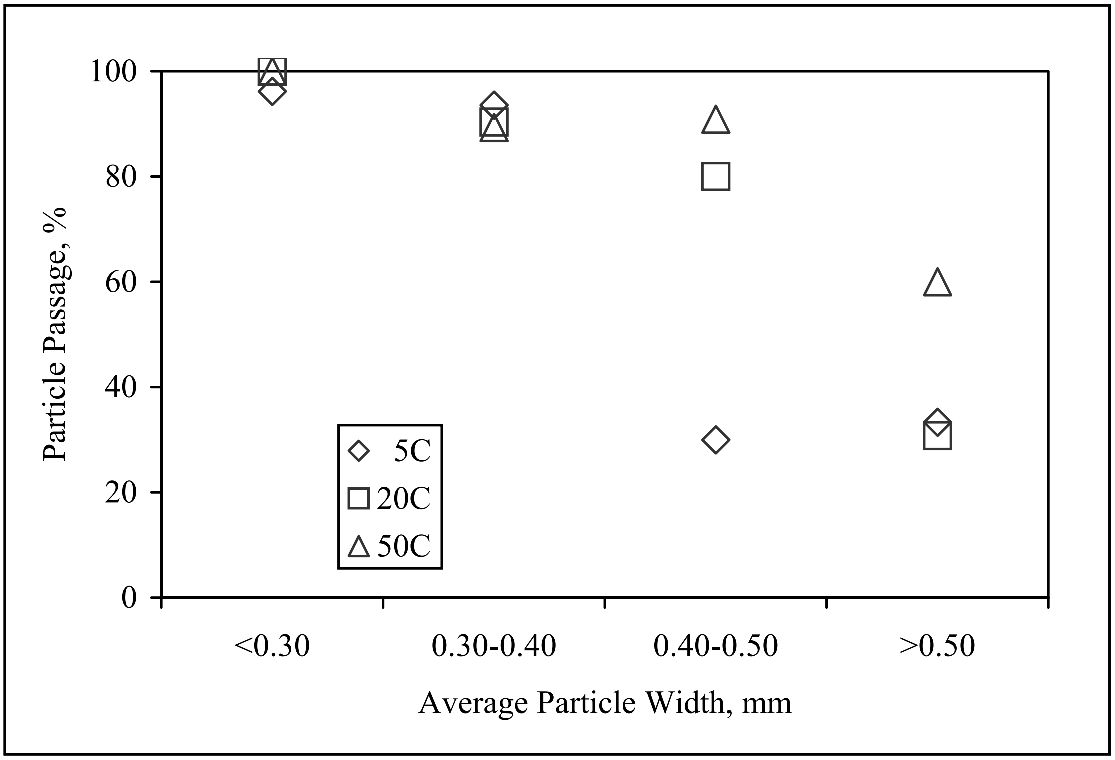

Figure 7-7. Particle Passage Versus Average Particle Width at Different Operating Temperatures

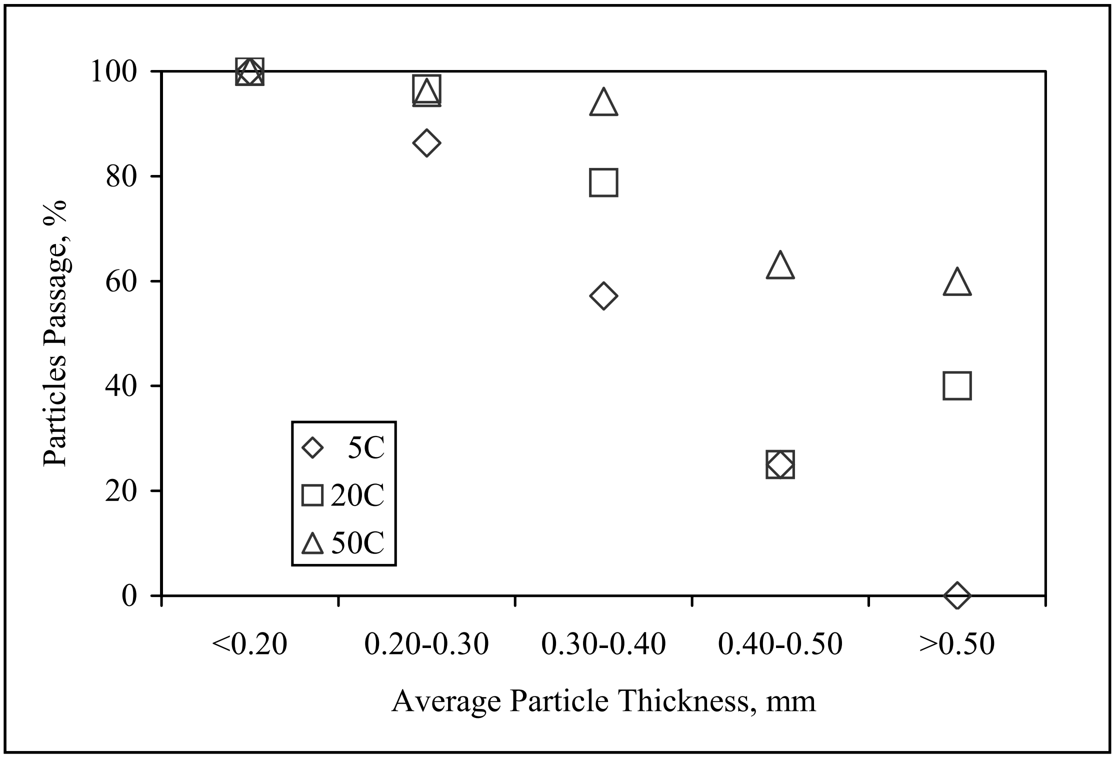

Figure 7-8. Particle Passage Versus Average Particle Thickness at Different Operating Temperatures

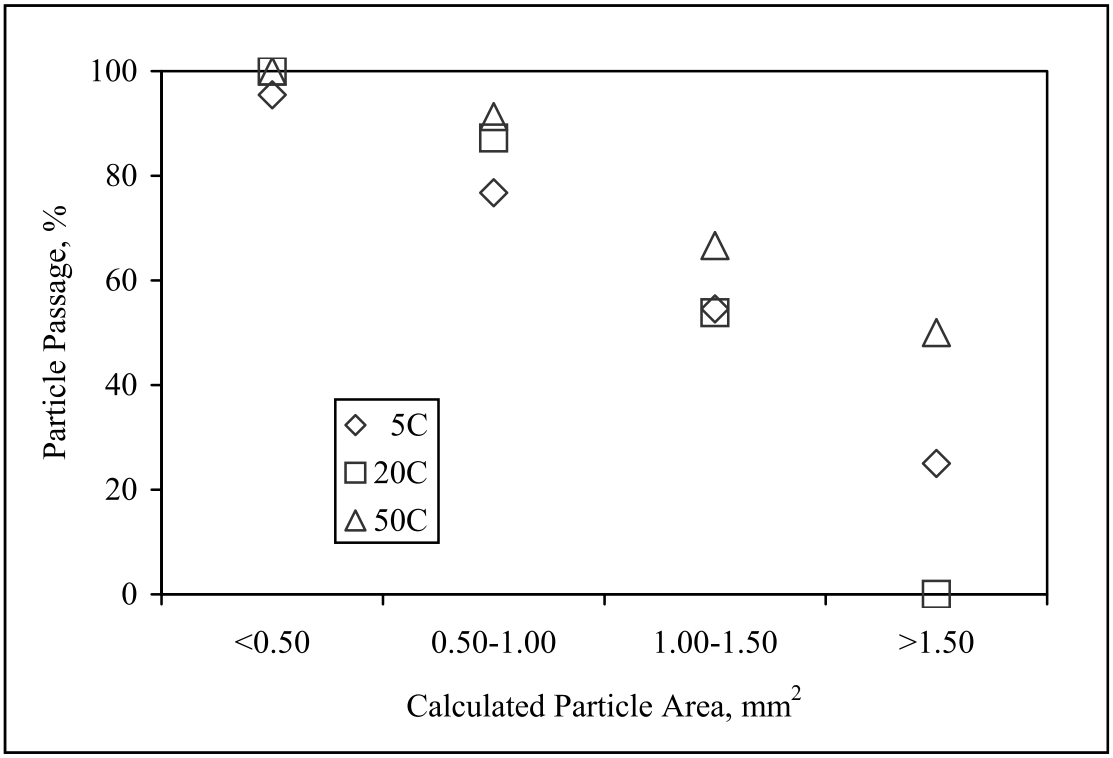

Figure 7-9. Particle Passage Versus Calculated Particle Area at Different Operating Temperatures

For the different pulping times, a plot of cumulative particle passage versus particle area is shown in **Figure 7-10**. As the particle area increased, particle passage decreased, and all of the pulping times generally followed a single curve of particle passage versus particle area. For the 0 minute particles, the particle area was larger than for the other pulping times, resulting in a lower overall particle passage.

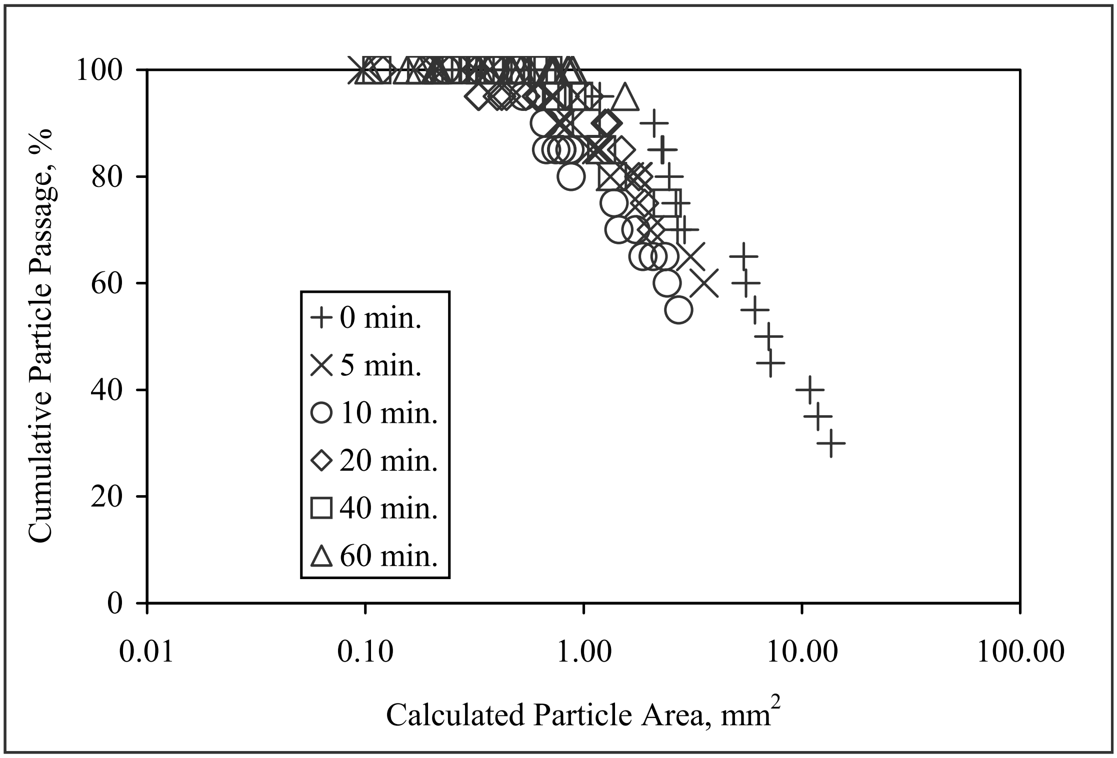

Figure 7-10. Cumulative Particle Passage Versus Particle Area for Different Pulping Times

Figure 7-11 shows the cumulative particle passage versus pressure difference across the slot for different operating temperatures. The data shows that increasing both the pressure difference and operating temperature increases the percentage of particles that pass through the slot, as previously reported [10].

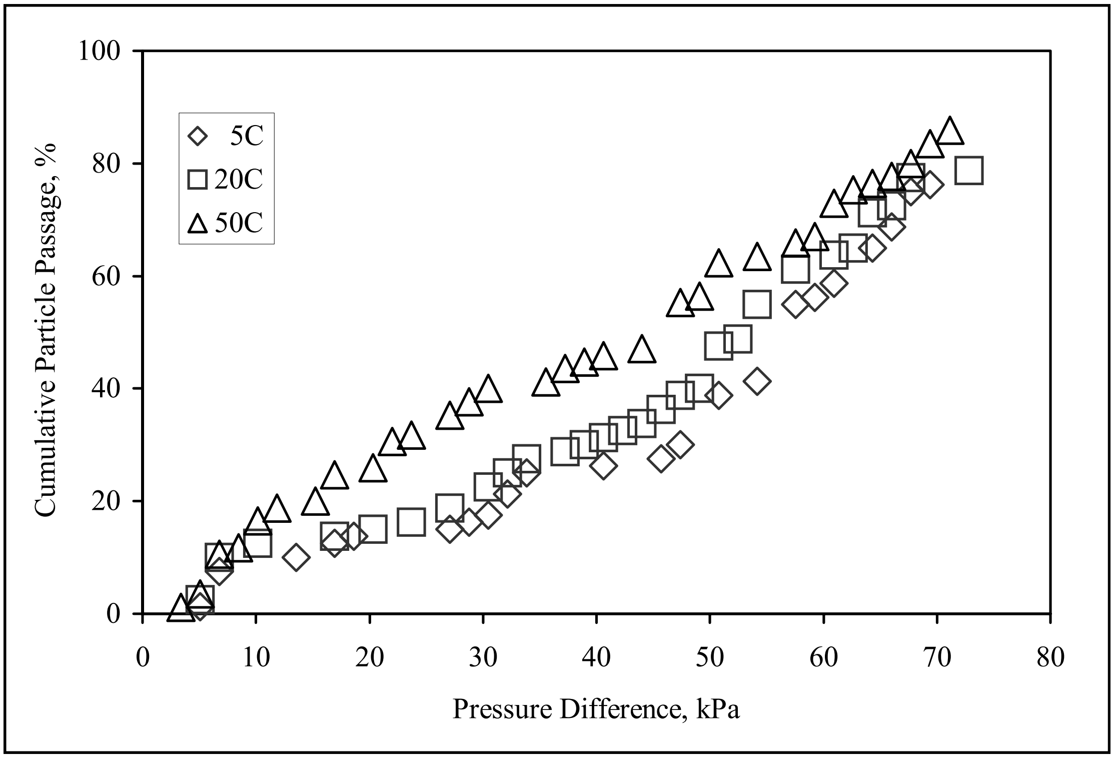

Figure 7-11. Cumulative Particle Passage Versus Pressure Difference for Different Operating Temperatures

Changes in Particle Dimensions Upon Passage

Comparisons of the particle dimensions before and after the particles passed through the slot at 50°C are shown in **Figure 7-12** through **Figure 7-15**. These figures indicate that the particle length, width, and area generally decreased upon passage, whereas the thickness generally remained the same.

By observation, no particle broke into two separate pieces due to the forces acting on it during the single slot experiments. This suggests that breakage in an industrial pressure screen is not due to the pressure difference across the slot, but is due to shear occurring in the region between the foil and screen plate.

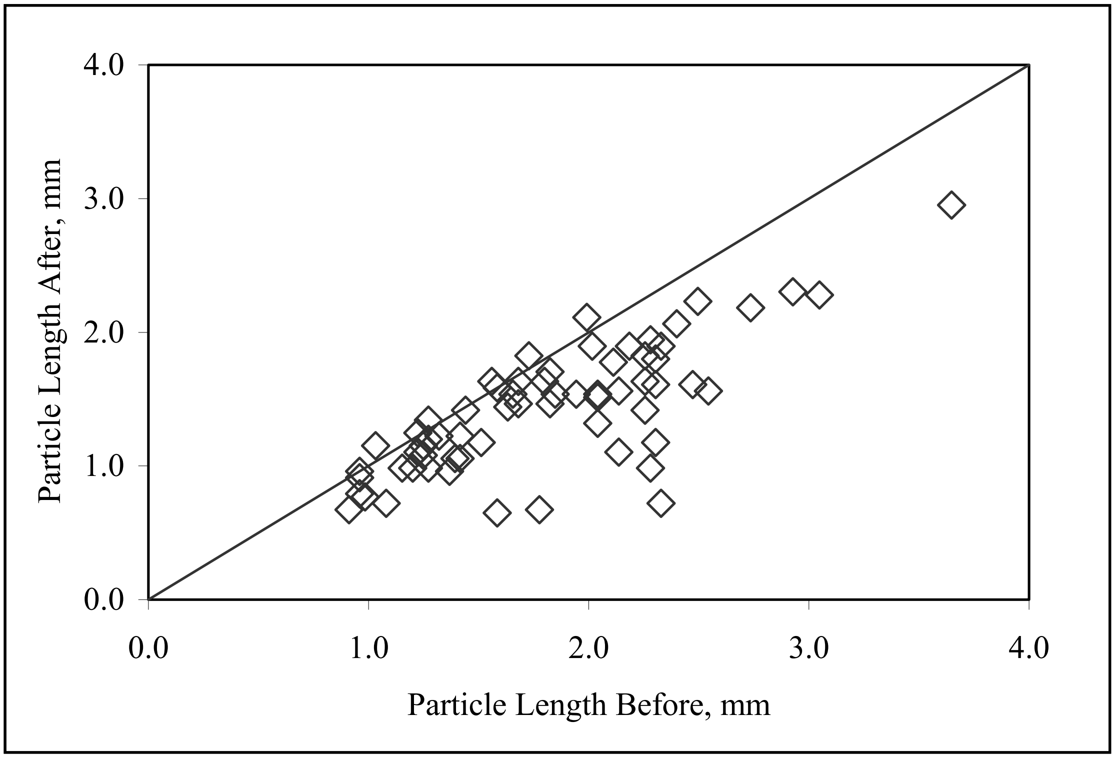

Figure 7-12. Particle Length Before and After Particle Passage Through the Slot (50°C)

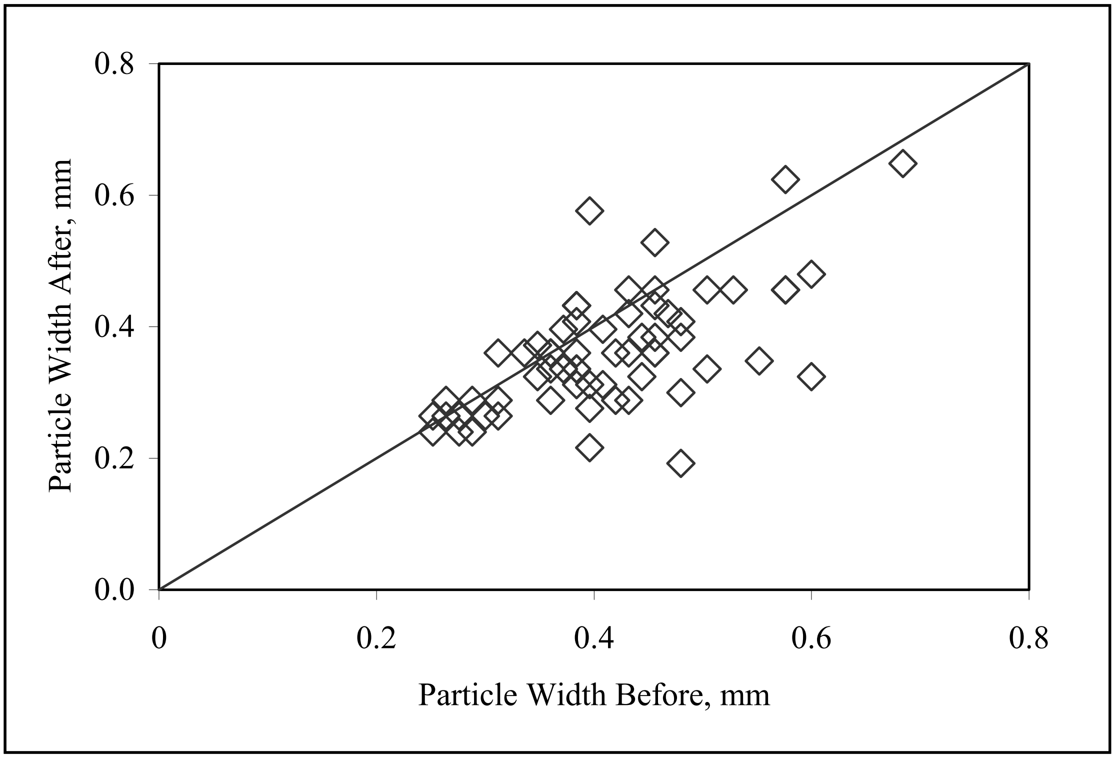

Figure 7-13. Particle Width Before and After Particle Passage Through the Slot (50°C)

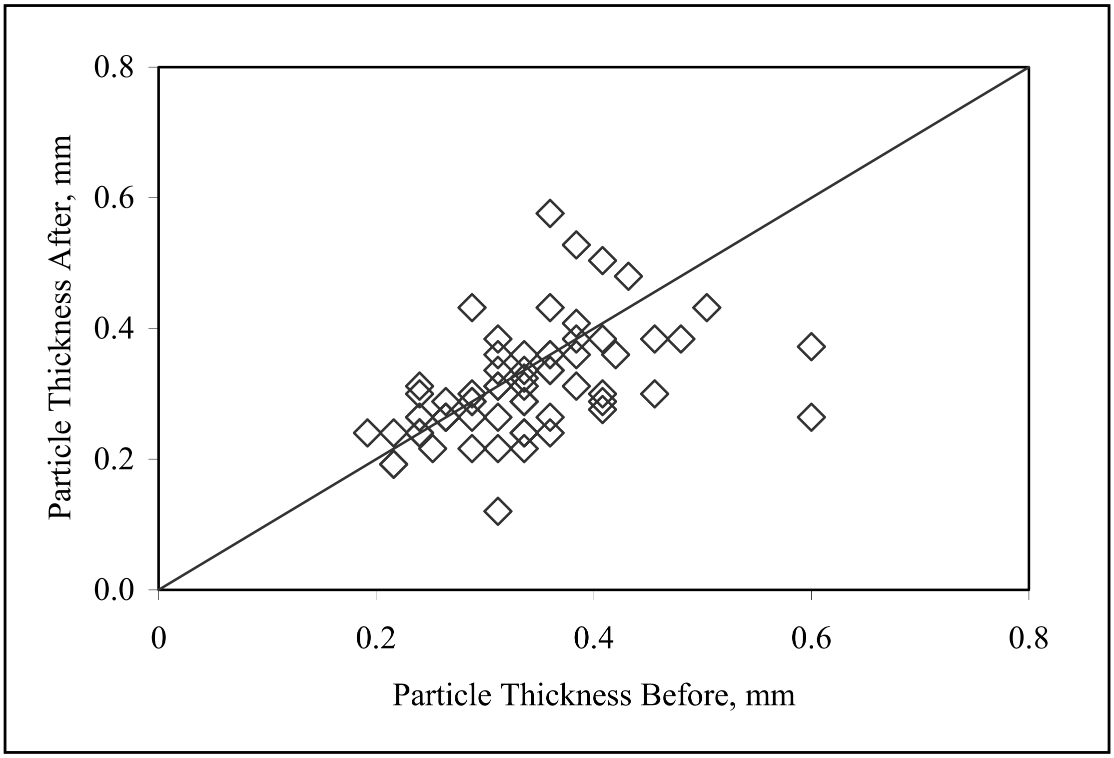

Figure 7-14. Particle Thickness Before and After Particle Passage Through the Slot (50^{o}C)

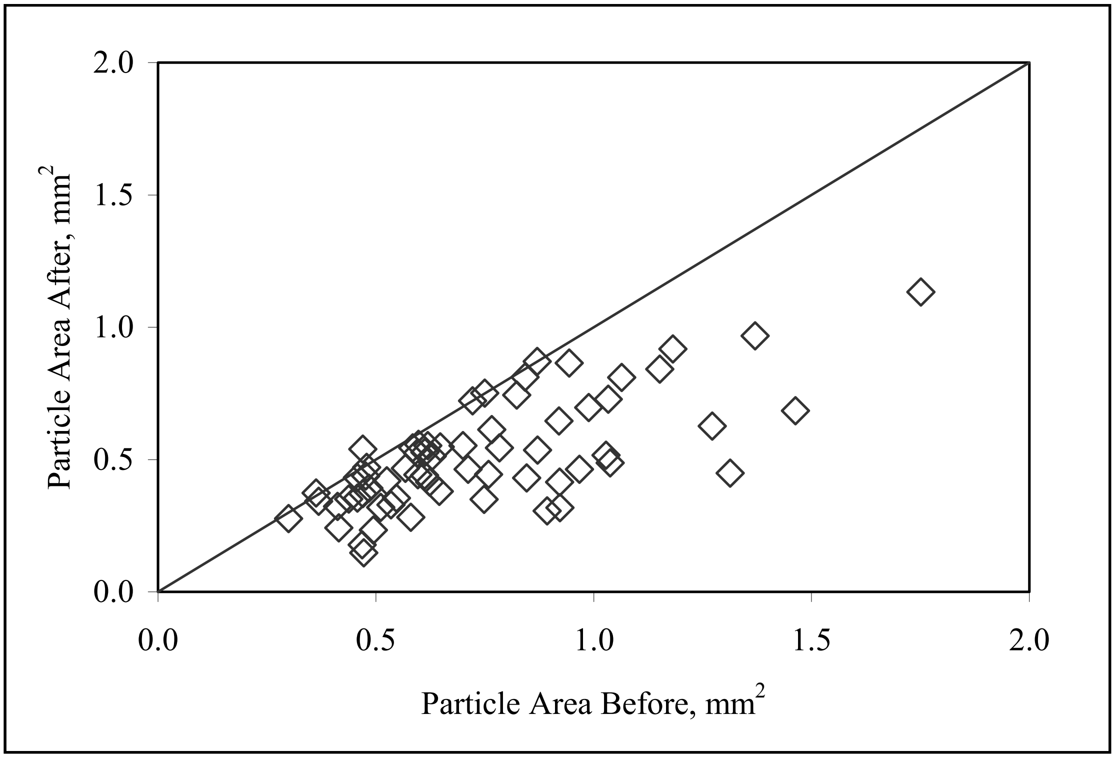

Figure 7-15. Particle Area Before and After Particle Passage Through the Slot (50^{o}C)

The statistical values for the dimensions of the particles before passage through the slot and the changes in the dimensions as a result of passing through the slot are shown in **Table 7-1**. The particle length and area decreased for all three temperatures considered and the change was greater at higher temperatures. The particle width and thickness generally did not show a strong change due to the magnitude of scatter in the data (i.e., the standard deviation of change was greater than the magnitude of the change).

Table 7-1. Statistical Values for Particle Dimensions Before and After Particle Passage Through the Slot

Temperature, °C		Length, mm	Width, mm	Thickness, mm	Area, mm^2
5	Average Before Passage	2.02	0.34	0.27	0.71
	Average Change	-0.30	+0.00	+0.02	-0.10
	St. Dev. of Change	0.23	0.08	0.06	0.20
20	Average Before Passage	1.87	0.38	0.31	0.69
	Average Change	-0.31	-0.02	+0.02	-0.14
	St. Dev. of Change	0.23	0.06	0.07	0.15
50	Average Before Passage	1.81	0.41	0.34	0.74
	Average Change	-0.38	-0.05	-0.02	-0.23
	St. Dev. of Change	0.37	0.08	0.09	0.21

How all three dimensions could decrease or stay the same after passage may be explained by the following two possible explanations. First, the apparent density of the adhesive particle could increase (i.e., the folded adhesive structure could be more compact after passage). Second, there may have been increases in the smallest dimension (thickness) that were outside of the measuring ability of our procedure.

A majority of the adhesive particles analyzed in these experiments had a "string-like" shape before and after passage through the slot. **Table 7-1** confirms this in that the average length is more than four times the average width and thickness for the adhesive particles.

CONCLUSIONS

Automated image analysis correlated well with manual analysis of the adhesive particles. Increases in pulping time increased the number of particles and decreased the average particle size. The length of the particles changed significantly versus pulping time, whereas the width and thickness remained relatively constant. Particle passage through a single slot was shown to be facilitated by increases in pressure difference across the slot, increases in operating temperature, and decreases in particle width, thickness, and area. Particle length did not correlate with particle passage. For the same particle size, pulping time did not correlate with particle passage. The passage of particles through the slot was accompanied by significant decreases in the length and area of the particles. Particles did not break down due to the forces acting on them in the single slot device.

ACKNOWLEDGEMENTS

Support for this research has been provided by Ecosynthetix. Donations of equipment by Apogee Systems are also greatly appreciated.

REFERENCES

1. Friberg, T., "Cost Impact of Stickies", *Progress in Paper Recycling*, 6(1):70-72, 1996.

2. Heise, O., "Screening Foreign Material and Stickies", *Tappi Journal*, 75(2):78-81, 1992.

3. Heise, O., Schabel, S., Cao, B., and Lorenz, K., "Deformation and Disintegration Physics of Stickies in Pressure Screens: A compromise between pulp quality and capital investment", *5th Research Forum on Recycling Proceedings*, Ottawa, ON, Canada, pp. 187-195, September 1999.

4. Heise, O., Cao, B., and Schabel, S., "A Novel Application of TAPPI T 277 to Determine Macro Stickies Disintegration and Agglomeration in the Recycle Process", *2000 Tappi Recycling Symposium Proceedings*, Washington, D.C., TAPPI Press, pp. 631-644, March 2000.

5. Lucas, B. E., Venditti, R. A., and Jameel, H., "The Breakage of Pressure Sensitive Adhesive Contaminants in Paper Recycling Operations", *2000 Tappi Pulping Conference Proceedings*, Boston, MA, TAPPI Press, November 2000.

6. Lucas, B. E., Venditti, R. A., and Jameel, H., "Breakage and Extrusion of Pressure Sensitive Adhesives in Industrial and Laboratory Screening Processes", *2001 Tappi Pulping Conference Proceedings*, Seattle, WA, TAPPI Press, November 2001.

7. Lucas, B. E., Venditti, R. A., and Jameel, H., "Behavior of Pressure Sensitive Adhesive Material in Industrial Pressure Screens and Laboratory Screens", *Tappi Journal*, 84(5):70, 2001.

8. Huo, X., Venditti, R. A., and Chang, H.-m., "Use of Deposition and Extraction Techniques to Track Adhesive Contaminants (Stickies) in a Papermill", *Progress in Paper Recycling*, 10(2):15-23, 2001.

9. Bliss, T., and Ostoja-Starzewski, M., "Debris Characteristics and Removal Techniques", *1997 Tappi Korea Recycling Symposium Proceedings*, TAPPI Press, Seoul, Korea, October 1997.

10. Flanagan, J., Venditti, R., Jameel, H., Wilson, N., Weaver, N., and Lucas, B., "Passage of Pressure Sensitive Adhesive Particles Through a Fine Slot", *Progress in Paper Recycling*, 11(3):17-23, 2002.

CHAPTER 8

THE EFFECTS OF ADHESIVE PROPERTIES ON ADHESIVE PARTICLE BREAKAGE AND PASSAGE DURING PAPER RECYCLING OPERATIONS

ABSTRACT

One of the major concerns in paper recycling is the presence of pressure sensitive adhesives in the recycled material. One useful process in the paper industry to remove the pressure sensitive adhesive from the recycled material is pressurized screening. The objective of this research was to understand how adhesive formulation affects the mechanical properties of pressure sensitive adhesives, and thus their behavior in the pulper and pressure screen. Eight different pressure sensitive adhesive materials were analyzed in this study. The glass transition temperature, contact angle, yield strain, yield stress, and modulus were measured for each of the eight different adhesive materials. Each pressure sensitive adhesive material was applied to copy paper and pulped in a laboratory pulper separately. Adhesive particles for each of the materials were analyzed in a pressurized single slot device with a 0.007 inches wide slot, which is within the range of typical slot widths for industrial pressure screens. Yield strain, yield stress, and modulus were significant in determining the average particle size produced by pulping. The particle size after pulping increased as the yield strain and modulus increased, and decreased as the yield stress increased. Yield stress and average particle area were significant in determining particle passage through the slot of the pressurized single slot device. Particle passage decreased as the yield stress and average particle area increased, and increased as the interaction between yield stress and average particle area increased.

It was concluded that the mechanical properties of adhesive materials, which depend on the adhesive formulation, are important in predicting particle breakage and passage in industrial recycling operations.

INTRODUCTION

There are several contaminants in recycled paper, but a major contaminant is adhesive material, or more specifically, pressure sensitive adhesive (PSA) material [1]. Adhesive contaminants have been reported to cost the paper industry about $700 million annually [2]. The best device for adhesive contaminant removal from recycled pulp is considered to be the pressurized screen [3]. Typically for adhesive contaminant removal, the screens contain narrow slots with slot widths of 0.006 inches to 0.012 inches (0.15 mm to 0.30 mm) [3].

One of the major generators of pressure sensitive adhesive material in paper recycling is the United States Postal Service (USPS) [4]. In 1994, the USPS started a program to develop “environmentally benign adhesives” [4]. In connection with the USPS, the Forest Product Laboratory (FPL) participated in developing “environmentally benign pressure sensitive adhesives” [4,5]. Adhesives from eight different adhesive companies were analyzed for their performance in a recycling process involving a hydropulper, primary pressure screen, secondary pressure screen, forward cleaner, through-flow cleaner, flotation, washing, and pressing [5]. The pressure screens provided removal efficiencies ranging from –44.7 to 99.5%. A negative removal efficiency suggests breakage of adhesive particles because a larger area of adhesive material was detected after the operation than before the operation. The wide range of removal efficiencies found in that study indicates that the PSA formulation has a significant impact on the screenability.

A pilot plant investigation was conducted at this facility to compare the behavior of pressure sensitive adhesives in industrial versus laboratory screens [6,7]. The laboratory screens removed almost all of the adhesive material, while the industrial pressure screen removed only 40 to 70%, depending on the reject flow rate. An important finding in this work was that the PSA particles broke down into smaller particles in the industrial pressure screen, which caused the removal efficiencies to be lower than expected. Other industrial pressure screening experiments have also found that PSA particles break down under the conditions of pressure screening [8,9].

Since the break down of PSA particles had an effect on the removal efficiency, a study was performed involving the effect of operating conditions on the particle size in a high shear laboratory device [10]. The operating conditions of consistency, residence time, rotor speed, and initial temperature were considered. Consistency, residence time, and initial temperature were significant and particle size decreased as consistency, residence time, or initial temperature increased.

Previous research has been done at this facility involving the passage of pressure sensitive adhesive particles through a pressurized single slot device [11,12]. In these studies, particle passage was compared to the operating parameters and the particle dimensions. Particle passage increased as the operating temperature or pressure drop increased and as the particle width, thickness, or area decreased.

Also, the behavior of various commercial pressure sensitive adhesive materials has been investigated in a laboratory pulper and a laboratory screen [6]. The different materials provided different particle sizes out of the pulper and different removal efficiencies out of the laboratory screen. Not surprisingly, there was a trend of the removal efficiency increasing as the average particle size increased for the different materials.

Some research has been done comparing the removal efficiency to the properties of pressure sensitive adhesive materials [13]. The removal efficiency increased with loop tack, stretch index, and contact angle. However, the addition of one of the tackifiers produced an increase in the tack and a decrease in the removal efficiency, which contradicts the removal efficiency increasing with loop tack. Also in that study, the removal efficiency was compared to peel strength, shear strength, and tensile strength, but there did not appear to be a clear correlation between removal efficiency and these properties. One drawback to that research was that a non-pressurized laboratory screen was utilized [13]. Therefore, the screenability of the particles reported there was strongly related to the size of the particles, but was not sensitive to the physical properties of the material. It is expected that in an industrial pressure screen PSA particle screenability is both a function of particle size and physical properties.

In an industrial recycling project, various adhesive materials were tracked through recycling equipment and the number of particles out of each operation was reported [1]. The adhesives analyzed consisted of an acrylate, a styrene acrylate, two styrene butadiene rubbers, and a styrene isoprene copolymer. The process equipment that was evaluated consisted of a pulper, primary screens, secondary screens, and flotation. The acrylate adhesive had the most particles out of the pulper and after the screens, while the styrene isoprene copolymer had the fewest particles out of the pulper and after the screens. The screens removed about 55% of the acrylate adhesive and 100% of the styrene isoprene copolymer adhesive. This again illustrates that the PSA formulation significantly affects the behavior of PSA particles in screening operations.

The purpose of this research is to understand how adhesive formulation and physical properties of PSA materials affect their behavior in two critical recycling operations, pulping and screening. It is hypothesized that adhesive materials with different adhesive formulations will have different mechanical properties and will behave differently in pulpers and screens. In this study, pressure sensitive adhesives of known adhesive formulations will be prepared and processed in a laboratory pulper and a pressurized single slot device. The physical properties of the adhesive materials will be measured and compared to the performance of the adhesive materials in the laboratory pulper and the pressurized single slot device.

EXPERIMENTAL

Adhesive Formulation

Pressure sensitive adhesive (PSA) solutions were prepared containing two different base polymers and two different tackifiers. The two base polymers from Union Carbide were UCAR9165 (see **APPENDIX 5**) and UCAR9175 (see **APPENDIX 6**). The two tackifiers from Akzo Nobel were Snowtack 775A (Tack A) and Snowtack 780G (Tack G). UCAR9165 contains 92% butyl acrylate (BA) and UCAR9175 contains 50% butyl acrylate and 50% 2-ethylhexyl acrylate (BA-EA). Six different adhesive formulations were considered and are shown in **Table 8-1**. The concentrations of the base polymers and tackifiers in **Table 8-1** are based on the solids content of the adhesive solution. The values for base polymer and tackifier concentration were selected from typical acrylic PSA formulations [14].

Table 8-1. Concentrations of Base Polymers and Tackifiers in Adhesive Solutions

Sample	BA, %	BA-EA, %	Tack A, %	Tack G, %
BA	100	0	0	0
BA:A	60	0	40	0
BA:G	60	0	0	40
BA-EA	0	100	0	0
BA-EA:A	0	60	40	0
BA-EA:G	0	60	0	40

The adhesive solutions were prepared in 200 g batches with solids concentrations of 50%. The solutions were stirred for 15 minutes in 400 mL beakers before being poured into 500 mL labeled plastic bottles until film preparation.

Also considered in these experiments were two industrial pressure sensitive adhesives, an acrylic (AC) adhesive film and a styrene-isoprene-styrene (SIS) block copolymer adhesive film, both provided by Avery Dennison. The exact formulation for these two adhesive films is unknown. Both of these adhesives were provided as films in rolls with the adhesive film between two release liners and wound around a core.

Adhesive Film Preparation

Adhesive films were prepared for each of the six different adhesive solutions by applying the adhesive solution to paper using a coating draw down apparatus. The rod used in the apparatus was a 0.5 inches diameter, #28 wire rod. A sheet of litho paper was secured on the draw down apparatus and a thin strip of adhesive solution was slowly poured in front of the rod. The bar was then drawn over the sheet of litho paper, distributing the adhesive solution into a thin film over the sheet. The adhesive film coated sheet of paper was removed from the coating draw down apparatus and placed in an oven at 60°C to dry for 30 minutes. A sheet of release liner was applied to the adhesive film to protect it until use. Three sheets of adhesive film were prepared for each of the six adhesive solutions. The adhesive films were allowed to condition before being cut into 10 cm by 10 cm labels.

Physical Property Analysis

Some of the mechanical properties, such as the modulus, were determined for each of the adhesive formulations using the Reometrics Solids Analyzer II (RSAII). A sample containing about 0.030 g of an adhesive solution was applied to the end of a stainless steel rod with a diameter of 7.9 mm. The sample was dried in an oven at 60°C. The rod containing the dried sample was inserted into the top fixture of the RSAII with another rod in the bottom fixture (see **APPENDIX 7**). The two rods were forced together. The distance between the rods with the sample in the middle was measured to be 0.45 mm with a feeler gauge. The system was set up in cylindrical tension/compression mode. A dynamic strain sweep in log sweep mode was conducted at a temperature of 50°C, a frequency of 1.0 rad/second, an initial strain of 0.1%, and a final strain of 80.0%. Stress-strain curves were obtained from the RSAII for each of the eight different adhesive samples. Two samples were analyzed for each of the adhesive formulations containing Tack A and four samples were analyzed for the BA-EA base polymer adhesive. The yield strain, yield stress, and modulus were determined from the stress-strain data for each of the adhesive samples.

The glass transition temperature (T_g) was determined by Differential Scanning Calorimetry (DSC) for each of the adhesive formulations using a DSC Q1000 system. Samples of the adhesive formulations were prepared for the DSC by placing drops of the solution on pieces of Teflon for the six adhesive solutions or by removing adhesive film from the release liner for the two adhesive films. The samples were then placed in a vacuum oven at a temperature of 50^oC overnight. The next day, the samples were placed in a drying pistol for overnight. About 5 mg of material was removed from a dried sample and sealed in a DSC pan. The DSC pan was then placed in the DSC device for analysis of the sample. The temperature of the system was decreased to -90^oC and then increased to 100^oC at a rate of 10^oC/minute. Heat flow and the first derivative of heat flow were plotted versus temperature to determine the T_g for each of the adhesive formulations. Two samples of each of the base polymer formulations were analyzed to determine repeatability.

The contact angle was determined for each of the eight different adhesive formulations. A 10 cm by 5 cm sample of an adhesive film on paper was secured on the horizontal surface in a goniometer. A drop containing 2 mL of deionized water was dropped onto the surface of the adhesive film using a 100 cm^3 syringe. The lines in the scope were aligned with the surface of the film and the edge of the drop of water. The contact angle was recorded at 10, 20, and 30 seconds after the water was dropped onto the adhesive film surface. The contact angle was determined for two samples of each adhesive formulation.

Pulping

Six 10 cm by 10 cm adhesive labels were applied to copy paper and then pulped in the 450H pulper. The operating parameters for the 450H pulper were 450 OD g of pulp, 12% consistency, 50°C, and 415 rpm, for 30 minutes. Pulp samples were removed from the 450H pulper at 10 and 30 minutes of pulping time. Handsheets were prepared from the pulp samples for dyeing followed by image analysis.

The dyeing procedure that was used is as follows. Each handsheet in a set was submerged in Morplas Blue-Heptane solution for ten seconds and then hung up to dry. Once the set of handsheets was dry, each handsheet was submerged in 95% Heptane for ten seconds and then hung up to dry. Once the set of dyed and rinsed handsheets was dry, the set was removed and placed in a labeled plastic bag.

Image analysis was used to determine the stickies content of the samples for the different sets of handsheets. For image analysis, the SpecScan 2000 program by Apogee Systems Inc. was used to scan each set of handsheets. The scanner was a UMAX PowerLook III with a 600 dpi resolution. Both the felt and wire sides of each of the handsheets in a set were scanned. The parts per million (ppm), the number of particles in 1 m^2, and the average particle size were determined for each side of each handsheet. Also, a histogram of particle sizes in terms of area and count were recorded. Particle size was compared to the physical properties of the different adhesive materials using SAS version 8 from the SAS Institute.

Single Slot Experiments

Individual PSA particles for each of the adhesive formulations were analyzed in a single slotted screening device for particle passage. The single slotted screening device consists of a metal plate, a plastic Buchner funnel, a vacuum flask, and a vacuum pressure gauge [11,12]. The metal plate has a slot cut in the middle that is 0.007 inches (0.18 mm) wide and 1 inch long. The metal plate containing the slot is 0.25 inches thick. The metal plate is secured to the Buchner funnel, with the middle cut out of it, by silicone and all of the holes around the metal plate are filled with silicone. The Buchner funnel fits in the tip of the vacuum flask. The vacuum flask is attached to a house vacuum valve by rubber tubing, with the vacuum gauge in between the flask and the valve.

Adhesive particles were removed from a pulp sample produced in the pulping experiments. The length, width, and thickness were measured for each adhesive particle under a microscope. Each adhesive particle was then allowed to soak in deionized water at 50^{o}C for five minutes, before being placed on the 0.007 inches wide slot of the single slot device. The length of the particle was aligned with the length of the slot. The device was then filled with 1000 mL of deionized water at 50^{o}C. A vacuum was applied to the single slot by slowly opening the vacuum line. If the particle passed through the slot, the vacuum pressure at which the particle passed was recorded and the particle was recovered from the device. The particle passage was determined for each of the adhesive formulations, based on the number of particles that passed through the slot compared to the total number of particles that were analyzed. Particle passage was compared to the physical and mechanical properties of the different adhesive materials using SAS version 8 from the SAS Institute.

RESULTS AND DISCUSSION

Pulping of Pressure Sensitive Adhesive Films

The image analysis results from the pulping experiments for the eight different PSA films are shown in **Table 8-2**. The results consist of the parts per million, number of particles in 1 m^2, and average particle size for particles larger than 0.040 mm^2. In comparing the two base polymers, BA-EA produced significantly larger particles than BA. AC produced the largest average particle size out of the pulper after 10 and 30 minutes. The average particle size of SIS did not change between 10 and 30 minutes in the pulper, while the average particle size decreased for all of the other adhesive films between 10 and 30 minutes in the pulper.

Table 8-2. Image Analysis Results for Eight Different PSA Materials

Sample	Pulping Time, minutes	Parts Per Million, ppm	Number of Particles in 1 m^2	Average Particle Size, mm^2
BA	10	1710	1210	1.41
	30	2040	1880	1.08
BA:A	10	2580	3020	0.86
	30	2880	5570	0.52
BA:G	10	1800	1870	0.96
	30	2140	2860	0.75
BA-EA	10	2260	1130	2.00
	30	2480	1690	1.47
BA-EA:A	10	2670	3690	0.72
	30	2510	5000	0.50
BA-EA:G	10	2620	3210	0.82
	30	2470	3620	0.68
AC	10	2510	1130	2.21
	30	2660	1660	1.60
SIS	10	860	950	0.90
	30	1160	1280	0.91

In comparing the AC and SIS adhesive films to the adhesive films with known formulations, AC had the largest average particle size and SIS had the fewest number of particles in 1 m^2 (**Table 8-2**). The SIS film has a different base material than all of the other materials considered, so it is not surprising that its behavior is significantly different than the other formulations. In a study where the number of particles was compared among different adhesive formulations, the SIS had the fewest particles and the acrylate had the most particles [1].

Figure 8-1 is a plot of cumulative particle size distribution from the image analysis data for the pulps out of the pulper at 30 minutes. This plot shows that BA-EA and AC had the fewest particles less than 0.50 mm^2 of the eight different adhesives analyzed. The adhesive formulations containing the same tackifier had similar particle size distributions, regardless of the base polymer. Also, the adhesives containing tackifiers had fewer large particles than the base polymer or commercial adhesives.

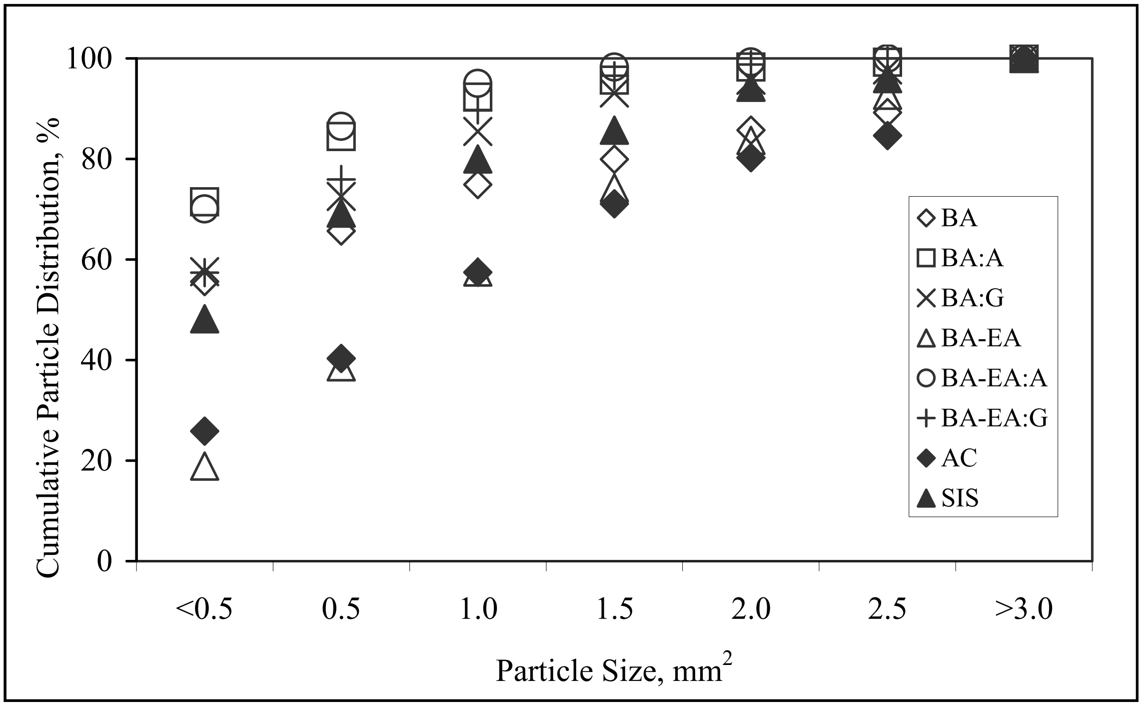

Figure 8-1. Cumulative Number of Particles Versus Particle Size Based on Image Analysis of Dyed Handsheets

Figure 8-2 and **Figure 8-3** are microscopic images representative of an AC and SIS adhesive particle, respectively. The images were captured using ImagePro with a microscope at 50x magnification. The two images show a considerable difference in the shape of the particles for the two different adhesives. The AC particle is significantly longer and more string like than the SIS adhesive particle, characteristics that should have an impact on screening. The SIS particle has a fiber attached to it (**Figure 8-3**). From inspection of many particles it was determined that the majority of the SIS particles had fibers attached. In contrast, a small minority of the AC particles had fibers attached. It was found that the tack for the SIS film was higher than the tack for the acrylic film (**APPENDIX 8**). The higher tack could contribute to the higher number of fibers attached to the SIS particles than to the acrylic particles. Microscopic images of other AC and SIS particles are available in **APPENDIX 9** and **APPENDIX 10**, respectively.

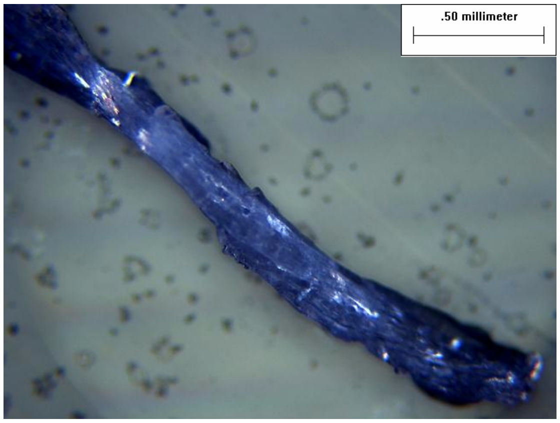

Figure 8-2. AC Adhesive Particle Image

Figure 8-3. SIS Adhesive Particle Image

Physical Properties of the Pressure Sensitive Adhesive Films

The physical analysis results for the eight different PSA films are shown in **Table 8-3**. The contact angle values are those measured at 10 seconds after the drop was on the sample surface. In comparing the two base polymers, BA-EA has a lower T_g and a lower modulus than BA. However, BA-EA has a higher yield strain and a higher yield stress than BA. In fact, BA-EA has the highest yield stress and yield strain of any of the adhesive materials analyzed. In comparing the adhesive formulations containing tackifiers, the samples containing the same tackifier have similar T_g, yield strain, and yield stress values. In general, the addition of a tackifier reduces the strength properties of the adhesive material. Among all eight of the adhesives, SIS has the highest modulus. In comparing the average particle size in **Table 8-2** and the properties in **Table 8-3**, there does not appear to be a direct relationship between the average particle size out of the pulper at 30 minutes and any single property by itself. The differential scanning calorimetry results to determine the T_g for the two base polymer materials are available in **APPENDIX 11**. Stress versus strain curves for all eight of the adhesive formulations are available in **APPENDIX 12**.

Table 8-3. Properties for Eight Different PSA Materials

Sample	T_g, °C	Contact Angle, °	Yield Strain, %	Yield Stress, kPa	Modulus, MPa
BA	-37	80	2.9	25	0.84
BA:A	-20	67	0.78	3.0	0.38
BA:G	-12	78	3.5	18	0.51
BA-EA	-49	98	19	56	0.30
BA-EA:A	-23	75	0.67	1.5	0.22
BA-EA:G	-16	92	6.4	20	0.31
AC	-28	80	0.86	6.0	0.69
SIS	-27	92	3.1	44	1.4
Tack A	17	70	-	-	-
Tack G	33	74	-	-	-

Particle Breakage in the Pulper

Average particle size out of the pulper at 30 minutes was compared to the mechanical properties of the adhesive materials using SAS, a statistical analysis package. The SAS input file and output for average particle size are available in **APPENDIX 13**. No individual mechanical property alone could significantly predict the average particle size out of the pulper. However, an equation containing yield strain, yield stress, and modulus could predict the average particle size. The equation for average particle size is:

$$\text{Particle Size} = -0.43 + 0.34*\text{Yield Strain} - 0.10*\text{Yield Stress} + 3.22*\text{Modulus}$$

where the units are mm^2 for average particle size, percent for yield strain, kPa for yield stress, and MPa for modulus. The calculated versus actual particle size is plotted in **Figure 8-4**. For this equation, the R^2 value is 0.86 and the F value is 8.15. With an R^2 value of 0.86, the model can predict 86% of the data. The partial R^2 values for the individual terms of the equation are 0.20, 0.53, and 0.12 for yield strain, yield stress, and modulus, respectively. T_g and contact angle have partial R^2 values of 0.04 and 0.01, respectively, and are not significant for particle size. The statistical model shows correlation between particle size and the three mechanical properties, but not cause and effect. It is unclear as to how the three mechanical properties may affect particle size with respect to the model.

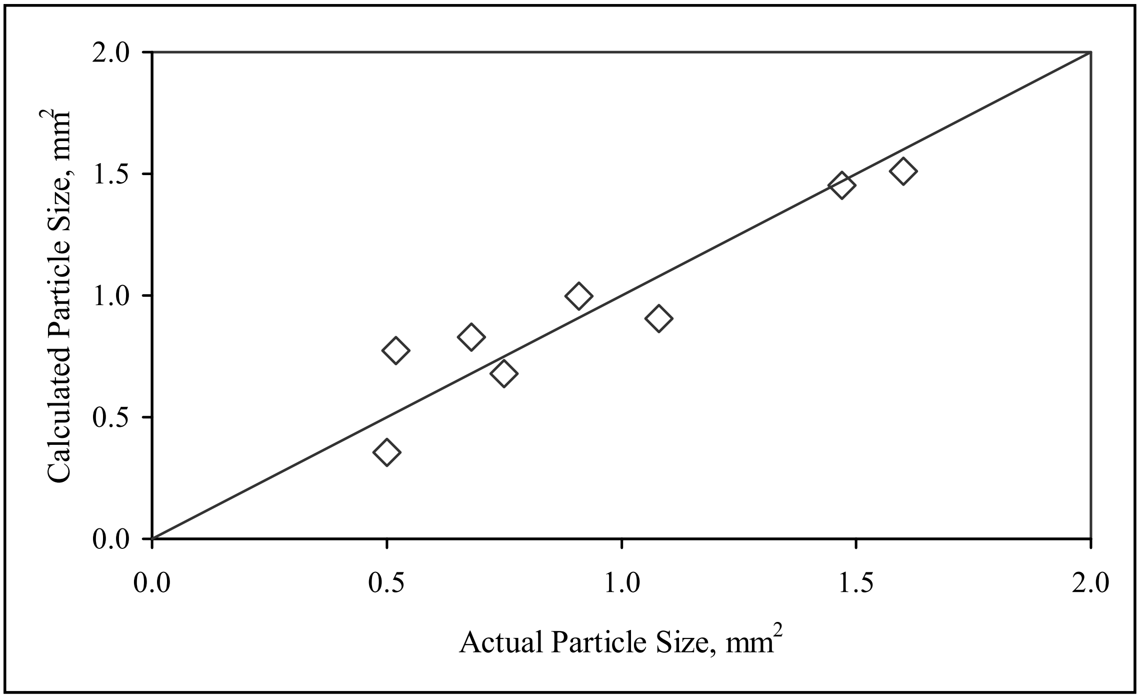

Figure 8-4. Calculated Average Particle Size Versus Actual Average Particle Size

Passage of the Pressure Sensitive Adhesive Particles Through a Slot

The percentage of particles passing through the slot and some average size characteristics are listed in **Table 8-4**. Particle area is the particle length times the particle width, as viewed under the microscope. Particle volume is the particle area times the particle thickness. Among the six adhesives with known formulations, this data shows that the base polymers had the longest and widest particles out of the pulper, and they provided the largest average particle area and the largest average particle volume. Also, the BA-EA particles provided the lowest particle passage of 5%. The adhesive formulations containing the same tackifier resulted in similar particle passage, regardless of the base polymer. The vacuum pressure for particle passage data appears in **APPENDIX 14**.

Table 8-4. Particle Passage and Average Particle Dimensions for Eight Different Adhesive Formulations

Sample	Length, mm	Width, mm	Thickness, mm	Area, mm^2	Volume, mm^3	Particle Passage, %
BA	3.08	0.36	0.31	1.15	0.38	38
BA:A	1.91	0.35	0.32	0.68	0.22	70
BA:G	2.21	0.33	0.27	0.77	0.22	30
BA-EA	2.72	0.38	0.33	1.06	0.38	5
BA-EA:A	1.61	0.31	0.27	0.50	0.14	75
BA-EA:G	1.44	0.35	0.30	0.48	0.16	30
AC	2.68	0.46	0.36	1.27	0.50	30
SIS	1.31	0.44	0.37	0.57	0.22	10

Figure 8-5 is a plot of cumulative particle size distribution for the particles used in the single slot experiments, with the dimensions measured manually under a microscope. This data is similar to that obtained by the image analysis of handsheets (**Figure 8-1**). This plot shows that the base polymer adhesives and AC had larger particles than the other adhesive materials. Also, the base polymer adhesives and AC had wider ranges of particle sizes than the adhesives containing tackifiers or SIS.

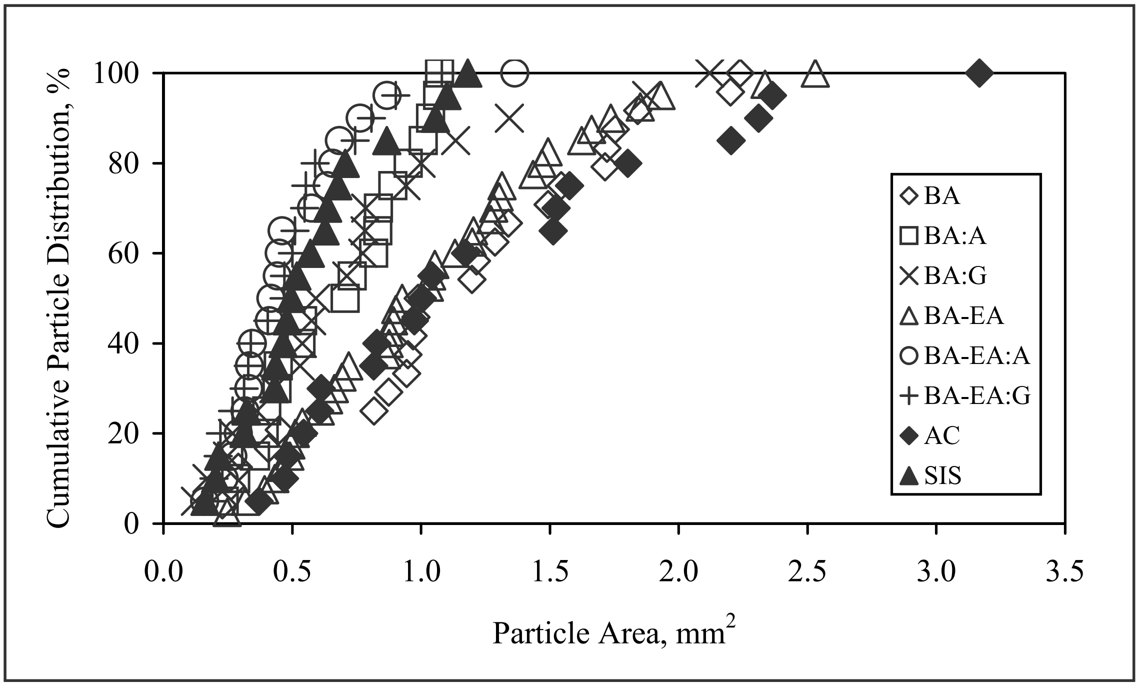

Figure 8-5. Cumulative Particle Size Distribution for Particle Area Measured Manually Using a Microscope

Figure 8-6 is a plot of cumulative particle passage versus particle area for the eight different adhesive formulations considered in the single slot. For a given formulation, as the particle area increases, particle passage decreases, which is to be expected (**Figure 8-6**). This indicates that particle size is an important factor in particle passage. A comparison between **Figure 8-5** and **Figure 8-6** shows that the particle area correlates well with the particle passage. However, as the particle area increases, the particle passage decreases at different rates for different adhesive formulations due to the different particle size distributions. The SIS particle passage is considerably lower than other formulations at the same particle size (**Figure 8-6**). It is possible that the attached fibers observed on the SIS particles play a role in the lower particle passage.

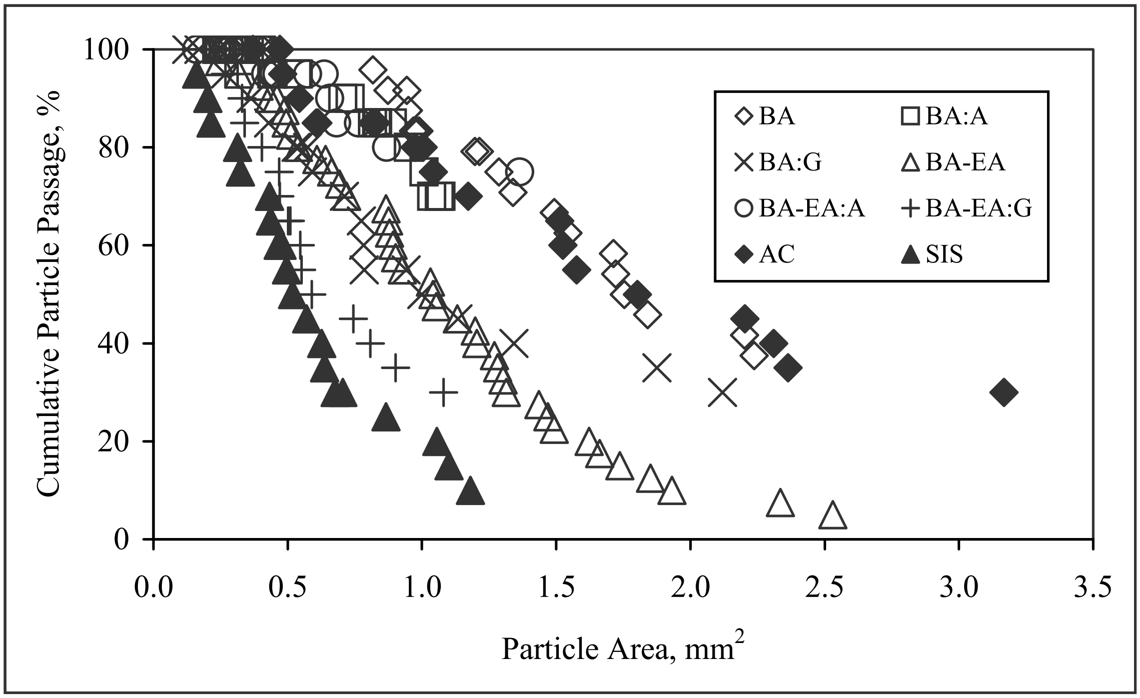

Figure 8-6. Cumulative Particle Passage Versus Particle Area

Plots of particle passage versus adhesive material yield strain, yield stress, and modulus are shown in **Figure 8-7**, **Figure 8-8**, and **Figure 8-9**, respectively. The material with the lowest yield strain has the highest particle passage and the material with the highest yield strain has the lowest particle passage (**Figure 8-7**). The material with the lowest yield stress has the highest particle passage and the material with the highest yield stress has the lowest particle passage (**Figure 8-8**). There does not appear to be a direct correlation between particle passage and modulus (**Figure 8-9**). Therefore, particle passage tends to decrease as either the yield strain increases or as the yield stress increases, but does not appear to be affected by the modulus.

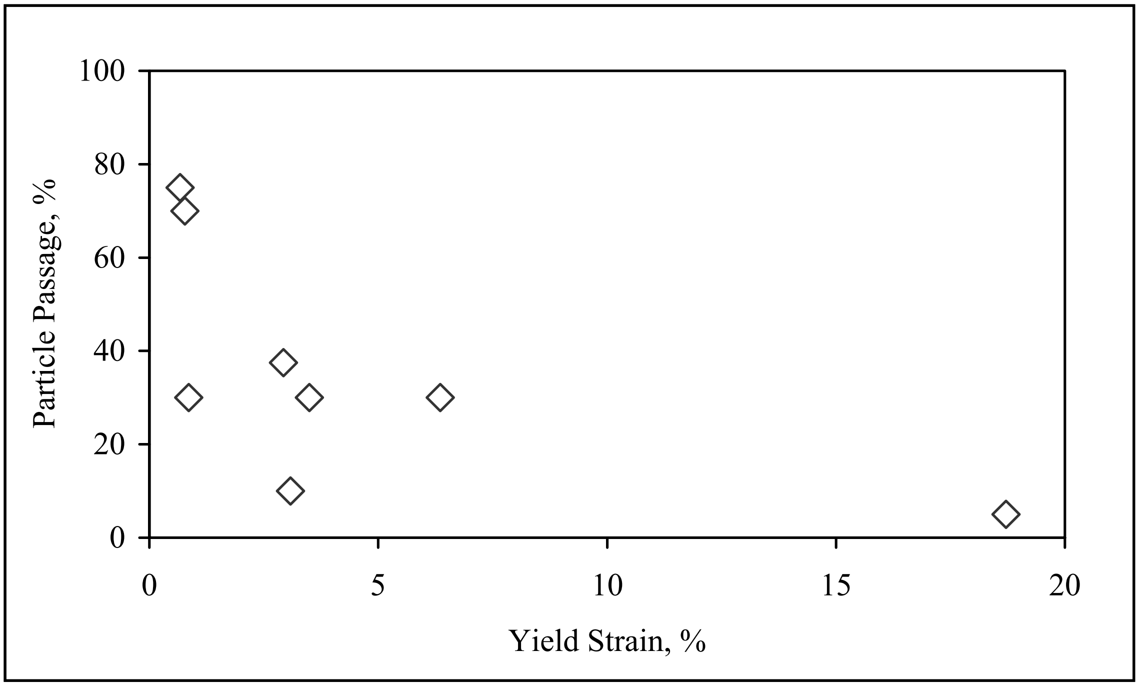

Figure 8-7. Particle Passage Versus Adhesive Material Yield Strain

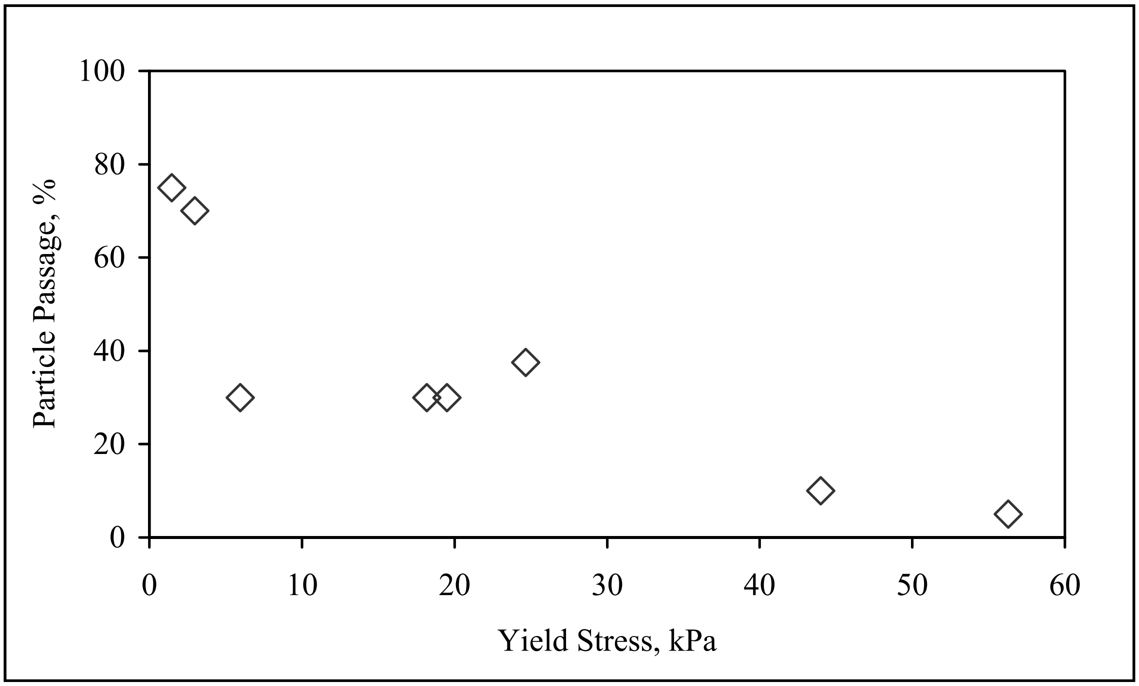

Figure 8-8. Particle Passage Versus Adhesive Material Yield Stress

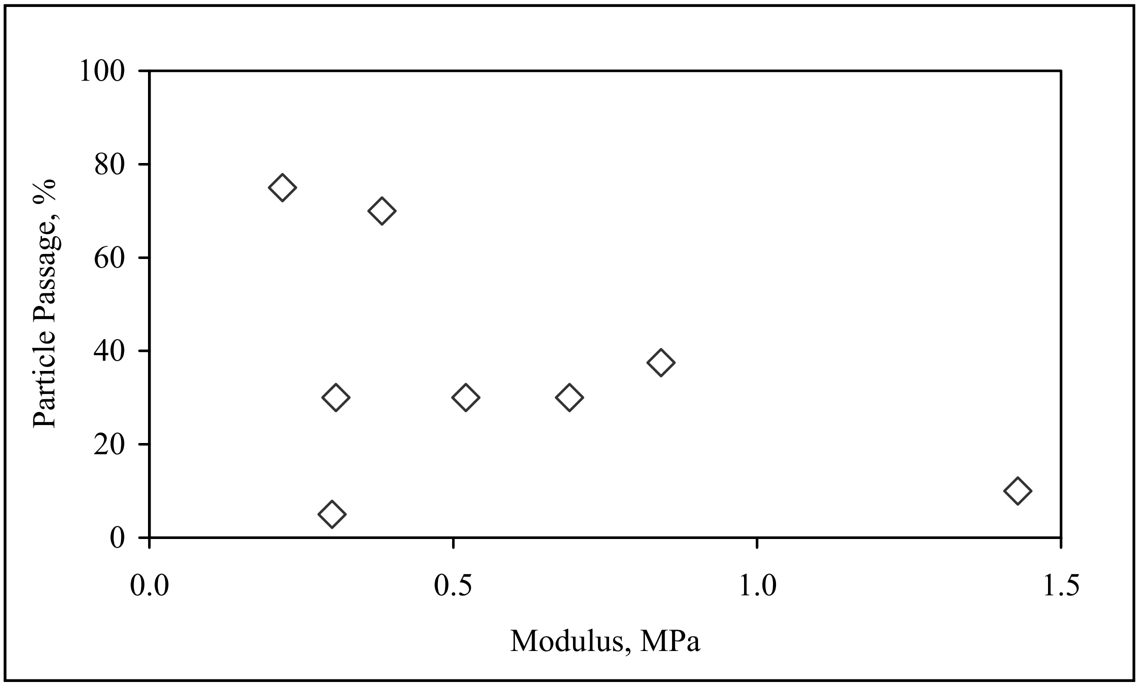

Figure 8-9. Particle Passage Versus Adhesive Material Modulus

Particle passage was compared to the overall average dimensions of the particles and the physical properties of the adhesive materials using SAS. The SAS input file and output for particle passage are available in **APPENDIX 15**. The overall average dimensions of the particles alone were not significant in the prediction of particle passage. Note that this does not mean that the size of individual particles is not a major factor in particle passage. Also, the T_g and contact angle were not significant in predicting particle passage. It was interesting to note that herein contact angle was not significantly related to particle passage under pressurized screening conditions, but previous work by Yan et. al. [13] found a trend between screenability in a non-pressurized screen and contact angle. However, for the mechanical properties, yield stress was the best individual property that was significant in predicting the particle passage. The equation for particle passage as a function of the yield stress is:

$$\text{Particle Passage} = 59.25 - 1.08*\text{Yield Stress}$$

where the units are percent for particle passage and kPa for yield stress. For this equation, the R^2 value is 0.72 and the F value is 15.30. The calculated versus actual particle passage based on this model is shown in **Figure 8-10**.

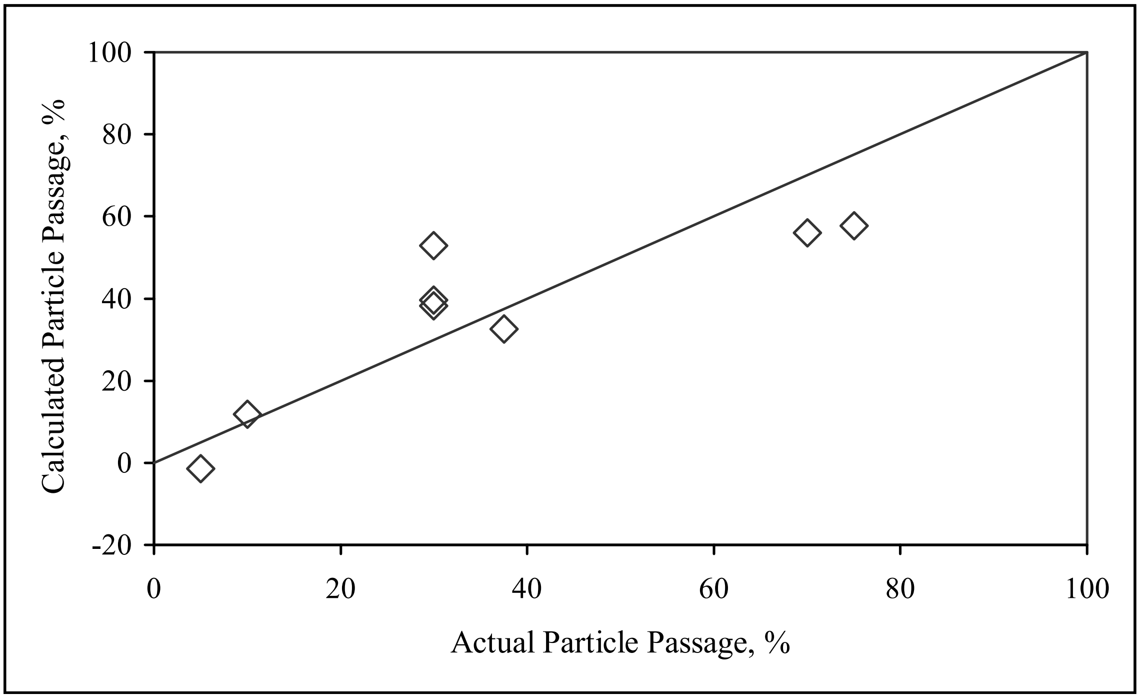

Figure 8-10. Calculated Versus Actual Particle Passage Using Yield Stress

The best model containing two variables consisted of yield stress and average particle area. The equation for particle passage as a function of yield stress and average particle area is:

$$\text{Particle Passage} = 99.52 - 2.54*\text{Yield Stress} + 1.74*\text{Yield Stress}*\text{Area} - 50.18*\text{Area}$$

where the units are percent for particle passage, kPa for yield stress, and mm^2 for average particle area. For this equation, the R^2 value is 0.90 and the F value is 21.41. The calculated versus actual particle passage based on this model is shown in **Figure 8-11**. Since the model containing both yield stress and average particle area has the higher R^2 value of the two models, it will have a better fit to the data, as seen in **Figure 8-11** relative to **Figure 8-10**.

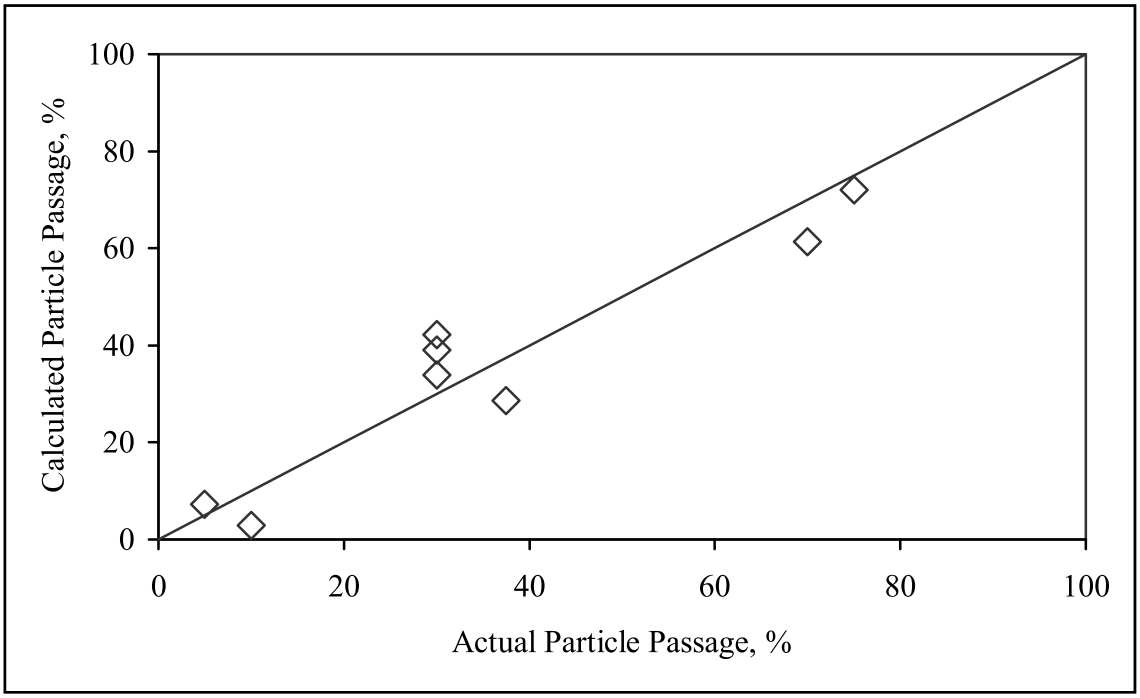

Figure 8-11. Calculated Versus Actual Particle Passage Using Yield Stress and Area

This model of particle passage as a function of yield stress and average particle area is to be expected. The particle passage decreases as the yield stress increases because particles with a higher yield stress are less likely to deform in order to pass through the slot than particles with a lower yield stress. The particle passage decreases as the average particle area increases because larger particles require more deformation than smaller particles in order to pass through the slot.

In a theoretical investigation of debris removal by pressure screens, particle passage was proposed to involve particle bending or particle extrusion [15]. The models developed for particle bending were functions of the pressure drop and modulus. The bending models required that particles have a thickness less than half the slot width in order to bend and pass through the slot. However, in the laboratory work shown here, none of the particles had a thickness less than half the slot width, but particles were still able to pass through the slot. Therefore, the bending models do not apply to our pressurized screening system. The alternative particle passage model, based on the particle extrusion phenomena [15], indicated that particle passage would decrease with increased yield stress at a constant opening size and pressure drop. The particle extrusion model is in agreement with the statistical model developed herein.

CONCLUSIONS

Adhesive formulation impacts the particle size out of the pulper and the screenability, as measured using a pressurized laboratory screening device, of the adhesive particles. Tackifiers have a significant effect on the properties of the adhesive material and its behavior in the pulper and screen. Statistical modeling determined that the particle size after pulping was significantly related to the yield strain, yield stress, and modulus of the adhesive formulations. Statistical modeling determined that particle passage in a pressurized screen was negatively related to both yield stress and particle area.

REFERENCES

1. Pikulin, M. A., “Stickies and Their Impact on Recycled Fiber Content Fine Paper”, *Joint Conference to Address Pressure Sensitive Adhesive Issues Proceedings*, United States Postal Service and American Forest & Paper Association, Washington, D.C., June 1996.

2. Friberg, T., “Cost Impact of Stickies”, *Progress in Paper Recycling*, 6(1):70-72, 1996.

3. Heise, O., “Screening Foreign Material and Stickies”, *Tappi Journal*, 75(2):78-81, 1992.

4. Peng, J. Y., “United States Postal Service Efforts to Develop an Environmentally Benign Pressure-Sensitive Adhesive for Postage Stamp Applications”, *2000 Tappi Recycling Symposium Proceedings*, Washington, D.C., TAPPI Press, March 2000.

5. Sutherland, N. R., “Stickies Dirt Count and Laboratory Methods”, *Environmentally Benign Pressure-Sensitive Adhesives for Postal Application Conference Proceedings*, United States Postal Service, Potomac, MD, July 1997.

6. Lucas, B. E., Venditti, R. A., and Jameel, H., “Breakage and Extrusion of Pressure Sensitive Adhesives in Industrial and Laboratory Screening Processes”, *2001 Tappi Pulping Conference Proceedings*, Seattle, WA, TAPPI Press, November 2001.

7. Lucas, B. E., Venditti, R. A., and Jameel, H., “Behavior of Pressure Sensitive Adhesive Material in Industrial Pressure Screens and Laboratory Screens”, *Tappi Journal*, 84(5):70, 2001.

8. Heise, O., Schabel, S., Cao, B., and Lorenz, K., “Deformation and Disintegration Physics of Stickies in Pressure Screens: A compromise between pulp quality and capital investment”, *5th Research Forum on Recycling Proceedings*, Ottawa, ON, Canada, pp. 187-195, September 1999.

9. Heise, O., Cao, B., and Schabel, S., “A Novel Application of TAPPI T 277 to Determine Macro Stickies Disintegration and Agglomeration in the Recycle Process”, *2000 Tappi Recycling Symposium Proceedings*, Washington, D.C., TAPPI Press, pp. 631-644, March 2000.

10. Lucas, B. E., Venditti, R. A., and Jameel, H., “The Breakage of Pressure Sensitive Adhesive Contaminants in Paper Recycling Operations”, *2000 Tappi Pulping/Process & Product Quality Conference Proceedings*, Boston, MA, TAPPI Press, November 2000.

11. Flanagan, J., Venditti, R., Jameel, H., Wilson, N., Weaver, N., and Lucas, B., "Passage of Pressure Sensitive Adhesive Particles Through a Fine Slot", *Progress in Paper Recycling*, 11(3):17-23, 2002.

12. Lucas, B. E., Venditti, R. A., and Jameel, H., "Factors in the Passage of Pressure Sensitive Adhesive Particles Through a Slot", *2002 Tappi Fall Conference & Trade Fair Proceedings*, San Diego, CA, TAPPI Press, November 2002.

13. Yan, Z., Zhao, Y., Deng, Y., and Yang, J., "The Effect of Pressure-Sensitive Adhesive Properties on Screenability", *2nd International Symposium on Emerging Technology of Pulping & Papermaking Proceedings*, Guanzhou, China, October 2002.

14. Leppanen, A., "The Role of Pressure Sensitive Labels in Paper Recycling", *Adhesive and Sealant Council 1999 Spring Convention and Expo Proceedings*, Toronto, ON, Canada, April 1999.

15. Bliss, T. and Ostoja-Starzewski, M., "Debris Characteristics and Removal Techniques", *1997 Tappi Korea Recycling Symposium Proceedings*, Seoul, Korea, TAPPI Press, October 1997.

CHAPTER 9

OVERALL CONCLUSIONS

The conclusions from this dissertation are as follows:

Industrial pressure screens can break down pressure sensitive adhesive particles, generating significant amounts of small adhesive particles and lowering the removal efficiency of the screens. Non-pressurized laboratory screens do not break down the adhesive particles, contributing to the laboratory screens having a much higher screening efficiency than industrial pressure screens. Therefore, laboratory screens are not good indicators of the screenability of pressure sensitive adhesive particles.

Experiments with a laboratory high shear device were useful in determining the effect of operating conditions on the breakage of PSA contaminants. Statistical analysis determined that increasing the consistency, time, or initial temperature significantly increased the breakage of the PSA contaminants. Rotor speed in the range evaluated did not have a significant effect. At consistencies less than about 6%, breakage of the particles was not detected. However, at consistencies greater than 6%, breakage increased with increasing consistency. Increases in operating temperature caused increases in the breakage of the PSA contaminants.

Lab-scale pulping of pressure sensitive adhesive labels and copy paper generated PSA particles that typically had one long dimension and two shorter dimensions. The two shorter dimensions were of approximately equal magnitude. PSA particles with their smallest dimension greater than approximately four times the slot width did not pass through the slot of a single slot device for pressure differences of up to 80 kPa. However, a significant percentage of PSA particles with their smallest dimension between the slot width and four times the slot width passed through the slot at moderate pressure differences. These particles were observed to deform and pass through the slot. Particle passage through a single slot was shown to be facilitated by increases in pressure drop across the slot, increases in operating temperature, and decreases in particle width, thickness, or area. Particle length did not correlate with particle passage.

The pressure difference across the slot in the single slot device did not break any of the adhesive particles. This indicates that particle breakage in an industrial pressure screen does not occur due to the forces associated with the pressure difference across the slot. Particle breakage is due to the forces in the region between the foil and the screen plate.

Adhesive formulation impacts the particle size out of the pulper and the screenability, as measured using a single slot device, of the adhesive particles. Tackifiers have a significant effect on the properties of the adhesive material and its behavior in the pulper and screen. Statistical modeling determined that the particle size after pulping was positively related to the yield strain and modulus and negatively related to the yield stress. Statistical modeling predicted particle passage in a pressurized screen was negatively related to yield stress and particle area. This agrees with the results of a mathematical model that yield stress and particle width are the key parameters (see **APPENDIX 16**).

CHAPTER 10

SUGGESTIONS FOR FUTURE RESEARCH

This dissertation focused on the passage of pressure sensitive adhesive particles through the slots of industrial pressure screens, non-pressurized laboratory screens, and a pressurized single slot device. In the cases of the industrial and laboratory screens, the process is dynamic, that is, the forces on the particles are not constant, whereas in the case of the single slot device, the process is not dynamic at all. A laboratory method needs to be developed in order to analyze the passage of single pressure sensitive adhesive particles through a slot in a dynamic system with a pressure pulse across the slot, instead of just a pressure difference. A potential avenue of investigation would be to use a dynamic flow process. An apparatus that could be modified for this investigation has been used by Hubbe [1] to study the retention of small particles on forming fabrics in the papermaking process. The device utilizes two pumps, a peristaltic pump to develop a main positive flow through the forming fabric, and a bellows pump to develop a secondary oscillating flow. A study utilizing this dynamic flow phenomenon with a slot may reveal more mechanistic details about the passage behavior of adhesive particles in an industrial screen.

Also, the effects of adhesive formulation need to further be investigated so that the adhesive manufacturer can produce adhesive particles that can be screened more effectively from pulp. This would involve a broader supply of adhesive samples from industry for investigation.

This study has determined that pressure sensitive adhesive materials that have high yield stress and that produce large particles out of the pulper are more screenable. Future research may involve the development of pressure sensitive adhesive materials with these characteristics, but that also have the traditional properties of tack and strength required for the product purpose. For instance, a composite structure that has a tacky surface, but higher yield stress in the middle might serve this purpose.

This research has shown that intense mechanical actions on the adhesive particles can break and extrude the particles. Future research should be performed to develop new screening techniques that reduce breakage and extrusion in screens. Possible avenues to explore are placing the foils on the accepts side of the screen or reducing the shear within the device by decreasing the consistency or altering the speed or gap of the foil.

REFERENCES

1. Tripattharanan, T., Hubbe, M. A., Venditti, R. A., and Heitmann, J. A., "Effect of Idealized Flow Conditions on Retention Aid Performance. 1. Cationic Acrylamide Copolymer", *Appita Journal*, accepted for publication, 2004.

APPENDIX

APPENDIX 1

FOURIER TRANSFORM INFRARED ANALYSIS OF ADHESIVE FILMS

For the investigation of pressure sensitive adhesive (PSA) material in a pilot plant paper recycling system, large amounts of commercial PSA films were needed. Five different sets of labels by Avery Dennison were selected for analysis. The product numbers of the five different sets of labels were 5164, 5263, 5265, 6465, and 8165.

It was desired to use only acrylate based PSA material, therefore the contents of the five sets of labels were determined by infrared analysis. Sample labels were removed from each of the five sets of Avery Dennison labels and placed in labeled vials. About 1 mL of dichloromethane was added to each vial. The vials were shaken vigorously and then allowed to soak over night. The next day, samples of the solutions were poured out of the vials onto calcium fluoride plates and the dichloromethane was allowed to evaporate off of the plates, leaving a film of the sample on the surface of the plate.

The calcium fluoride plates were analyzed in a Fourier Transform InfraRed (FTIR) spectrometer for the films on their surfaces. For each of the samples, a second calcium fluoride plate was place on top of the film, so that the film was between the plates. A background was established for the FTIR spectrometer by scanning two calcium fluoride plates without a sample between them. Then, all five of the samples were scanned in the FTIR spectrometer and spectrums were produced. The spectra for the five samples are shown in **Figure A1-1** through **Figure A1-5**. The five spectra were compared to FTIR spectra for an acrylate based PSA film (**Figure A1-6**) and a SIS based

PSA film (**Figure A1-7**). All five samples have spectra similar to that for an acrylate based PSA film, so all five samples are acrylate based PSA films.

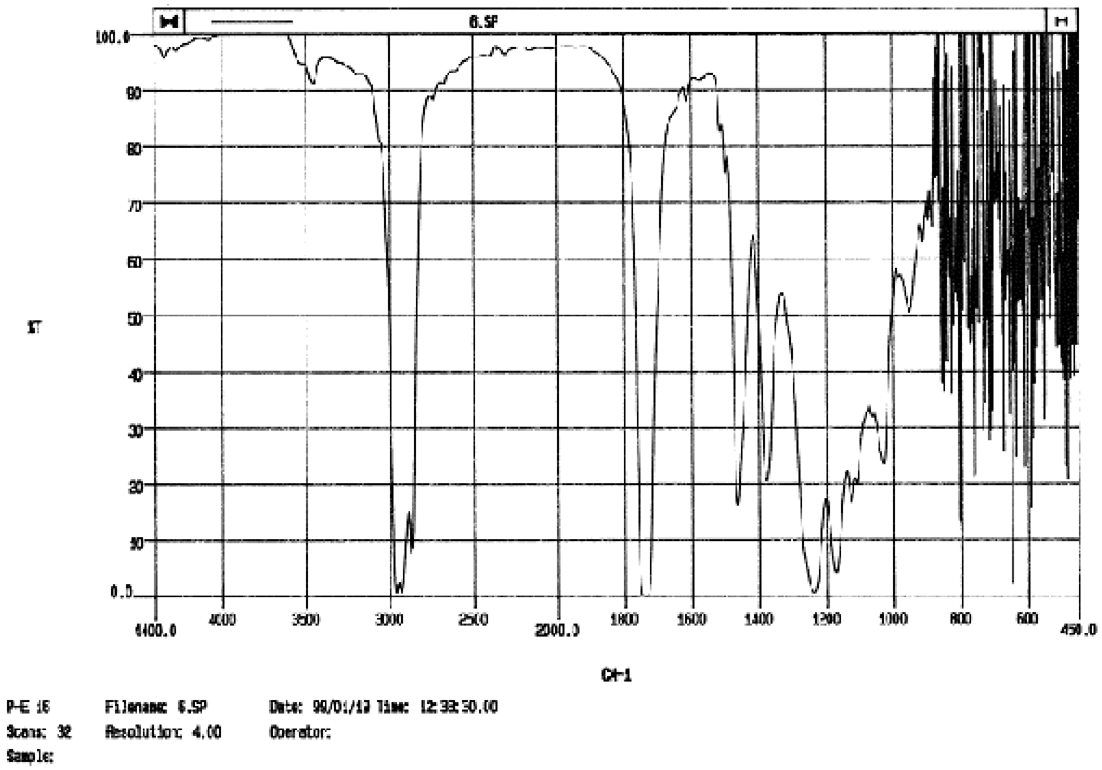

Figure A1-1. FTIR Spectrum for Avery Dennison Product Number 5164

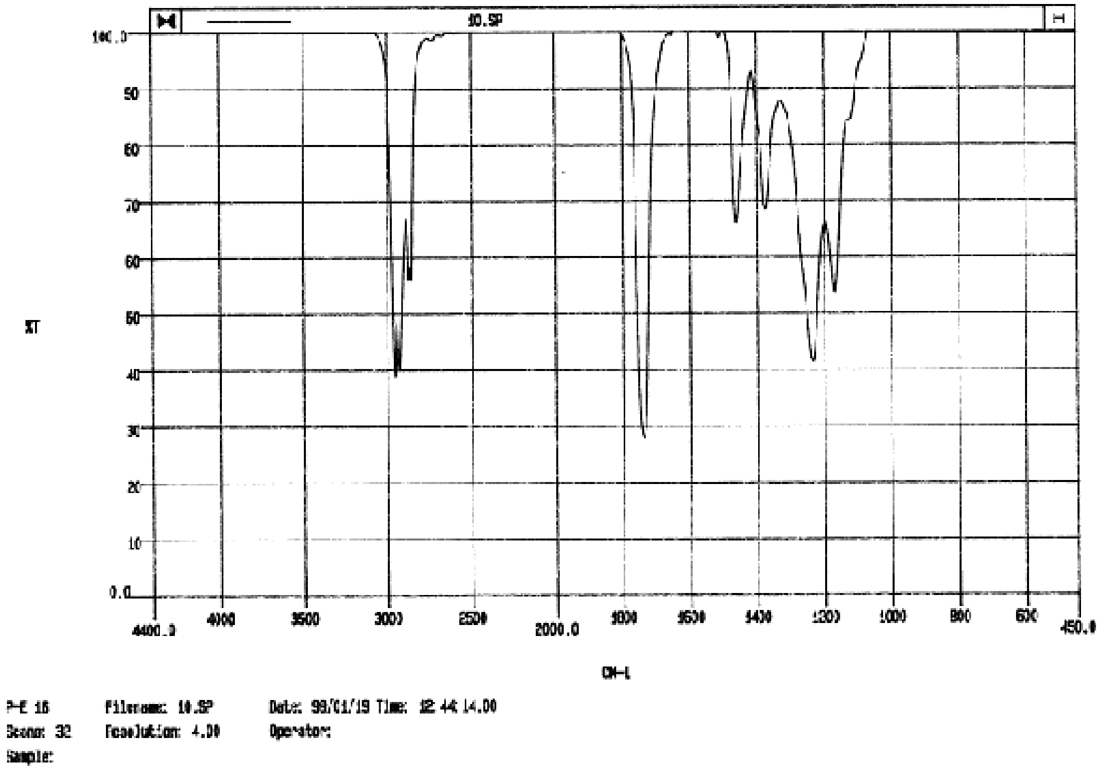

P-E 16 Filename: 10.SP Date: 98/01/19 Time: 12 44 14.00
Scans: 32 Resolution: 4.00 Operator:
Sample:

Figure A1-2. FTIR Spectrum for Avery Dennison Product Number 5263

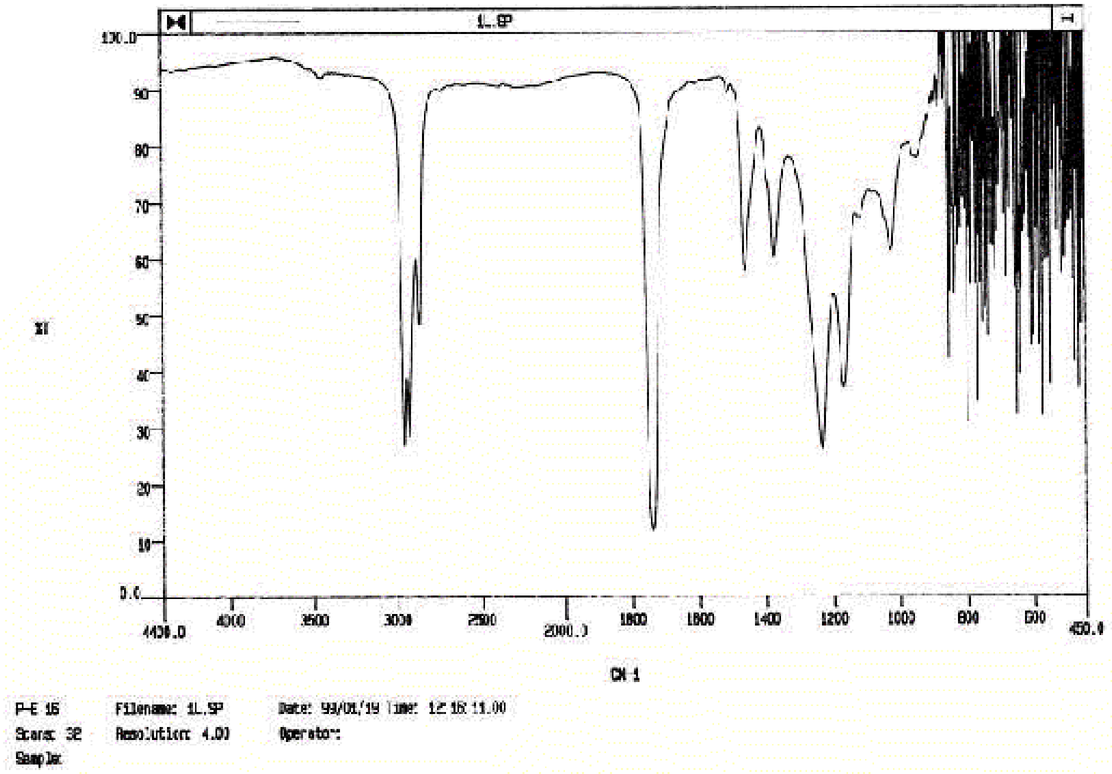

P-E 16 Filename: 1L.SP Date: 99/01/19 Time: 12:16:11.00
Scans: 32 Resolution: 4.00 Operator:
Sample:

Figure A1-3. FTIR Spectrum for Avery Dennison Product Number 5265

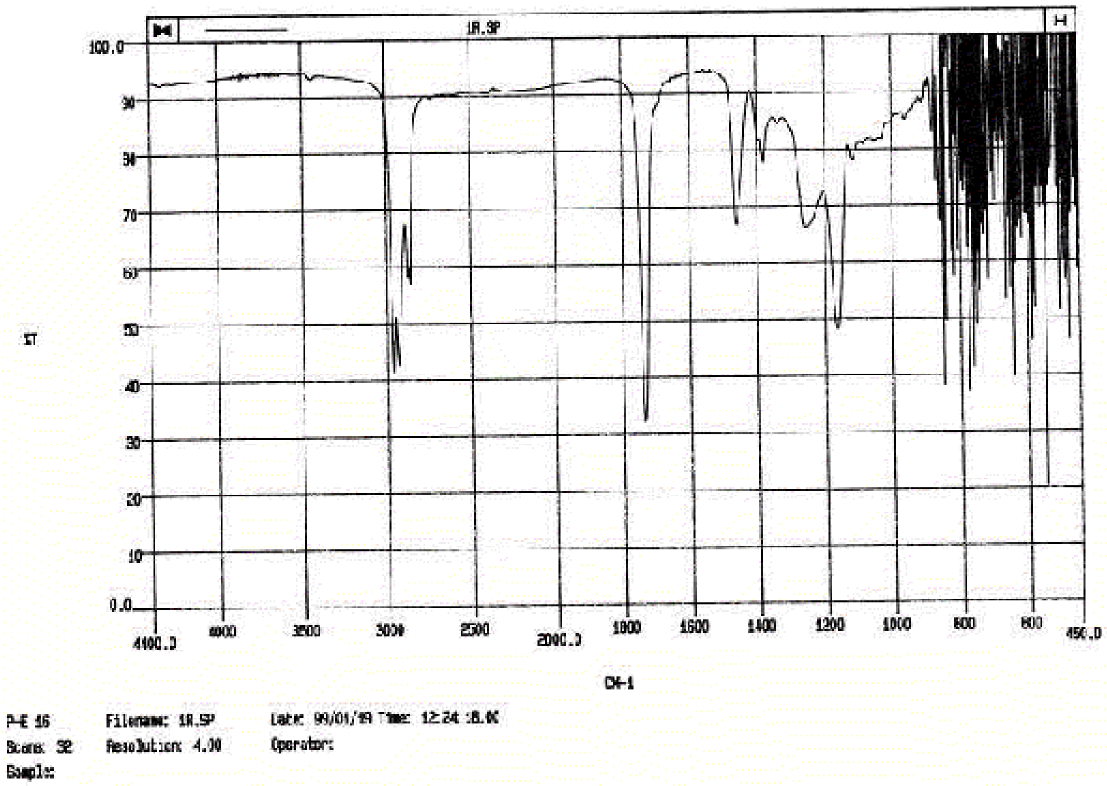

Figure A1-4. FTIR Spectrum for Avery Dennison Product Number 6465

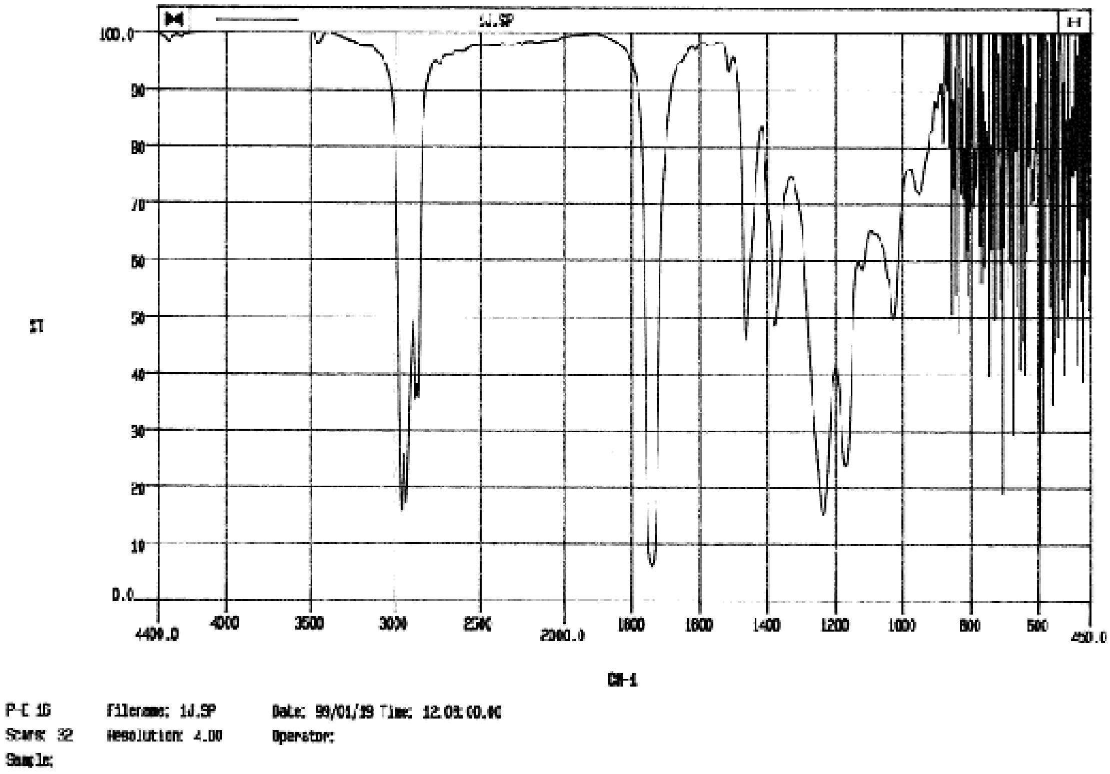

Figure A1-5. FTIR Spectrum for Avery Dennison Product Number 8165

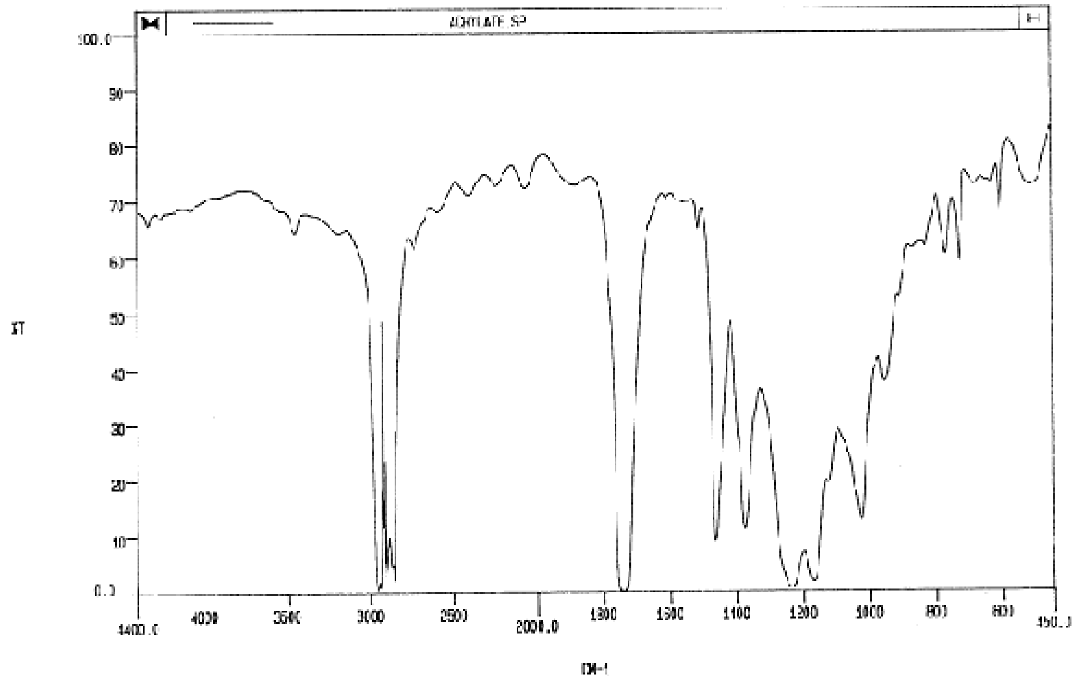

P-E 16 Filename: ACRYLATE.SP Date: 98/12/29 Time: 13:58:56.00
Scans: 32 Resolution: 4.00 Operator:
Sample:

Figure A1-6. FTIR Spectrum for an Acrylate Based PSA Film

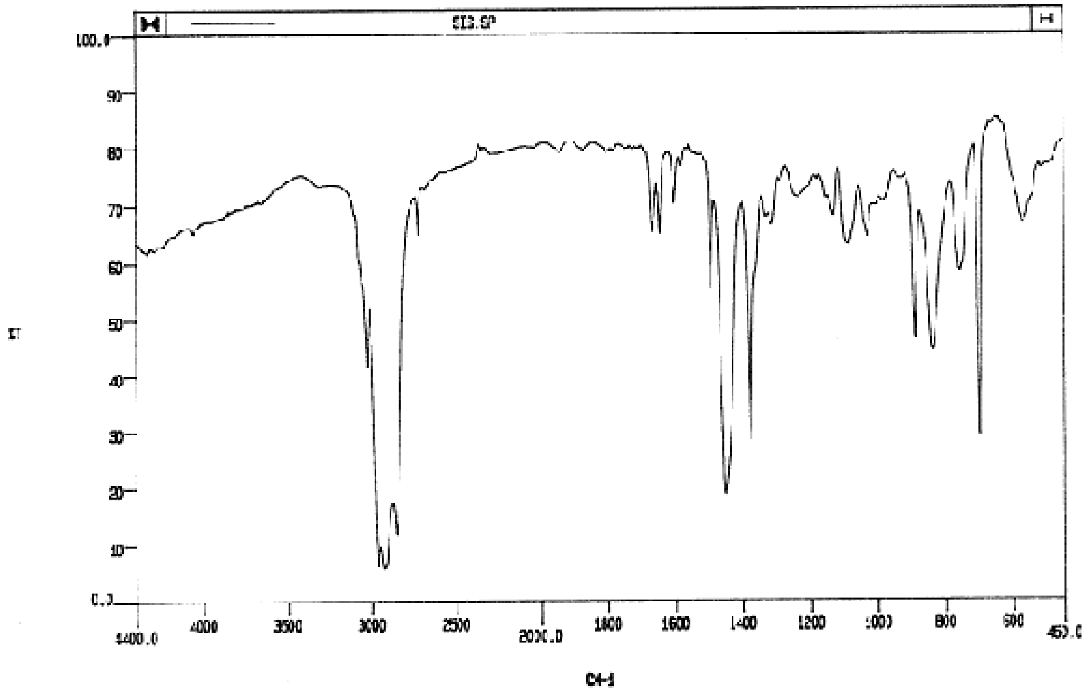

```
P-E 16        Filename: SIS.SP       Date: 99/04/04 Time: 12:08:41.30
Scans: 32     Resolution: 4.00       Operator: CH2Cl2 cased on KBr
Sample: SIS block copolymer from Shell Chemicals
```

Figure A1-7. FTIR Spectrum for a SIS Based PSA Film

APPENDIX 2

DYEING METHODS FOR THE ANALYSIS OF ADHESIVE CONTAMINANTS IN PULP

There are several methods available for analyzing adhesive contaminants. The methods include image analysis, dyeing, reaction to heat, spectroscopic analysis, adsorption, screening, and weighing [28]. One method used in this laboratory is dyeing followed by image analysis. Basically, the dye preferentially stains the adhesive and not the fibers to enhance the contrast between the adhesive particles and the paper fibers.

In preliminary research, two dye solutions and several dyeing methods were compared to determine which was the best method. All of the methods involved the dyeing of handsheets followed by image analysis. The two dye solutions considered were Morplas Blue-Heptane and Drew's Blue Stickies Dye-Ethanol. The three dyeing methods considered for Morplas Blue-Heptane were applying the adhesive with a roller to each handsheet, dipping each handsheet in the dye solution, and dyeing the adhesive film before application. Also, each handsheet was rinsed in Heptane once or twice. The two dyeing methods considered for Drew's Blue Stickies Dye-Ethanol were dyeing the pulp followed by making the handsheets and making the handsheets from the pulp followed by dyeing the handsheets. The pulp and handsheets were rinsed in water and then Ethanol or in Ethanol and then water.

Image analysis was used to determine the stickies content of the samples for the different sets of handsheets. For image analysis, the SpecScan 2000 program by Apogee Systems Inc. was used to scan each set handsheets. The scanner was a Hewlett

Packard Scanjet 4c with a 600 dpi resolution. Both the felt and wire sides of each of the handsheets in a set were scanned. The parts per million (ppm) of stickies, the average particle size, and the number of particles in 1 m^2 were determined for each side of each handsheet. Also, a histogram of particle sizes in terms of area and count was recorded. Using a stereomicroscope and a dissecting probe, the results from image analysis were confirmed manually on selected samples.

The procedures were compared based on the results from image analysis. In comparing the different dyeing methods for the same type of pulp and adhesive, the best method would have the most contrast between the adhesive particles and the background. The dyeing method in which handsheets were dipped in Morplas Blue-Heptane and rinsed once in Heptane was determined to be the best dyeing method.

The best dyeing procedure is as follows. Each handsheet was submerged in Morplas Blue-Heptane solution for 10 seconds and then hung up to dry over night. The next day, each handsheet was submerged in 95% Heptane for 10 seconds and then hung up to dry. Each handsheet was removed as soon as it was dry.

APPENDIX 3

EXAMPLE OF IMAGE ANALYSIS OUTPUT

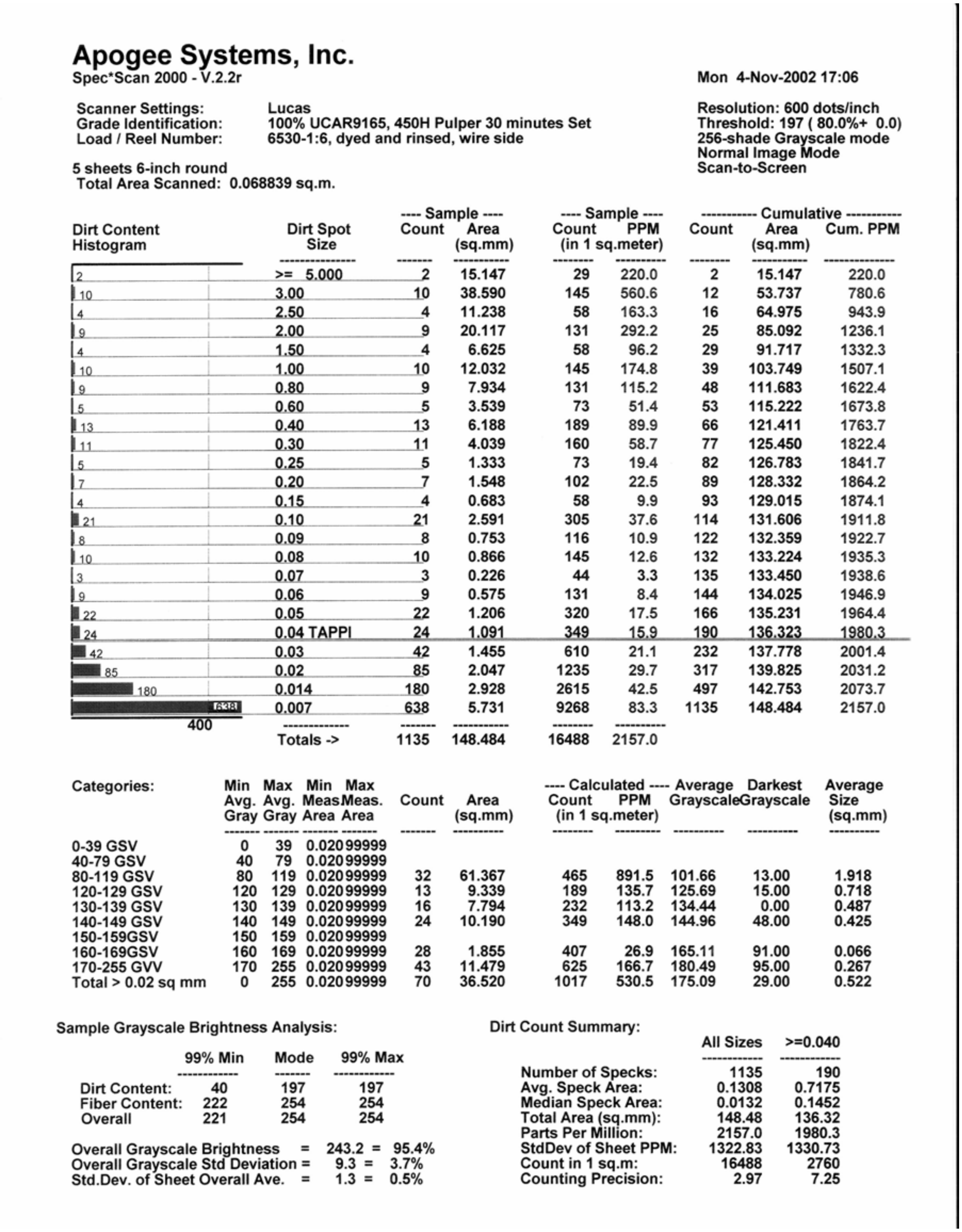

```
Apogee Systems, Inc.
Spec*Scan 2000 - V.2.2r                                                      Mon  4-Nov-2002 17:06

 Scanner Settings:          Lucas                                            Resolution: 600 dots/inch
 Grade Identification:      100% UCAR9165, 450H Pulper 30 minutes Set        Threshold: 197 ( 80.0%+  0.0)
 Load / Reel Number:        6530-1:6, dyed and rinsed, wire side             256-shade Grayscale mode
                                                                             Normal Image Mode
5 sheets 6-inch round                                                        Scan-to-Screen
 Total Area Scanned:  0.068839 sq.m.

                                  ---- Sample ----     ---- Sample ----     ----------- Cumulative -----------
Dirt Content          Dirt Spot   Count    Area        Count      PPM       Count     Area       Cum. PPM
Histogram               Size              (sq.mm)     (in 1 sq.meter)                (sq.mm)
                    -------------  -------  ----------  --------  --------  --------  ----------  -------------
2                   >=  5.000          2    15.147         29     220.0         2     15.147      220.0
10                  3.00              10    38.590        145     560.6        12     53.737      780.6
4                   2.50               4    11.238         58     163.3        16     64.975      943.9
9                   2.00               9    20.117        131     292.2        25     85.092     1236.1
4                   1.50               4     6.625         58      96.2        29     91.717     1332.3
10                  1.00              10    12.032        145     174.8        39    103.749     1507.1
9                   0.80               9     7.934        131     115.2        48    111.683     1622.4
5                   0.60               5     3.539         73      51.4        53    115.222     1673.8
13                  0.40              13     6.188        189      89.9        66    121.411     1763.7
11                  0.30              11     4.039        160      58.7        77    125.450     1822.4
5                   0.25               5     1.333         73      19.4        82    126.783     1841.7
7                   0.20               7     1.548        102      22.5        89    128.332     1864.2
4                   0.15               4     0.683         58       9.9        93    129.015     1874.1
21                  0.10              21     2.591        305      37.6       114    131.606     1911.8
8                   0.09               8     0.753        116      10.9       122    132.359     1922.7
10                  0.08              10     0.866        145      12.6       132    133.224     1935.3
3                   0.07               3     0.226         44       3.3       135    133.450     1938.6
9                   0.06               9     0.575        131       8.4       144    134.025     1946.9
22                  0.05              22     1.206        320      17.5       166    135.231     1964.4
24                  0.04 TAPPI        24     1.091        349      15.9       190    136.323     1980.3
42                  0.03              42     1.455        610      21.1       232    137.778     2001.4
85                  0.02              85     2.047       1235      29.7       317    139.825     2031.2
180                 0.014            180     2.928       2615      42.5       497    142.753     2073.7
638                 0.007            638     5.731       9268      83.3      1135    148.484     2157.0
        400         -------------  -------  ----------  --------  --------
                    Totals ->       1135   148.484      16488    2157.0

Categories:          Min  Max  Min  Max                       ---- Calculated ---- Average  Darkest     Average
                     Avg. Avg. MeasMeas.   Count    Area      Count     PPM    GrayscaleGrayscale   Size
                     Gray Gray Area Area           (sq.mm)    (in 1 sq.meter)                        (sq.mm)
                     ---- ---- ---- ----   -----   --------   -------  -------  --------  --------  --------
0-39 GSV               0   39  0.02099999
40-79 GSV             40   79  0.02099999
80-119 GSV            80  119  0.02099999    32    61.367      465    891.5   101.66     13.00      1.918
120-129 GSV          120  129  0.02099999    13     9.339      189    135.7   125.69     15.00      0.718
130-139 GSV          130  139  0.02099999    16     7.794      232    113.2   134.44      0.00      0.487
140-149 GSV          140  149  0.02099999    24    10.190      349    148.0   144.96     48.00      0.425
150-159GSV           150  159  0.02099999
160-169GSV           160  169  0.02099999    28     1.855      407     26.9   165.11     91.00      0.066
170-255 GVV          170  255  0.02099999    43    11.479      625    166.7   180.49     95.00      0.267
Total > 0.02 sq mm     0  255  0.02099999    70    36.520     1017    530.5   175.09     29.00      0.522

Sample Grayscale Brightness Analysis:                   Dirt Count Summary:
                                                                                  All Sizes    >=0.040
                 99% Min      Mode     99% Max                                  -----------  -----------
                 ---------   -------  ---------          Number of Specks:          1135        190
 Dirt Content:      40         197       197             Avg. Speck Area:         0.1308     0.7175
 Fiber Content:    222         254       254             Median Speck Area:       0.0132     0.1452
 Overall           221         254       254             Total Area (sq.mm):      148.48     136.32
                                                         Parts Per Million:       2157.0     1980.3
 Overall Grayscale Brightness  =   243.2 =  95.4%        StdDev of Sheet PPM:    1322.83    1330.73
 Overall Grayscale Std Deviation =   9.3 =   3.7%        Count in 1 sq.m:          16488       2760
 Std.Dev. of Sheet Overall Ave.  =   1.3 =   0.5%        Counting Precision:        2.97       7.25
```

Apogee Systems, Inc.

Spec*Scan 2000 - V.2.2r

Mon 4-Nov-2002 17:06

Scanner Settings:	Lucas
Grade Identification:	100% UCAR9165, 450H Pulper 30 minutes Set
Load / Reel Number:	6530-1:6, dyed and rinsed, wire side

Resolution: 600 dots/inch
Threshold: 197 (80.0%+ 0.0)
256-shade Grayscale mode
Normal Image Mode
Scan-to-Screen

5 sheets 6-inch round
Total Area Scanned: 0.068839 sq.m.

Sheet	Speck Data			Overall Gray		Dirt Grayscale				Fiber Grayscale			
Number	Count	Area	PPM	Ave.	StdDev	2σ Min	Mode	2σ Max	Ave.	2σ Min	Mode	2σ Max	Ave.
1	303	25.75	1870.5	244.89	8.96	53	197	197	141.5	230	254	254	245.1
2	221	26.30	1909.9	243.87	8.80	40	196	197	138.6	230	254	254	244.1
3	190	11.85	860.9	242.65	8.08	54	197	197	151.3	228	254	254	242.7
4	204	60.51	4395.2	241.43	11.40	33	197	197	130.8	226	254	254	241.9
5	217	24.07	1748.3	243.31	8.65	43	195	197	139.2	229	254	254	243.5
Sample	1135	148.48	2157.0	243.23	9.32	40	197	197	137.2	229	254	254	243.5

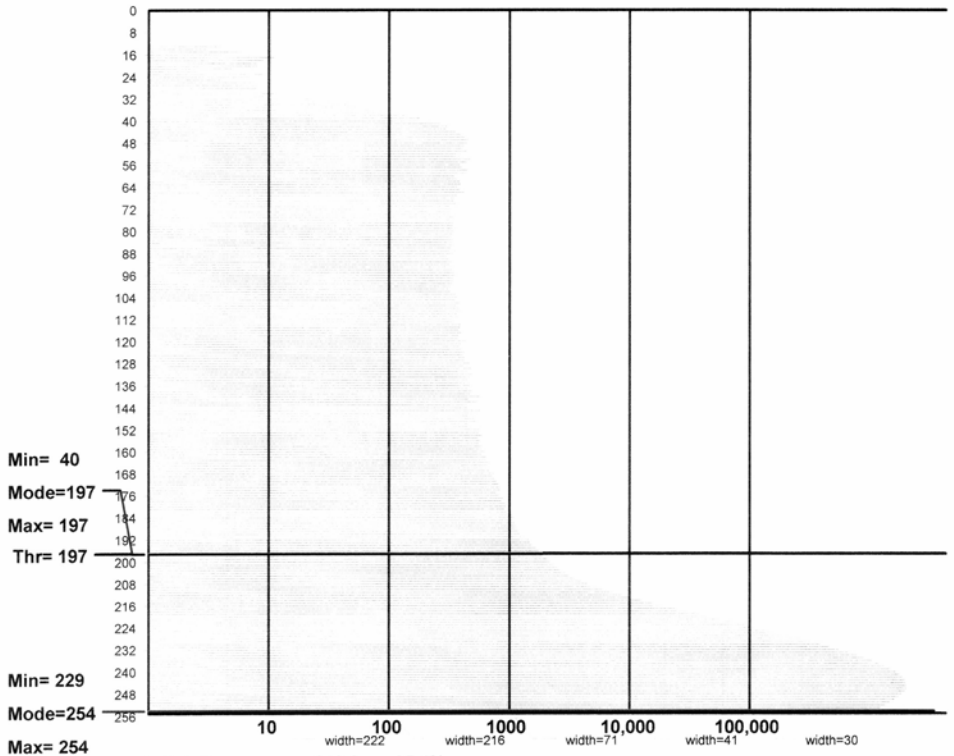

Overall Grayscale Brightness = 243.2 = 95.4%
Overall Grayscale Std Deviation = 9.3 = 3.7%

APPENDIX 4

STATISTICAL ANALYSIS USING SAS SYSTEMS

One computer package available for experimental data analysis is provided by SAS Systems. Models may be developed for each of the dependent variables in terms of all of the dependent variables involved in the experiments. For this package, all of the independent and dependent variables involved in the experiments must be listed as the input. The values for the independent variables must be converted into a scale of –1 to +1 so that all of the independent variables are in the same range. Interactions between the independent variables may be considered by setting up the multiplication equations for the variables involved in each interaction combination.

Models involving the independent variables and their interactions can be analyzed by forward, backward, or maximum R^2 mode. In forward mode, the model begins with the most significant variable or interaction and adds a variable or interaction with each step until all of the variables and interactions are in the model. In backward mode, the model begins with all of the variables and interactions in the model and removes a variable or interaction with each step until all of the variables and interactions in the model are significant at the 0.1000 level. In maximum R^2 mode, the model considers all of the variables and interactions that contribute to the R^2 value.

The R^2 value and the F value are used to determine the validity of a model. The R^2 value indicates the fraction of the experimental data that can be explained by the model, so the closer the R^2 value is to 1, the better the model. The F value indicates the ratio between the model and the error, so the higher the F value is, the better the model.

```
DATA QUANTUM;
INPUT CONS TIME TEMP ROTOR PPM SIZE NUMBER;
CARDS;
-1 -1 -1 -1 3116 0.634 4917
1 -1 -1 -1 2605 0.669 3894
-1 1 -1 -1 1914 0.438 4373
1 1 -1 -1 1962 0.173 11346
-1 -1 1 -1 3062 0.620 4939
1 -1 1 -1 2048 0.333 6145
-1 1 1 -1 2261 0.447 5056
1 1 1 -1 1936 0.133 14520
-1 -1 -1 1 2689 0.679 3958
1 -1 -1 1 2064 0.470 4395
-1 1 -1 1 2173 0.962 2259
1 1 -1 1 1919 0.219 8767
-1 -1 1 1 2195 0.670 3276
1 -1 1 1 2258 0.384 5876
-1 1 1 1 2697 0.378 7133
1 1 1 1 1965 0.145 13590
0 0 0 0 2346 0.765 3066
0 0 0 0 2388 0.612 3901
0 0 0 0 2626 0.465 5643
0 0 0 0 2765 0.552 5012
PROC PRINT DATA = QUANTUM;
DATA ANAL; SET QUANTUM;
CONSTIME = CONS * TIME;
CONSTEMP = CONS * TEMP;
CONSROTOR = CONS * ROTOR;
TIMETEMP = TIME * TEMP;
TIMEROTOR = TIME * ROTOR;
TEMPROTOR = TEMP * ROTOR;
COTITE = CONS * TIME * TEMP;
COTIRO = CONS * TIME * ROTOR;
COTERO = CONS * TEMP * ROTOR;
TITERO = TIME * TEMP * ROTOR;
COTITERO = CONS * TIME * TEMP * ROTOR;
PROC CORR;
PROC REG;
        MODEL PPM = CONS TIME
                    TEMP ROTOR
                    CONSTIME CONSTEMP
                    CONSROTOR TIMETEMP
                    TIMEROTOR TEMPROTOR
                    COTITE COTIRO
                    COTERO TITERO
                    COTITERO / SELECTION = BACKWARD;
        MODEL SIZE = CONS TIME
                     TEMP ROTOR
                     CONSTIME CONSTEMP
                     CONSROTOR TIMETEMP
                     TIMEROTOR TEMPROTOR
                     COTITE COTIRO
                     COTERO TITERO
                     COTITERO / SELECTION = BACKWARD;
        MODEL NUMBER = CONS TIME
                          TEMP ROTOR
                       CONSTIME CONSTEMP
                       CONSROTOR TIMETEMP
                       TIMEROTOR TEMPROTOR
                       COTITE COTIRO
                       COTERO TITERO
                       COTITERO / SELECTION = BACKWARD;
RUN;
```

```
                The SAS System        07:42 Friday, April 28, 2000  1

              Obs    CONS    TIME    TEMP    ROTOR     PPM     SIZE    NUMBER

                1     -1      -1      -1      -1      3116    0.634      4917
                2      1      -1      -1      -1      2605    0.669      3894
                3     -1       1      -1      -1      1914    0.438      4373
                4      1       1      -1      -1      1962    0.173     11346
                5     -1      -1       1      -1      3062    0.620      4939
                6      1      -1       1      -1      2048    0.333      6145
                7     -1       1       1      -1      2261    0.447      5056
                8      1       1       1      -1      1936    0.133     14520
                9     -1      -1      -1       1      2689    0.679      3958
               10      1      -1      -1       1      2064    0.470      4395
               11     -1       1      -1       1      2173    0.962      2259
               12      1       1      -1       1      1919    0.219      8767
               13     -1      -1       1       1      2195    0.670      3276
               14      1      -1       1       1      2258    0.384      5876
               15     -1       1       1       1      2697    0.378      7133
               16      1       1       1       1      1965    0.145     13590
               17      0       0       0       0      2346    0.765      3066
               18      0       0       0       0      2388    0.612      3901
               19      0       0       0       0      2626    0.465      5643
               20      0       0       0       0      2765    0.552      5012

                                 The CORR Procedure

  18  Variables:  CONS      TIME      TEMP      ROTOR     PPM       SIZE      NUMBER
CONSTIME
                  CONSTEMP  CONSROTOR TIMETEMP  TIMEROTOR TEMPROTOR COTITE    COTIRO
COTERO
                  TITERO    COTITERO


                                    Simple Statistics

  Variable             N          Mean       Std Dev           Sum       Minimum
Maximum

  CONS                20             0       0.91766             0      -1.00000
1.00000
  TIME                20             0       0.91766             0      -1.00000
1.00000
  TEMP                20             0       0.91766             0      -1.00000
1.00000
  ROTOR               20             0       0.91766             0      -1.00000
1.00000
  PPM                 20          2349     379.38114         46989          1914
3116
  SIZE                20       0.48740       0.22115       9.74800       0.13300
0.96200
  NUMBER              20          6103          3403        122066          2259
14520
  CONSTIME            20             0       0.91766             0      -1.00000
1.00000
  CONSTEMP            20             0       0.91766             0      -1.00000
1.00000
  CONSROTOR           20             0       0.91766             0      -1.00000
1.00000
  TIMETEMP            20             0       0.91766             0      -1.00000
1.00000
  TIMEROTOR           20             0       0.91766             0      -1.00000
1.00000
  TEMPROTOR           20             0       0.91766             0      -1.00000
1.00000
  COTITE              20             0       0.91766             0      -1.00000
1.00000
  COTIRO              20             0       0.91766             0      -1.00000
1.00000
  COTERO              20             0       0.91766             0      -1.00000
1.00000
  TITERO              20             0       0.91766             0      -1.00000
1.00000
  COTITERO            20             0       0.91766             0      -1.00000
1.00000


                         Pearson Correlation Coefficients, N = 20
                                Prob > |r| under H0: Rho=0
```

```
                  CONS        TIME        TEMP       ROTOR         PPM        SIZE
NUMBER

 CONS          1.00000     0.00000     0.00000     0.00000    -0.50644    -0.59702
0.54973
                            1.0000      1.0000      1.0000      0.0227      0.0054
0.0120

 TIME          0.00000     1.00000     0.00000     0.00000    -0.48528    -0.40562
0.49954
                1.0000                  1.0000      1.0000      0.0301      0.0760
0.0249

 TEMP          0.00000     0.00000     1.00000     0.00000    -0.00302    -0.29410
0.28017
                1.0000      1.0000                  1.0000      0.9899      0.2082
0.2315

 ROTOR         0.00000     0.00000     0.00000     1.00000    -0.14271     0.11930    -
0.10003
                1.0000      1.0000      1.0000                  0.5484      0.6164
0.6748

 PPM          -0.50644    -0.48528    -0.00302    -0.14271     1.00000     0.49835    -
0.42426
                0.0227      0.0301      0.9899      0.5484                  0.0253
0.0623

 SIZE         -0.59702    -0.40562    -0.29410     0.11930     0.49835     1.00000    -
0.87455
                0.0054      0.0760      0.2082      0.6164      0.0253
<.0001

 NUMBER        0.54973     0.49954     0.28017    -0.10003    -0.42426    -0.87455
1.00000
                0.0120      0.0249      0.2315      0.6748      0.0623      <.0001

 CONSTIME      0.00000     0.00000     0.00000     0.00000     0.12457    -0.20955
0.44121
                1.0000      1.0000      1.0000      1.0000      0.6008      0.3752
0.0515

 CONSTEMP      0.00000     0.00000     0.00000     0.00000    -0.10068     0.01608
0.11513
                1.0000      1.0000      1.0000      1.0000      0.6728      0.9464
0.6289

 CONSROTOR     0.00000     0.00000     0.00000     0.00000     0.03840    -0.16598    -
0.01041
                1.0000      1.0000      1.0000      1.0000      0.8723      0.4843
0.9652

 TIMETEMP      0.00000     0.00000     0.00000     0.00000     0.27242    -0.06328
0.17664
                1.0000      1.0000      1.0000      1.0000      0.2452      0.7910
0.4563

 TIMEROTOR     0.00000     0.00000     0.00000     0.00000     0.34862     0.14679    -
0.01948
                1.0000      1.0000      1.0000      1.0000      0.1320      0.5369
0.9350

 TEMPROTOR     0.00000     0.00000     0.00000     0.00000     0.08466    -0.09648
0.07357
                1.0000      1.0000      1.0000      1.0000      0.7227      0.6858
0.7579

 COTITE        0.00000     0.00000     0.00000     0.00000    -0.15662     0.22304    -
0.03289
                1.0000      1.0000      1.0000      1.0000      0.5096      0.3445
0.8905

 COTIRO        0.00000     0.00000     0.00000     0.00000    -0.25277    -0.03994    -
0.10660
                1.0000      1.0000      1.0000      1.0000      0.2823      0.8672
0.6546

 COTERO        0.00000     0.00000     0.00000     0.00000     0.16418     0.20852    -
0.04395
                1.0000      1.0000      1.0000      1.0000      0.4891      0.3777
0.8540
```

```
 TITERO          0.00000      0.00000      0.00000      0.00000     -0.00937     -0.22874
0.12325
                  1.0000       1.0000       1.0000       1.0000       0.9687       0.3320
0.6047

 COTITERO        0.00000      0.00000      0.00000      0.00000     -0.19593      0.08144    -
0.04172
                  1.0000       1.0000       1.0000       1.0000       0.4078       0.7329
0.8613

                CONSTIME       CONSTEMP       CONSROTOR       TIMETEMP       TIMEROTOR
TEMPROTOR

 CONS            0.00000        0.00000         0.00000        0.00000         0.00000
0.00000
                  1.0000         1.0000          1.0000         1.0000          1.0000
1.0000

 TIME            0.00000        0.00000         0.00000        0.00000         0.00000
0.00000
                  1.0000         1.0000          1.0000         1.0000          1.0000
1.0000

 TEMP            0.00000        0.00000         0.00000        0.00000         0.00000
0.00000
                  1.0000         1.0000          1.0000         1.0000          1.0000
1.0000

 ROTOR           0.00000        0.00000         0.00000        0.00000         0.00000
0.00000
                  1.0000         1.0000          1.0000         1.0000          1.0000
1.0000

 PPM             0.12457       -0.10068         0.03840        0.27242         0.34862
0.08466
                  0.6008         0.6728          0.8723         0.2452          0.1320
0.7227

 SIZE           -0.20955        0.01608        -0.16598       -0.06328         0.14679        -
0.09648
                  0.3752         0.9464          0.4843         0.7910          0.5369
0.6858

 NUMBER          0.44121        0.11513        -0.01041        0.17664        -0.01948
0.07357
                  0.0515         0.6289          0.9652         0.4563          0.9350
0.7579

 CONSTIME        1.00000        0.00000         0.00000        0.00000         0.00000
0.00000
                                 1.0000          1.0000         1.0000          1.0000
1.0000

 CONSTEMP        0.00000        1.00000         0.00000        0.00000         0.00000
0.00000
                  1.0000                         1.0000         1.0000          1.0000
1.0000

 CONSROTOR       0.00000        0.00000         1.00000        0.00000         0.00000
0.00000
                  1.0000         1.0000                         1.0000          1.0000
1.0000

 TIMETEMP        0.00000        0.00000         0.00000        1.00000         0.00000
0.00000
                  1.0000         1.0000          1.0000                         1.0000
1.0000

 TIMEROTOR       0.00000        0.00000         0.00000        0.00000         1.00000
0.00000
                  1.0000         1.0000          1.0000         1.0000
1.0000

 TEMPROTOR       0.00000        0.00000         0.00000        0.00000         0.00000
1.00000
                  1.0000         1.0000          1.0000         1.0000          1.0000

 COTITE          0.00000        0.00000         0.00000        0.00000         0.00000
0.00000
```

```
                  1.0000         1.0000          1.0000         1.0000          1.0000
1.0000

 COTIRO          0.00000        0.00000         0.00000        0.00000         0.00000
0.00000
                  1.0000         1.0000          1.0000         1.0000          1.0000
1.0000

 COTERO          0.00000        0.00000         0.00000        0.00000         0.00000
0.00000
                  1.0000         1.0000          1.0000         1.0000          1.0000
1.0000

 TITERO          0.00000        0.00000         0.00000        0.00000         0.00000
0.00000
                  1.0000         1.0000          1.0000         1.0000          1.0000
1.0000

 COTITERO        0.00000        0.00000         0.00000        0.00000         0.00000
0.00000
                  1.0000         1.0000          1.0000         1.0000          1.0000
1.0000
                                  COTITE         COTIRO         COTERO         TITERO       COTITERO

         CONS                    0.00000        0.00000        0.00000        0.00000        0.00000
                                  1.0000         1.0000         1.0000         1.0000         1.0000

         TIME                    0.00000        0.00000        0.00000        0.00000        0.00000
                                  1.0000         1.0000         1.0000         1.0000         1.0000

         TEMP                    0.00000        0.00000        0.00000        0.00000        0.00000
                                  1.0000         1.0000         1.0000         1.0000         1.0000

         ROTOR                   0.00000        0.00000        0.00000        0.00000        0.00000
                                  1.0000         1.0000         1.0000         1.0000         1.0000

         PPM                    -0.15662       -0.25277        0.16418       -0.00937       -0.19593
                                  0.5096         0.2823         0.4891         0.9687         0.4078

         SIZE                    0.22304       -0.03994        0.20852       -0.22874        0.08144
                                  0.3445         0.8672         0.3777         0.3320         0.7329

         NUMBER                 -0.03289       -0.10660       -0.04395        0.12325       -0.04172
                                  0.8905         0.6546         0.8540         0.6047         0.8613

         CONSTIME                0.00000        0.00000        0.00000        0.00000        0.00000
                                  1.0000         1.0000         1.0000         1.0000         1.0000

         CONSTEMP                0.00000        0.00000        0.00000        0.00000        0.00000
                                  1.0000         1.0000         1.0000         1.0000         1.0000

         CONSROTOR               0.00000        0.00000        0.00000        0.00000        0.00000
                                  1.0000         1.0000         1.0000         1.0000         1.0000

        TIMETEMP                0.00000        0.00000        0.00000        0.00000        0.00000
                                  1.0000         1.0000         1.0000         1.0000         1.0000

         TIMEROTOR               0.00000        0.00000        0.00000        0.00000        0.00000
                                  1.0000         1.0000         1.0000         1.0000         1.0000

         TEMPROTOR               0.00000        0.00000        0.00000        0.00000        0.00000
                                  1.0000         1.0000         1.0000         1.0000         1.0000

         COTITE                  1.00000        0.00000        0.00000        0.00000        0.00000
                                                 1.0000         1.0000         1.0000         1.0000

         COTIRO                  0.00000        1.00000        0.00000        0.00000        0.00000
                                  1.0000                        1.0000         1.0000         1.0000

         COTERO                  0.00000        0.00000        1.00000        0.00000        0.00000
                                  1.0000         1.0000                        1.0000         1.0000

         TITERO                  0.00000        0.00000        0.00000        1.00000        0.00000
                                  1.0000         1.0000         1.0000                        1.0000

         COTITERO                0.00000        0.00000        0.00000        0.00000        1.00000
                                  1.0000         1.0000         1.0000         1.0000
```

```
                             The REG Procedure
                                 Model: MODEL1
                            Dependent Variable: PPM

                          Backward Elimination: Step 0

               All Variables Entered: R-Square = 0.8579 and C(p) = 15.0000


                              Analysis of Variance

                                        Sum of           Mean
         Source                  DF        Squares         Square    F Value    Pr > F

         Model                   14        2345984         167570       2.16    0.2033
         Error                    5         388687          77737
         Corrected Total         19        2734671


                     Parameter     Standard
               Variable      Estimate        Error   Type II SS  F Value  Pr > F

               Intercept   2349.45000     62.34476    110398306  1420.14  <.0001
               CONS        -209.37500     69.70356       701406     9.02  0.0300
               TIME        -200.62500     69.70356       644006     8.28  0.0347
               TEMP          -1.25000     69.70356     25.00000     0.00  0.9864
               ROTOR        -59.00000     69.70356        55696     0.72  0.4359
               CONSTIME      51.50000     69.70356        42436     0.55  0.4932
               CONSTEMP     -41.62500     69.70356        27722     0.36  0.5764
               CONSROTOR     15.87500     69.70356   4032.25000     0.05  0.8289
               TIMETEMP     112.62500     69.70356       202950     2.61  0.1671
               TIMEROTOR    144.12500     69.70356       332352     4.28  0.0935
               TEMPROTOR     35.00000     69.70356        19600     0.25  0.6369
               COTITE       -64.75000     69.70356        67081     0.86  0.3956
               COTIRO      -104.50000     69.70356       174724     2.25  0.1941
               COTERO        67.87500     69.70356        73712     0.95  0.3749
               TITERO        -3.87500     69.70356    240.25000     0.00  0.9578

                          Bounds on condition number: 1, 196
-----------------------------------------------------------------------------------------
-------
```

```
                                  The REG Procedure
                                     Model: MODEL1
                                 Dependent Variable: PPM

                                Backward Elimination: Step 9

                    Variable COTERO Removed: R-Square = 0.7516 and C(p) = 0.7375


                                   Analysis of Variance

                                               Sum of           Mean
         Source                      DF        Squares         Square    F Value    Pr > F

         Model                        5        2055439         411088       8.47    0.0007
         Error                       14         679232          48517
         Corrected Total             19        2734671


                          Parameter     Standard
               Variable    Estimate        Error   Type II SS  F Value  Pr > F

               Intercept  2349.45000     49.25270   110398306  2275.48  <.0001
               CONS       -209.37500     55.06619      701406    14.46  0.0019
               TIME       -200.62500     55.06619      644006    13.27  0.0027
               TIMETEMP    112.62500     55.06619      202950     4.18  0.0601
               TIMEROTOR   144.12500     55.06619      332352     6.85  0.0203
               COTIRO     -104.50000     55.06619      174724     3.60  0.0785

                             Bounds on condition number: 1, 25
-----------------------------------------------------------------------------------------
-------


              All variables left in the model are significant at the 0.1000 level.



                              Summary of Backward Elimination

              Variable     Number     Partial      Model
      Step    Removed      Vars In    R-Square    R-Square      C(p)      F Value    Pr >
F

        1     TEMP            13       0.0000      0.8579     13.0003        0.00
0.9864
        2     TITERO          12       0.0001      0.8578     11.0034        0.00
0.9534
        3     CONSROTOR       11       0.0015      0.8563      9.0553        0.07
0.7954
        4     TEMPROTOR       10       0.0072      0.8491      7.3074        0.40
0.5452
        5     CONSTEMP         9       0.0101      0.8390      5.6640        0.60
0.4567
        6     CONSTIME         8       0.0155      0.8235      4.2099        0.96
0.3494
        7     ROTOR            7       0.0204      0.8031      2.9264        1.27
0.2839
        8     COTITE           6       0.0245      0.7786      1.7893        1.50
0.2449
        9     COTERO           5       0.0270      0.7516      0.7375        1.58
0.2305
```

```
                              The REG Procedure
                                Model: MODEL2
                          Dependent Variable: SIZE

                          Backward Elimination: Step 0

             All Variables Entered: R-Square = 0.8754 and C(p) = 15.0000


                              Analysis of Variance

                                       Sum of           Mean
Source                     DF         Squares         Square    F Value    Pr > F

Model                      14         0.81344        0.05810       2.51    0.1582
Error                       5         0.11577        0.02315
Corrected Total            19         0.92921


            Parameter     Standard
Variable     Estimate        Error   Type II SS  F Value  Pr > F

Intercept     0.48740      0.03402      4.75118   205.20  <.0001
CONS         -0.14388      0.03804      0.33120    14.30  0.0129
TIME         -0.09775      0.03804      0.15288     6.60  0.0501
TEMP         -0.07088      0.03804      0.08037     3.47  0.1215
ROTOR         0.02875      0.03804      0.01323     0.57  0.4838
CONSTIME     -0.05050      0.03804      0.04080     1.76  0.2417
CONSTEMP      0.00388      0.03804   0.00024025     0.01  0.9228
CONSROTOR    -0.04000      0.03804      0.02560     1.11  0.3412
TIMETEMP     -0.01525      0.03804      0.00372     0.16  0.7051
TIMEROTOR     0.03537      0.03804      0.02002     0.86  0.3951
TEMPROTOR    -0.02325      0.03804      0.00865     0.37  0.5678
COTITE        0.05375      0.03804      0.04623     2.00  0.2168
COTIRO       -0.00962      0.03804      0.00148     0.06  0.8103
COTERO        0.05025      0.03804      0.04040     1.74  0.2437
TITERO       -0.05512      0.03804      0.04862     2.10  0.2070

                   Bounds on condition number: 1, 196
```

```
                              The REG Procedure
                                Model: MODEL2
                          Dependent Variable: SIZE

                         Backward Elimination: Step 11

             Variable TITERO Removed: R-Square = 0.6075 and C(p) = 3.7539

                             Analysis of Variance

                                         Sum of           Mean
         Source                   DF    Squares         Square    F Value    Pr > F

         Model                     3    0.56445        0.18815       8.25    0.0015
         Error                    16    0.36476        0.02280
         Corrected Total          19    0.92921

                        Parameter     Standard
           Variable      Estimate        Error   Type II SS  F Value  Pr > F

           Intercept      0.48740      0.03376      4.75118   208.41  <.0001
           CONS          -0.14388      0.03775      0.33120    14.53  0.0015
           TIME          -0.09775      0.03775      0.15288     6.71  0.0198
           TEMP          -0.07088      0.03775      0.08037     3.53  0.0788

                          Bounds on condition number: 1, 9
-----------------------------------------------------------------------------------------
-------

          All variables left in the model are significant at the 0.1000 level.



                          Summary of Backward Elimination

            Variable     Number     Partial     Model
      Step    Removed      Vars In    R-Square    R-Square     C(p)      F Value    Pr >
F

         1    CONSTEMP        13       0.0003      0.8752    13.0104       0.01
0.9228
         2    COTIRO          12       0.0016      0.8736    11.0744       0.08
0.7912
         3    TIMETEMP        11       0.0040      0.8696     9.2351       0.22
0.6521
         4    TEMPROTOR       10       0.0093      0.8602     7.6087       0.57
0.4716
         5    ROTOR            9       0.0142      0.8460     6.1798       0.92
0.3634
         6    TIMEROTOR        8       0.0215      0.8245     5.0446       1.40
0.2642
         7    CONSROTOR        7       0.0276      0.7969     4.1503       1.73
0.2156
         8    COTERO           6       0.0435      0.7534     3.8952       2.57
0.1349
         9    CONSTIME         5       0.0439      0.7095     3.6575       2.32
0.1521
        10    COTITE           4       0.0497      0.6598     3.6540       2.40
0.1438
        11    TITERO           3       0.0523      0.6075     3.7539       2.31
0.1496
```

```
                              The REG Procedure
                                Model: MODEL3
                          Dependent Variable: NUMBER

                         Backward Elimination: Step 0

               All Variables Entered: R-Square = 0.9148 and C(p) = 15.0000


                             Analysis of Variance

                                        Sum of           Mean
Source                   DF            Squares         Square    F Value    Pr > F

Model                    14          201348270       14382019       3.84    0.0728
Error                     5           18743814        3748763
Corrected Total          19          220092084


             Parameter     Standard
Variable      Estimate        Error   Type II SS  F Value  Pr > F

Intercept   6103.30000    432.94127    745005418   198.73  <.0001
CONS        2038.87500    484.04305     66512180    17.74  0.0084
TIME        1852.75000    484.04305     54922921    14.65  0.0123
TEMP        1039.12500    484.04305     17276492     4.61  0.0846
ROTOR       -371.00000    484.04305      2202256     0.59  0.4780
CONSTIME    1636.37500    484.04305     42843570    11.43  0.0197
CONSTEMP     427.00000    484.04305      2917264     0.78  0.4181
CONSROTOR    -38.62500    484.04305        23870     0.01  0.9395
TIMETEMP     655.12500    484.04305      6867020     1.83  0.2339
TIMEROTOR    -72.25000    484.04305        83521     0.02  0.8872
TEMPROTOR    272.87500    484.04305      1191372     0.32  0.5973
COTITE      -122.00000    484.04305       238144     0.06  0.8110
COTIRO      -395.37500    484.04305      2501142     0.67  0.4512
COTERO      -163.00000    484.04305       425104     0.11  0.7500
TITERO       457.12500    484.04305      3343412     0.89  0.3883

                      Bounds on condition number: 1, 196
```

```
                                     The REG Procedure
                                       Model: MODEL3
                                Dependent Variable: NUMBER

                               Backward Elimination: Step 10


                 Variable TIMETEMP Removed: R-Square = 0.8249 and C(p) = 0.2799


                                       Analysis of Variance

                                              Sum of           Mean
         Source                     DF       Squares         Square    F Value    Pr > F

         Model                       4      181555164       45388791      17.67    <.0001
         Error                      15       38536920        2569128
         Corrected Total            19      220092084


                            Parameter      Standard
               Variable      Estimate         Error   Type II SS  F Value  Pr > F

               Intercept   6103.30000     358.40815    745005418   289.98  <.0001
               CONS        2038.87500     400.71249     66512180    25.89  0.0001
               TIME        1852.75000     400.71249     54922921    21.38  0.0003
               TEMP        1039.12500     400.71249     17276492     6.72  0.0204
               CONSTIME    1636.37500     400.71249     42843570    16.68  0.0010

                                Bounds on condition number: 1, 16
------------------------------------------------------------------------------------------
-------


              All variables left in the model are significant at the 0.1000 level.


                                 Summary of Backward Elimination

              Variable     Number     Partial      Model
      Step    Removed      Vars In    R-Square     R-Square     C(p)      F Value    Pr >
F

        1     CONSROTOR       13        0.0001      0.9147     13.0064       0.01
0.9395
        2     TIMEROTOR       12        0.0004      0.9143     11.0286       0.03
0.8756
        3     COTITE          11        0.0011      0.9133      9.0922       0.09
0.7748
        4     COTERO          10        0.0019      0.9113      7.2056       0.18
0.6841
        5     TEMPROTOR        9        0.0054      0.9059      5.5234       0.55
0.4774
        6     ROTOR            8        0.0100      0.8959      4.1108       1.06
0.3267
        7     COTIRO           7        0.0114      0.8846      2.7780       1.20
0.2965
        8     CONSTEMP         6        0.0133      0.8713      1.5562       1.38
0.2633
        9     TITERO           5        0.0152      0.8561      0.4481       1.53
0.2374
       10     TIMETEMP         4        0.0312      0.8249      0.2799       3.04
0.1034
```

APPENDIX 5

UCAR LATEX 9165 MATERIAL SAFETY DATA SHEET

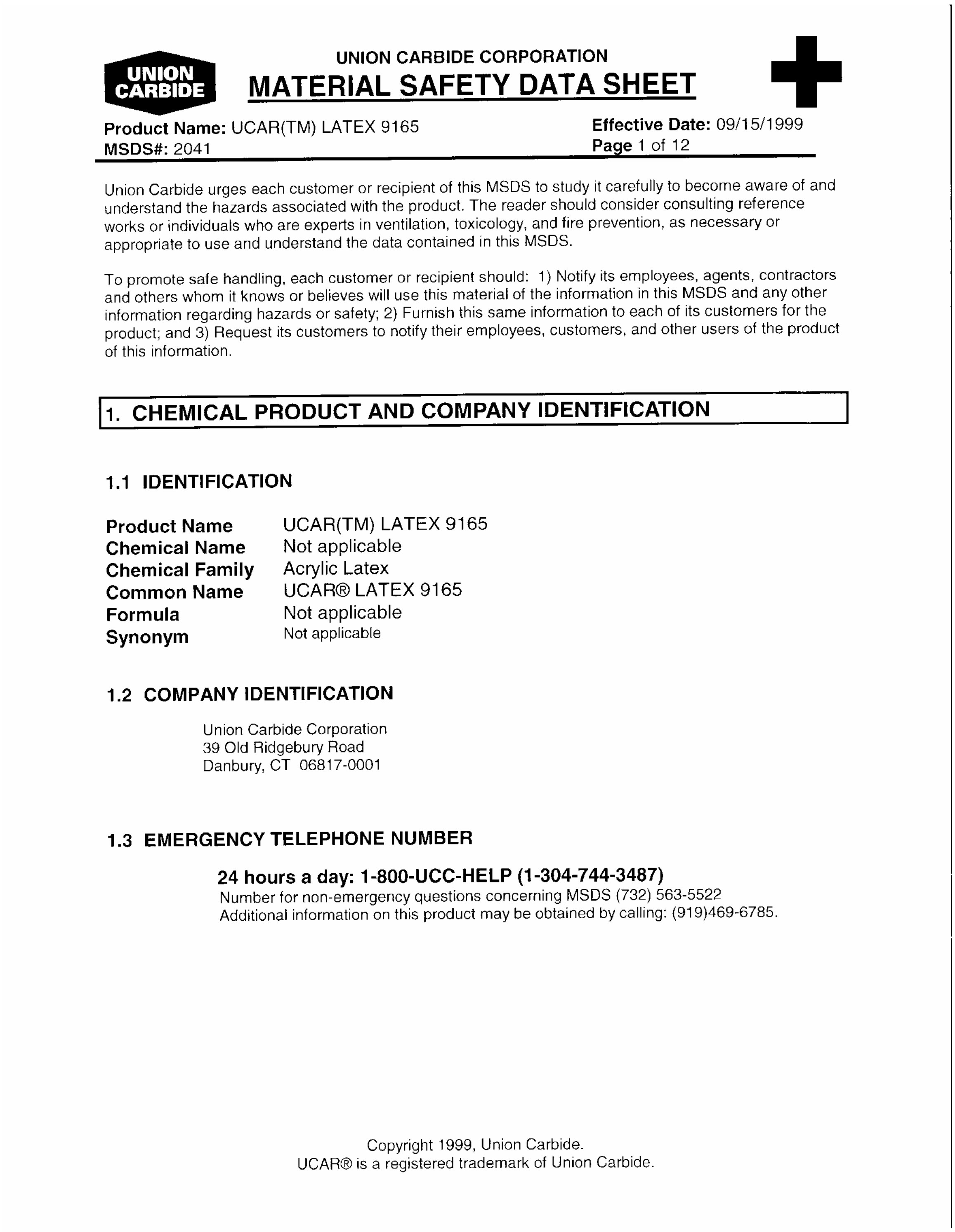

UNION CARBIDE CORPORATION

MATERIAL SAFETY DATA SHEET

Product Name: UCAR(TM) LATEX 9165
MSDS#: 2041

Effective Date: 09/15/1999
Page 1 of 12

Union Carbide urges each customer or recipient of this MSDS to study it carefully to become aware of and understand the hazards associated with the product. The reader should consider consulting reference works or individuals who are experts in ventilation, toxicology, and fire prevention, as necessary or appropriate to use and understand the data contained in this MSDS.

To promote safe handling, each customer or recipient should: 1) Notify its employees, agents, contractors and others whom it knows or believes will use this material of the information in this MSDS and any other information regarding hazards or safety; 2) Furnish this same information to each of its customers for the product; and 3) Request its customers to notify their employees, customers, and other users of the product of this information.

1. CHEMICAL PRODUCT AND COMPANY IDENTIFICATION

1.1 IDENTIFICATION

Product Name	UCAR(TM) LATEX 9165
Chemical Name	Not applicable
Chemical Family	Acrylic Latex
Common Name	UCAR® LATEX 9165
Formula	Not applicable
Synonym	Not applicable

1.2 COMPANY IDENTIFICATION

Union Carbide Corporation
39 Old Ridgebury Road
Danbury, CT 06817-0001

1.3 EMERGENCY TELEPHONE NUMBER

24 hours a day: 1-800-UCC-HELP (1-304-744-3487)
Number for non-emergency questions concerning MSDS (732) 563-5522
Additional information on this product may be obtained by calling: (919)469-6785.

Copyright 1999, Union Carbide.
UCAR® is a registered trademark of Union Carbide.

2. COMPOSITION INFORMATION

Component	CAS #	Amount
Butyl acrylate, methyl methacrylate, hydroxyethyl acrylate polymer	25951-38-6	< 53.%
Water	7732-18-5	47. %
Ammonia	7664-41-7	0.2 %

3. HAZARDS IDENTIFICATION

3.1 EMERGENCY OVERVIEW

Appearance	White	
Physical State	Liquid	
Odor	Mild	
Hazards of product	WARNING!	VAPOR MAY BE HARMFUL IF INHALED. MAY CAUSE SKIN IRRITATION.

3.2 POTENTIAL HEALTH EFFECTS

Effects of Single Acute Overexposure

Inhalation May cause irritation of the respiratory tract, experienced as burning sensation of eyes, nose, and throat, sneezing, coughing, and nausea.

Eye Contact Liquid may cause discomfort in the eye with slight excess redness and possibly swelling of the conjunctiva.

Skin Contact Brief contact is not irritating. Prolonged contact, as from clothing wet with the material, may cause mild irritation, experienced as discomfort, and seen as local redness.

Skin Absorption No evidence of harmful effects from available information.

Swallowing No evidence of harmful effects from available information.

Chronic, Prolonged or Repeated Overexposure

Effects of Repeated Overexposure No adverse effects anticipated from available information.

Other Effects of Overexposure None currently known.

Medical Conditions Aggravated by Exposure

A knowledge of available toxicology information and of the physical and chemical properties of the material suggests that overexposure is unlikely to aggravate existing medical conditions.

3.3 POTENTIAL ENVIRONMENTAL EFFECTS

See Section 12 for Ecological Information.

4. FIRST AID PROCEDURES

4.1 INHALATION

Remove to fresh air. Give artificial respiration if not breathing. Oxygen may be given by qualified personnel if necessary. Call a physician.

4.2 EYE CONTACT

Immediately flush eyes with water and continue washing for several minutes. Remove contact lenses, if worn. Obtain medical attention

4.3 SKIN CONTACT

Remove contaminated clothing. Wash skin with soap and water. If irritation persists or if contact has been prolonged, obtain medical attention.

4.4 SWALLOWING

No harmful effects expected.

4.5 NOTES TO PHYSICIAN

Toxicology studies have shown similar material to be of very low acute toxicity. There is no specific antidote. Treatment of overexposure should be directed at the control of symptoms and the clinical condition of the patient.

5. FIRE FIGHTING MEASURES

5.1 FLAMMABLE PROPERTIES

Flash Point - Closed Cup: *Not applicable.*

Flash Point - Open Cup: *Not applicable.*

Autoignition Temperature: *Not currently available.*

Flammable Limits In Air:

Lower	*Not Determined, Aqueous System*
Upper	*Not Determined, Aqueous System*

5.2 EXTINGUISHING MEDIA

Non-flammable (aqueous solution): After water evaporates, remaining material will burn. Apply alcohol-type or all-purpose-type foam by manufacturers' recommended techniques for large fires. Use water spray, carbon dioxide or dry chemical media for small fires.

5.3 EXTINGUISHING MEDIA TO AVOID

No information currently available.

5.4 SPECIAL FIRE FIGHTING PROCEDURES

No information currently available.

5.5 SPECIAL PROTECTIVE EQUIPMENT FOR FIREFIGHTERS

Use self-contained breathing apparatus when fighting fires in enclosed areas.

5.6 UNUSUAL FIRE AND EXPLOSION HAZARDS

Product will not burn but may spatter if temperature exceeds boiling point of water.

5.7 HAZARDOUS COMBUSTION PRODUCTS

Burning can produce the following products: Carbon monoxide and carbon dioxide. Carbon monoxide is highly toxic if inhaled; carbon dioxide in sufficient concentrations can act as an asphyxiant.

6. ACCIDENTAL RELEASE MEASURES

Steps to be taken if Material is Released or Spilled:

Small spills can be flushed with large amounts of water; larger spills should be collected for disposal.

Personal Precautions: Wear suitable protective equipment. See Section 8.2 - Personal Protection.

Environmental Precautions: Not toxic to fish or plants.

7. HANDLING AND STORAGE

7.1 HANDLING

General Handling

Avoid breathing vapor from container opening.
Avoid contact with skin and clothing.
Keep container closed.
Use with adequate ventilation.
Wash thoroughly after handling.

FOR INDUSTRY USE ONLY.

Ventilation

General (mechanical) room ventilation is expected to be satisfactory for use at room temperature.

7.2 STORAGE

Store above 4 °C (40 °F). Do not freeze.

8. EXPOSURE CONTROLS AND PERSONAL PROTECTION

8.1 EXPOSURE LIMITS

Component	Exposure Limits	Skin	Form
Ammonia	17 mg/m3 TWA8 ACGIH 25 ppm TWA8 ACGIH 24 mg/m3 STEL ACGIH 35 ppm STEL ACGIH 27 mg/m3 STEL OSHA-Vacated 35 ppm STEL OSHA-Vacated 50 ppm TWA8 OSHA 35 mg/m3 TWA8 OSHA		

In the Exposure Limits Chart above, if there is no specific qualifier (i.e., Aerosol) listed in the Form Column for a particular limit, the listed limit includes all airborne forms of the substance that can be inhaled.

A "Yes" in the Skin Column indicates a potential significant contribution to overall exposure by the cutaneous (skin) route, including mucous membranes and the eyes, either by contact with vapors or by direct skin contact with the substance. A "Blank" in the Skin Column indicates that exposure by the cutaneous (skin) route is not a potential significant contributor to overall exposure.

8.2 PERSONAL PROTECTION

Respiratory Protection:	None required if airborne concentrations are maintained below listed exposure limits. If airborne concentrations exceed listed exposure limits, select respiratory protection equipment in accordance with OSHA Standard 29 CFR 1910.134. If necessary, use NIOSH approved mist respirator in poorly ventilated areas.
Ventilation:	General (mechanical) room ventilation is expected to be satisfactory for use at room temperature.
Eye Protection:	Safety glasses or monogoggles, as appropriate
Protective Gloves:	Polyvinyl chloride coated

8.3 ENGINEERING CONTROLS

Avoid inhalation of product spray through the use of engineering controls. General (mechanical) room ventilation is expected to be satisfactory. Use local exhaust if needed to control mist or vapor.

9. PHYSICAL AND CHEMICAL PROPERTIES

Physical State: Liquid

Appearance: White

pH: 9 Approx.

Solubility in Water (by weight): Completely miscible

Odor: Mild

Boiling Point (760 mmHg): ~ 100 °C ~ 212 °F

Freezing Point: 0 °C 32 °F

Specific Gravity (H2O = 1): 1.1

Vapor Pressure at 20°C: 2.4 kPa 18 mmHg

Vapor Density (air = 1): 0.6

Evaporation Rate (Butyl Acetate = 1): 0.8

Dynamic Viscosity: 350 cps Approx.

Melting Point: *Not applicable.*

10. STABILITY AND REACTIVITY

10.1 STABILITY/INSTABILITY Stable

10.2 HAZARDOUS POLYMERIZATION Will Not Occur.

10.3 INHIBITORS/STABILIZERS Not applicable.

11. TOXICOLOGICAL INFORMATION

Information on analogous products shows minimal toxicity concerns.

ACUTE TOXICITY

Peroral: Rat LD50 > 2000 mg/kg

Percutaneous: Rat LD50 > 2000 mg/kg

SIGNIFICANT DATA WITH POSSIBLE RELEVANCE TO HUMANS

Trace amounts of formaldehyde may be generated under acid conditions. Maintain adequate ventilation under these conditions to prevent exposure above the current OSHA limits.

12. ECOLOGICAL INFORMATION

12.1 ENVIRONMENTAL FATE

Not toxic to fish or plants., Does not inhibit bacteria in waste treatment facilities., Polymer is not biodegradable., Product is not RCRA hazardous., The following information is based on analogy with a similar material.

BOD (% Oxygen consumption)

	Day 5	Day 10	Day 15	Day 20	Day 30
				1 - 8 %	

12.2 ECOTOXICITY

Toxicity to Micro-organisms: IC50 > 2000 mg/l

Toxicity to Aquatic Invertebrates: Daphnia EC50 > 1000 mg/l
Toxicity to Fish: Fathead Minnow LC50 > 1000 mg/l

12.3 FURTHER INFORMATION

None.

13. DISPOSAL CONSIDERATIONS

13.1 WASTE DISPOSAL METHOD

Incinerate in a furnace or otherwise dispose of in accordance with applicable Federal, State and local requirements. Dispose in accordance with all applicable Federal, State, and local environmental regulations. Empty containers should be recycled or disposed of through an approved waste management facility.

13.2 DISPOSAL CONSIDERATIONS

Does not inhibit bacteria in waste treatment facilities. Polymer is not biodegradable. Product is not RCRA hazardous. See Section 13.1

Disposal methods identified are for the product as sold. For proper disposal of used material, an assessment must be completed to determine the proper and permissible waste management options permissible under applicable rules, regulations and/or laws governing your location.

14. TRANSPORT INFORMATION

14.1 U.S. D.O.T.

NON-BULK
Proper Shipping Name : NOT REGULATED

BULK
Proper Shipping Name : NOT REGULATED

This information is not intended to convey all specific regulatory or operational requirements/information relating to this product. Additional transportation system information can be obtained through an authorized sales or customer service representative. It is the responsibility of the transporting organization to follow all applicable laws, regulations and rules relating to the transportation of the material.

15. REGULATORY INFORMATION

15.1 FEDERAL/NATIONAL

COMPREHENSIVE ENVIRONMENTAL RESPONSE, COMPENSATION, AND LIABILITY ACT OF 1980 SECTION 103 (CERCLA)

The following components of this product are specifically listed as hazardous substances in 40 CFR 302.4 (unlisted hazardous substances are not identified) and are present at levels which could require reporting:

None.

SUPERFUND AMENDMENTS AND REAUTHORIZATION ACT OF 1986 (SARA) TITLE III SECTIONS 302 AND 304

The following components of this product are listed as extremely hazardous substances in 40 CFR Part 355 and are present at levels which could require reporting and emergency planning:

None.

SUPERFUND AMENDMENTS AND REAUTHORIZATION ACT OF 1986 (SARA) TITLE III SECTION 313

The following components of this product are listed as toxic chemicals in 40 CFR 372.65 and are present at levels which could require reporting and customer notification under Section 313 and 40 CFR Part 372:

This product does not contain toxic chemicals at levels which require reporting under the statute.

SUPERFUND AMENDMENTS AND REAUTHORIZATION ACT OF 1986 (SARA) TITLE III SECTIONS 311 AND 312

Delayed Hazard : No
Fire Hazard : No
Immediate Health Hazard : No
Reactive Hazard : No
Sudden Release of Pressure Hazard : No

TOXIC SUBSTANCES CONTROL ACT (TSCA)

All components of this product are on the TSCA Inventory or are exempt from TSCA Inventory requirements.

CEPA - DOMESTIC SUBSTANCES LIST (DSL)

The components of this product are on the DSL.

15.2 STATE/LOCAL

PENNSYLVANIA (WORKER AND COMMUNITY RIGHT-TO-KNOW ACT)

This product is subject to the Worker and Community Right-to-Know Act. The following components of this product are at levels which could require identification in the MSDS:
None.

MASSACHUSETTS (HAZARDOUS SUBSTANCES DISCLOSURE BY EMPLOYERS)

The following components of this product appear on the Massachusetts Substance List and are present at levels which could require identification in the MSDS:

Component	CAS #	Amount
Ammonia	7664-41-7	<= 0.2000%

CALIFORNIA PROPOSITION 65 (SAFE DRINKING WATER AND TOXIC ENFORCEMENT ACT OF 1986)

This product contains no listed substances known to the State of California to cause cancer, birth defects or other reproductive harm, at levels which would require a warning under the statute.

CALIFORNIA SCAQMD RULE 443.1 (SOUTH COAST AIR QUALITY MANAGEMENT DISTRICT RULE 443.1, LABELING OF MATERIALS CONTAINING ORGANIC SOLVENTS)

VOC: Not applicable.

This section provides selected regulatory information on this product including its components. This is not intended to include all regulations. It is the responsibility of the user to know and comply with all applicable rules, regulations and laws relating to the product being used.

16. OTHER INFORMATION

16.1 AVAILABLE LITERATURE AND BROCHURES

Additional information on this product may be obtained by calling: (919)469-6785.

16.2 SPECIFIC HAZARD RATING SYSTEM

HMIS ratings for this product are:	H - 0	F - 1	S - 0
NFPA ratings for this product are:	H - 1	F - 1	S - 0

These ratings are part of specific hazard communications program(s) and should be disregarded where individuals are not trained in the use of these hazard rating systems. You should be familiar with the hazard communication applicable to your workplace.

16.3 RECOMMENDED USES AND RESTRICTIONS

FOR INDUSTRY USE ONLY

16.4 REVISION

Version: 1.
Revision: 09/15/1999
Most recent revision(s) are noted by the bold, double bars in left-hand margin throughout this document.

16.5 LEGEND

TS	Trade Secret
N/A	Not available
W/W	Weight/Weight

The opinions expressed herein are those of qualified experts within Union Carbide. We believe that the information contained herein is current as of the date of this Material Safety Data Sheet. Since the use of this information and the conditions of the use of the product are not under the control of Union Carbide, it is the user's obligation to determine conditions of safe use of the product.

APPENDIX 6

UCAR LATEX 9175 MATERIAL SAFETY DATA SHEET

UNION CARBIDE CORPORATION

MATERIAL SAFETY DATA SHEET

Product Name: UCAR™ Latex 9175
MSDS#: 26523

Effective Date: 08/30/2000
Page 1 of 13

Union Carbide urges each customer or recipient of this MSDS to study it carefully to become aware of and understand the hazards associated with the product. The reader should consider consulting reference works or individuals who are experts in ventilation, toxicology, and fire prevention, as necessary or appropriate to use and understand the data contained in this MSDS.

To promote safe handling, each customer or recipient should: 1) Notify its employees, agents, contractors and others whom it knows or believes will use this material of the information in this MSDS and any other information regarding hazards or safety; 2) Furnish this same information to each of its customers for the product; and 3) Request its customers to notify their employees, customers, and other users of the product of this information.

1. CHEMICAL PRODUCT AND COMPANY IDENTIFICATION

1.1 IDENTIFICATION

Product Name	UCAR™ Latex 9175
Chemical Name	Not available
Chemical Family	Acrylic Latex
Formula	Not available
Synonym	None

1.2 COMPANY IDENTIFICATION

Union Carbide Corporation
39 Old Ridgebury Road
Danbury, CT 06817-0001

1.3 EMERGENCY TELEPHONE NUMBER

24 hours a day: 1-800-UCC-HELP (1-304-744-3487)
Number for non-emergency questions concerning MSDS (732) 563-5522
Additional information on this product may be obtained by calling: (919)469-6785.

Copyright© 2000, Union Carbide Chemicals & Plastics Technology Corporation.
UCAR is a trademark of Union Carbide.

2. COMPOSITION INFORMATION

Component	CAS #	Amount (%W/W)
Butyl acrylate, 2-ethylhexyl acrylate, methacrylic acid polymer C	31071-53-1	< 58%
Water	7732-18-5	42 %
Ammonia	7664-41-7	0.07 %
2-Ethylhexyl acrylate	103-11-7	0.04 %

3. HAZARDS IDENTIFICATION

3.1 EMERGENCY OVERVIEW

Appearance	White	
Physical State	Liquid	
Odor	Mild	
Hazards of product	WARNING!	VAPOR MAY BE HARMFUL IF INHALED. MAY CAUSE SKIN IRRITATION.

3.2 POTENTIAL HEALTH EFFECTS

Effects of Single Acute Overexposure

Inhalation May cause irritation of the respiratory tract, experienced as burning sensation of eyes, nose, and throat, sneezing, coughing, and nausea.

Eye Contact Liquid may cause discomfort in the eye with slight excess redness and possibly swelling of the conjunctiva.

Skin Contact Brief contact is not irritating. Prolonged contact, as from clothing wet with the material, may cause mild irritation, experienced as discomfort, and seen as local redness.

Skin Absorption No evidence of harmful effects from available information.

Swallowing No evidence of harmful effects from available information.

Chronic, Prolonged or Repeated Overexposure

Effects of Repeated Overexposure No adverse effects anticipated from available information.

Other Effects of Overexposure None currently known.

Medical Conditions Aggravated by Exposure

A knowledge of the available toxicology information and of the physical and chemical properties of the material suggests that overexposure is unlikely to aggravate existing medical conditions.

3.3 POTENTIAL ENVIRONMENTAL EFFECTS

See Section 12 for Ecological Information.

4. FIRST AID PROCEDURES

4.1 INHALATION

Remove to fresh air. Give artificial respiration if not breathing. Oxygen may be given by qualified personnel if necessary. Call a physician.

4.2 EYE CONTACT

Immediately flush eyes with water and continue washing for several minutes. Remove contact lenses, if worn. Obtain medical attention

4.3 SKIN CONTACT

Remove contaminated clothing. Wash skin with soap and water. If irritation persists or if contact has been prolonged, obtain medical attention.

4.4 SWALLOWING

No harmful effects expected.

4.5 NOTES TO PHYSICIAN

Toxicology studies have shown similar material to be of very low acute toxicity. There is no specific antidote. Treatment of overexposure should be directed at the control of symptoms and the clinical condition of the patient.

5. FIRE FIGHTING MEASURES

5.1 FLAMMABLE PROPERTIES

Flash Point - Closed Cup: *Not applicable.*

Flash Point - Open Cup: *Not applicable.*

Autoignition Temperature: *Not currently available.*

Flammable Limits In Air:

Lower	*Not Determined, Aqueous System*
Upper	*Not Determined, Aqueous System*

5.2 EXTINGUISHING MEDIA

Non-flammable (aqueous solution): After water evaporates, remaining material will burn. Apply alcohol-type or all-purpose-type foam by manufacturers' recommended techniques for large fires. Use water spray, carbon dioxide or dry chemical media for small fires.

5.3 EXTINGUISHING MEDIA TO AVOID

No information currently available.

5.4 SPECIAL FIRE FIGHTING PROCEDURES

No information currently available.

5.5 SPECIAL PROTECTIVE EQUIPMENT FOR FIREFIGHTERS

Use self-contained breathing apparatus when fighting fires in enclosed areas.

5.6 UNUSUAL FIRE AND EXPLOSION HAZARDS

Product will not burn but may spatter if temperature exceeds boiling point of water.

5.7 HAZARDOUS COMBUSTION PRODUCTS

Burning can produce the following products: Carbon monoxide and carbon dioxide. Carbon monoxide is highly toxic if inhaled. Carbon dioxide in sufficient concentrations can act as an asphyxiant.

6. ACCIDENTAL RELEASE MEASURES

Steps to be Taken if Material is Released or Spilled:
Small spills can be flushed with large amounts of water; larger spills should be collected for disposal.

Personal Precautions: Wear suitable protective equipment. See Section 8.2 - Personal Protection.

Environmental Precautions: Not toxic to fish or plants.

7. HANDLING AND STORAGE

7.1 HANDLING

General Handling
Avoid breathing vapor from container opening.
Avoid contact with skin and clothing.
Keep container closed.
Use with adequate ventilation.
Wash thoroughly after handling.

FOR INDUSTRY USE ONLY.

Ventilation
General (mechanical) room ventilation is expected to be satisfactory for use at room temperature.

7.2 STORAGE

Store above 4 °C (40 °F). Do not freeze.

8. EXPOSURE CONTROLS AND PERSONAL PROTECTION

8.1 EXPOSURE LIMITS

Component	Exposure Limits	Skin	Form
Ammonia	17 mg/m3 TWA8 ACGIH		

	25 ppm TWA8 ACGIH 24 mg/m3 STEL ACGIH 35 ppm STEL ACGIH 27 mg/m3 STEL OSHA-Vacated 35 ppm STEL OSHA-Vacated 50 ppm TWA8 OSHA 35 mg/m3 TWA8 OSHA
2-Ethylhexyl acrylate	5 ppm TWA8 UCC

In the Exposure Limits Chart above, if there is no specific qualifier (i.e., Aerosol) listed in the Form Column for a particular limit, the listed limit includes all airborne forms of the substance that can be inhaled.

A "Yes" in the Skin Column indicates a potential significant contribution to overall exposure by the cutaneous (skin) route, including mucous membranes and the eyes, either by contact with vapors or by direct skin contact with the substance. A "Blank" in the Skin Column indicates that exposure by the cutaneous (skin) route is not a potential significant contributor to overall exposure.

8.2 PERSONAL PROTECTION

Respiratory Protection:	None required if airborne concentrations are maintained below listed exposure limits. If airborne concentrations exceed listed exposure limits, select respiratory protection equipment in accordance with OSHA Standard 29 CFR 1910.134. If necessary, use NIOSH approved mist respirator in poorly ventilated areas.
Ventilation:	General (mechanical) room ventilation is expected to be satisfactory for use at room temperature.
Eye Protection:	Safety glasses or monogoggles, as appropriate
Protective Gloves:	Polyvinyl chloride coated

8.3 ENGINEERING CONTROLS

Avoid inhalation of product spray through the use of engineering controls. General (mechanical) room ventilation is expected to be satisfactory. Use local exhaust if needed to control mist or vapor.

9. PHYSICAL AND CHEMICAL PROPERTIES

Physical State: Liquid

Appearance: White

pH: 7 Approx.

Solubility in Water (by weight): Completely miscible

Odor: Mild

Boiling Point (760 mmHg): ~ 100 °C ~ 212 °F

Freezing Point: 0 °C 32 °F

Specific Gravity (H2O = 1): 1.1

Vapor Pressure at 20°C: 2.4 kPa 18 mmHg

Vapor Density (air = 1): 0.6

Evaporation Rate (Butyl Acetate = 1): 0.8

Dynamic Viscosity: 1,000 cps Approx.

Melting Point: *Not applicable.*

10. STABILITY AND REACTIVITY

10.1 STABILITY/INSTABILITY Stable

10.2 HAZARDOUS POLYMERIZATION Will Not Occur.

10.3 INHIBITORS/STABILIZERS

Not applicable.

11. TOXICOLOGICAL INFORMATION

Information on analogous products shows minimal toxicity concerns.

ACUTE TOXICITY

Peroral

Rat; LD50 = > 2000 mg/kg

Percutaneous

Rat; LD50 = > 2000 mg/kg

SIGNIFICANT DATA WITH POSSIBLE RELEVANCE TO HUMANS

2-Ethylhexyl acrylate (EHA), used in the manufacture of this product, has been shown to cause cancer in laboratory animals, based on chronic skin painting studies in mice. Although there is no evidence that EHA causes cancer in humans, skin contact should be avoided, and the material should be handled with ventilation adequate to keep the atmospheric concentration of EHA below 5 ppm.

12. ECOLOGICAL INFORMATION

12.1 ENVIRONMENTAL FATE

Not toxic to fish or plants. Does not inhibit bacteria in waste treatment facilities. Polymer is not biodegradable. Product is not RCRA hazardous. The following information is based on analogy with a similar material.

BOD (% Oxygen consumption)

	Day 5	Day 10	Day 15	Day 20	Day 30
				1 - 8 %	

12.2 ECOTOXICITY

Toxicity to Micro-organisms
IC50
Result value: > 2000 mg/l

Toxicity to Aquatic Invertebrates
Daphnia; EC50
Result value: > 1000 mg/l

Toxicity to Fish
Fathead Minnow; LC50
Result value: > 1000 mg/l

12.3 FURTHER INFORMATION

None.

13. DISPOSAL CONSIDERATIONS

13.1 WASTE DISPOSAL METHOD

Incinerate in a furnace or otherwise dispose of in accordance with applicable Federal, State and local requirements. Dispose in accordance with all applicable Federal, State, and local environmental regulations. Empty containers should be recycled or disposed of through an approved waste management facility.

13.2 DISPOSAL CONSIDERATIONS

Does not inhibit bacteria in waste treatment facilities. Polymer is not biodegradable. Product is not RCRA hazardous. See Section 13.1

Disposal methods identified are for the product as sold. For proper disposal of used material, an assessment must be completed to determine the proper and permissible waste management options permissible under applicable rules, regulations and/or laws governing your location.

14. TRANSPORT INFORMATION

14.1 U.S. D.O.T.

NON-BULK
Proper Shipping Name : NOT REGULATED

BULK
Proper Shipping Name : NOT REGULATED

This information is not intended to convey all specific regulatory or operational requirements/information relating to this product. Additional transportation system information can be obtained through an authorized sales or customer service representative. It is the responsibility of the transporting organization to follow all applicable laws, regulations and rules relating to the transportation of the material.

15. REGULATORY INFORMATION

15.1 FEDERAL/NATIONAL

COMPREHENSIVE ENVIRONMENTAL RESPONSE, COMPENSATION, AND LIABILITY ACT OF 1980 SECTION 103 (CERCLA)

The following components of this product are specifically listed as hazardous substances in 40 CFR 302.4 (unlisted hazardous substances are not identified) and are present at levels which could require reporting:

None.

SUPERFUND AMENDMENTS AND REAUTHORIZATION ACT OF 1986 TITLE III (EPCRA) SECTIONS 302 AND 304

The following components of this product are listed as extremely hazardous substances in 40 CFR Part 355 and are present at levels which could require reporting and emergency planning:

None.

SUPERFUND AMENDMENTS AND REAUTHORIZATION ACT OF 1986 TITLE III (EPCRA) SECTION 313

The following components of this product are listed as toxic chemicals in 40 CFR 372.65 and are present at levels which could require reporting and customer notification under Section 313 and 40 CFR Part 372:

This product does not contain toxic chemicals at levels which require reporting under the statute.

SUPERFUND AMENDMENTS AND REAUTHORIZATION ACT OF 1986 TITLE III (EPCRA) SECTIONS 311 AND 312

Delayed Hazard : No
Fire Hazard : No
Immediate Health Hazard : No
Reactive Hazard : No
Sudden Release of Pressure Hazard : No

TOXIC SUBSTANCES CONTROL ACT (TSCA)

All components of this product are on the TSCA Inventory or are exempt from TSCA Inventory requirements.

CEPA - DOMESTIC SUBSTANCES LIST (DSL)

The components of this product are on the DSL or are exempt from reporting under the New Substances Notification Regulations.

15.2 STATE/LOCAL

PENNSYLVANIA (WORKER AND COMMUNITY RIGHT-TO-KNOW ACT)

This product is subject to the Worker and Community Right-to-Know Act. The following components of this product are at levels which could require identification in the MSDS:
None.

MASSACHUSETTS (HAZARDOUS SUBSTANCES DISCLOSURE BY EMPLOYERS)

The following components of this product appear on the Massachusetts Substance List and are present at levels which could require identification in the MSDS:

Component	CAS #	Amount
Ammonia	7664-41-7	<= 0.0700%

CALIFORNIA PROPOSITION 65 (SAFE DRINKING WATER AND TOXIC ENFORCEMENT ACT OF 1986)

This product contains no listed substances known to the State of California to cause cancer, birth defects or other reproductive harm, at levels which would require a warning under the statute.

CALIFORNIA SCAQMD RULE 443.1 (SOUTH COAST AIR QUALITY MANAGEMENT DISTRICT RULE 443.1, LABELING OF MATERIALS CONTAINING ORGANIC SOLVENTS)

VOC: Not applicable.

This section provides selected regulatory information on this product including its components. This is not intended to include all regulations. It is the responsibility of the user to know and comply with all applicable rules, regulations and laws relating to the product being used.

16. OTHER INFORMATION

16.1 AVAILABLE LITERATURE AND BROCHURES

Additional information on this product may be obtained by calling: (919)469-6785.

16.2 SPECIFIC HAZARD RATING SYSTEM

HMIS ratings for this product are: **H** - 0 **F** - 1 **R** - 0

NFPA ratings for this product are: **H** - 1 **F** - 1 **R** - 0

These ratings are part of specific hazard communications program(s) and should be disregarded where individuals are not trained in the use of these hazard rating systems. You should be familiar with the hazard communication applicable to your workplace.

16.3 RECOMMENDED USES AND RESTRICTIONS

FOR INDUSTRY USE ONLY

16.4 REVISION

Version: 1.
Revision: 08/30/2000
Most recent revision(s) are noted by the bold, double bars in left-hand margin throughout this document.

16.5 LEGEND

TS	Trade Secret
N/A	Not available
W/W	Weight/Weight
VOL/VOL	Volume/Volume
NFPA	National Fire Protection Association
HMIS	Hazardous Materials Information System
H	Health
F	Fire
R	Reactivity
W	Water Reactive
O	Oxidizer
A	Asphyxiant
P	Peroxide Former

The opinions expressed herein are those of qualified experts within Union Carbide. We believe that the information contained herein is current as of the date of this Material Safety Data Sheet. Since the use of this information and the conditions of the use of the product are not under the control of Union Carbide, it is the user's obligation to determine conditions of safe use of the product.

APPENDIX 7

RHEOMETRICS SOLIDS ANALYZER II (RSA II)

A system consisting of two sample holder fixtures was used to analyze pressure sensitive adhesive samples in the Rheometrics Solids Analyzer II (RSA II). The pressure sensitive adhesive film is the white area in between the two gray cylindrical fixtures in **Figure A7-1**. The diameters of the plate surfaces for the top and bottom fixtures in **Figure A7-1** are 7.9 mm and 25 mm, respectively. The shaft diameter and plate thickness for the two fixtures in **Figure A7-1** are 6.2 mm and 3.1 mm, respectively. For analysis in the RSA II, the fixtures were secured in the RSA II and then the fixtures were forced together. The distance between the two fixtures in the RSA II is 0.45 mm, which is the same as the thickness of the adhesive film sample during analysis.

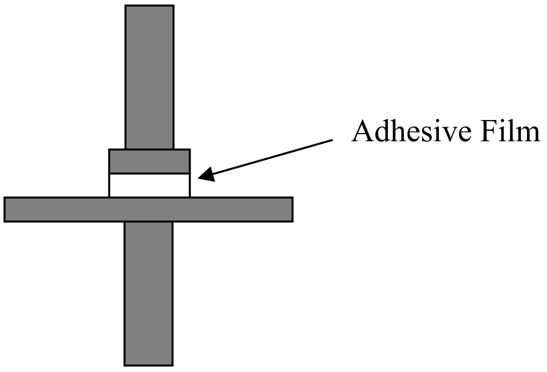

Figure A7-1. Two RSA II Sample Holder Fixtures with an Adhesive Film in Between Them

APPENDIX 8

TACK OF ACRYLIC AND SIS ADHESIVE FILMS

The tack was evaluated for an acrylic and a SIS pressure sensitive adhesive film. The adhesive films, between two sheets of silicone release liner, were cut into 2.0 cm wide strips. One sheet of release liner was removed from a 2.0 cm wide adhesive film. The strip was applied to a square area of 2.0 cm x 2.0 cm on a 1.2 kg stainless steel weight. The combination of the adhesive strip and weight were placed on a balance. The adhesive strip was slowly pulled up from the weight, without the weight lifting off of the balance surface, until the adhesive released from the weight. When the adhesive released from the weight, the reading on the balance was recorded. The measurement was conducted five times for each of the adhesive films. The tack was calculated as the force required for the adhesive film to release from the weight per unit area of the adhesive film in contact with the weight. The average and standard deviation were calculated for the tack of the two adhesive films. For the acrylic adhesive film, the average tack was 2.5 kN/m^2 with a standard deviation of 0.2 kN/m^2. For the SIS adhesive film, the average tack was 4.4 kN/m^2 with a standard deviation of 0.2 kN/m^2. The tack for the SIS was almost twice that for the acrylic, while the standard deviations were the same. Therefore, the SIS adhesive film is tackier than the acrylic adhesive film.

APPENDIX 9

MICROSCOPIC IMAGES OF ACRYLIC ADHESIVE PARTICLES

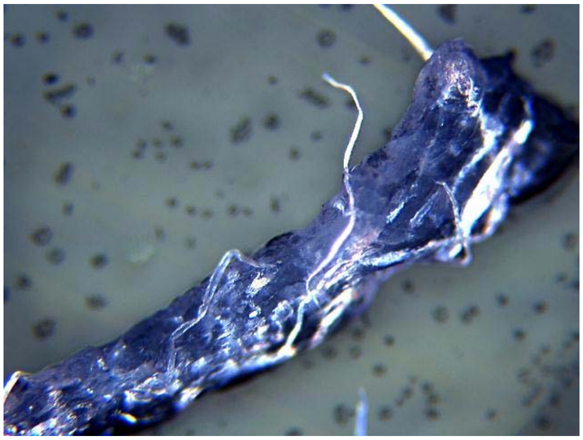

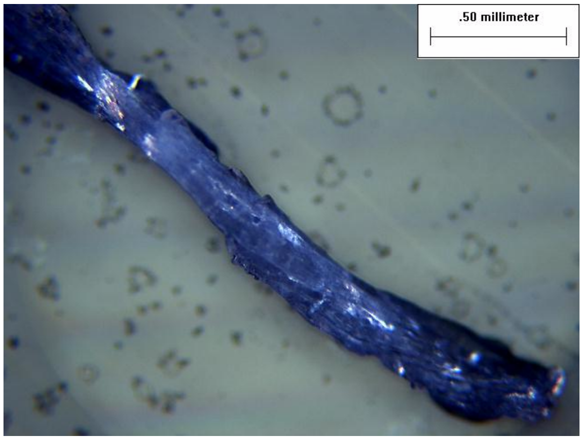

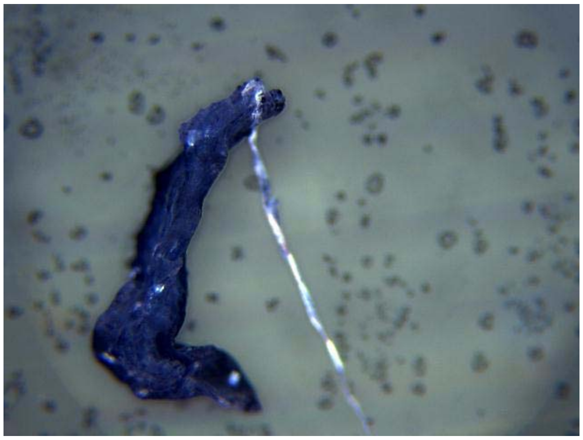

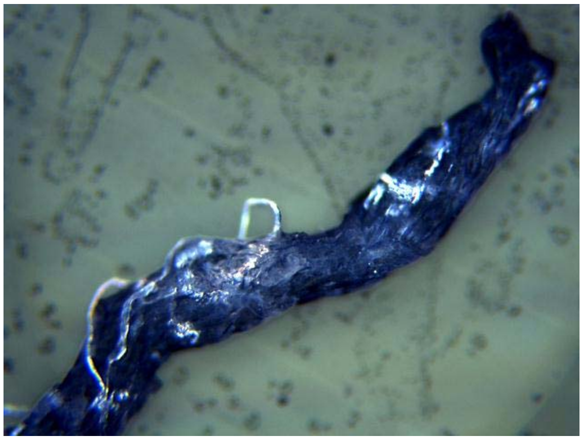

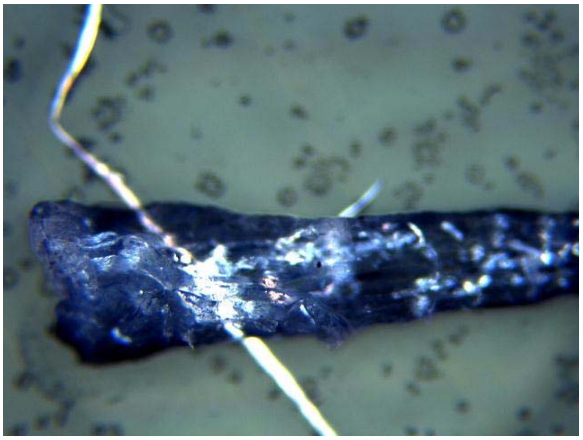

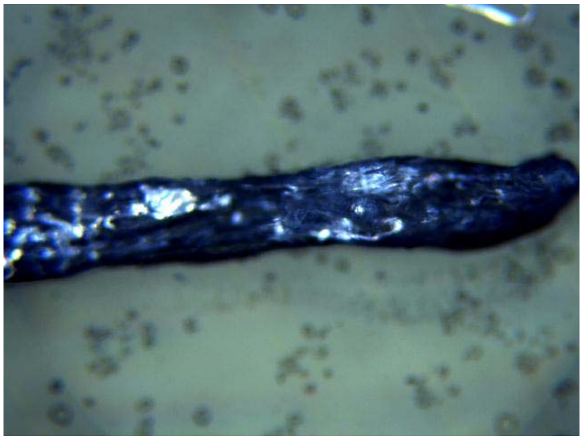

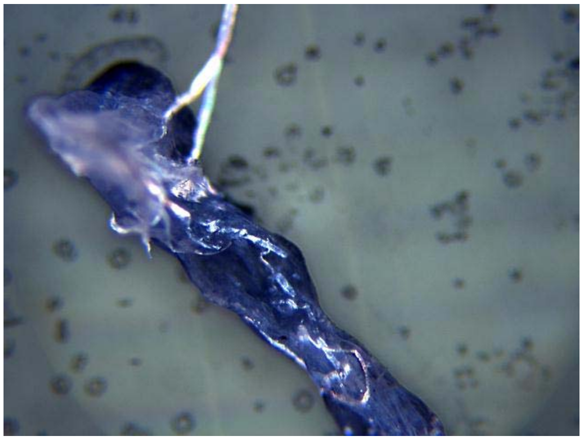

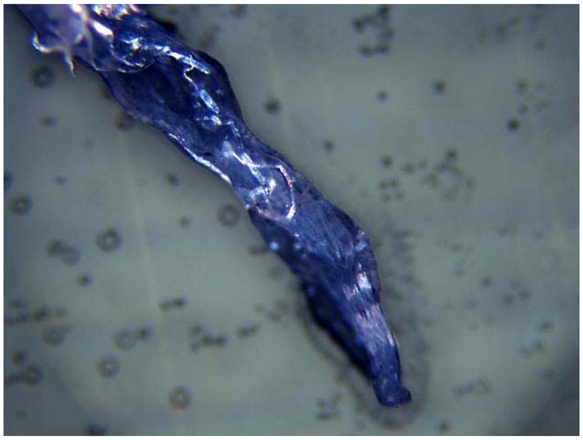

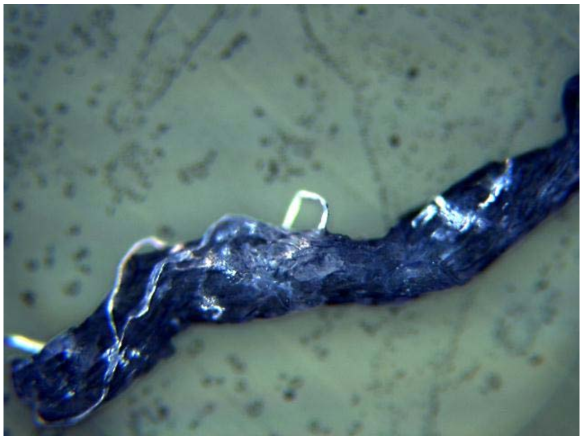

APPENDIX 10

MICROSCOPIC IMAGES OF SIS ADHESIVE PARTICLES

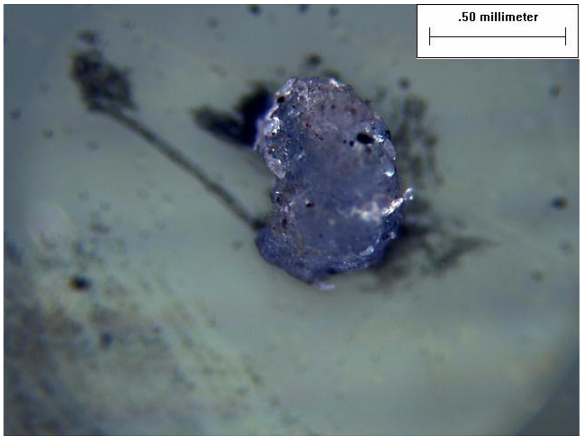

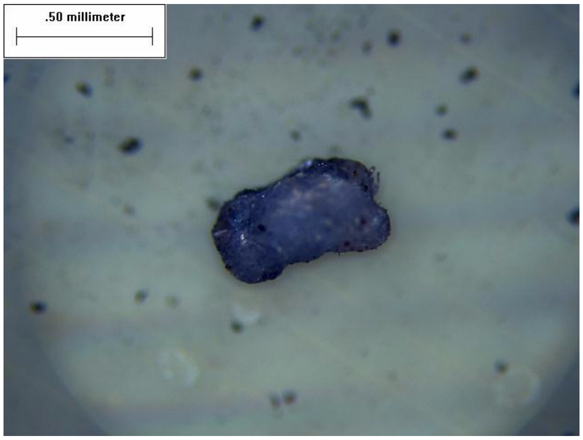

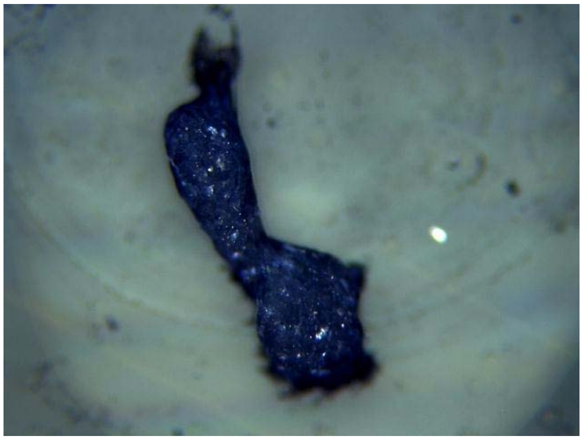

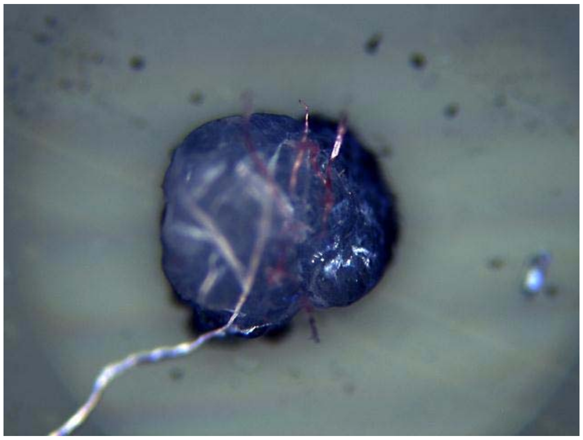

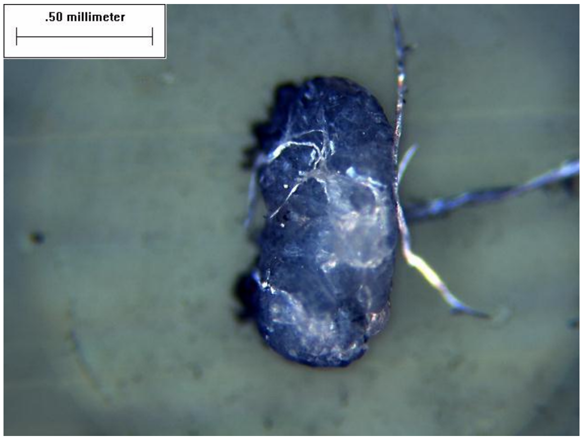
.50 millimeter

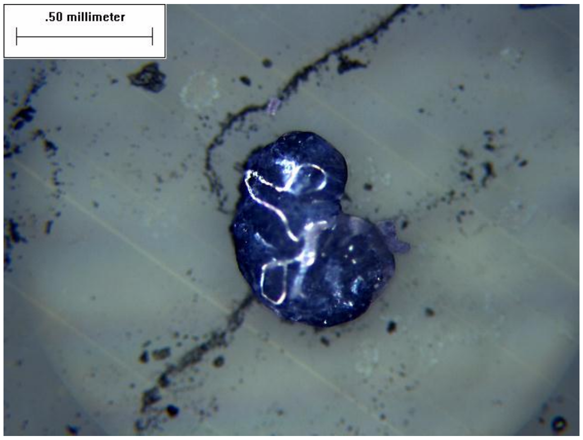
.50 millimeter

APPENDIX 11

DIFFERENTIAL SCANNING CALORIMETRY OUTPUT FOR UCAR FILMS

Differential scanning calorimetry (DSC) is used to determine the glass transition temperature (T_g) of a material by analyzing plots of heat flow versus temperature and the derivative heat flow versus temperature. The T_g occurs where the slope of the heat flow versus temperature curve changes. The T_g is interpreted from the plots by applying straight lines to the curves and finding their intersection point of the with the heat flow versus temperature curve (see **Figure A11-1** through **Figure A11-4**).

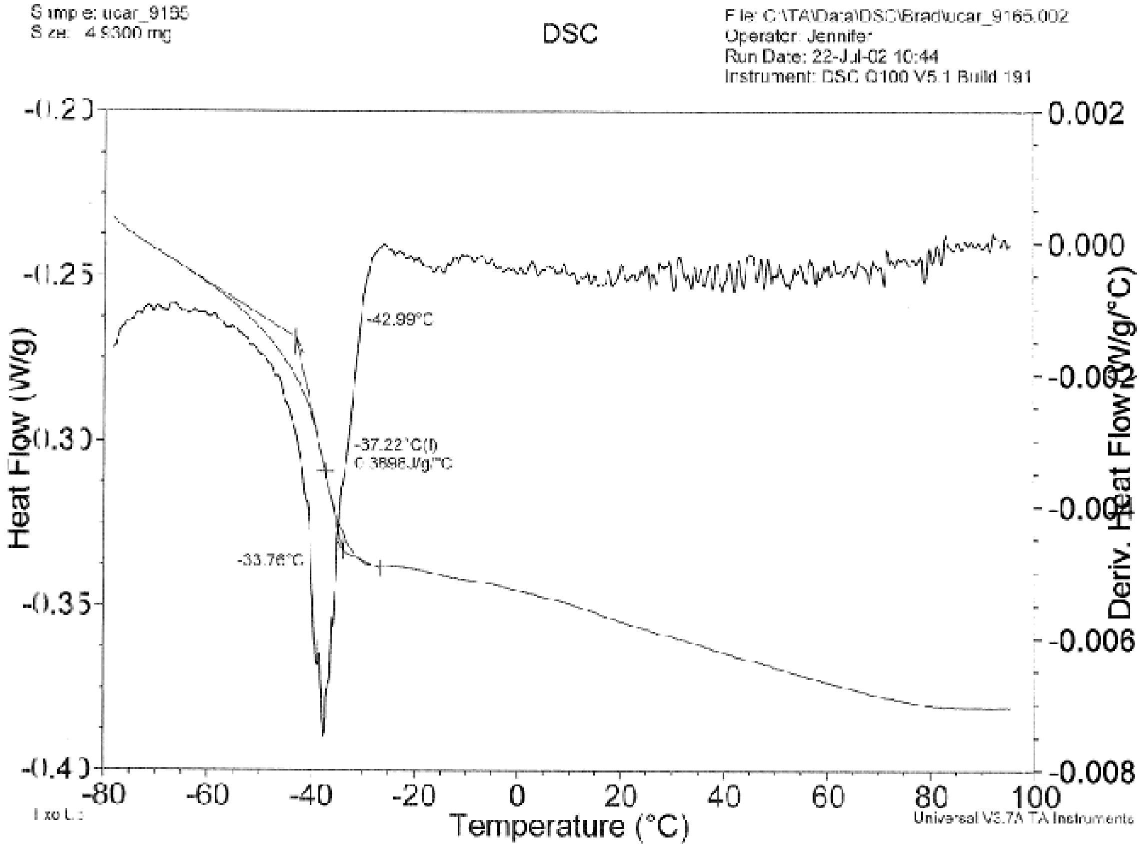

Figure A11-1. Differential Scanning Calorimetry Output for UCAR 9165

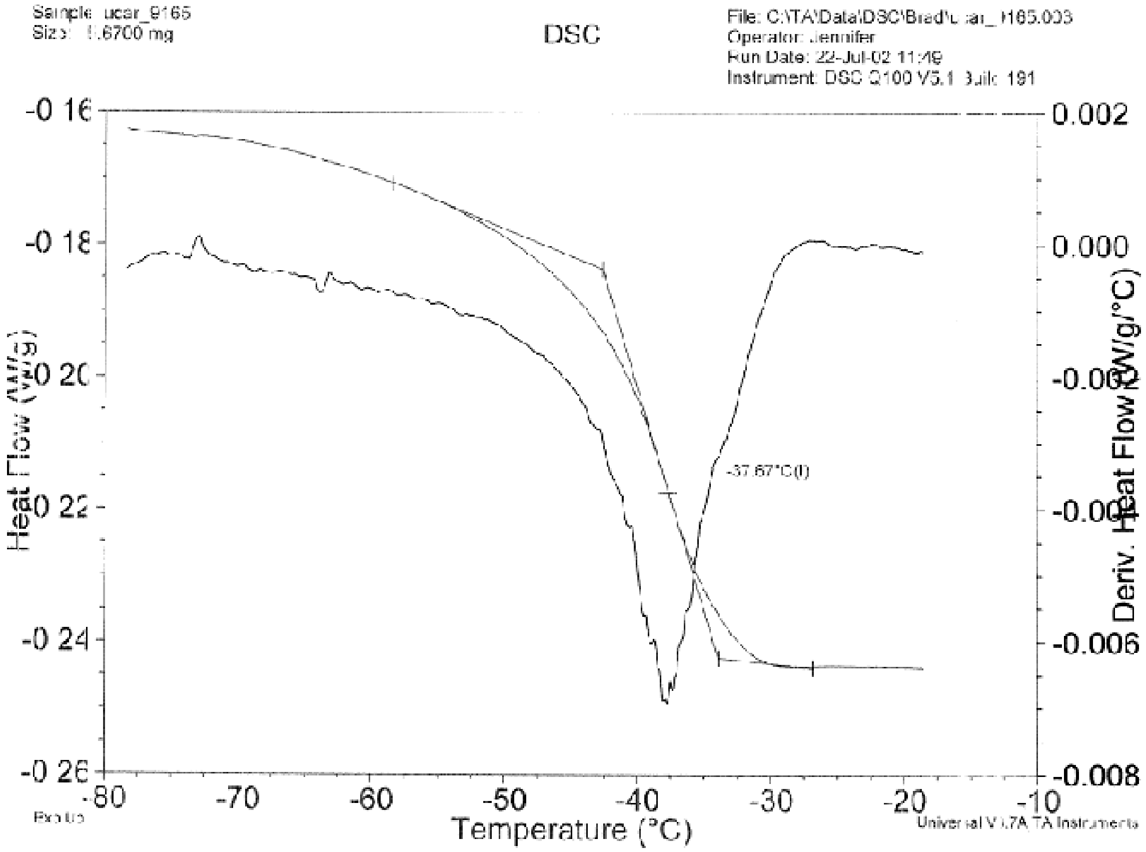

Figure A11-2. Differential Scanning Calorimetry Output for UCAR 9165

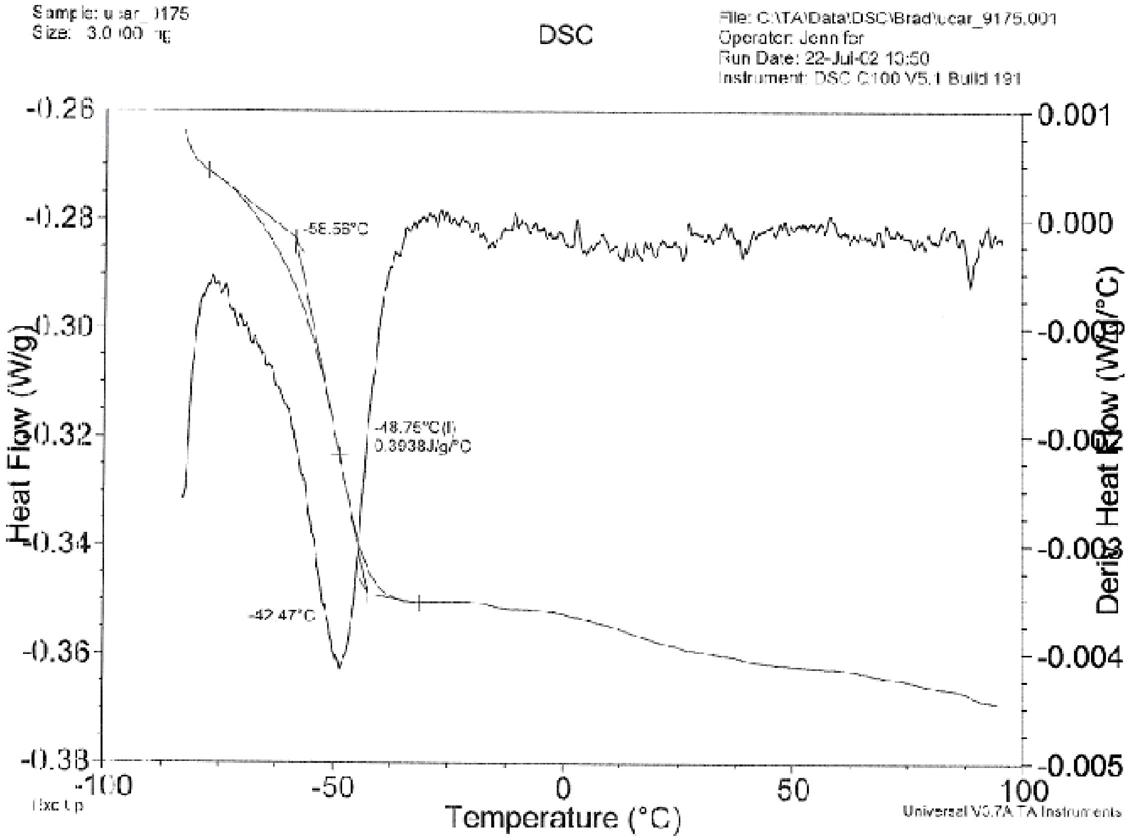

Figure A11-3. Differential Scanning Calorimetry Output for UCAR 9175

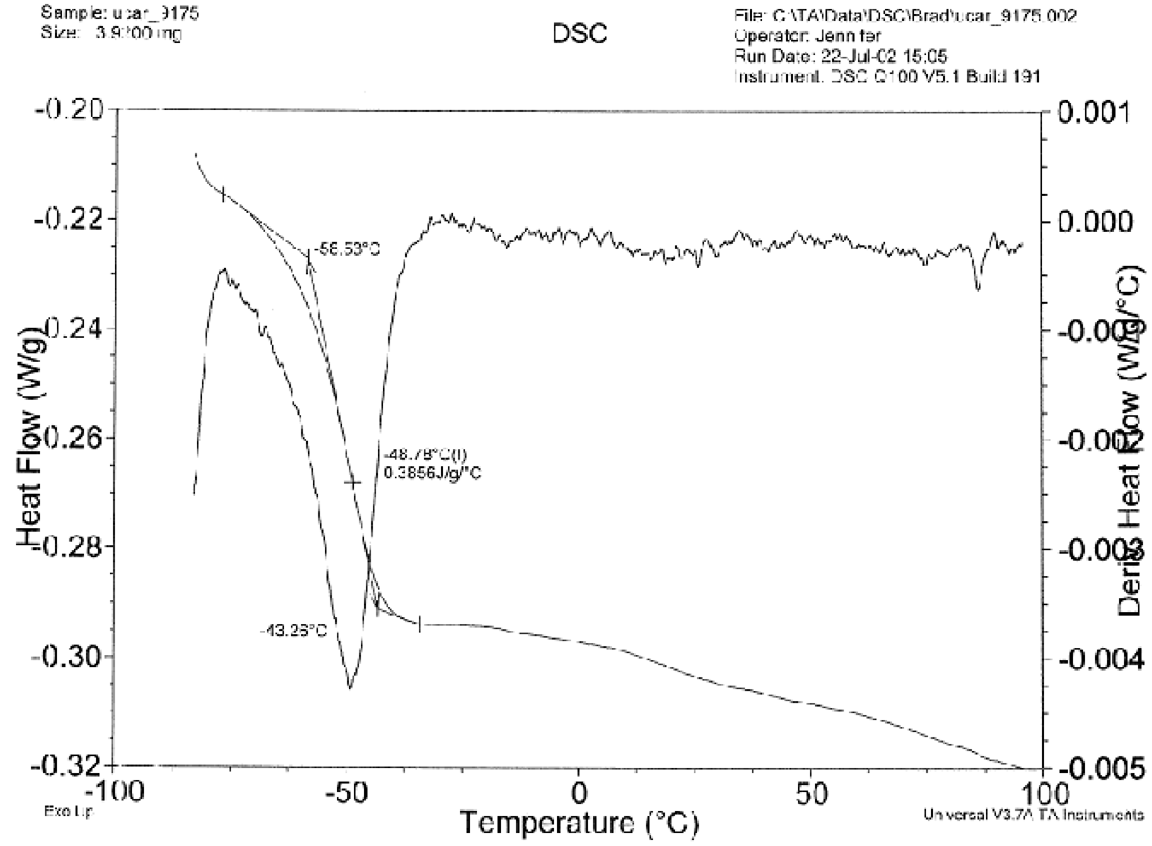

Figure A11-4. Differential Scanning Calorimetry Output for UCAR 9175

APPENDIX 12

STRESS VERSUS STRAIN CURVES FOR ADHESIVE FILMS

Below are the plots of stress versus strain from the RSAII for the adhesive films containing BA as the base material (**Figure A12-1**), containing BA-EA as the base material (**Figure A12-2**), and with AC and SIS as the adhesive films (**Figure A12-3**).

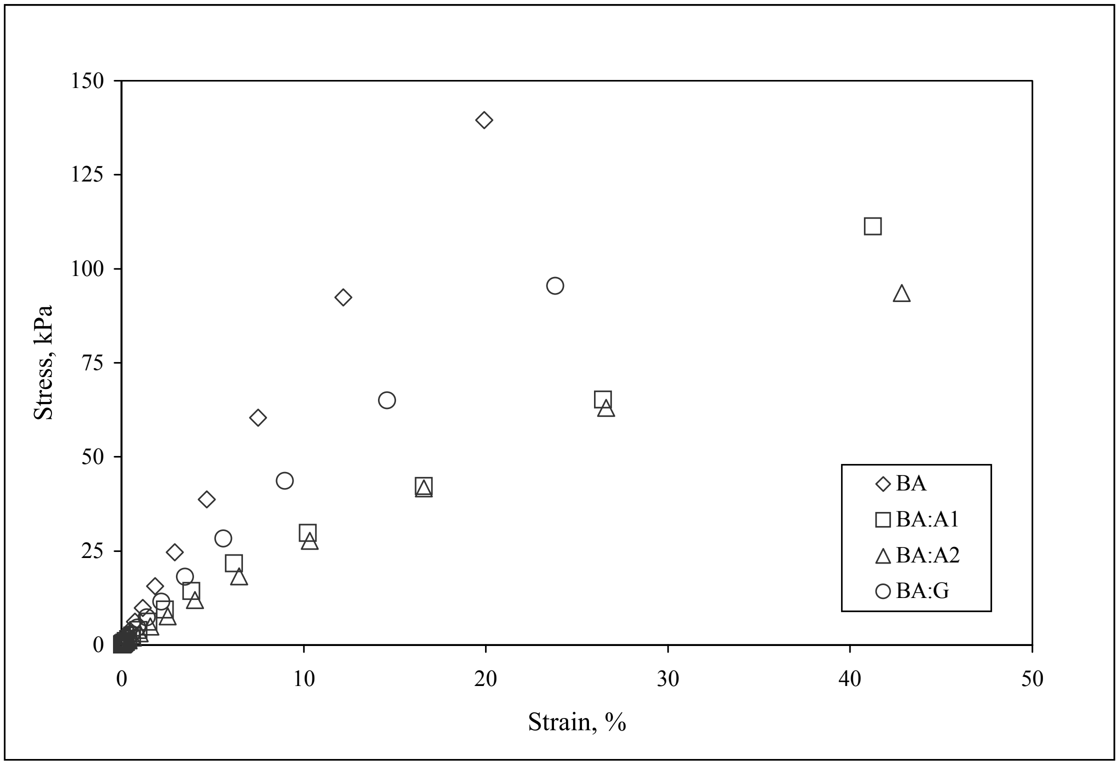

Figure A12-1. Stress Versus Strain for Adhesive Films Containing BA

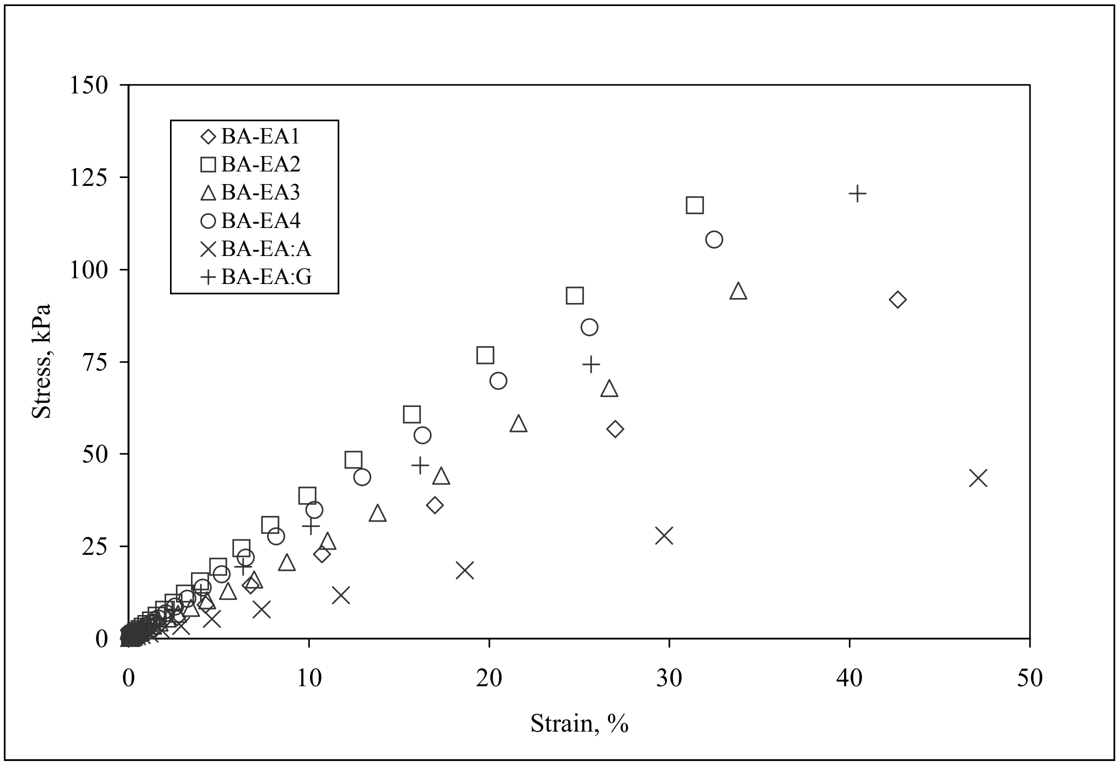

Figure A12-2. Stress Versus Strain for Adhesive Films Containing BA-EA

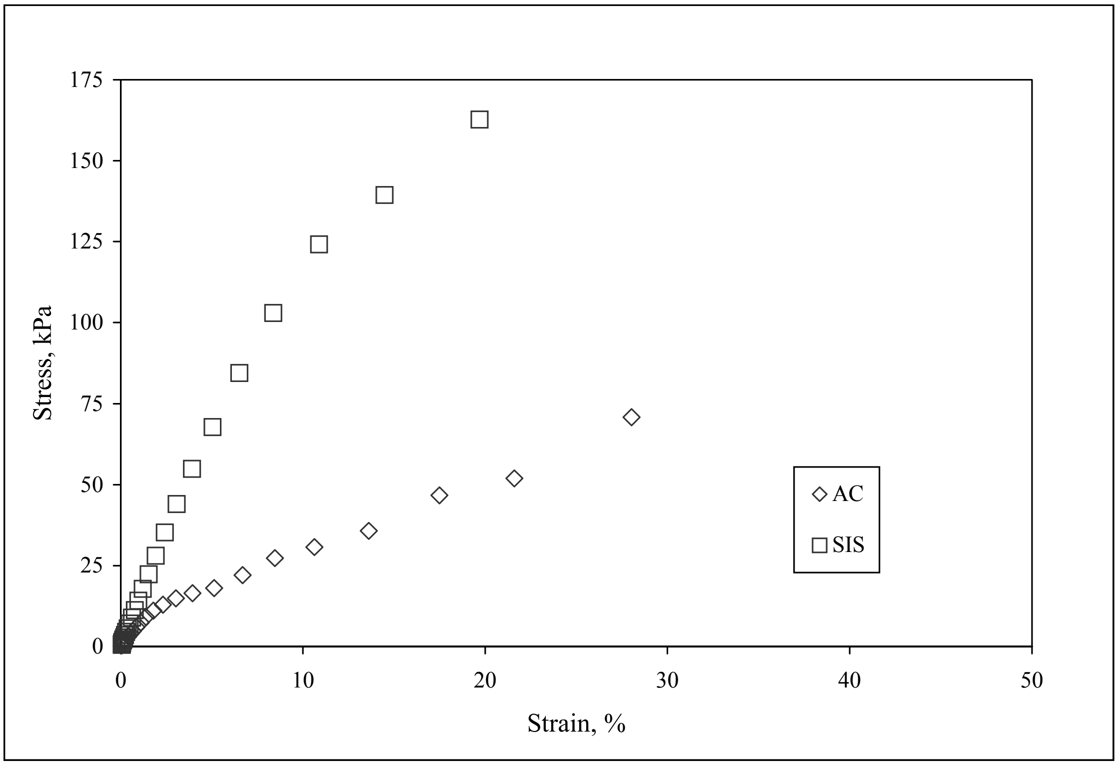

Figure A12-3. Stress Versus Strain for AC and SIS Adhesive Films

APPENDIX 13

ADHESIVE FORMULATION PARTICLE SIZE SAS VERSION 8 RESULTS

```
DATA UCARSIZE;
INPUT STRAIN STRESS MODULUS SIZE;
CARDS;
-0.75 -0.15 0.03 1.08
-0.99 -0.95 -0.73 0.52
-0.69 -0.39 -0.50 0.75
1.00 1.00 -0.87 1.47
-1.00 -1.00 -1.00 0.50
-0.37 -0.34 -0.85 0.68
-0.98 -0.84 -0.22 1.60
-0.73 0.55 1.00 0.91
PROC PRINT DATA = UCARSIZE;
DATA ANAL; SET UCARSIZE;
SS = STRAIN * STRESS;
SM = STRESS * MODULUS;
S2 = STRESS * STRESS;
STR2 = STRAIN * STRAIN;
PROC CORR;
PROC REG;
        MODEL SIZE = STRAIN STRESS
                     MODULUS / SELECTION = FORWARD;
RUN;
```

```
Obs    STRAIN    STRESS    MODULUS    SIZE

 1      -0.75     -0.15      0.03     1.08
 2      -0.99     -0.95     -0.73     0.52
 3      -0.69     -0.39     -0.50     0.75
 4       1.00      1.00     -0.87     1.47
 5      -1.00     -1.00     -1.00     0.50
 6      -0.37     -0.34     -0.85     0.68
 7      -0.98     -0.84     -0.22     1.60
 8      -0.73      0.55      1.00     0.91
```

```
                                   The SAS System                              8
                                                11:37 Wednesday, October 15, 2003

                                 The CORR Procedure

  8  Variables:     STRAIN   STRESS   MODULUS  SIZE     SS       SM       S2
                    STR2


                                 Simple Statistics

Variable          N         Mean      Std Dev          Sum      Minimum      Maximum

STRAIN            8     -0.56375      0.66616     -4.51000     -1.00000      1.00000
STRESS            8     -0.26500      0.72101     -2.12000     -1.00000      1.00000
MODULUS           8     -0.39250      0.66323     -3.14000     -1.00000      1.00000
SIZE              8      0.93875      0.41588      7.51000      0.50000      1.60000
SS                8      0.48370      0.52815      3.86960     -0.40150      1.00000
SM                8      0.25473      0.55767      2.03780     -0.87000      1.00000
S2                8      0.52510      0.42004      4.20080      0.02250      1.00000
STR2              8      0.70611      0.32514      5.64890      0.13690      1.00000


                      Pearson Correlation Coefficients, N = 8
                             Prob > |r| under H0: Rho=0

                          STRAIN         STRESS        MODULUS           SIZE

       STRAIN            1.00000        0.79546       -0.25701        0.45252
                                         0.0182         0.5389         0.2602

       STRESS            0.79546        1.00000        0.36019        0.44638
                          0.0182                        0.3808         0.2676

       MODULUS          -0.25701        0.36019        1.00000        0.22093
                          0.5389         0.3808                        0.5990

       SIZE              0.45252        0.44638        0.22093        1.00000
                          0.2602         0.2676         0.5990

                      Pearson Correlation Coefficients, N = 8
                             Prob > |r| under H0: Rho=0

                              SS             SM             S2           STR2

       STRAIN            0.17060       -0.85694        0.20310        0.05476
                          0.6863         0.0066         0.6295         0.8975

       STRESS           -0.35449       -0.71597       -0.12853       -0.16111
                          0.3889         0.0458         0.7616         0.7031

       MODULUS          -0.75794        0.08364       -0.46478       -0.25453
                          0.0293         0.8439         0.2459         0.5430

       SIZE              0.12169       -0.73742        0.09570        0.27045
                          0.7741         0.0368         0.8217         0.5171
```

```
                        The CORR Procedure

              Pearson Correlation Coefficients, N = 8
                     Prob > |r| under H0: Rho=0

                  STRAIN        STRESS       MODULUS          SIZE

SS               0.17060      -0.35449      -0.75794       0.12169
                  0.6863        0.3889        0.0293        0.7741

SM              -0.85694      -0.71597       0.08364      -0.73742
                  0.0066        0.0458        0.8439        0.0368

S2               0.20310      -0.12853      -0.46478       0.09570
                  0.6295        0.7616        0.2459        0.8217

STR2             0.05476      -0.16111      -0.25453       0.27045
                  0.8975        0.7031        0.5430        0.5171

              Pearson Correlation Coefficients, N = 8
                     Prob > |r| under H0: Rho=0

                      SS            SM            S2          STR2

SS               1.00000      -0.08916       0.85921       0.81085
                                0.8337        0.0063        0.0146

SM              -0.08916       1.00000       0.02779      -0.02267
                  0.8337                      0.9479        0.9575

S2               0.85921       0.02779       1.00000       0.89755
                  0.0063        0.9479                      0.0025

STR2             0.81085      -0.02267       0.89755       1.00000
                  0.0146        0.9575        0.0025
```

```
                              The REG Procedure
                                Model: MODEL1
                          Dependent Variable: SIZE

                          Forward Selection: Step 1

         Variable STRAIN Entered: R-Square = 0.2048 and C(p) = 18.6189


                             Analysis of Variance

                                    Sum of           Mean
 Source                   DF       Squares         Square    F Value    Pr > F

 Model                     1       0.24791        0.24791       1.54    0.2602
 Error                     6       0.96277        0.16046
 Corrected Total           7       1.21069


                 Parameter     Standard
      Variable    Estimate        Error   Type II SS  F Value  Pr > F

      Intercept    1.09801      0.19098      5.30390    33.05  0.0012
      STRAIN       0.28250      0.22728      0.24791     1.54  0.2602

                        Bounds on condition number: 1, 1
--------------------------------------------------------------------------------

                          Forward Selection: Step 2


         Variable MODULUS Entered: R-Square = 0.3265 and C(p) = 17.1552


                             Analysis of Variance

                                    Sum of           Mean
 Source                   DF       Squares         Square    F Value    Pr > F

 Model                     2       0.39534        0.19767       1.21    0.3722
 Error                     5       0.81534        0.16307
 Corrected Total           7       1.21069


                 Parameter     Standard
      Variable    Estimate        Error   Type II SS  F Value  Pr > F

      Intercept    1.21954      0.23109      4.54141    27.85  0.0033
      STRAIN       0.34044      0.23708      0.33625     2.06  0.2105
      MODULUS      0.22642      0.23813      0.14743     0.90  0.3854

                   Bounds on condition number: 1.0707, 4.2829
--------------------------------------------------------------------------------

                          Forward Selection: Step 3
```

```
                               The REG Procedure
                                 Model: MODEL1
                           Dependent Variable: SIZE

                           Forward Selection: Step 3

          Variable STRESS Entered: R-Square = 0.8594 and C(p) = 4.0000


                              Analysis of Variance

                                     Sum of           Mean
 Source                   DF        Squares         Square    F Value    Pr > F

 Model                     3        1.04043        0.34681       8.15    0.0353
 Error                     4        0.17026        0.04257
 Corrected Total           7        1.21069


                    Parameter     Standard
       Variable      Estimate        Error   Type II SS  F Value  Pr > F

       Intercept      2.71922      0.40291      1.93874    45.55  0.0025
       STRAIN         3.03327      0.70224      0.79415    18.66  0.0125
       STRESS        -2.61661      0.67214      0.64508    15.16  0.0176
       MODULUS        1.94615      0.45820      0.76789    18.04  0.0132

                   Bounds on condition number: 38.623, 269.4
--------------------------------------------------------------------------------


                All variables have been entered into the model.


                         Summary of Forward Selection

        Variable    Number    Partial     Model
 Step   Entered     Vars In   R-Square   R-Square    C(p)     F Value   Pr > F

   1    STRAIN          1      0.2048     0.2048    18.6189      1.54   0.2602
   2    MODULUS         2      0.1218     0.3265    17.1552      0.90   0.3854
   3    STRESS          3      0.5328     0.8594     4.0000     15.16   0.0176
```

APPENDIX 14

PRESSURE DIFFERENCE AT PASSAGE VERSUS PARTICLE DIMENSIONS

Figure A14-1, **Figure A14-2**, **Figure A14-3**, and **Figure A14-4** are plots of pressure difference across the slot of the single slot device at particle passage versus the particle dimensions for eight different adhesive formulations. The particle dimensions for **Figure A14-1**, **Figure A14-2**, **Figure A14-3**, and **Figure A14-4** are particle length, average particle width, average particle thickness, and particle area, respectively. Particle area is calculated as the particle length times the average particle width.

These plots show considerable scatter in the pressure differences required for particles with the same particle dimension values. Also, the plots only show data for particles that did pass through the slot of the single slot device. The dimensions of particles that did not pass through the slot are not shown here because they do not have a value for pressure difference at passage.

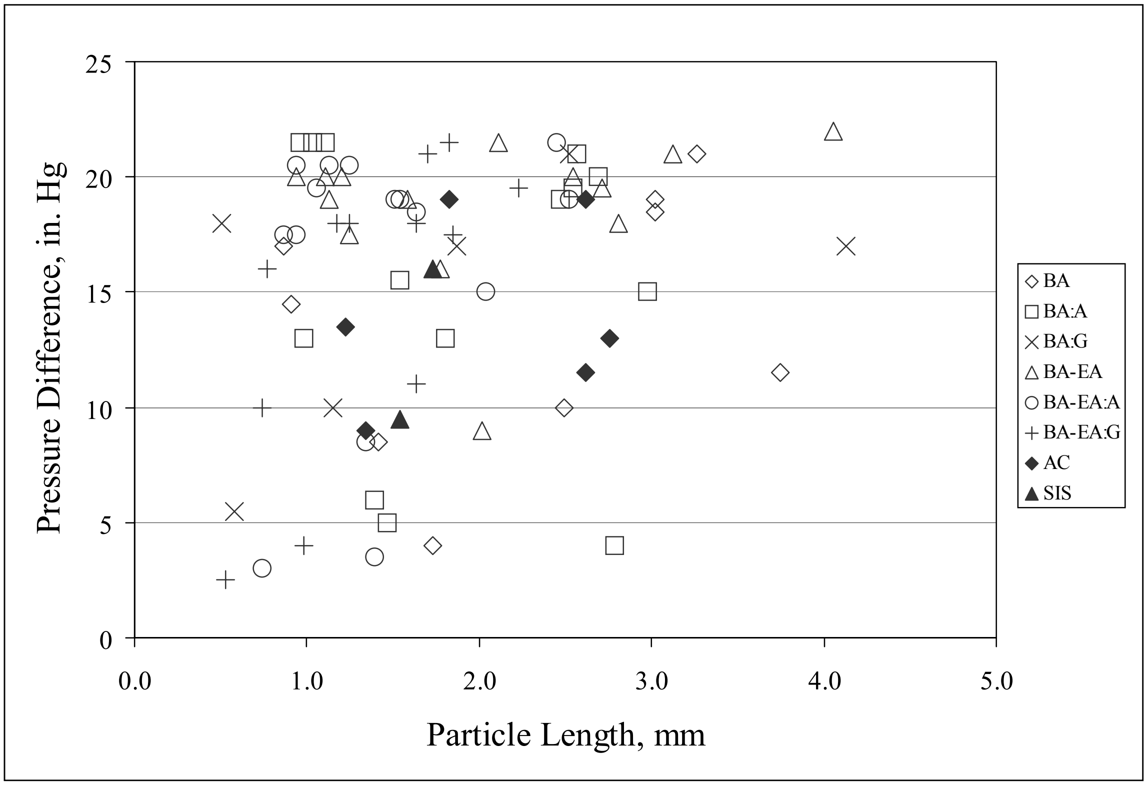

Figure A14-1. Pressure Difference at Passage Versus Particle Length

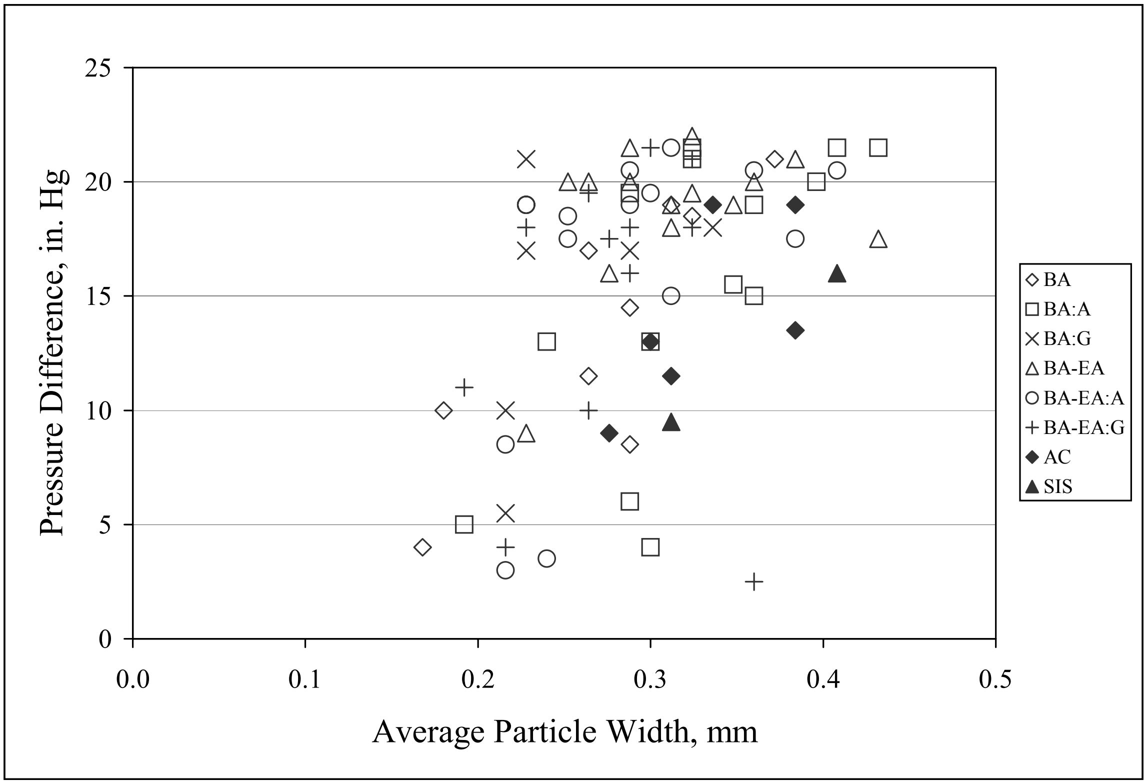

Figure A14-2. Pressure Difference at Passage Versus Average Particle Width

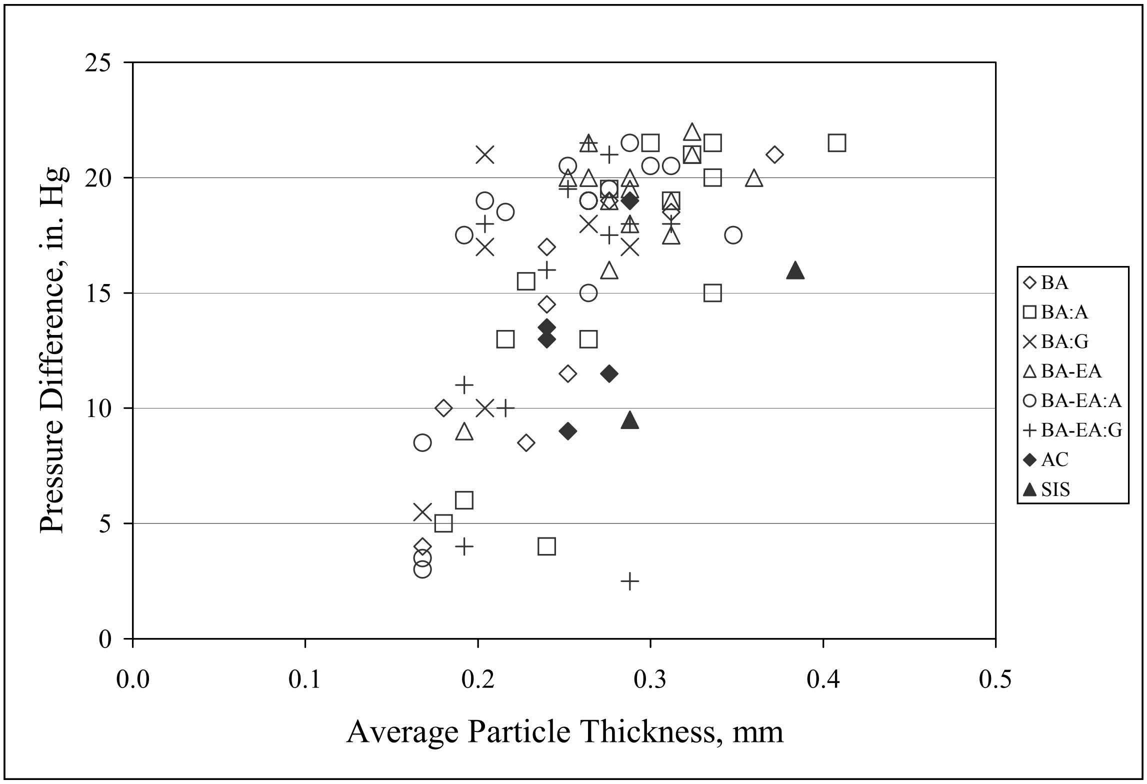

Figure A14-3. Pressure Difference at Passage Versus Average Particle Thickness

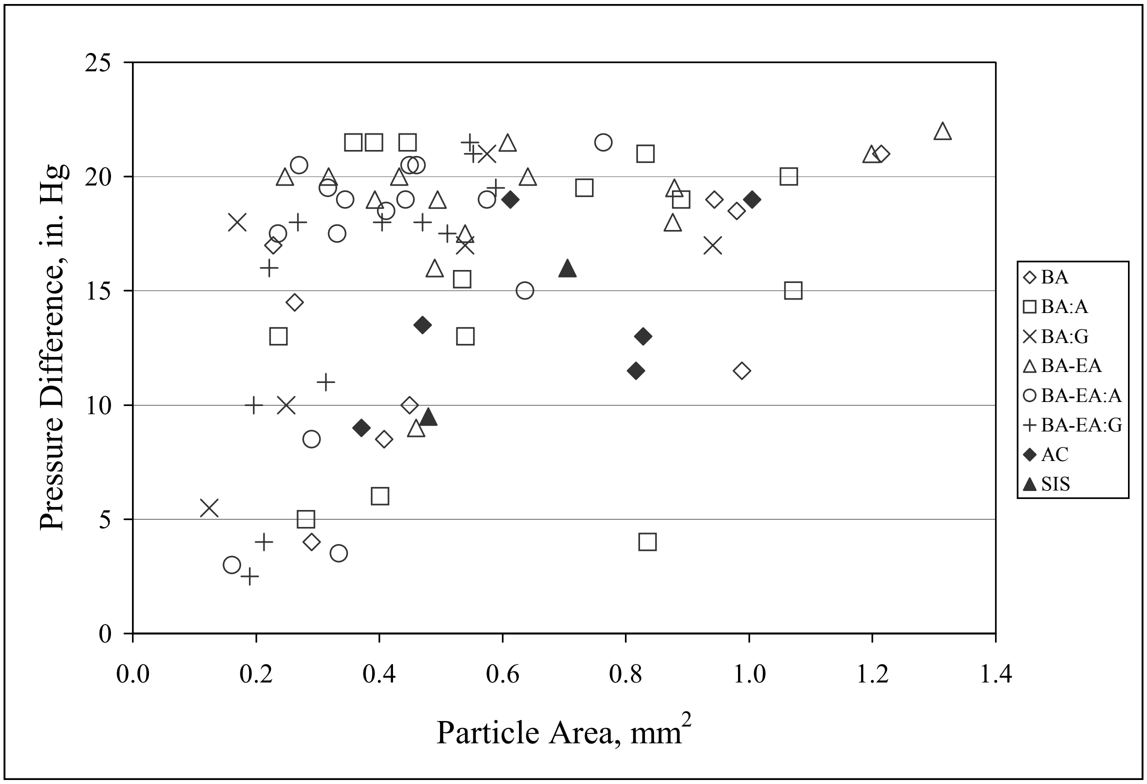

Figure A14-4. Pressure Difference at Passage Versus Particle Area

APPENDIX 15

ADHESIVE FORMULATION PARTICLE PASSAGE SAS VERSION 8 RESULTS

```
DATA UCAR;
INPUT LENGTH WIDTH THICK AREA STRAIN STRESS MODULUS PASSAGE;
CARDS;
1.00 -0.39 -0.20 0.70 -0.75 -0.15 0.03 37.5
-0.32 -0.44 -0.07 -0.49 -0.99 -0.95 -0.73 70
0.02 -0.80 -0.97 -0.27 -0.69 -0.39 -0.50 30
0.60 -0.10 0.30 0.47 1.00 1.00 -0.87 5
-0.66 -1.00 -1.00 -0.95 -1.00 -1.00 -1.00 75
-0.86 -0.57 -0.34 -1.00 -0.37 -0.34 -0.85 30
0.55 1.00 0.78 1.00 -0.98 -0.84 -0.22 30
-1.00 0.66 1.00 -0.77 -0.73 0.55 1.00 10
PROC PRINT DATA = UCAR;
DATA ANAL; SET UCAR;
LT = LENGTH * THICK;
WT = WIDTH * THICK;
VOLUME = AREA * THICK;
SS = STRAIN * STRESS;
SM = STRESS * MODULUS;
S2 = STRESS * STRESS;
LOAD = AREA * STRESS;
LS = LENGTH * STRAIN;
STR2 = STRAIN * STRAIN;
PROC CORR;
PROC REG;
      MODEL PASSAGE = LENGTH AREA
                      STRAIN STRESS
                      MODULUS LOAD
                      / SELECTION = FORWARD;
RUN;
```

```
Obs    LENGTH    WIDTH    THICK     AREA    STRAIN    STRESS    MODULUS    PASSAGE

 1       1.00    -0.39    -0.20     0.70     -0.75     -0.15      0.03       37.5
 2      -0.32    -0.44    -0.07    -0.49     -0.99     -0.95     -0.73       70.0
 3       0.02    -0.80    -0.97    -0.27     -0.69     -0.39     -0.50       30.0
 4       0.60    -0.10     0.30     0.47      1.00      1.00     -0.87        5.0
 5      -0.66    -1.00    -1.00    -0.95     -1.00     -1.00     -1.00       75.0
 6      -0.86    -0.57    -0.34    -1.00     -0.37     -0.34     -0.85       30.0
 7       0.55     1.00     0.78     1.00     -0.98     -0.84     -0.22       30.0
 8      -1.00     0.66     1.00    -0.77     -0.73      0.55      1.00       10.0
```

```
                                The CORR Procedure

  17  Variables:    LENGTH   WIDTH    THICK    AREA     STRAIN   STRESS
                    MODULUS  PASSAGE  LT       WT       VOLUME   SS       SM
                    S2       LOAD     LS       STR2


                                Simple Statistics

 Variable          N        Mean     Std Dev         Sum     Minimum     Maximum

 LENGTH            8    -0.08375     0.74492    -0.67000    -1.00000     1.00000
 WIDTH             8    -0.20500     0.69898    -1.64000    -1.00000     1.00000
 THICK             8    -0.06250     0.73373    -0.50000    -1.00000     1.00000
 AREA              8    -0.16375     0.78420    -1.31000    -1.00000     1.00000
 STRAIN            8    -0.56375     0.66616    -4.51000    -1.00000     1.00000
 STRESS            8    -0.26500     0.72101    -2.12000    -1.00000     1.00000
 MODULUS           8    -0.39250     0.66323    -3.14000    -1.00000     1.00000
 PASSAGE           8    35.93750    25.14023   287.50000     5.00000    75.00000
 LT                8     0.04555     0.50169     0.36440    -1.00000     0.66000
 WT                8     0.43608     0.40890     3.48860    -0.03000     1.00000
 VOLUME            8     0.19965     0.53583     1.59720    -0.77000     0.95000
 SS                8     0.48370     0.52815     3.86960    -0.40150     1.00000
 SM                8     0.25473     0.55767     2.03780    -0.87000     1.00000
 S2                8     0.52510     0.42004     4.20080     0.02250     1.00000
 LOAD              8     0.12029     0.56657     0.96230    -0.84000     0.95000
 LS                8     0.16528     0.55611     1.32220    -0.75000     0.73000
 STR2              8     0.70611     0.32514     5.64890     0.13690     1.00000


                      Pearson Correlation Coefficients, N = 8
                             Prob > |r| under H0: Rho=0

                LENGTH       WIDTH       THICK        AREA      STRAIN      STRESS

LENGTH         1.00000     0.15849     0.08430     0.93678     0.27190     0.13540
                            0.7078      0.8427      0.0006      0.5148      0.7492

WIDTH          0.15849     1.00000     0.94319     0.48341     0.00143     0.27516
                0.7078                  0.0004      0.2249      0.9973      0.5095

THICK          0.08430     0.94319     1.00000     0.37622     0.15728     0.44629
                0.8427      0.0004                  0.3583      0.7099      0.2677

AREA           0.93678     0.48341     0.37622     1.00000     0.21330     0.15542
                0.0006      0.2249      0.3583                  0.6120      0.7132

STRAIN         0.27190     0.00143     0.15728     0.21330     1.00000     0.79546
                0.5148      0.9973      0.7099      0.6120                  0.0182

STRESS         0.13540     0.27516     0.44629     0.15542     0.79546     1.00000
                0.7492      0.5095      0.2677      0.7132      0.0182

MODULUS       -0.07558     0.64013     0.64297     0.11004    -0.25701     0.36019
                0.8588      0.0873      0.0855      0.7953      0.5389      0.3808

PASSAGE       -0.19850    -0.54052    -0.57179    -0.33094    -0.62992    -0.84752
                0.6375      0.1666      0.1387      0.4233      0.0941      0.0079
```

```
                                The SAS System                               27
                                          08:53 Monday, October 13, 2003

                              The CORR Procedure

                       Pearson Correlation Coefficients, N = 8
                              Prob > |r| under H0: Rho=0

                 LENGTH        WIDTH        THICK         AREA       STRAIN       STRESS

 LT             0.18343     -0.37370     -0.50094      0.10099      0.02908     -0.54380
                 0.6637       0.3618       0.2060       0.8119       0.9455       0.1636

 WT            -0.32822      0.07924     -0.17091     -0.21601     -0.52741     -0.39114
                 0.4274       0.8521       0.6857       0.6074       0.1792       0.3380

 VOLUME         0.12606     -0.27794     -0.47728      0.09271     -0.13861     -0.62631
                 0.7661       0.5051       0.2317       0.8272       0.7434       0.0966

 SS             0.30032     -0.19086     -0.22476      0.24333      0.17060     -0.35449
                 0.4698       0.6507       0.5926       0.5615       0.6863       0.3889

 SM            -0.66395     -0.20947     -0.27042     -0.63651     -0.85694     -0.71597
                 0.0726       0.6186       0.5171       0.0897       0.0066       0.0458

 S2             0.00672      0.03550      0.07458      0.04225      0.20310     -0.12853
                 0.9874       0.9335       0.8607       0.9209       0.6295       0.7616

 LOAD          -0.28675     -0.85174     -0.70684     -0.54916      0.23251     -0.11731
                 0.4911       0.0073       0.0500       0.1586       0.5795       0.7820

 LS            -0.72992     -0.19235     -0.01917     -0.72863      0.31674      0.30405
                 0.0398       0.6481       0.9641       0.0403       0.4446       0.4641

 STR2           0.32385      0.16382      0.14707      0.36033      0.05476     -0.16111
                 0.4339       0.6983       0.7282       0.3806       0.8975       0.7031

                       Pearson Correlation Coefficients, N = 8
                              Prob > |r| under H0: Rho=0

                MODULUS      PASSAGE           LT           WT       VOLUME           SS

 LENGTH        -0.07558     -0.19850      0.18343     -0.32822      0.12606      0.30032
                 0.8588       0.6375       0.6637       0.4274       0.7661       0.4698

 WIDTH          0.64013     -0.54052     -0.37370      0.07924     -0.27794     -0.19086
                 0.0873       0.1666       0.3618       0.8521       0.5051       0.6507

 THICK          0.64297     -0.57179     -0.50094     -0.17091     -0.47728     -0.22476
                 0.0855       0.1387       0.2060       0.6857       0.2317       0.5926

 AREA           0.11004     -0.33094      0.10099     -0.21601      0.09271      0.24333
                 0.7953       0.4233       0.8119       0.6074       0.8272       0.5615

 STRAIN        -0.25701     -0.62992      0.02908     -0.52741     -0.13861      0.17060
                 0.5389       0.0941       0.9455       0.1792       0.7434       0.6863

 STRESS         0.36019     -0.84752     -0.54380     -0.39114     -0.62631     -0.35449
                 0.3808       0.0079       0.1636       0.3380       0.0966       0.3889

 MODULUS        1.00000     -0.45907     -0.87120      0.16377     -0.73827     -0.75794
                              0.2525       0.0048       0.6984       0.0365       0.0293
```

```
                               The CORR Procedure

                   Pearson Correlation Coefficients, N = 8
                          Prob > |r| under H0: Rho=0

                MODULUS     PASSAGE          LT          WT      VOLUME          SS

PASSAGE    -0.45907     1.00000     0.48062     0.18974     0.48214     0.46822
             0.2525                  0.2280      0.6527      0.2263      0.2420

LT         -0.87120     0.48062     1.00000     0.13720     0.96048     0.78098
             0.0048      0.2280                  0.7460      0.0001      0.0221

WT          0.16377     0.18974     0.13720     1.00000     0.39691    -0.04590
             0.6984      0.6527      0.7460                  0.3303      0.9141

VOLUME     -0.73827     0.48214     0.96048     0.39691     1.00000     0.70645
             0.0365      0.2263      0.0001      0.3303                  0.0501

SS         -0.75794     0.46822     0.78098    -0.04590     0.70645     1.00000
             0.0293      0.2420      0.0221      0.9141      0.0501

SM          0.08364     0.72709     0.01890     0.54689     0.15054    -0.08916
             0.8439      0.0410      0.9646      0.1607      0.7220      0.8337

S2         -0.46478     0.34195     0.47144     0.04836     0.42952     0.85921
             0.2459      0.4071      0.2383      0.9095      0.2882      0.0063

LOAD       -0.72405     0.51741     0.43208    -0.16322     0.29241     0.44408
             0.0423      0.1891      0.2850      0.6994      0.4822      0.2703

LS         -0.12851    -0.00719    -0.11647     0.08105    -0.15076     0.06495
             0.7617      0.9865      0.7836      0.8487      0.7216      0.8786

STR2       -0.25453     0.33598     0.35211     0.08331     0.35102     0.81085
             0.5430      0.4158      0.3923      0.8445      0.3939      0.0146

                   Pearson Correlation Coefficients, N = 8
                          Prob > |r| under H0: Rho=0

                   SM            S2          LOAD            LS          STR2

  LENGTH     -0.66395       0.00672      -0.28675      -0.72992       0.32385
               0.0726        0.9874        0.4911        0.0398        0.4339

  WIDTH      -0.20947       0.03550      -0.85174      -0.19235       0.16382
               0.6186        0.9335        0.0073        0.6481        0.6983

  THICK      -0.27042       0.07458      -0.70684      -0.01917       0.14707
               0.5171        0.8607        0.0500        0.9641        0.7282

  AREA       -0.63651       0.04225      -0.54916      -0.72863       0.36033
               0.0897        0.9209        0.1586        0.0403        0.3806

  STRAIN     -0.85694       0.20310       0.23251       0.31674       0.05476
               0.0066        0.6295        0.5795        0.4446        0.8975

  STRESS     -0.71597      -0.12853      -0.11731       0.30405      -0.16111
               0.0458        0.7616        0.7820        0.4641        0.7031
```

```
                             The CORR Procedure

                 Pearson Correlation Coefficients, N = 8
                        Prob > |r| under H0: Rho=0

                 SM            S2          LOAD            LS          STR2

MODULUS     0.08364      -0.46478      -0.72405      -0.12851      -0.25453
             0.8439        0.2459        0.0423        0.7617        0.5430

PASSAGE     0.72709       0.34195       0.51741      -0.00719       0.33598
             0.0410        0.4071        0.1891        0.9865        0.4158

LT          0.01890       0.47144       0.43208      -0.11647       0.35211
             0.9646        0.2383        0.2850        0.7836        0.3923

WT          0.54689       0.04836      -0.16322       0.08105       0.08331
             0.1607        0.9095        0.6994        0.8487        0.8445

VOLUME      0.15054       0.42952       0.29241      -0.15076       0.35102
             0.7220        0.2882        0.4822        0.7216        0.3939

SS         -0.08916       0.85921       0.44408       0.06495       0.81085
             0.8337        0.0063        0.2703        0.8786        0.0146

SM          1.00000       0.02779       0.15821       0.19137      -0.02267
                           0.9479        0.7083        0.6498        0.9575

S2          0.02779       1.00000       0.40036       0.43418       0.89755
             0.9479                      0.3257        0.2824        0.0025

LOAD        0.15821       0.40036       1.00000       0.55611       0.15661
             0.7083        0.3257                      0.1523        0.7111

LS          0.19137       0.43418       0.55611       1.00000       0.09746
             0.6498        0.2824        0.1523                      0.8184

STR2       -0.02267       0.89755       0.15661       0.09746       1.00000
             0.9575        0.0025        0.7111        0.8184
```

```
                               The REG Procedure
                                 Model: MODEL1
                          Dependent Variable: PASSAGE

                           Forward Selection: Step 1

         Variable STRESS Entered: R-Square = 0.7183 and C(p) = 176035.2


                              Analysis of Variance

                                     Sum of           Mean
 Source                   DF        Squares         Square    F Value    Pr > F

 Model                     1     3177.88236     3177.88236      15.30    0.0079
 Error                     6     1246.33639      207.72273
 Corrected Total           7     4424.21875


                    Parameter     Standard
       Variable      Estimate        Error   Type II SS  F Value  Pr > F

       Intercept     28.10638      5.47485   5474.56900    26.36  0.0021
       STRESS       -29.55139      7.55529   3177.88236    15.30  0.0079

                        Bounds on condition number: 1, 1
--------------------------------------------------------------------------------

                           Forward Selection: Step 2


          Variable LOAD Entered: R-Square = 0.8954 and C(p) = 65335.88


                              Analysis of Variance

                                     Sum of           Mean
 Source                   DF        Squares         Square    F Value    Pr > F

 Model                     2     3961.63434     1980.81717      21.41    0.0035
 Error                     5      462.58441       92.51688
 Corrected Total           7     4424.21875


                    Parameter     Standard
       Variable      Estimate        Error   Type II SS  F Value  Pr > F

       Intercept     26.30366      3.70589   4660.88880    50.38  0.0009
       STRESS       -27.81777      5.07725   2777.20829    30.02  0.0028
       LOAD          18.80601      6.46127    783.75198     8.47  0.0334

                   Bounds on condition number: 1.014, 4.0558
--------------------------------------------------------------------------------

                           Forward Selection: Step 3
```

```
                            The REG Procedure
                              Model: MODEL1
                       Dependent Variable: PASSAGE

                         Forward Selection: Step 3

        Variable MODULUS Entered: R-Square = 0.9412 and C(p) = 36724.17


                           Analysis of Variance

                                    Sum of           Mean
Source                   DF        Squares         Square    F Value    Pr > F

Model                     3     4164.21602     1388.07201      21.35    0.0063
Error                     4      260.00273       65.00068
Corrected Total           7     4424.21875


               Parameter     Standard
      Variable      Estimate        Error   Type II SS  F Value  Pr > F

      Intercept     29.22040      3.51833   4483.49200    68.98  0.0011
      STRESS       -31.11467      4.64748   2913.48385    44.82  0.0026
      MODULUS       12.84201      7.27431    202.58169     3.12  0.1523
      LOAD          29.19843      7.99908    866.07869    13.32  0.0218

                  Bounds on condition number: 2.5067, 17.783
--------------------------------------------------------------------------------

                         Forward Selection: Step 4

          Variable AREA Entered: R-Square = 0.9803 and C(p) = 12293.44


                           Analysis of Variance

                                    Sum of           Mean
Source                   DF        Squares         Square    F Value    Pr > F

Model                     4     4337.19685     1084.29921      37.38    0.0068
Error                     3       87.02190       29.00730
Corrected Total           7     4424.21875


               Parameter     Standard
      Variable      Estimate        Error   Type II SS  F Value  Pr > F

      Intercept     31.67548      2.55634   4453.65977   153.54  0.0011
      AREA           9.50806      3.89356    172.98083     5.96  0.0923
      STRESS       -34.33314      3.37281   3005.72543   103.62  0.0020
      MODULUS       21.66182      6.05464    371.29582    12.80  0.0373
      LOAD          43.42053      7.90396    875.40221    30.18  0.0119

                  Bounds on condition number: 4.8393, 49.63
--------------------------------------------------------------------------------

                         Forward Selection: Step 5
```

```
                                  The REG Procedure
                                    Model: MODEL1
                             Dependent Variable: PASSAGE

                              Forward Selection: Step 5

          Variable STRAIN Entered: R-Square = 0.9976 and C(p) = 1507.911


                                Analysis of Variance

                                         Sum of           Mean
 Source                        DF       Squares         Square    F Value    Pr > F

 Model                          5    4413.57124      882.71425     165.81    0.0060
 Error                          2      10.64751        5.32376
 Corrected Total                7    4424.21875


                   Parameter     Standard
       Variable     Estimate        Error   Type II SS  F Value  Pr > F

       Intercept    71.82829     10.65752    241.82245    45.42  0.0213
       AREA          7.47636      1.75215     96.92928    18.21  0.0508
       STRAIN       69.15205     18.25746     76.37438    14.35  0.0632
       STRESS     -101.17076     17.70546    173.82558    32.65  0.0293
       MODULUS      75.19165     14.36895    145.78316    27.38  0.0346
       LOAD         58.36350      5.19909    670.88215   126.02  0.0078

                      Bounds on condition number: 214.28, 2710.4
--------------------------------------------------------------------------------

                              Forward Selection: Step 6


           Variable LENGTH Entered: R-Square = 1.0000 and C(p) = 7.0000


                                Analysis of Variance

                                         Sum of           Mean
 Source                        DF       Squares         Square    F Value    Pr > F

 Model                          6    4424.21167      737.36861     104150    0.0024
 Error                          1       0.00708        0.00708
 Corrected Total                7    4424.21875


                   Parameter     Standard
       Variable     Estimate        Error   Type II SS  F Value  Pr > F

       Intercept    98.72257      0.79518    109.12491  15413.4  0.0051
       LENGTH       17.08523      0.44071     10.64043  1502.91  0.0164
       AREA        -13.13874      0.53559      4.26060   601.79  0.0259
       STRAIN      117.78417      1.42020     48.69708  6878.23  0.0077
       STRESS     -147.34989      1.35492     83.73316  11826.9  0.0059
       MODULUS     110.02819      1.04022     79.21030  11188.1  0.0060
       LOAD         58.47258      0.18962    673.24389  95092.5  0.0021
```

```
                              The REG Procedure
                                Model: MODEL1
                         Dependent Variable: PASSAGE

                          Forward Selection: Step 6

                   Bounds on condition number: 943.59, 15549
--------------------------------------------------------------------------------


                All variables have been entered into the model.


                         Summary of Forward Selection

       Variable     Number    Partial     Model
 Step  Entered      Vars In   R-Square    R-Square     C(p)     F Value   Pr > F

   1   STRESS          1       0.7183      0.7183     176035      15.30   0.0079
   2   LOAD            2       0.1772      0.8954    65335.9       8.47   0.0334
   3   MODULUS         3       0.0458      0.9412    36724.2       3.12   0.1523
   4   AREA            4       0.0391      0.9803    12293.4       5.96   0.0923
   5   STRAIN          5       0.0173      0.9976    1507.91      14.35   0.0632
   6   LENGTH          6       0.0024      1.0000     7.0000    1502.91   0.0164
```

APPENDIX 16

PARTICLE PASSAGE THROUGH A SLOT BY PARTICLE BENDING OR PARTICLE EXTRUSION

INTRODUCTION

Recycled paper contains several different contaminants that must be removed by various operations in the recycling process in order to produce a marketable product [1]. One such contaminant is pressure sensitive adhesive (PSA) material [1]. The primary operation in the recycling process for removing pressure sensitive adhesive material is the pressure screen [2]. However, the pressure screen does not remove all of the adhesive material from the pulp [2-5]. Therefore, it is of interest to understand how pressure sensitive adhesive particles are able to pass through the slot of a pressurized screen. Two proposed methods for particle passage are particle bending and particle extrusion [6]. Elastic beam theory could explain particle bending and the theory of combined loads on a bar could explain particle extrusion.

Particle Bending

When a beam is subjected to a load, stresses occur within the beam and the beam changes shape by deflection [7]. There are two simple loading situations for a beam that is only supported at both ends. Either the load occurs at the center of the beam or the load is evenly distributed along the length of the beam. Also, the load can cause elastic or plastic deformation to occur in the beam, depending on the stress-strain relationship.

When the load occurs at the center of the beam, all of the force is focused at one point equidistant from both ends of the beam [7]. The equation relating the load and deflection in the beam is:

$$\delta = \frac{WL^3}{48EI}$$

where δ is the deflection in the beam, *W* is the load on the beam, *L* is the length of the beam, *E* is the modulus of the beam, and *I* is the moment of inertia for the beam [7]. Deflection is how far the center of the beam moves after the load is applied to the beam. The equation for the moment of inertia, *I*, for a rectangular beam, is:

$$I = \frac{bd^3}{12}$$

where *b* is the width of the beam and *d* is the height of the beam [7].

When the load is evenly distributed along the length of the beam, the force is spread out over the length of the beam [7]. The equation relating the load and deflection is:

$$\delta = \frac{5}{384}\frac{wL^4}{EI}$$

where δ is the deflection in the beam, *w* is the load divided by the length of the beam, *L* is the length of the beam, *E* is the modulus of the beam, and *I* is the moment of inertia for the beam [7]. However, both of these equations for δ assume that the deflections are so small that changes do not occur in the geometry of the beam.

In the case of large deflections, the equations are non-linear because the beam changes from a straight beam to a curved beam [7]. Due to the changes in the geometry when the load is applied the load that can be supported by the beam reaches a maximum.

When δ/L is equal to 0.24, the load is at a maximum and WL^2/EI equals 6.72. However, when δ/L is small, the equations are linear and take the form of the equation for small deflections with a central load.

When a beam is subjected to a load, the load can occur in the elastic or plastic region of the stress-strain relationship [7]. If the load is in the plastic region, that is at a stress greater than the yield stress of the material, permanent deformation can occur and there is a maximum load that the beam can support before the beam fails and collapses. The maximum load that a centrally loaded, simply supported beam can sustain is given by the equation:

$$W_P = \frac{bd^2}{L}\sigma_Y$$

where W_p is the maximum load, b is the width of the beam, d is the height of the beam, L is the length of the beam, and σ_Y is the tensile yield stress of the beam [7]. The equation for the load at first yield is:

$$W_E = \frac{2}{3}W_P$$

where W_E is the load at first yield [7]. As the load increases above the load at first yield, the beam begins to deform plastically until the load reaches the maximum load.

In a theoretical investigation of debris removal in screens by Bliss, particle passage was proposed to involve particle bending or particle extrusion [6]. Two models were developed for particle bending that were functions of the pressure drop and modulus. One model was for the maximum deflection and the equation is:

$$\delta_{\max} = \frac{60dpL^4}{384Ez^3}$$

where δ_{max} is the maximum deflection, dp is the pressure drop, E is the modulus, L is the particle length, and z is the particle thickness [6]. The other model for particle bending was for the maximum angle of deflection and the equation is:

$$\theta_{\max} = \frac{dpL^3}{2Ez^3}$$

where θ_{max} is the maximum angle of deflection, dp is the pressure drop, E is the modulus, L is the particle length, and z is the particle thickness [6]. However, in order for the particle to bend and pass through the slot of the pressure screen, the particle thickness must be less than half the slot width.

Particle Extrusion – Beam Deformation

The above beam theory involves only one force being applied to a beam, but multiple forces can occur at different locations on the same beam at the same time. In theory, combined loads on a bar involve two independent forces being applied to a non-rigid bar [8]. If one of the surfaces is under tension and the other compression, plastic yielding can occur. The equation relating the two forces to each other for plastic yielding is:

$$F_1 - F_2 = \pm 2\sigma_Y A$$

where F_1 and F_2 are the loads acting on opposite ends of the bar, σ_Y is the yield stress of the material, and A is the cross-sectional area of the bar [8]. The sign on the right side of the equation is positive if the top surface is under compression and the bottom surface is under tension and negative if the top surface is under tension and the bottom surface is under compression.

For particle extrusion, a model was developed involving a pressure screen with a screen plate containing tapered holes [6]. The equation for particle extrusion through the hole of a contoured screen plate is:

$$\frac{F_1}{A_1}+\frac{F_2}{A_2}=2\sigma_Y \ln\frac{D_1}{D_2}$$

where F_1/A_1 is the pressure on the inlet side of the screen, F_2/A_2 is the pressure on the accept side of the screen, σ_Y is the yield stress of the material, D_1 is the widest diameter of the hole, and D_2 is the smallest diameter of the hole [6]. From this equation and typical values for pressure screen operations and yield stress, it was predicted that extrusion could not occur. However, this model does not take into account the dimensions of the particle that is passing through the hole, only the dimensions of the hole itself. This model is similar to the above model for plastic yielding with combined loads.

The objective of this research is to determine a model that can represent the passage of pressure sensitive adhesive particles through the slot of a pressurized screen. Equations will be developed relating the pressures at points within a pressurized screening system to measurable variables. The way in which the particle enters and passes through a pressurized single slot device will be compared to determine how particle bending and particle extrusion affect particle passage.

EXPERIMENTAL PROCEDURE

Single Slot Experiments Involving Particle Orientation

Six 10 cm by 10 cm adhesive labels were applied to copy paper and then pulped in the 450H pulper. The operating parameters for the 450H pulper were 450 OD g of pulp, 12% consistency, 50°C, and 415 rpm, for 30 minutes. The adhesive formulations considered for these experiments were BA-EA and BA-EA:A.

Individual PSA particles for each of the adhesive formulations were analyzed in a single slotted screening device for particle passage involving particle orientation with respect to the slot. The two orientations that were considered were aligned and perpendicular and are shown in **Figure A16-1**. Aligned particles have their length aligned with the length of the slot and perpendicular particles have their length perpendicular to the length of the slot.

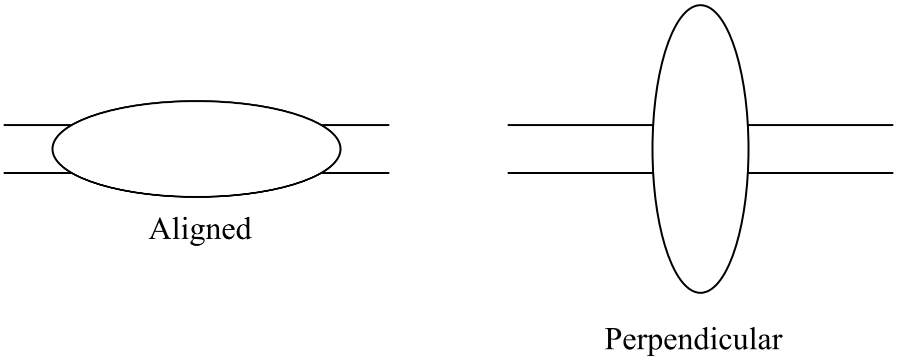

Figure A16-1. Particle Orientation with Respect to the Slot Length

BA-EA or BA-EA:A adhesive particles were removed from a pulp sample. The length, width, and thickness were measured for each adhesive particle under a microscope. The length was the largest dimension, width was the second largest dimension, and thickness was the shortest dimension of a particle. Each adhesive particle was then allowed to soak in deionized water at 50°C for five minutes, before being placed on the 0.007 inches wide slot of the single slot device. The length of the particle was either aligned with or perpendicular to the length of the slot. The remainder of the slot was covered with duct tape. The device was then filled with 1000 mL of deionized water at 50°C. A vacuum was applied to the single slot by slowly opening the vacuum line. The method by which the particles entered the slot was observed. If the particle passed through the slot, the vacuum pressure at which the particle passed was recorded and the particle was recovered from the device. If the particle did not pass through the slot, the vacuum pressure at which the particle started to enter the slot and the percentage of the particle that entered the slot were recorded. The particle passage was determined for each of the adhesive formulations and orientations considered, based on the number of particles that passed through the slot compared to the total number of particles that were analyzed.

RESULTS AND DISCUSSION

Single Slot Experiments Involving Particle Orientation

The single slotted screening results for adhesive particles for two different PSA formulations and two different particle orientations are shown in **Table A16-1**. Aligned with the slot and perpendicular to the slot in **Table A16-1** correspond to (A) and (P), respectively. The results consist of average particle length, average particle width, average particle thickness, average particle area, particle entering, and particle passage. Particle area is the particle length times the particle width. Particle entering and particle passage are the percentage of the analyzed particles that entered the slot and the percentage of particles that passed through the slot, respectively.

Table A16-1. Single Slotted Screening Results for Two Different Slot Orientations

Sample	Length, mm	Width, mm	Thickness, mm	Area, mm^2	Particle Entering, %	Particle Passage, %
BA-EA (A)	3.24	0.45	0.39	1.46	70	0
BA-EA (P)	3.24	0.42	0.38	1.43	90	0
BA-EA:A (A)	1.45	0.36	0.33	0.52	95	65
BA-EA:A (P)	1.35	0.42	0.35	0.64	90	55

The BA-EA particles were unable to pass through the slot regardless of their orientation with respect to the slot. The BA-EA:A particles were able to pass through the slot, but fewer particles passed through the slot when perpendicular to the slot, than when aligned with the slot.

A majority of the particles entered the slot, but the way in which the particles entered the slot depended on their orientation to the slot. For the particles that were aligned with the slot, the center of the particle slid into the slot first and then the particle would continue to enter until the ends of the particle entered the slot. For the particles that were perpendicular to the slot, the particle folded on itself perpendicular to its width and entered the slot.

Note that the particle width and thickness were both larger than the slot width of 0.007 inches (0.18 mm). It has been predicted that only particles with a thickness less than half the slot width may pass through the slot by particle bending. However, particles were able to pass through the slot even with a thickness greater than the slot width. Therefore, the particles must pass through the slot by extrusion whether or not bending occurs.

The theory of bending to solely account for particle passage is not useful here. For bending to be the main mechanism, it is required that the smallest dimension of the particle be less than half the slot width, but the data in **Table A16-1** show that this is not the case for these particles.

Single Slot Energy Balances

In operations involving the pressurized single slot device, the only values that can be measured are the dimensions of the device, the water level in the funnel, and the vacuum gauge pressure in the vacuum line of the device. Equations must be developed relating the forces on a particle at the slot of the device to the water level and vacuum gauge pressure.

The forces acting on a particle at the slot of the single slot device consist of drag and pressure forces. The drag forces involve interaction between the particle and fluid flow around it. The pressure forces involve the pressure difference across the particle. However, the drag forces were found to be negligible for the single slot device (see **APPENDIX 17**).

A model of the single slot device was set up with four points of interest. Point 0 is the surface of the water in the funnel, point 1 is the top of the slot, point two is inside the slot, and point 3 is the bottom of the slot. **Figure A16-2** is a drawing of the model single slot device. The dimensions of the device are a funnel diameter of 17 cm, a top slot width of 0.007 inches, a bottom slot width of 0.014 inches, a slot length of 1 inch, and a slot height of 0.25 inches. The water level in the funnel is 1.6 cm.

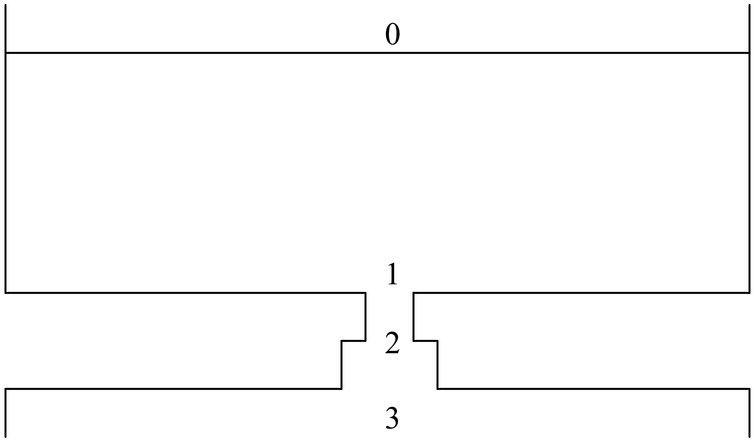

Figure A16-2. Model of Pressurized Single Slot Device

Energy balance equations and mass balance equations will be used to determine the pressures at points 1 and 2 in **Figure A16-2** in terms of the device dimensions, water level, gauge pressure. These equations will then be used to determine the forces acting on a particle at the slot of a pressurized single slot device.

The application of energy balance equations and mass balance equations to the pressurized single slot device provided equations for the pressures above and below the slot opening. The equation for the pressure at point 1 in **Figure A16-2** is:

$$P_1 = P_{atm} + \rho g\left(z_0 - z_1\right)$$

where P_1 is the pressure at point 1, P_{atm} is atmosphere pressure, ρ is the density of water at 50°C, g is acceleration due to gravity, z_0 is the water level in the funnel, and z_1 is the slot height. All of the variables on the right side of the P_1 equation are constant, so P_1 is constant. The equation for the pressure at point 2 in **Figure A16-2** is:

$$P_2 = P_{atm} + \frac{3}{2}P_{3gauge} - \frac{\rho g}{2}\left(z_0 + z_1\right)$$

where P_2 is the pressure at point 2, P_{atm} is atmosphere pressure, P_{3gauge} is pressure reading from the pressure gauge in the vacuum line, ρ is the density of water at 50°C, g is acceleration due to gravity, z_0 is the water level in the funnel, and z_1 is the slot height. The only variable on the right side of the P_2 equation that is not constant is P_{3gauge}.

Model for Particle Passage Through a Slot

Since extrusion must occur in order for particles to pass through a pressurized slot, the equation for yielding with combined loads will be used for particle passage. The conditions with the top surface under compression and the bottom surface under tension would be similar to the conditions of a particle on an opening of a pressure screen, so the sign in the equation would be positive. By assuming that the forces on the particle are only due to pressure on the particle, the equation relating the pressures to yielding in the single slot device is:

$$P_1 W_{Part} - P_2 W_{Slot} = 2\sigma_Y W_{Part}$$

where P_1 is the pressure above the slot, P_2 is the pressure inside the slot, σ_Y is the yield stress of the material, W_{Part} is the particle width, and W_{Slot} is the slot width. The equation relating the vacuum gauge pressure required for a particle to extrude through the slot is:

$$P_{3gauge} = -\frac{2}{3}\left\{ P_{atm} - \frac{\rho g}{2}(z_0 + z_1) + \left[2\sigma_Y - P_{atm} - \rho g(z_0 - z_1)\right]\frac{W_{Part}}{W_{Slot}} \right\}$$

where P_{3gauge} is the vacuum gauge pressure in the vacuum line, P_{atm} is atmospheric pressure, ρ is the density of water at 50^{o}C, g is acceleration due to gravity, z_0 is the water level in the funnel, z_1 is the slot height, σ_Y is the yield stress of the material, W_{Part} is the particle width, and W_{Slot} is the slot width. The only variables on the right side of the equation that are not constant for the pressurized single slot device are the yield stress of the material and the particle width. Previous research involving the pressurized single slot device found that particle passage through the slot correlated with the yield stress of the material and the average particle area [9].

The calculated gauge pressure using the above equation can be compared to the pressures in the single slot device. The minimum gauge pressure that can be obtained by the single slot device is –73 kPa. If the gauge pressure is less than –73 kPa, then the adhesive particle should not pass through the slot of the single slot device. If the gauge pressure is between the minimum gauge pressure, –73 kPa, and atmospheric gauge pressure, 0 kPa, the particle should pass through the slot of the single slot device.

A total of 224 particles were analyzed with the particle aligned with the slot in the previous research [9] and the above research. Eight different adhesive formulations were analyzed, each with a different yield stress [9]. Of the 224 total particles, 60 particles had calculated gauge pressure values less than –73 kPa, and should not have passed through the slot, while 164 particles had calculated gauge pressure values greater than –73 kPa, and should have passed through the slot. All 60 of the particles that had calculated gauge pressure values less than –73 kPa were from the BA-EA adhesive formulation. BA-EA had the highest yield stress, 56 kPa, of all of the adhesive formulations considered [9]. Of the 60 particles that should not have passed, 58 of the particles did not pass, so 97% of the particles were predicted correctly. Of the 164 particles that should have passed, only 77 of the particles did pass through the slot, so only 47% of the particles were predicted correctly.

CONCLUSIONS

Particle bending may occur when a particle is on the slot of a pressurized screen, but extrusion must occur in order for the particle to pass through the slot. The gauge pressure required for a particle to pass through the slot can be determined based on the yield stress of the material and the width of the particle.

REFERENCES

1. Pikulin, M. A., "Stickies and Their Impact on Recycled Fiber Content Fine Paper", *Joint Conference to Address Pressure Sensitive Adhesive Issues Proceedings*, United States Postal Service and American Forest & Paper Association, Washington, D.C., June 1996.

2. Heise, O., "Screening Foreign Material and Stickies", *Tappi Journal*, 75(2):78-81, 1992.

3. Sutherland, N. R., "Stickies Dirt Count and Laboratory Methods", *Environmentally Benign Pressure-Sensitive Adhesives for Postal Application Conference Proceedings*, United States Postal Service, Potomac, MD, July 1997.

4. Lucas, B. E., Venditti, R. A., and Jameel, H., "Breakage and Extrusion of Pressure Sensitive Adhesives in Industrial and Laboratory Screening Processes", *2001 Tappi Pulping Conference Proceedings*, Seattle, WA, TAPPI Press, November 2001.

5. Lucas, B. E., Venditti, R. A., and Jameel, H., "Behavior of Pressure Sensitive Adhesive Material in Industrial Pressure Screens and Laboratory Screens", *Tappi Journal*, 84(5):70, 2001.

6. Bliss, T., and Ostoja-Starzewski, M., "Debris Characteristics and Removal Techniques", *1997 Tappi Korea Recycling Symposium Proceedings*, Seoul, Korea, TAPPI Press, pp. 1-17, October 1997.

7. Williams, J. G., *Stress Analysis of Polymers*, 2nd edition, Ellis Horwood Limited Publishers, Chichester, England, 1980.

8. Zyczkowski, M., *Combined Loadings in the Theory of Plasticy*, Polish Scientific Publishers, Warsaw, Poland, 1981.

9. Lucas, B. E., Venditti, R. A., and Jameel, H., “The Effects of Adhesive Properties on Adhesive Particle Breakage and Passage During Paper Recycling Operations”, <u>*Progress in Paper Recycling*</u>, accepted for publication, 2004.

APPENDIX 17

DRAG FORCES ON AN OBJECT

When an object is immersed in a fluid there is an interaction between the object and the fluid [1]. If the fluid is moving or the object is moving, resultant forces occur at the interface between the object and fluid. The forces are called shear stresses and normal stresses. The normal stresses are due to the pressure on the object. The distribution of the resultant forces is determined in relation to the upstream velocity. The forces that are parallel with the upstream velocity are the drag forces and the forces that are normal to the upstream velocity are the lift forces.

The drag forces on an object can be separated into friction drag and form drag [1]. The friction drag is due to the shear stresses on the object and the form drag is due to the pressure on the object. The drag forces can generally only be determined for simple situations, such as for smooth spheres and smooth circular cylinders. The equation used to calculate the form drag force on an object is:

$$D = \frac{1}{2}\rho U^2 A C_D$$

where D is the drag force in N, ρ is the density of the fluid in kg/m^3, U is the upstream velocity of the fluid in m/s, A is the area of the object perpendicular to the fluid flow in m^2, and C_D is the drag coefficient [1].

The distributions of shear stresses and pressure usually cannot be determined analytically, so a drag coefficient is used [1]. The main factors for the drag coefficient are the shape of the object and the Reynolds number. The drag coefficient also depends on the Mach number, the Froude number, and the relative surface roughness. All of the factors for the drag coefficient affect the characteristics of fluid flow around the object.

The shape of the object affects how the pressure forces are oriented with respect to the surface of the object. Parts of the surface may be parallel or normal to the upstream velocity, but most of the surface would be in between parallel and normal.

The Reynolds number is used to determine if the fluid flow is laminar or turbulent [1]. As the Reynolds number increases, the drag coefficient generally decreases. When the Reynolds number is very low, there is a balance between the viscous and pressure forces on the object and fluid separation does not occur. As the Reynolds number increases, fluid separation occurs, creating a wake in the fluid flow beyond the object. At moderate Reynolds numbers, a laminar boundary layer is formed on the object, with a wide turbulent wake beyond the object. At very large Reynolds numbers, the boundary layer becomes turbulent and the wake becomes narrow.

In **APPENDIX 16**, the theoretical model for fluid flow through a slot involves velocities as functions of the gauge pressure of the device. The equation for the velocity through the slot of the single slot device is:

$$v_2^{\ 2} = 2\left(gz_0 - \frac{P_{3gauge}}{\rho}\right)$$

where v_2 is the velocity through the slot in m/s, g is acceleration due to gravity in m/s^2, z_0 is the water level within the device in meters, P_{3gauge} is the gauge pressure of the device in Pa, and ρ is the density of water in kg/m^3. The equation for the velocity providing the drag force on a particle is:

$$v_1 = v_2 \frac{A_{Slot}}{A_{Funnel}}$$

where v_1 is the velocity above the slot providing the drag force in m/s, v_2 is the velocity through the slot in m/s, A_{Slot} is the cross-sectional area of the slot in cm^2, and A_{Funnel} is the cross-sectional area of the funnel in cm^2. The cross-sectional area of the slot is 0.045 cm^2 and the cross-sectional area of the funnel is 235 cm^2.

Theoretical calculations of the drag force as pressure as a function of the single slot gauge pressure are shown in **Table A17-1**. The maximum drag force per unit area that can be achieved in the single slot device is 0.035 Pa. Notice that the units for drag pressure are Pa, while the units for the gauge pressure are kPa. The drag force is negligible compared to the yield stresses of pressure sensitive adhesive films (see **CHAPTER 8**), the single slot device gauge pressure of –73 kPa (**APPENDIX 16**), and the atmospheric pressure of 101 kPa. Therefore, drag forces are negligible for pressure sensitive adhesive particles in the single slot device.

Table A17-1. Theoretical Drag Force Data

Gauge Pressure. kPa	Drag Velocity, m/s	Drag Coefficient	Drag Pressure, Pa
-10	0.00087	25	0.0094
-20	0.0012	20	0.012
-30	0.0015	18	0.020
-40	0.0017	16	0.024
-50	0.0019	15	0.028
-60	0.0021	14	0.031
-70	0.0023	13	0.034
-73	0.0023	13	0.035

REFERENCES

1. Geankoplis, C. J., Transport Processes and Unit Operations, 3rd edition, Prentice-Hall, Englewood Cliffs, NJ, 1993.